Environmental determinants of antibiotic resistance and virulence of *Acinetobacter baumannii* and development of novel molecular tools for genetic manipulations of *Acinetobacter baumannii*

BY

Pawuththuwadura Malaka Pulinda De Silva

A thesis submitted to the Faculty of Graduate Studies of The University of Manitoba in partial fulfilment of the requirements of the degree of

DOCTOR OF PHILOSOPHY

Department of Microbiology

University of Manitoba

Winnipeg

ABSTRACT

Acinetobacter baumannii is a notorious pathogen in health-care settings around the world, primarily due to its reduced susceptibility to antibiotics. It also shows impressive capabilities to adapt to harsh conditions in clinics, which contributes to its persistence in such conditions. Following their traditional role, the Two Component Systems (TCSs) present in *A. baumannii* play a crucial role in sensing and adapting to the changing environmental conditions. AdeRS TCS has been shown to modulate a key RND efflux pump, AdeABC which can result in antibiotic resistance. In-frame deletion of *adeRS* resulted in reduced expression of AdeB as demonstrated previously confirming the regulatory role of AdeRS in expression of AdeABC. Deletion of *adeRS* affected biofilm formation and motility of *A. baumannii* demonstrating the multi-faceted nature of regulatory networks controlled by AdeRS. Interestingly, the *adeRS* deletion mutant was sensitive to saline stress and surface associated motility was adversely affected at higher NaCl concentrations suggesting AdeRS could be a part of salinity stress adaptation in *A. baumannii*.

Investigations into the adaptation of *A. baumannii* to incubation temperatures of 28˚C and 37˚C revealed potentially clinically relevant phenotypic changes. Specifically, motility was reduced at 28˚C while biofilm formation significantly increased at 28˚C. Proteomic analysis showed an upregulation of 366 proteins and downregulation of 263 proteins at 28˚C.

An uncharacterized orphan response regulator, A1S_2006 displayed significantly higher expression levels in a MDR *A. baumannii* clinical isolate AB030. A deletion mutant of *A1S_2006* displayed decreased biofilm formation, motility, and virulence in *Galleria mellonella* model. However, deletion of *A1S_2006* resulted in significantly higher attachment of *A.*

baumannii in A549 cells. RNA-Seq analysis of the deletion mutant revealed upregulation of 116 genes and downregulation of 42 genes.

Finally, to address the lack of molecular tools available for *A. baumannii*, a set of novel mini-Tn*7* based vectors were to rejuvenate the current mini-Tn*7* based vectors. These can be used for genetic manipulations in clinical isolates with reduced susceptibility to commonly used markers. These results show the role of environmental determinants in modulating clinically relevant characteristics of *A. baumannii* as well as adding new components to the molecular toolkit for *A. baumannii*.

ACKNOWLEDGEMENTS

First, I want to thank my supervisor, Dr. Ayush Kumar for giving me a chance to pursue my PhD with him and also for his guidance, mentorship, and advice all throughout my PhD journey. It has taught me so much not only about science but also about life in general. This would not have been possible without you.

I would also like to thank my committee members Drs. Ann Karen Brassinga, W.G.Dilantha Fernanado, and Denice Bay for their time guiding me and their invaluable input to make my projects a success. I really appreciate all your efforts and guidance given to me over the last few years.

A special mention to Dr. Dinesh Fernando and Yasser Alsaadi who were my first points of contact in Kumar Lab back in 2014 for helping me settle in and also for their previous work on my projects that I took over for my PhD. All the past and present members of Kumar Lab have been an awesome bunch to hang out with, discuss science and also it has been a lot of fun to be around you guys in the last few years. There are too many to name individually but I would like to thank each one of you for being great people to have crossed paths with me and I have learned so much from all of you.

Finally, I would like to acknowledge the awesome people of the Department of Microbiology from professors, graduate students, undergraduate students, and other staff for being so supportive and making me feel welcome in the Buller building. I have made great friendships with you that I hope will last a life time. I also would like to acknowledge the funding received from the NSERC, Research Manitoba, University of Manitoba, Faculty of Science, and UMGF that enable me to carry out this research.

DEDICATION

I would like to dedicate this thesis to my dad P. Indrasiri De Silva and my mum D. Ayesha Sendrika De Silva. I am truly fortunate to be raised by you and I cannot thank you enough for moulding me into the person I am today. I could not have asked for better parents ever. Also to my brother P. Tharaka Lalinda De Silva who has not only been an awesome brother but also a dear friend who I could share everything with. I wish you all the very best in your life. A huge thank you to my wife, Dulya Thathsarani Senarathane Uhanovitage for being with me, supporting me, and sharing the highs and lows of my life for the past 13 years. You have been an amazing life partner.

Also to my extended family; parents-in-law - Dharmasena Uhanovitage and Padmini Rupalatha, Sister-in-law – Gayani De Silva and my sweet little niece Thea De Silva and all my cousin brothers and sisters, aunts and uncles. Also to my late grandparents, especially to my dear grandma Yasawathie De Silva along with P. Goman De Silva, Kalumin Weeranona, D. Mahindapala De Silva and Kusumawathie De Silva. I would never forget the love and care you have given me throughout the years and I am forever grateful for that.

Finally, to all my teachers, mentors, and colleagues that I have met throughout the years for your extended help and support (especially Andy J., Jon, Gary, Andy C., Matt, Mark, Emily, Simone, and Rob from my time studying for Master's).

I am truly fortunate to have you in my life and it is an honour to dedicate this thesis to all of you.

CONTRIBUTION OF AUTHORS

Work presented in chapters 3, 4, and 5 are the products of collective efforts by multiple authors as stated in the journal articles.

Chapter 3.2

Dr. Dinesh Fernando grew and prepared the strains to be sent for proteomic analysis while Drs. Patrick Chong and Garret Westmacott carried out the sample preparation, proteomic analysis, and differential expression analysis of the samples at the National Microbiology Laboratory in Winnipeg.

Chapter 4

Christopher I. Graham maintained and prepared A549 cells to be infected with *A. baumannii* in the laboratory of Dr. Ann Karen Brassinga with her help and guidance at the University of Manitoba.

Chapter 5

pFLP2^{ab} plasmid was created by Dr. Dinesh Fernando and the remaining plasmids were created by undergraduate honours student Kaleigh Ducas-Mowchun under the direct supervision of P. Malaka De Silva while Leandro Crisostomo carried out the fluorescent image acquisition in the laboratory of Dr. Peter Pelka with his help and guidance at the University of Manitoba. Parent plasmids that were used in this study were gifted to us by Dr. Tzu-Chiao Chao of University of Regina and Dr. Herbert P. Schweizer of University of Florida.

LIST OF COPYRIGHTED MATERIAL FOR WHICH PERMISSION WAS OBTAINED

Chapter 1 (Parts of the text and all the figures from the article)

Frontiers in Microbiology, P. Malaka De Silva and Ayush Kumar (2019) Signal Transduction Proteins in *Acinetobacter baumannii*: Role in Antibiotic Resistance, Virulence, and Potential as drug Targets https://doi.org/10.3389/fmicb.2019.00049. Frontiers in Microbiology permits the use, distribution or reproduction in other forums is permitted, provided the original author(s) and the copyright owner(s) are credited and that the original publication in this journal is cited, in accordance with accepted academic practice.

Chapter 3.1 (Full article)

Journal of Membrane Biology, P. Malaka De Silva and Ayush Kumar (2018). Effect of sodium chloride on surface-associated motility of *Acinetobacter baumannii* and the role of AdeRS two-component system. doi: 10.1007/s00232-017-9985-7.

License number: 4555711469217

Chapter 3.2 (Full article)

Antimicrobial Agents and Chemotherapy, P. Malaka De Silva, Patrick Chong, Dinesh M. Fernando, Garrett Westmacott, and Ayush Kumar (2018). Effect of incubation temperature on antibiotic resistance and virulence factors of *Acinetobacter baumannii* ATCC 17978. doi: 10.1128/AAC.01514-17. ASM authorizes an advanced degree candidate to republish the requested material in his/her doctoral thesis or dissertation.

Chapter 5 (Full article)

Applied and Environmental Microbiology, Kaleigh Ducas-Mowchun‡, P. Malaka De Silva‡, Leandro Crisostomo, Dinesh M. Fernando, Tzu-Chiao Chao, Peter Pelka, Herbert P. Schweizer, and Ayush Kumar (2019). Next generation of Tn7-based single copy insertion elements for use

in multi- and pandrug resistant strains of *Acinetobacter baumannii*. doi: 10.1128/AEM.00066-19. ASM authorizes an advanced degree candidate to republish the requested material in his/her doctoral thesis or dissertation.

TABLE OF CONTENTS

LIST OF TABLES

LIST OF FIGURES

LIST OF ABBREVIATIONS

˚C	degrees celcius
A_{600}	Absorbance at 600nm
aac-3-(IV)	Aminoglycoside N(3)-acetyltransferase encoding gene (aprmaycin resistance)
aacC1	Gentamycin 3-N-acetyletransferase encoding gene (gentamycin resistance)
Amp	Ampicillin
Apr	Apramycin
ATCC	American Type Culture Collection
ATP	Adenosine Triphosphate
BCA	bicinchoninic acid
bla	beta-lactamase gene (ampicillin resistance)
ble	Bleomycin reisitance protein encoding gene (zeocin resistance)
bp	base pair
BSA	Bovine Serum Albumin
CA	Catalytic ATP binding
cDNA	complementary DNA
CFU	Colony Forming Unit
COG	Clusters of Orthologous Groups
DHp	Dimerization and Histidine phosphtransfer
DNA	Deoxyribonucleic acid
FRT	Flp Recombinase Target
g	gram(s)
gDNA	Genomic DNA
Gm	Gentamycin
GFP	Green Fluorescent Protein
HK	Histidine Kinase
kb	kilo base pairs
kV	kilovolt
L	Litre(s)
LB	Lysogeny Broth
LC	Liquid Chromatography
LPS	Lipopolysaccharide
M	Molar
mg	milligram(s)
MHB	Mueller Hinton Broth
MIC	Minimum Inhibitory Concentration
mM	milimolar
MRSA	Methicillin Resistant Staphylococcus aureus
ng	nanogram

PCR	Polymerase Chain Reaction
qRT-PCR	quantitative Real Time - PCR
REC	Receiver
RNA	Ribonucleic acid
RNA-Seq	RNA sequencing
RR	Response Regulator
SOEing	Splice Overlap Extension
TCS	Two Component System
v/v	volume/volume
VBMM	Vogel-Bonner Minimal Media
WHO	World Heath Organization
w/v	weight/volume
x g	G-Force
µg	microgram(s)
µM	micromolar

CHAPTER 1

LITERATURE REVIEW

Parts of this chapter were published in Frontiers in Microbiology, 2019: P. Malaka De Silva and Ayush Kumar (2019) Signal Transduction Proteins in *Acinetobacter baumannii*: Role in Antibiotic Resistance, Virulence, and Potential as drug Targets https://doi.org/10.3389/fmicb.2019.00049

1.1 *Acinetobacter baumannii* – A SUCCESSFUL OPPORTUNISTIC PATHOGEN

Acinetobacter baumannii is a Gram-negative coccobacillus, which has earned a notorious reputation for being an important opportunistic human pathogen (Peleg et al., 2012; Peleg, Seifert, & Paterson, 2008; Visca, Seifert, & Towner, 2011; Wong et al., 2017). Clinical importance of *A. baumannii* is emphasised by the fact that it is listed by the World Health Organization (WHO) as the 'top priority' pathogen that urgently needs novel and effective therapeutic options (http://www.who.int/medicines/publications/WHO-PPL-Short_Summary_25Feb-ET_NM_WHO.pdf). The success of *A. baumannii* in hospital environments can be mainly attributed to its ability to display multi–drug resistant (MDR) phenotypes due to the rather robust acquisition of antibiotic resistance mechanisms (Antunes, Visca, & Towner, 2014) (Dijkshoorn, Nemec, & Seifert, 2007). These include antibiotic modifying enzymes, decreased permeability to antibiotic molecules, and efflux pumps that extrude the antibiotic molecules out to the periplasm and outside the cell (Gordon & Wareham, 2010; C. R. Lee et al., 2017).

Multi- and pan-drug resistant *A. baumannii* is an alarming development for healthcare facilities around the world (Agodi et al., 2010; Labarca, Salles, Seas, & Guzman-Blanco, 2016; Rodriguez-Bano et al., 2004; Sievert et al., 2013). As some infections caused by multi-drug resistant *A. baumannii* have become virtually untreatable with our current arsenal of antibiotics. Further, without any new antibiotics for Gram-negative bacteria such as *A. baumannii* in the developmental pipeline (Lakemeyer, Zhao, Mandl, Hammann, & Sieber, 2018), we are on the verge of a post-antibiotic era where even a minor infection could have lethal consequences for the patient (https://amr-review.org/sites/default/files/160518_Final%20paper_with%20cover.pdf)

Apart from its multidrug resistance, the success of *A. baumannii* can also be attributed to its ability to survive and persist in the harsh conditions found within hospital environmental niches (Jawad, Seifert, Snelling, Heritage, & Hawkey, 1998). Constant and prolonged exposure to antiseptics and desiccating agents, endurance of less than optimal temperatures, and sudden changes of environmental and nutritional conditions when transferred into the human body from an abiotic surface are some of the challenges that *A. baumannii* faces in its role as an opportunistic human pathogen. Therefore, in order to be a successful pathogen, *A. baumannii* needs to sense and adapt to these changes in an efficient and timely manner.

Signal transduction mechanisms in bacteria play a crucial role in adapting to environmental changes. TCSs are one of the most ubiquitous signal transduction systems present in bacteria that help them sense and adapt to the environmental conditions (Alm, Huang, & Arkin, 2006). Therefore TCSs play a role in bacterial adaptive responses which can lead to the modulation of their antibiotic susceptibility and virulence. These systems are vital to study in order to understand the mechanisms of antibiotic resistance and virulence in bacteria (Kroger, Kary, Schauer, & Cameron, 2016). Further, TCSs can also serve as an attractive target when developing anti-virulence therapeutics (Gotoh, Eguchi, et al., 2010).

1.2 MECHANISMS OF RESISTANCE IN *A. baumannii*

Global success of *A. baumannii* as an opportunistic pathogen has been heavily dependent on its ability to display decreased susceptibility to a large number of antibiotics in use (Esterly, Richardson, Eltoukhy, Qi, & Scheetz, 2011). *A. baumannii* is well known for acquiring and displaying resistance mechanisms to all available antibiotics. Ability of *Acinetobacter* genus in general to acquire novel antibiotic resistance mechanisms mainly revolves around its genome plasticity compared to other pathogens. For example, *Acinetobacter baylyi* strain ADP1, is

remarkably naturally competent for the uptake of foreign DNA and as such is up to a 100 times more competent than calcium chloride treated *E. coli* (Metzgar et al., 2004). In addition to that, computational sequence analysis has revealed the presence of an 86kb resistance island AbaR1 in *A. baumannii* strain AYE where 45 resistance genes and transposition machinery has been observed (Fournier et al., 2006).Most of these resistance genes have been previously identified in other Gram-negative pathogens such as *Pseudomonas* spp and *Salmonella* spp. further establishing the plasticity of *A. baumannii* genome. This together with horizontal gene transfer contributes in a large scale to the decreased susceptibility of *A. baumannii* on a global scale especially in clinical isolates. In fact, a sequence analysis of the type strain *A. baumannii* ATCC 17978, which is used in the bulk of the studies presented in this thesis, revealed 74 potential drug resistance genes (including 32 efflux pump genes and 11 permease genes) in the genome (M. G. Smith et al., 2007). Analysis of whole genome sequence data from a different clinical isolate of *A. baumannii* isolated form France revealed 88 open reading frames encoding for potential resistance mechanisms (Fournier et al., 2006). This goes to show the inherent ability of *A. baumannii* to acquire resistance genes especially in clinical surroundings where it is exposed to other pathogens with resistance mechanisms. Inactivating enzymes such as beta-lactamases and carbapenamases, Efflux pump proteins such as AdeABC top the list of resistance genes associated with *A. baumannii* (Perez et al., 2007) Below are some of the mechanisms of resistance displayed by *A. baumannii* to known classes of antibiotics:

1.2.1. BETA-LACTAMS

In addition to the expression of beta-lactamases, decreased porin expression limiting the chances of the drug molecule entering into the cell and the expression of efflux pumps which extrude the beta-lactams are deployed by *A. baumannii* to resist the action of beta-lactams. *A. baumannii* is

shown to express a vast array of beta-lactamases ranging from the chromosomally encoded bla_{ampC} encoding an AmpC cephalosporinase and $bla_{OXA\text{-}51}$ encoding an OXA-51 group of Ambler class oxacillinase to the extended spectrum beta-lactamases (ESBL) and metallo-beta-lactamases (MBL) (Bonomo & Szabo, 2006; Brown, Young, & Amyes, 2005). Usually the basal level expression of AmpC through the chromosomal copy is not enough to elicit a decreased susceptibility. However, the acquisition of ISAbaI insertion sequence upstream of the *ampC* gene has been observed to act as a promoter to drive higher levels of AmpC expression conferring decreased susceptibility to all penicillins and also to most extended-spectrum cephalosporins (Corvec et al., 2003; Jacoby, 2009). Apart from these Class C beta-lactamases, other classes of beta-lactamases such as Class B MBLs which differ from the other beta-lactamases by having a metal ion in the active site have been found in *A. baumannii* which has the capacity to hydrolyze carbapenems and all beta-lactams except aztreonam.(Chu et al., 2001; Gales, Tognim, Reis, Jones, & Sader, 2003; Walsh, 2005). Class D OXA beta-lactamses which are usually efficient penicillinases are able to hydrolyze extended spectrum cephalosporins. These are also described to be present in *A. baumannii* isolates from various parts of the world (Brown & Amyes, 2006).

In addition to the hydrolyzing enzymes, several porins or outer membrane proteins (OMPs) have been associated with the decreased susceptibility towards beta-lactams. Of note is the observation of reduced expression of 37 kDa, 44 kDa and 47 kDa OMPs together with Class C cephalosporinases in a carbapenem resistant clinical isolate (Quale, Bratu, Landman, & Heddurshetti, 2003). Also reduced expression of 22 kDa and 33 kDa OMPs coupled with OXA-24 production in another carbapenem resistant isolate of *A. baumannii* demonstrate the role of reduced expression of OMPs in decreased susceptibility to beta-lactams and also carbapenems (Bou, Cervero, Dominguez, Quereda, & Martinez-Beltran, 2000). Another resistance mechanism

towards beta-lactams is the expression of efflux pumps by *A. baumannii*. A classic example is the role of AdeABC efflux pump where overexpression of AdeABC combined with carbapenem hydrolyzing oxacillinase resulted in resistance to carbapenems (Marque et al., 2005). AdeABC ellux pump however, is also known to efflux a wide variety of other antibiotic molecules such as aminoglycosides, tetracyclines, trimethoprim, and fluoroquinolones (Magnet, Courvalin, & Lambert, 2001).

1.2.2 QUINOLONES AND AMINOGLYCOSIDES

Resistance to quinolone antibiotics such as ciprofloxacin is mediated by target site mutations in *gyrA* and *parC* genes whereby modifying the structure of DNA gyrase and topoisomerase (Seward & Towner, 1998). These mechanisms have been reported in clinical isolates of *A. baumannii* where decreased susceptibility towards quinolones has been observed (Vila, Ruiz, Goni, & Jimenez de Anta, 1997; Vila, Ruiz, Goni, Marcos, & Jimenez de Anta, 1995). In addition to that, efflux pumps such as AdeABC and novel efflux pump AbeM are also known to mediate resistance for flouroquinolones (Magnet et al., 2001; Su, Chen, Mizushima, Kuroda, & Tsuchiya, 2005). Of note, however, is the absence of plasmid mediated quinolone resistance gene (*qnr* genes) in *A. baumannii* which is present in other Gram-negative pathogens such as *Klebsiella* spp and *Enterobacter* spp (Nordmann & Poirel, 2005; Robicsek, Sahm, Strahilevitz, Jacoby, & Hooper, 2005).

Aminoglycoside modifying enzymes and efflux pumps such as AdeABC that are described above are the main mechanisms of resistance against aminoglycosides in *A. baumannii*. Genes encoding aminoglycoside phosphotransferases, aminoglycoside acetyltransferases, and aminoglycoside nucleotidyltransferases are reported in *A. baumannii* clinical isolates from

different parts of the world (Nemec, Dolzani, Brisse, van den Broek, & Dijkshoorn, 2004; Turton et al., 2006). Interestingly, aminoglycoside modifying enzymes that confer resistance to more than one type of aminoglycoside have not been reported in *A. baumannii* as in other pathogens (Kim, Hesek, Zajicek, Vakulenko, & Mobashery, 2006).

1.2.3. TETRACYCLINE AND POLYMIXINS

Two common mechanisms of resistance against tetracyclines are TetA / TetB mediated efflux pumps and *tet(M)* encoded ribosomal protection protein. TetA mediated efflux pumps are shown to be active against tetracycline whereas TetB mediated efflux pump is seen to be active against both tetracycline and minocycline in *A. baumannii* (Guardabassi, Dijkshoorn, Collard, Olsen, & Dalsgaard, 2000). TetM ribosomal protection protein, which is homologous to that of *Staphylococcus aureus* provides protection against tetracycline, doxycycline, and minocycline in *A. baumannii* (Ribera, Ruiz, & Vila, 2003). However, neither of the above mechanisms were reported to confer resistance to the relatively novel glycylcyline, tigecyline and it was only recently that it was described as a substrate for AdeABC efflux pump in *A. baumannii* (Ruzin, Keeney, & Bradford, 2007).

Polymixins are considered the "last resort" antibiotics and worryingly the number of *A. baumannii* clinical isolates displaying decreased susceptibility to polymixins are on the rise (Li et al., 2006; Reis, Luz, Tognim, Sader, & Gales, 2003). The main mechanism of resistance against polymixins such as colistin is considered to be modifications in the lipopolysaccharides of *A. baumannii* (Peterson, Fesik, & McGroarty, 1987). This modification of lipopolysaccharides has been reported to be under the regulation of PmrAB TCS in *A. baumannii* as described elsewhere in this thesis (Arroyo et al., 2011).

1.3 VIRULENCE FACTORS OF *A. baumannii*

A. baumannii posses only a limited number of well known virulence factors compared to some other Gram-negative pathogens. These virulence factors may not always be present across different strains of *A. baumannii* as well (Morris, Dexter, Kostoulias, Uddin, & Peleg, 2019). Out of the known virulence factors observed in *A. baumannii*, the best characterized virulence factor at present is outer membrane protein A (OmpA). It is also the most abundant outer membrane protein (OMP) in *A. baumannii* and has been implicated in a number of virulence related mechanisms in *A. baumannii* (C. H. Choi et al., 2005). One significant characteristic of OmpA is its reduced permeability compared to the other OMPs such as OmpF and OmpC from *E. coli* thereby reducing the overall permeability of *A. baumannii* membrane (Sugawara & Nikaido, 2012). OmpA has been seen to concentrate into outer membrane vesicles during the in-vivo growth of *A. baumannii* where it induces cytotoxicity in eukaryotic cells by binding to the cell surface death receptors (C. H. Choi et al., 2005; D. C. Moon et al., 2012). OmpA also plays a role in adherence and invasion of epithelial cells potentially contributing to the dissemination of *A. baumannii* in human hosts (C. H. Choi, Lee, Lee, Park, & Lee, 2008). In addition to that, OmpA is also implicated in assisting biofilm formation and surface motility demonstrating that it is one of the main virulence factors in *A. baumannii* (Gaddy, Tomaras, & Actis, 2009).

Lipopolysaccharide (LPS) comprised of a lipid A anchor, a carbohydrate core, and a repetitive O-antigen is also a known virulence factor in *A. baumannii* Lipid A acts as the immunostimulatory component of the LPS in *A. baumannii* and until recently thought to be essential in Gram-negative bacteria (Moffatt et al., 2013). However, recently it was shown that colistin exposure inactivated *lpxA*, *lpxC*, and *lpxD* resulting in a Lipid A deficient strain of *A. baumannii* (Moffatt et al., 2013). In light of this evidence of Lipid A being non-essential, it

partially explains the PmrAB TCS mediated Lipid A modifications as a sensible modification to induce decreased susceptibility to colistin by *A. baumannii*.

In addition to the LPS, capsule has also been recognized as a virulence factor in *A. baumannii*. There have been studies demonstrating that the capsule deficient strains to have decreased growth in human serum and being less capable than the capsule positive strain to cause soft tissue infection (Russo et al., 2010). Presence or absence of capsule was also implicated in phenotypic switching in *A. baumannii* whereby the capsule positive strain was

more virulent further emphasizing the role of capsule as a virulence factor (Chin et al., 2018).

1.4 ANIMAL MODELS USED IN *A. baumannii* STUDIES

Since *A. baumannii* is a pathogenic bacterium, it is necessary to study its virulence capabilities using *in-vivo* animal models. In addition to that, animal models are helpful and often crucial in development and assessment of novel therapeutics prior to clinical trials. Traditionally as with other human pathogens, the best-suited animal model to assess human infections and therapeutics is another mammalian system where mice are usually used. The first animal model used with *A. baumannii* is also a mouse model of acute pneumonia (Joly-Guillou, Wolff, Pocidalo, Walker, & Carbon, 1997). The most commonly used mouse strains in the laboratory are BALB/c and C57BL/6 However, clinical strains of *A. baumannii* are often unable to immunocompetent mice (Renckens et al., 2006). Therefore, immunocompromised mice or mice treated with mucin or agar have also been used with *A. baumannii* studies (Knapp et al., 2006). Despite these issues, mice models have been used for years and also with clinical isolates of *A. baumannii* (G. Harris et al., 2013). However, there are reports of other animal models used in *A. baumannii* infection assays where a more diverse range of animals have been used. Amount of

preparation work required to start and maintain mice in laboratory conditions and the costs associated with that may be the contributing factors among others for this diversification. Even though the infection pathologies have to be characterized for novel infection models before they are used and accepted, there have been various published records of rodent, non-rodents such as rabbits, and non-mammalian models being used for *A. baumannii* virulence models (McConnell, Actis, & Pachon, 2013). Rabbit models were recently used as a model for *A. baumannii* meningitis where the inoculum was instilled into the intracisternal space (Pachon-Ibanez et al., 2010). On another instance, a rabbit endocarditis model has been developed following a staphylococcal endocarditis model using New Zealand rabbits (Rodriguez-Hernandez et al., 2004). In addition to that, a zebra fish model was recently employed to assess the neutrophil migratory patterns during *A. baumannii* infection (Bhuiyan et al., 2016) However, the same limitations may apply for these animal models and due to the ease of handling, storage and costs involved, non-mammalian models such as *Galleria. mellonella* and *Caenorhabditis elegans* models have recently emerged. However, one drawback of using these small animal models is the inability to sample the same animal at multiple time points as usually end-point readings of the bacterial load are obtained. Nonetheless, these systems offer a lucrative alternative to not only the above mentioned issues but also provide an alternative for ethical concerns using large animals for research (The mechanisms of disease caused by *Acinetobacter baumannii* (Morris et al., 2019). We used a *G. mellonella* infection model for the experiments described in this thesis based on a previously published protocol (Peleg et al., 2009) with minor modification if and when necessary. *G. mellonella* are the caterpillars of the greater wax moth and final-instar larvae were used in the studies described in this thesis. *G. mellonella* model when used with *A. baumannii* has demonstrated the inoculum load dependent larval mortality post infection as well

as the acinetobactin mediated iron acquisition (Gaddy et al., 2012). In addition to that, *G. mellonella* virulence assays have revealed that the mortality of the larvae also varied when different strains of *Acinetobacter* were used according to their levels of known pathogenicity in humans (McConnell et al., 2013). Therefore, *G. mellonella* is a tried and tested alternative to the larger animal models such as mice, which serves the purposes of this thesis to examine virulence of *A. baumannii*.

1.5 TWO COMPONENT SYSTEMS (TCSs)

TCSs are the most widespread signal transduction system present in bacterial and archeal kingdoms (Stock, Robinson, & Goudreau, 2000). A prototypical TCS is comprised of a membrane-bound sensory histidine kinase (HK) and a cytosolic response regulator (RR) protein (Figure 1). Since their first description in 1986 (Nixon, Ronson, & Ausubel, 1986), an enormous amount of both HK and RR proteins have been discovered and characterised in a wide variety of bacteria (Whitworth & Cock, 2009). It is estimated that an average bacterial genome can contain up to 50-60 TCS-encoding genes (Whitworth, 2008; Whitworth & Cock, 2008; Wuichet, Cantwell, & Zhulin, 2010). Given the advancement in bioinformatics and next generation sequencing techniques over the past couple of decades, the number of TCSs identified *in silico* based on the domain architecture homology with previously characterised TCSs has increased exponentially. This has resulted in the emergence of specific databases such as P2CS and MiST dedicated to TCSs (Barakat, Ortet, & Whitworth, 2011; Ulrich & Zhulin, 2007) that present the researchers with valuable information about these proteins.

The basic mechanism of action of a TCS involves the HK sensing the changes in the surrounding environment and relaying the message to the RR effectively through phosphorelays in order for the RR to initiate the necessary response. The RR protein is activated by the transfer of the phosphoryl group from the HK and the activated form of the RR most commonly binds to DNA to control transcription that allows the bacterial cell to mediate the appropriate response. A high level of specificity between the HK and the RR is observed within the TCSs of a bacterial cell and this is crucial for the adaptation and survival of the bacterial cell to the changing environmental conditions (Szurmant, White, & Hoch, 2007). However, there are instances where a single HK protein can have multiple cognate RR proteins (Lopez-Redondo et al., 2010) or when a single RR protein can be activated by multiple HK proteins (Laub & Goulian, 2007). A general architecture of a typical TCS is depicted in Figure 1. HK proteins, which usually exist as dimers, possess several conserved domains that are essential for their function such as the dimerization and histidine phosphotransfer (DHp) domain and catalytic ATP binding (CA) domain which make up the catalytic core of the HK (Bhate, Molnar, Goulian, & DeGrado, 2015). As shown in Figure 1, the DHp domain usually consists of parallel alpha-helices which are joined together by a length variable loop (DHp loop). One of these helices contain the H-box where the conserved histidine residue, that gets phosphorylated, is located (Casino, Rubio, & Marina, 2009, 2010). The catalytic core of the HK is connected to the upstream N-terminal and usually extra-cytoplasmic sensing domains through transmembrane helices (Figure 1). The DHp domain is also connected to the CA domain via a variable length loop called the DHp-CA linker (Albanesi et al., 2009). The CA domain, consists of a five-stranded beta-sheet flanked by three parallel alpha-helices on the side of the ATP pocket and it binds ATP and phosphorylates the HK at the conserved histidine residue; Thus, initiating the HK autophosphorylation (Zschiedrich,

Keidel, & Szurmant, 2016). The DHp and CA domains are conserved among all HK proteins and the sensory domains are variable conferring specificity of signal recognition. The phosphoryl group from the H-box of the HK is ultimately transferred to a conserved aspartate residue of the receiver (REC) domain of the cognate RR thus activating the RR (Yamamoto et al., 2005). The REC domain consists of a doubly wound alpha/beta fold with a five-stranded parallel beta-sheet encompassed by two alpha-helices on one side and three on the other. While the REC domain is highly conserved, the effector domains display variability conferring specificity to RR proteins (Zschiedrich et al., 2016). Following its activation, dephosphorylation of the RR is critical to maintain the efficient regulatory capacity of the TCSs (Kenney, 2010). This is achieved through the phosphatase activity of the HK where dephosphorylation of the RR is typically guided by a nucleophilic attack of a water molecule on the phosphoryl group (Hsing & Silhavy, 1997).

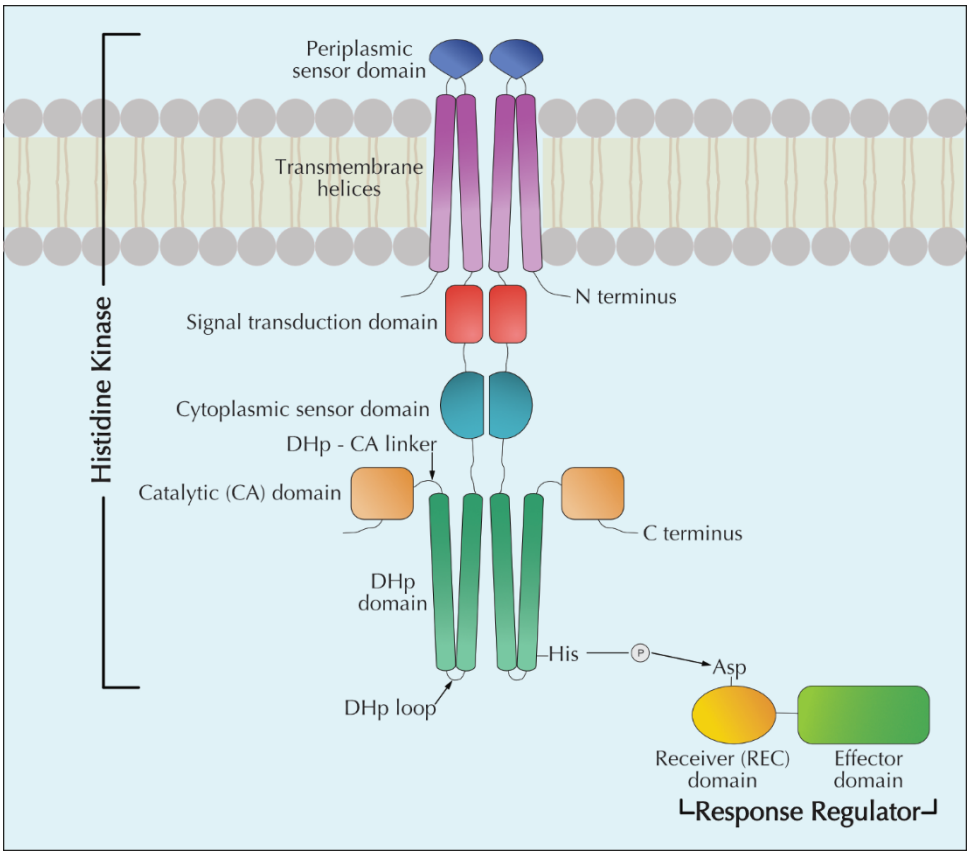

Figure 1. General arrangement of a TCS displaying the components of the HK and RR.

A prototypical TCS comprises of a membrane bound HK and a cytosolic RR. The dimeric HK component of a TCS is usually composed of several conserved domains such as DHp domain and CA domain. Activation of the RR is observed when a phosphryl group is transferred from the conserved histidine residue of the DHp domain of HK to the conserved aspartate residue of the REC domain of the RR.

The TCSs in bacterial systems have implications for a wide variety of regulatory functions relating to sensing and adapting to their environment. In pathogenic bacteria, these functions often include but are not limited to antibiotic susceptibility modulation and virulence-related phenotypes such as biofilm formation and motility (Tiwari et al., 2017).

1.6 TCSs IN *Acinetobacter baumannii*

Analysis of various genomes of well-characterized *A. baumannii* clinical isolates show the presence of about 20 different genes/operons that encode for TCSs. Most of these genes and operons have a high degree of conservation at the nucleotide level among the clinical isolates, indicating that they may be involved in important functions (Appendix I). However, as mentioned above, the effector domains of *A. baumannii* RR proteins can be quite diverse as shown in Figure 2. This is due to the various different effector domains that are present towards the C-terminal of the RR protein. The predicted effector domains are represented in Figure 2 for the RR proteins of *A. baumannii* ATCC 17978. The DNA binding OmpR_PhoB type effector domain was most commonly found in a conserved domain search of the annotated RR proteins of *A. baumannii* followed by the Lux_R type HTH domain.

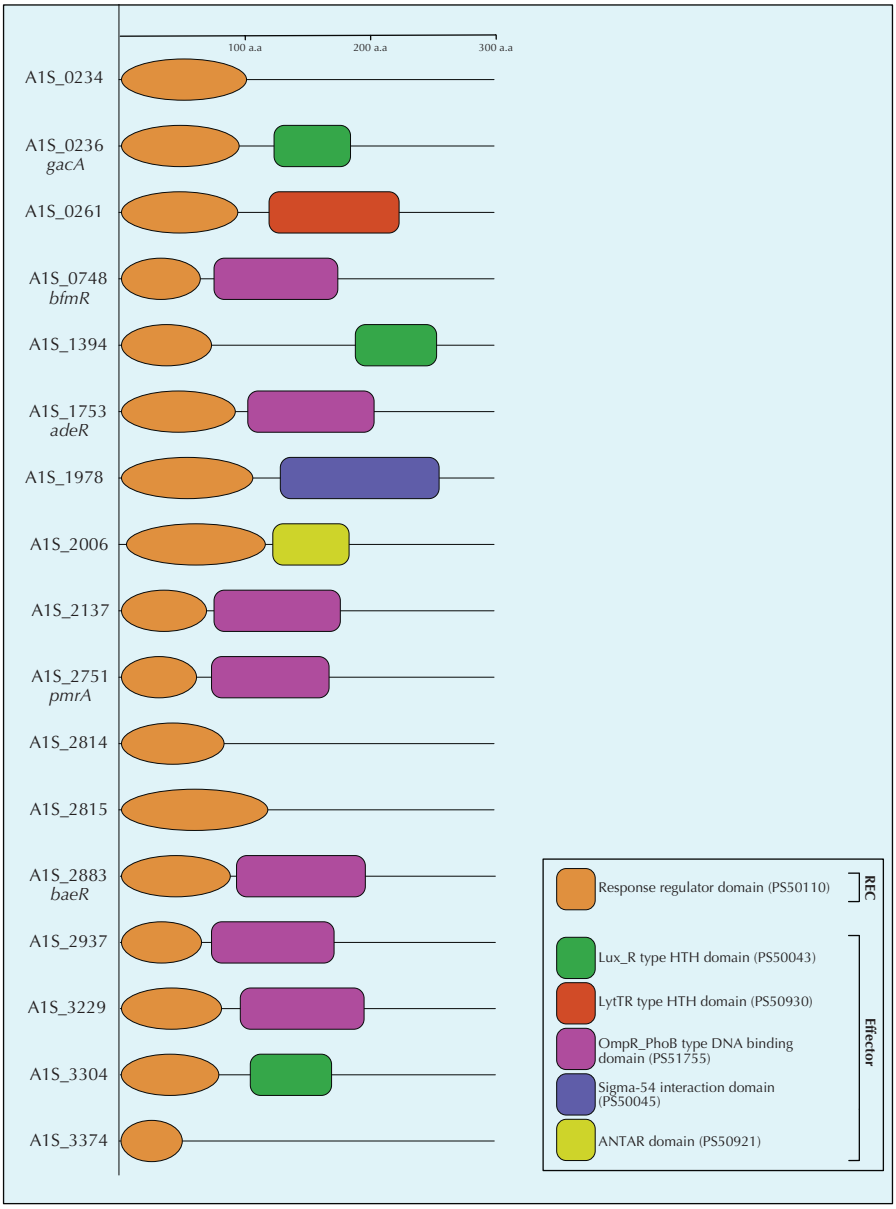

Figure 2. Schematic diagram of the conserved domains of the RRs of *A. baumannii* ATCC 17978. According to a ScanProsite (https://prosite.expasy.org/scanprosite/) search, predicted conserved effector domains demonstrate a high degree of variability among the RR of *A. baumannii*. The most commonly found effector domain was OmpR_PhoB type DNA binding domain where it was present in seven RR proteins followed by Lux_R type HTH domain, which was present in three RR proteins. The other types of effector domains were exclusive to a single RR protein.

Below are the TCS in *A. baumannii* that have been characterized to date. A summary of TCS characterized in *A. baumannii* to date is also provided in Figure 3.

1.6.1 AdeRS

AdeRS is the first characterised and also the most studied TCS in *A. baumannii* in a number of clinical isolates. The AdeRS system acts as an activator of the AdeABC efflux pump where the phosphorylated AdeR upregulates the expression of AdeABC (Yoon et al 2013). The AdeRS system was first described in a clinical strain of *A. baumannii* BM4454, where the inactivation of *adeRS* resulted in an increased susceptibility to aminoglycosides (Marchand, Damier-Piolle, Courvalin, & Lambert, 2004). The increased susceptibility to aminoglycosides is attributed to the downregulation of the RND efflux pump AdeABC in *A. baumannii* BM4454 upon insertion-inactivation of *adeS*. This demonstrated the requirement of AdeS for the expression of *adeABC* (Marchand et al., 2004). Two studies on the expression of the AdeABC pump have demonstrated that there is a direct relationship between the AdeABC overexpression and reduced tigecycline susceptibility in clinical isolates, linking the role of AdeRS in tigecycline susceptibility of *A. baumannii* (Sun et al., 2014; Yuhan, Ziyun, Yongbo, Fuqiang, & Qinghua, 2016). This is important since tigecycline is a last resort antibiotics for the treatment of multidrug resistant *A. baumannii* infections (Ni et al., 2016). Since AdeABC-independent mechanisms of tigecycline have also been reported recently (Yoon, Courvalin, & Grillot-Courvalin, 2013), it is believed that tigecycline susceptibility of *A. baumannii* is likely to be multifactorial.

A number of mutations in either *adeR*, *adeS,* or both may be directly responsible for the overexpression of the AdeABC pump by preventing dephosphrylation of AdeR (Ruzin et al., 2007; Sun et al., 2016). Several amino acid substitutions have been observed in the vicinity of

conserved His_{149} of the DHp domain (Figure 1) in AdeS (for example R152K, T153M, etc) or the conserved Asp_{63} of the REC domain (Figure 1) in AdeR (for example P56S, A91V, etc) in clinical isolates. The most common types of mutations in the *adeRS* genes that result in the overexpression of the AdeABC pump are associated with mutations in the conserved regions of both *adeR* and *adeS* causing increased expression of the pump (Yoon et al., 2013). While the exact mechanism of regulation of the AdeABC efflux pump by AdeRS remains to be determined, a recent study has shown that the response regulator AdeR binds to an intercistronic region between *adeR* and *adeABC* which consists of a 10 bp direct repeat DNA sequence containing a single random nucleotide in between (Wen et al., 2017). Interestingly, unphosphorylated AdeR, despite being in the inactive state, also retains binding affinity to its target DNA (Wen et al., 2017). This may indicate that AdeR helps maintain a basal level of expression of AdeABC in a non-stimulated condition and initiates an overexpression of AdeABC when antibiotic stress is encountered (Wen et al., 2017). However, further investigations are needed to delineate the exact mechanisms by which AdeRS regulates the expression of AdeABC.

Recent data suggest that the role of AdeRS extends well beyond the expression of the AdeABC efflux pump. A study in *A. baumannii* AYE showed that AdeRS controls the expression of almost 600 different genes (Richmond et al., 2016). A number of these genes are believed to play a role in virulence, biofilm formation and multi drug efflux activity. However, at least some phenotypes attributed to AdeRS appear to be strain-specific. For example, we observed that deletion of AdeRS in *A. baumannii* ATCC 17978 (widely used type strain originally isolated from a meningitis patient) results in a decrease in biofilm formation on plastic surfaces (De Silva & Kumar, 2017), whereas no change was observed in biofilm formation capabilities in *A.*

baumannii AYE (a multidrug resistant clinical isolate) upon the deletion of AdeRS (Richmond et al., 2016).

The multifaceted regulon of AdeRS remains to be explored further, especially in clinically relevant phenotypes of *A. baumannii*. Environmental signals that activate the sensor kinase, AdeS, remain mostly unknown. Thus a better understanding of the function of AdeRS can lead to its potential targeting as a drug candidate in *A. baumannii* because the regulon of AdeRS involves a number of clinically relevant phenotypes as discussed above (Figure 3). Therefore, regulating these phenotypes could potentially have a key benefit in controlling and/or eradicating infections caused by *A. baumannii*.

1.6.2 BaeSR

Overlapping regulons are a characteristic feature of several bacterial TCSs which leads to the regulation of a certain genes by more than one TCS. BaeSR, named for its homology with an *E. coli* TCS (Leblanc, Oates, & Raivio, 2011), is an example of that of TCSs in *A. baumannii*. BaeSR was initially thought to be associated with the regulation of AdeABC RND efflux pump expression and thus the modulation of tigecycline susceptibility of *A. baumannii* (Lin, Lin, Yeh, & Lan, 2014). Specifically, deletion of *baeR* resulted in a decreased expression of *adeABC* leading to an increased susceptibility to tigecycline. This is indicative of a possible overlapping regulons between BaeSR and AdeRS as they both regulate the expression of the AdeABC efflux pump. Further investigations into the BaeSR revealed that it may play a role in modulating the expression of the AdeIJK and MacAB-TolC efflux pumps as well (Henry et al., 2012). However, efforts to determine the DNA binding sites in the promoters corresponding to the observed target genes *in vitro* proved unsuccessful, leaving room for further explorations (Lin, Lin, & Lan,

2015). A phenotypic microarray screen revealed that the deletion of *baeR* resulted in reduced tolerance of *A. baumannii* to tannic acid (Lin et al., 2015). Tannic acid has long been known to have antibacterial properties (Henis, Tagari, & Volcani, 1964) and was recently shown to inhibit biofilm formation in *Staphylococcus aureus* (Payne et al., 2013). This study also showed an increased expression of *baeR* and *baeS* when *A. baumannii* was exposed to elevated sucrose (20%) concentrations. This suggests that BaeSR may very well be involved in modulating the antimicrobial susceptibility of *A. baumannii* in response to the environmental stimuli in the form of osmotic stress (Figure 3).

1.6.3 PmrAB

Due to *A. baumannii*'s increasing resistance to commonly used antibiotics in clinical settings, there is a greater use of "last resort" antibiotics, such as colistin, to treat such infections. However, with an increase in the use of colistin for treatment, emergence of colistin resistance is becoming more common among *A. baumannii* clinical isolates (Cai, Chai, Wang, Liang, & Bai, 2012; Lean, Yeo, Suhaili, & Thong, 2015). Investigations into the mechanisms of resistance to colistin in *A. baumannii* have revealed the involvement of PmrAB (Park, Choi, Shin, & Ko, 2011; Rolain et al., 2013). PmrAB has also been shown to play a role in colistin resistance of various Gram-negative pathogens including *E. coli* (Quesada et al., 2015), *Salmonella enterica* (Gunn, 2008), *Klebsiella pneumoniae* (Cheng, Chen, & Peng, 2010) and *Pseudomonas aeruginosa* (J. Y. Lee & Ko, 2014). Observations of mutations in both *pmrA* (RR) and *pmrB* (HK) lead to decreased susceptibility to colistin possibly through differential expression of the genes regulated by PmrAB regulon presented preliminary evidence of the connection between PmrAB and colistin resistance in *A. baumannii* (Adams et al., 2009). Investigations involving both colistin-resistant clinical isolates as well as laboratory generated spontaneous mutants that

showed phosphoethanolamine modification of lipid A species of lipopolysaccharide (LPS) within their outer membranes. (Arroyo et al., 2011; Beceiro et al., 2011). The modification of lipid A is mediated by PmrC (Lipid A phosphoethanolamine transferase), encoded frequently in the same operon as *pmrAB* (Raetz, Reynolds, Trent, & Bishop, 2007), and transfers phosphoethanolamine to lipid A at either the 1' or 4' phosphate of Lipid A (Tamayo, Choudhury, et al., 2005; Tamayo, Prouty, & Gunn, 2005). Mutations in both *pmrA* and *pmrB* cause overexpression of the *pmrCAB* operon. PmrC, as mentioned above, is responsible for the addition of phosphoethanolamine to either the 4' or 1' phosphate of Lipid A (Da Silva & Domingues, 2017). This modification of LPS leads to modifications of the Lipid A phosphate groups into positively charged molecules and prevent the binding of the cationic colistin at neutral pH (Arroyo et al., 2011).

Additionally, *A. baumannii* acquires resistance to colistin by a total loss of Lipid A production via mutations in *lpxA, lpxC,* and *lpxD* genes (Moffatt et al., 2010). However, acquiring colistin resistance by either *lpx* or *pmrABC* mutation mechanisms comes at a fitness and virulence cost to *A. baumannii*. Reduced growth fitness and attenuated virulence in colistin resistant mutants of *A. baumannii* were observed in both a *Caenorhabditis elegans* model and a mouse model (Beceiro et al., 2014). Interestingly, the attenuation of virulence as well as the reduction of growth fitness were less prominent in the *pmrB* mutant strains as compared to strains acquiring colistin resistance through the loss of LPS production via *lpx* genes (Beceiro et al., 2014; Mu et al., 2016). Therefore, colistin resistance mediated via the *pmrAB* system may have less of a fitness cost for *A. baumannii* than mutations in the *lpx* genes.

Colistin resistant *A. baumannii* clinical isolates have severely limited treatment options but combination therapy involving other antibiotics such as a glycopeptide, vancomycin, and

doripenem (O'Hara et al., 2013) as well as antimicrobial peptide derivatives (Oddo et al., 2015) have been effective against *A. baumannii*, albeit *in-vitro*. Vancomycin, which is used against Gram-positive bacteria, has been added in combination therapy with colistin in Gram-negatives due to the speculation that the membrane permeabilizing effect of colistin facilitates vancomycin to reach its target peptidoglycan (Gordon, Png, & Wareham, 2010). However, novel treatment options involving antimicrobial compounds, such as those above, always possess a risk of generating resistant mutants. Therefore, recent explorations into treatment options for colistin resistant *A. baumannii* have focused on downregulating *pmrAB* TCS and reversing the Lipid A modifications that lead to colistin resistance (T. L. Harris et al., 2014).

The environmental signals that activate PmrAB are still not known. An indirect observation of a rapid response to low pH and Fe^{3+} leading to colistin resistance may suggest that PmrB could be responding to those signals (Gunn, 2008). Expression of *pmrA* in colistin resistant mutants is constitutively higher suggesting autoregulation of *pmrCAB* promoter by PmrA. *A. baumannii* growth under low pH and supplementation of growth media with iron failed to alter the expression of *pmrA* albeit changing colistin susceptibility (Adams et al., 2009). Hence, the environmental signals to which PmrAB responds to in *A. baumannii* remain elusive (Figure 3).

1.6.4 GacSA

GacSA is a TCS that is well characterised in *Pseudomonas sp*. and provided much information about its regulatory pathways, which have been useful in the study of GacSA homologues in other organisms (Gooderham & Hancock, 2009). Identification of GacSA in *A. baumannii* ATCC19606 involved a screening of a transposon library. (Dorsey, Tomaras, & Actis, 2002). The transposon insertion in the *gacS* sensor kinase gene rendered those strains incapable of

utilizing citrate as the sole carbon source. This suggests that GacSA is involved in citrate metabolism (Dorsey et al., 2002). However, in *A. baumannii* ATCC 17978, the *gacS* gene is not linked to the response regulator-encoding gene, rather, it has both a HisKA domain and a REC domain suggesting that it could function as a hybrid sensor kinase. Although, there is also a possibility that in *A. baumannii* ATCC 17978, the response regulator for GacS is encoded elsewhere in the genome. This is not unusual as in other organisms, such as *Pseudomonas sp.* where an orphan response regulator gene located elsewhere in the genome was determined to be the cognate response regulator for GacS (Cerqueira et al., 2014). This does indicate that the organization of the *gacSA* genes may vary from strain to strain in *A. baumannii*.

In addition to the initially observed metabolic regulatory role of *gacS*, a transposon mutant with a disrupted *gacS* gene displayed significantly attenuated virulence in a *Candida albicans* virulence model (Peleg, Tampakakis, et al., 2008). The attenuation of virulence was also observed in a mouse model when a deletion mutant of *gacS* was used, which confirmed the involvement of GacS in virulence modulation of *A. baumannii* (Cerqueira et al., 2014). Deletion of *gacS* also determined its involvement in a number of other virulence related functions in *A. baumannii* (Figure 3). These include control of pili synthesis, motility, and biofilm formation, resistance against human serum, and metabolism of aromatic compounds (Cerqueira et al., 2014). GacSA is involved in the regulation of the aromatic compound catabolism through the *paa* operon, that encodes the components of the phenylacetic acid catabolic pathway. The *paa* gene cluster is significantly downregulated in the *gacSA* deletion mutants, leading to an attenuation of virulence of *A. baumannii* in a mouse septicaemia model (Cerqueira et al., 2014). The attenuated virulence of *gacSA* deletion mutants was observed in a later study involving a zebra fish as a virulence

model as well (Bhuiyan et al., 2016) and added to the repertoire of studies that suggest that GacSA may function as a global virulence regulator in *A. baumannii*.

1.6.5 BfmRS

Biofilm formation is an important virulence factor of pathogens such as *A. baumannii* that helps them survive harsh conditions present in hospital environments. The ability of *A. baumannii* to form biofilms starts with its attachment to surfaces that is mediated by the expression of pili. The expression of pili is mediated by the *csu* operon in *A. baumannii* and is under the regulatory control of BfmRS (Tomaras, Flagler, Dorsey, Gaddy, & Actis, 2008). Deletion of the response regulator *bfmR* in *A. baumannii* ATCC19606 resulted in the complete abolishment of biofilm formation capabilities (Tomaras et al., 2008). Even though the deletion of the sensor kinase component *bfmS* did show an appreciable reduction, it did not result in a complete loss of biofilm formation as seen for *bfmR* deletion. This suggests that BfmR may retain some activity even in the absence of BfmS, possibly due to its interaction with a hitherto unknown HK protein. While the role of the *csu* operon in the attachment of *A. baumannii* to abiotic surfaces is well established (K. H. Moon, Weber, & Feldman, 2017; Pakharukova et al., 2018; Tomaras, Dorsey, Edelmann, & Actis, 2003), its role in the adherence of *A. baumannii* to human epithelial cells remains ambiguous. It was observed that *A. baumannii* ATCC19606 strain, lacking *csuE*, adhered to bronchial epithelial cells better than the wild-type parent, making the role of these pili in adherence to epithelial cells unclear (de Breij et al., 2009). It is possible that this was a strain specific outcome and further investigations are required to draw definitive conclusions.

In addition to regulating biofilm formation, BfmRS also plays a role in regulating the exopolysaccharide production through the genes of the K locus (Geisinger, Mortman, Vargas-

Cuebas, Tai, & Isberg, 2018). Exopolysaccharide plays an important role in virulence of *A. baumannii,* as they are a component of the capsule, which helps protect *A. baumannii* against serum killing, thereby, increasing the virulence in animal models. BfmRS determines the expression levels of K locus transcriptionally where transcription – promoting effects of BfmR is negatively regulated by BfmS. However, under stresses introduced by sub lethal antibiotic concentrataions, the regulation is relieved causing overexpression of the K locus. (Geisinger & Isberg, 2015).

The crystal structure of the BfmR response regulator has presented valuable experimental evidence of BfmR self-regulatory mechanisms (Draughn et al., 2018). Experimental data from some studies show that BfmR binds to its own promoter with higher affinity in an inactive (dephosphorylated) state compared to the active (phosphorylated) state (Draughn et al., 2018). This is unusual for a response regulator as DNA-binding affinity is usually higher for the phosphorylated form and highlights a unique self-regulation strategy of the BfmRS system. Therefore, a better understanding of the functioning of the BfmRS system can not only provide novel insights on the mechanisms that regulate virulence factors in *A. baumannii* but also that of the functioning of the TCS systems in general.

1.6.6 A1S_2811

A1S_2811 is a recently characterized hybrid sensor kinase possessing four histidine–containing phosphotransfer domains as well as a regulatory CheA-like domain and a CheY-like receiver domain (Chen et al., 2017). CheA and CheY homologues in *E. coli* and *P. aeruginosa* have previously been associated with regulatory roles in controlling motility via regulation of either pili or flagella (Alon et al., 1998; Bertrand, West, & Engel, 2010; Li, Swanson, Simon, & Weis,

1995). This hybrid sensor kinase was expressed in an operon of five genes, where the four other genes upstream are *pilJ, pilI, pilH,* and *pilG*. Phenotypic analysis of the deletion mutant of *A1S_2811* revealed a significant reduction in surface motility and biofilm formation at the gas-liquid interface. More intriguingly, *abaI,* which encodes a N-acylhomoserine lactone synthase, involved in quorum sensing, was also significantly downregulated. Supplementation with synthetic homoserine lactone was able to complement the loss of biofilm and motility phenotypes. This suggests that A1S_2811 regulates biofilm formation and surface motility through an *AbaI*-associated quorum sensing pathway rather than the conventional pili associated pathway (Chen et al., 2017). This is in contrast to the BfmRS mediated regulon controlling biofilm formation in *A. baumannii* and is an example of one phenotype being under the control of multiple regulatory networks formed by different TCSs.

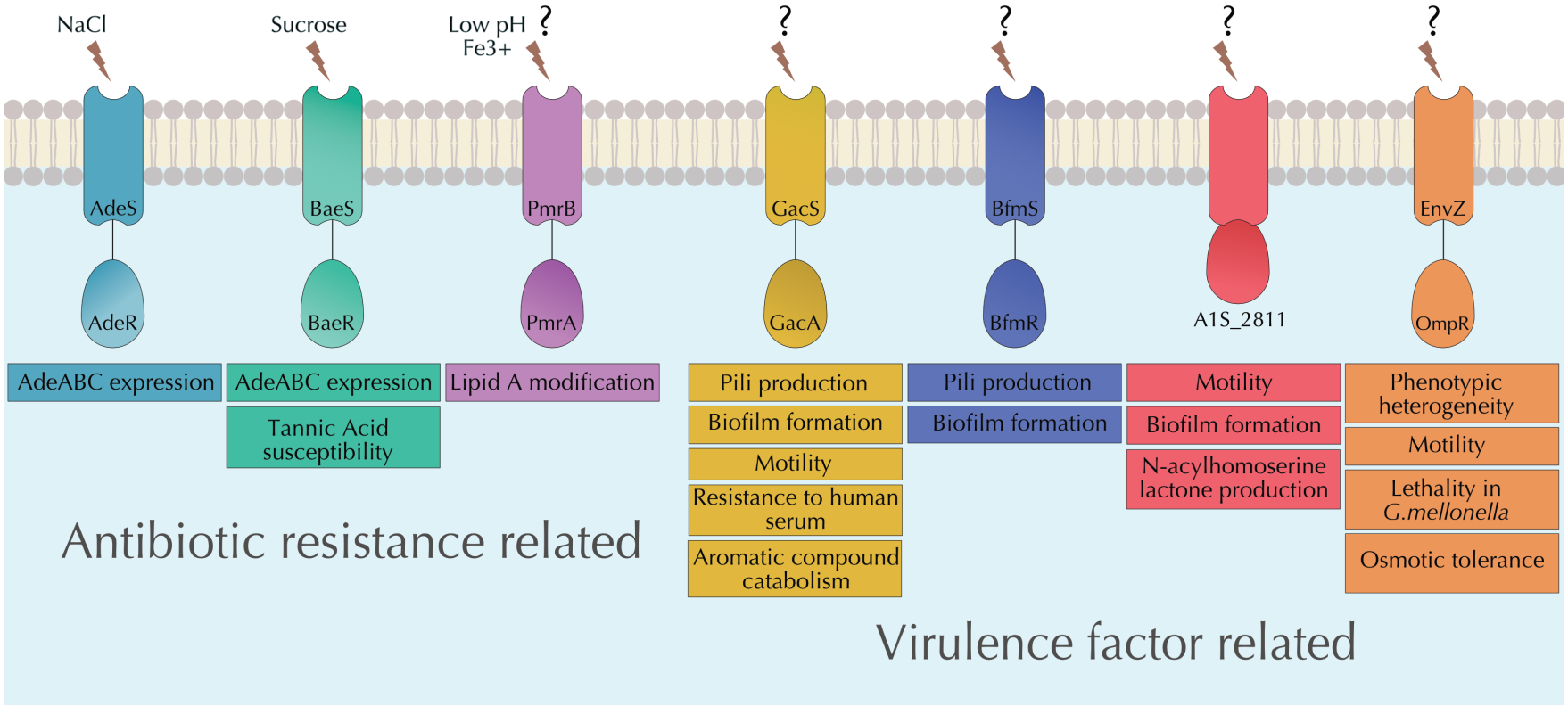

Figure 3. Summary of the characterized TCSs of *A. baumannii* type strains. Roles of the characterized TCSs of *A. baumannii* could be broadly categorised into antibiotic resistance related roles and virulence factor related roles. However, a high degree of overlap in different phenotypes could be observed among the TCSs indicating the complex nature of regulatory networks controlled by TCS signalling.

1.6.7 OmpR/EnvZ ORTHOLOG

A recent report described a phase variable colony opacity phenotypic switch in a clinical strain of *A. baumannii* (Tipton & Rather, 2016). This phase variation was associated with modulating virulence associated phenotypes in *A. baumannii* AB5075. The two variable colony types; opaque and translucent, possessed the capacity to interconvert between colony morphologies leading to phenotypic heterogeneity. In general, it was observed that the opaque variant had an increased capacity to form biofilms and to be more virulent in a *G. mellonella* model. An investigation into an opaque colony that resembled a translucent colony, having irregular edges and was speckled with papillae, revealed a transposon insertion 169 bp downstream from the start codon of the OmpR type RR gene. Further, characterisation involving an in-frame deletion mutant of the said RR gene and also the cognate EnvZ type HK gene revealed an increase in the switching frequency from opaque to translucent variant (Tipton & Rather, 2016). This TCS was involved in regulating motility and virulence, where the deletions of both TCS genes resulted in reduced surface associated motility and lethality in a *G. mellonella* model (Tipton & Rather, 2016). This study presented compelling evidence of the involvement of the OmpR/EnvZ TCS in regulating a multitude of phenotypes in *A. baumannii* AB5075. The homolog of this TCS in *A. baumannii* type strain ATCC 17978 (*A1S_3229* and *A1S_3230*) has not been studied to date. Microscopic investigations into the virulent opaque colonies revealed a two-fold thicker capsule as compared to the relatively avirulent translucent colonies. RNA-Seq studies revealed a TetR-type transcriptional regulator to be differentially expressed at a higher level between the two strains (Chin et al., 2018). This is an excellent example of the complex regulatory networks that govern the TCS signalling as well as the complicated signalling networks managed by TCSs and their potential to be used in clinical isolates as well.

1.7 TCSs AS POTENTIAL NOVEL DRUG TARGETS IN BACTERIAL PATHOGENS

Given the important role that TCSs play in regulating the clinically-relevant phenotypes (virulence and/or antibiotic resistance) of bacterial pathogens, it has been proposed that targeting them therapeutically can offer an alternative treatment strategy against multidrug resistant pathogens (J. F. Barrett & Hoch, 1998; Cardona, Choy, & Hogan, 2018; Gotoh, Eguchi, et al., 2010). TCSs in *A. baumannii* as well as other organisms offer novel potential drug targets for four reasons; (i) their conserved nature among bacteria, (ii) their involvement in modulating antibiotic resistance and virulence phenotypes, (iii) their absence in mammalian cells reducing off–target toxicity, (iv) lower potential of resistance development, as the focus of the approach is to supress virulence and/or antibiotic susceptibility rather than killing the cells.

Inhibition of signal transduction by TCSs using small molecules or other means as a novel therapeutic approach have been experimentally tested in bacterial pathogens. The first report of a TCS inhibitor is the use of thiazole derivatives to act against the AlgR1(RR)/AlgR2(HK) system of *P. aeruginosa* (Roychoudhury et al., 1993). A screen of ~25,000 synthetic compounds led to the identification of two thiazole-derivatives that inhibited AlgR1 phosphorylation as well as AlgR2 kinase-activity (Roychoudhury et al., 1993). Since then, studies that utilise approaches ranging from screening of compound libraries to structure-based virtual screening have been deployed in the search of TCS inhibitors. A few successful screening examples include inhibition of the essential TCS WalKR, quorum sensing regulation-associated QseCB, virulence and cationic antimicrobial peptide resistance-associated PhoPQ, and antibiotic resistance-associated VanSR among others (Gotoh, Eguchi, et al., 2010; Tiwari et al., 2017).

WalKR and its homologues have been described in different organisms including *S. aureus* (Martin, Li, Sun, Biek, & Schmid, 1999), *Streptococcus pneumoniae* (Lange et al., 1999), *Listeria monocytogenes* (Kallipolitis & Ingmer, 2001), *Bacillus subtilis* (Fabret & Hoch, 1998) and *Enterococcus faecalis* (Hancock & Perego, 2002). It is mainly associated with cell wall metabolism and is an essential TCS in most low G+C content Gram-positive bacteria (Ji et al., 2016) but in some instances their function remains unknown. Walkmycin B and Waldiomycin, both isolated from a *Streptomyces sp.* were shown to be potent in inhibiting the action of WalKR in both *S. aureus* and *B. subtilis* via the inhibition of auto phosphorylation of the sensor histidine kinase WalK by binding to its cytoplasmic domain (Igarashi et al., 2013; Okada et al., 2010). Importantly, the *S. aureus* strain used in these studies was methicillin resistant (MRSA), highlighting the effectiveness of this approach against antibiotic resistant pathogens. Furthermore, two novel inhibitors, walrycin A and walrycin B, were also identified as inhibitors of the response regulator WalR in *S. aureus* and *B. subtilis* through the inhibition of phosphotransfer (Gotoh, Doi, et al., 2010). Since the activity of the RR is driven through phosphotransfer to its conserved aspartate residue, inhibition of phosphotransfer in WalR results in changes in the expression of WalR regulon genes with effects similar to those observed when WalR is absent.

Potential of TCS inhibition in Gram-negative enteric pathogens has also been demonstrated. For example, QseCB present in Enterohemorrhagic *E. coli* (EHEC) O157:H7 is associated with virulence associated functions in EHEC. These include quorum sensing regulation of flagellar genes *flhDC*, and regulation of the genes located in the pathogenicity island locus of enterocyte effacement (LEE) (Sperandio, Torres, & Kaper, 2002). A high-throughput screen of a library of 150,000 compounds led to the identification of LED209, which was able to suppress the

expression of pathogenic genes under the regulation of QseC by blocking autophosphorylation of the sensor kinase QseC (Rasko et al., 2008). The efficacy of LED209 was demonstrated in a mouse model where bacterial proliferation was unaffected but the pathogenicity was suppressed demonstrating the potential of LED209 to be used as a therapeutic agent (Rasko et al., 2008). Hence, the presence of homologues of QseC in a number of other pathogenic bacteria adds to the value of LED209 to be used as an antivirulence therapeutic agent (Njoroge & Sperandio, 2009).

Yet another example is the PhoPQ system in *Salmonella sp*. This is a well characterized system that regulates various virulence factors such as invasion of epithelial cells, survival inside phagocytic cells, and resistance to antimicrobial peptides (Miller, Kukral, & Mekalanos, 1989). Since the ATP–binding Bergerat fold of the histidine kinase PhoQ is shared with the gyrase, Hsp90, and MutL (GHL) family, GHL inhibitors were tested for their ability to inhibit the catalytic domain of PhoQ (Guarnieri, Zhang, Shen, & Zhao, 2008). An Hsp90 inhibitor, radicicol, was identified with activity against sensor kinase PhoQ (Guarnieri et al., 2008). Since the targeted Bergerat fold is also observed in mammalian proteins, it is not suitable for therapeutic use. Nonetheless, radicicol can potentially be used as a lead compound to develop other potential agents which do not target mammalian proteins.

Similarly, VanSR is a TCS present in *S. aureus, Enterococcus faecalis,* and *E. faecium* that regulates genes responsible for vancomycin resistance (Hong, Hutchings, Buttner, Biotechnology, & Biological Sciences Research Council, 2008). Inhibition of the phosphotransfer to the VanR(RR) mediated by thiazole derivative halophenyl isothiazolone LY-266,400 was observed, which led to reduction of expression of the *vanHAXYZ* operon (Ulijasz & Weisblum, 1999). Due to the effect of these compounds on mitochondrial respiration, these compounds could not be used directly as a therapeutic option. Nevertheless, these compounds

can potentially act as platforms for the development of synthetic compounds without toxic effects.

1.7.1 POTENTIAL OF TCSs IN *A. baumannii* AS NOVEL DRUG TARGETS

As described in the above examples, TCSs have been tested as potential novel therapeutic target options in other pathogenic bacteria. TCSs present in *A. baumannii* also regulate a variety of biological functions often leading to antibiotic resistance and/or virulence associated phenotypes. Small molecule inhibitors of TCSs such as 2-aminoimidazole compounds have shown promise in inhibiting the action of both PmrA and BfmR in *A. baumannii*. The 2-aminoimidazole-based adjuvants used in combination with colistin were able to reverse colistin resistance up to 32-fold in *A. baumannii* clinical isolates by inhibiting PmrAB, thereby, abolishing lipid A modifications (Brackett et al., 2016). A promising feature of this strategy was that no resistance towards the PmrAB inhibitor was observed during the testing period of 7-days (T. L. Harris et al., 2014). This is certainly an advantage that TCS inhibitors offer over traditional antimicrobial compounds as development of resistance towards the latter is simply unavoidable. However, as with any other small molecule inhibitor, the cytotoxicity of the compound remains to be determined before the inhibitors could be deployed in a clinical setting.

Since BfmR plays a key role in several drug resistance and virulence associated phenotypes, studies have explored BfmR as a potential drug target using small molecule inhibitors. One such example is the use of 2-aminoimidazole derivatives to inhibit the functions of BfmR leading to a reduction of the BfmR–associated phenotypes (Thompson et al., 2012) . The 2-aminoimidazole derivatives used were able to penetrate the cell membrane of *A. baumannii* and were able to inhibit BfmR, thereby reducing the biofilm forming capacities (Milton et al., 2018). Despite the

success of the 2-aminoimidazole derivatives against BfmR, the toxicity of these compounds in human or similar animal models is yet to be determined and is critical to the application of these compounds in clinics.

Since bacterial TCSs are a part of an intricate regulatory network often modulating more than one biological function, it is challenging to characterise the complete regulons of TCSs. However, significant progress has been made in the last decade in terms of characterization efforts of the TCSs in *A. baumannii.* This has led to broadening our understanding of the regulatory networks controlled by these TCSs and in addition to that, it has further confirmed that these regulatory networks are often multi-factorial since there is an observable overlap of functions in TCSs as described above for AdeRS and BaeRS systems. Almost all TCSs described here are not confined to controlling one phenotype, but rather multiple biological functions that contribute to the virulence and/or antibiotic resistance of *A. baumannii.* An example of that is GacSA which directly or indirectly has an effect on the transcription of 674 genes (Cerqueira et al., 2014) with most of them associated with virulence phenotypes of *A. baumannii.* Therefore, inhibition of one TCS can potentially result in reversal of a myriad of virulence- and antibiotic susceptibility-associated phenotypes in *A. baumannii*.

1.7.2 CHALLENGES IN TARGETING TCS FOR THERAPEUTICS

Despite the fact that the investigations of the TCSs show an increasing amount of information being uncovered during the recent years, the majority of these efforts have focused on the cellular functions carried out by TCSs. This has left a void of information about the environmental signals that act as a trigger for the histidine kinase stimulation. The proposed stimuli for the already characterized TCSs include osmotic stress for BaeSR (Lin et al., 2014),

monovalent cations for AdeRS (De Silva & Kumar, 2017); and low pH and Fe^{3+} for PmrAB (Adams et al., 2009; Gunn, 2008). However, other TCSs described here do not have a defined environmental signal that activates their responses. Uncovering the environmental stimuli that activate a TCS response is critical in understanding the molecular pathways that are used for gene regulation by a particular TCS. These pathways can then be better exploited to render *A. baumannii* non-virulent and/or antibiotic susceptible. However, it is often difficult to determine these signals for many practical reasons including, but not limited to, the potential ability of sensor kinases to detect multiple stimuli and difficulty in expressing, purifying, and experimenting with histidine kinase proteins *in vitro* in their natural conformations.

1.7.3 CONCLUSIONS AND FUTURE PERSPECTIVES OF USING TCS AS DRUG TARGETS

Given the above examples, it is evident that the characterised TCSs present in *A. baumannii* are responsible for controlling a number of antibiotic resistance and virulence associated phenotypes. TCS provide a distinct advantage for *A. baumannii*, which is consistent with the success of this organism as a human pathogen. Research on TCSs in *A. baumannii* has extended our knowledge on virulence and resistance mechanisms in this organism over the last few years. However, there is still a considerable knowledge gap in comprehensive understanding of the complete TCS regulatory networks. Nonetheless, TCSs present themselves as potential targets for drug design. As some recent developments, such as the use of 2-aminoimidazole compounds, are encouraging towards these efforts. A better characterization of these systems both genetically and functionally is key for the potential use of TCS as therapeutic targets.

1. 8 MOLECULAR TOOLS FOR *A. baumannii*

The need for research based investigation into the mechanisms of resistance and virulence of *A. baumannii* is of critical importance to tackle the challenges observed in the clinic due to increasing *A. baumannii* infections. The success of such research often hinges on the molecular tools available to the researchers. However, the molecular tool kit available for *A. baumannii* is currently lagging behind, thus, restricting the options available for researchers (Biswas, 2015). One example is the use of plasmid – based complementation systems that are currently used in complementing gene deletions of *A. baumannii*. Often these plasmid systems rely on an antibiotic resistance marker for their maintenance in the host and constitute a need for a continued use of antibiotics in the growth medium. This is less than optimum and could pose certain challenges for some laboratory based experiments (Romero-Jimenez, Rodriguez-Carbonell, Gallegos, Sanjuan, & Perez-Mendoza, 2015). Another drawback of plasmid – based complementation systems is the multi – copy nature of the complemented gene due to the copy number of the plasmid being used. The presence of more than one copy of a complemented gene could result in the phenotypic observations leaning towards overexpression of the cloned gene rather than complementing the deficient gene. One of the alternatives to this is the use of Mini-Tn*7* plasmid systems based on the transposon Tn*7*.

1.8.1 TRANSPOSON Tn*7*

Transposons are mobile genetic elements with the capability to transpose between different genetic locations either within the same genome or between different genomes. Many of the transposable elements move at a low frequency and often display non – specific target sites. Bacterial transposon Tn*7* is a transposable element that moves with a high frequency and more importantly into a single specific site of the bacterial chromosome (Waddell & Craig, 1988).

This specific "insertion" site is called *att*Tn*7* and is widely conserved in the chromosomes of many bacterial species (Waddell & Craig, 1989). In the absence of the *att*Tn*7* site, Tn*7* transposons have been shown to transpose into other sites with a low frequency resembling other transposable elements (Kubo & Craig, 1990).

Since the first report of Tn*7* [originally named as Transposon C (TnC) and redesignated as Tn*7*] in 1976 (Barth, Datta, Hedges, & Grinter, 1976), Tn*7* transposons have been extensively studied in recent years and much detail about their molecular mechanisms and recombination machinery have come to light. Tn*7* is ~14 kb in size encoding a dihydrofolate reductase conferring trimethoprim resistance, an adenyl-transferase conferring resistance to aminoglycosides streptomycin and spectinomycin, and a transacetylase conferring resistance to streptothricin along with the transposition genes *tnsABCDE* (Craig, 1991). It also encodes a pseudo-integrase gene (*p-int*) which may mediate the rearrangement of drug resistance cassettes. Five of the transposon–encoded proteins (TnsA, TnsB, TnsC, TnsD, and TnsE) and the *cis*-acting left and right end sequences are responsible for Tn*7* transposition (Sarnovsky, May, & Craig, 1996) (summarized in Figure 4). TnsA and TnsB act as transposases while TnsD and TsnE are target specificity factors. TnsC is the key regulatory protein in transposition interacting with TnsAB transposase and the target specificity proteins (Gary, Biery, Bainton, & Craig, 1996).

1.8.2 TnsD MEDIATED TRANSPOSITION

Tn*7* can potentially display two different types of transposition. The type of transposition is determined by the two different target specificity factors TnsD and TnsE (Craig, 1991). The more frequent transposition into the *att*Tn*7* site of the bacterial chromosome is mediated by the target specificity factor TnsD when it functions with the core TnsABC machinery (Bainton, Kubo, Feng, & Craig, 1993; K. Y. Choi, Spencer, & Craig, 2014). With *att*Tn*7* directed

transposition, the specific point of insertion lies downstream of the *glmS* gene (Gay, Tybulewicz, & Walker, 1986). The essential *glmS* gene encodes for a glucosamine 6-phosphate synthase which catalyses the formation of glucosamine 6-phosphate from a fructose 6-phosphate precursor to produce N-acetylglucosamine, which is essential for cell wall formation (Walker, Gay, Saraste, & Eberle, 1984). TnsD binds to a conserved region of the coding region of the *glmS* gene but the Tn*7* directed transposition occurs at a neutral region 25bp downstream of the stop codon of the *glmS* gene, thereby, keeping the *glmS* gene intact (J. E. Peters & N. L. Craig, 2001b). The highly conserved nature of the *glmS* gene facilitates Tn*7* mediated transposition in a wide array of bacterial species (K. H. Choi et al., 2005). Also the neutral nature of the insertion site where the essential *glmS* gene is not disrupted adds to the efficacy of the Tn*7* transposition in bacterial hosts (McKenzie & Craig, 2006). One key importance of the TnsD mediated transposition, apart from its high frequency, is the fact that *att*Tn7 site driven transposition by TnsD also occurs at a specific site, thus avoiding random inactivation of genes in the chromosome.

1.8.3 TnsE-MEDIATED TRANSPOSITION

TnsE-mediated Tn*7* transposition does not depend on the presence of an *att*Tn7 attachment site in the host genome (Finn, Parks, & Peters, 2007). Rather it recognises unspecific non-*att*Tn*7* sites for transposition (J. E. Peters & N. L. Craig, 2001a). Although the non-specific integration of transposons carries the risk of being detrimental to the hosts, the ability of Tn*7* to not entirely depend on one conserved region for transposition may present an evolutionary advantage by facilitating horizontal transfer into other bacteria (Kubo & Craig, 1990). One of the key observations on the TnsE mediated transposition is its preferential transposition onto conjugal plasmids thus facilitating horizontal transfer among bacteria (Peters, 2014).

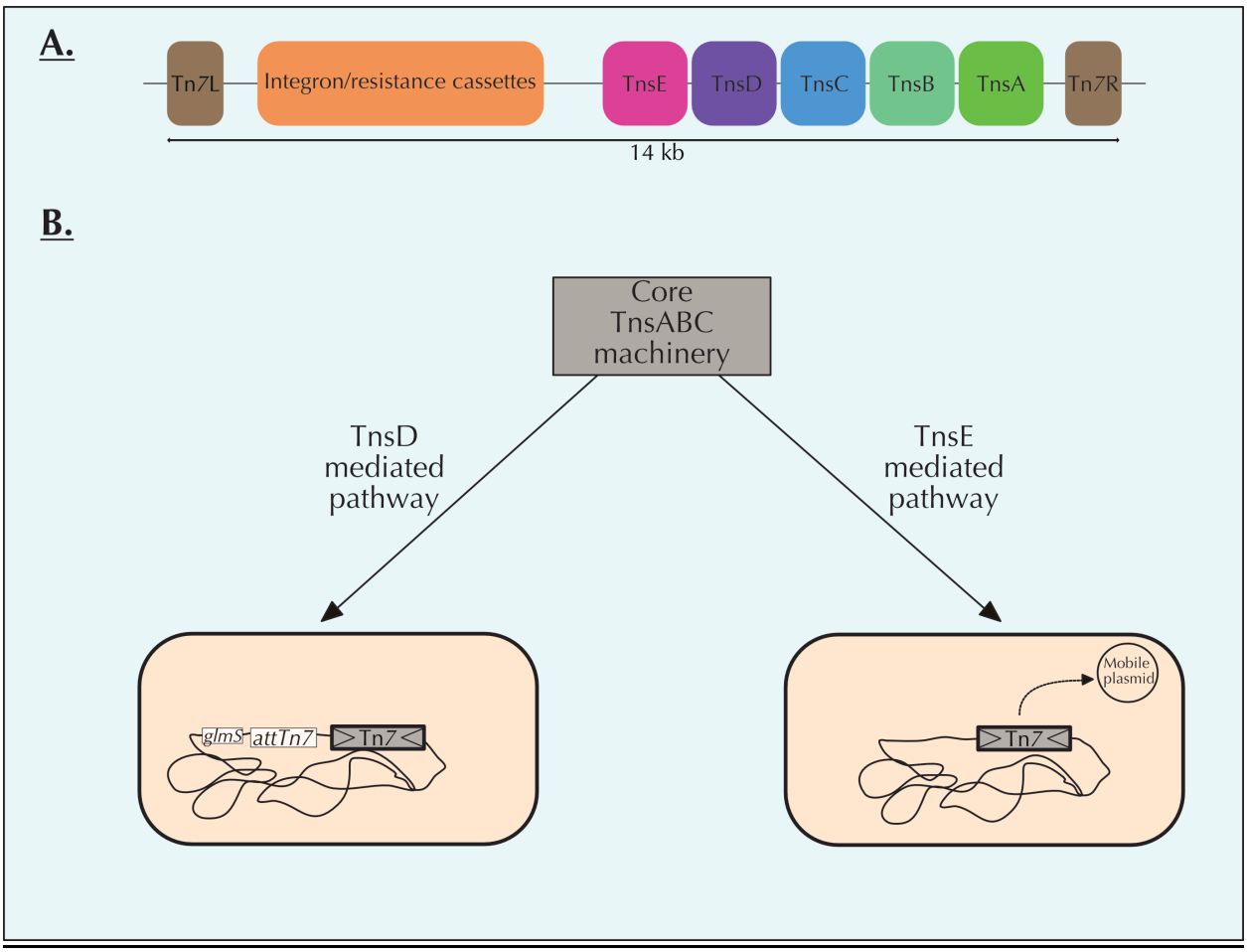

Figure 4. Organization and the machinery of action of Tn*7* transposon. (A) Tn*7* transposon is comprised of *tnsABCDE* genes followed by the integron and resistance cassettes region where resistance genes could be found sandwiched between the right (Tn*7*R) and left (Tn*7*L) ends. (B) The integration of Tn*7* could be two-fold based on the target specificity factor involved. TnsD mediated pathway recognizes *att*Tn*7* site and transposes downstream of the *glmS* gene where as TnsE mediated pathway does not depend on the *att*Tn*7* site and transposes into conjugative plasmids.

1.8.4 Mini-Tn*7* VECTORS

Mini-Tn*7* vectors that are based on the Tn*7* transposon system are excellent alternatives to the above mentioned plasmid based complementation issues. Firstly, Mini-Tn*7* systems would bypass the multi-copy effects of because they insert a single copy of the desired gene onto a known position of the genome. Secondly, since these vectors promote a stable insertion onto the bacterial chromosome, they circumvent the need of continued antibiotic selection to maintain the complementation. Mini-Tn*7* based plasmid systems have been successfully used in *Pseudomonas* spp. and *Burkholderia* spp. previously(K. H. Choi, DeShazer, & Schweizer, 2006; K. H. Choi et al., 2005; K. H. Choi et al., 2008a; K. H. Choi & Schweizer, 2006b). The use of mini-Tn*7* based plasmids has previously been shown in *A. baumannii* as well (Kumar, Dalton, Cortez-Cordova, & Schweizer, 2010b). The mini-Tn*7* plasmid systems utilise the left (Tn*7*L) and the right (Tn*7*R) ends, which are less than 200bp of the Tn*7* transposon cloned into the pUC18T based vectors (McKown, Orle, Chen, & Craig, 1988). That enables the mini-Tn*7* vectors to possess the elements essential for the transposition as well as general functions of the pUC18T vectors. For example, the mini-Tn*7* vectors possess a ColE1 origin of replication from pUC18T vectors that allows it to only replicate in *Enterobacteriaceae* thus maintaining the possibility of maintaining the plasmid in *E. coli* strains for storage and also acting as suicide delivery vectors for the other strains (Leung, Chen, Cachianes, & Goeddel, 1985). Since the mini-Tn*7* vectors do not have the Tn*7* encoded Tns proteins, they are usually supplied *in-trans* using the pTNS2 plasmid, which contains the *tnsABCD* genes that are necessary for the integration of the desired gene that is cloned between Tn*7*L and Tn*7*R of the mini-Tn*7* vector (K. H. Choi et al., 2005). Another useful additional feature of the mini-Tn*7* vectors is the presence of flippase recognition target (FRT) sites sandwiching the antibiotic resistance marker that is used for selection of the

transposition of the desired gene. This allows for the removal of the antibiotic resistance marker with the help of the yeast Flp recombinase encoded on another plasmid (pFLP2) after the successful insertion of the desired gene (Andrews, Proteau, Beatty, & Sadowski, 1985) (summarized in Figure 5). Therefore, mini-Tn*7* vector system proves to be an extremely useful molecular tool for genetic manipulations and are particularly useful in genetic manipulations of *A. baumannii* as shown in one previous study (Kumar et al., 2010b).

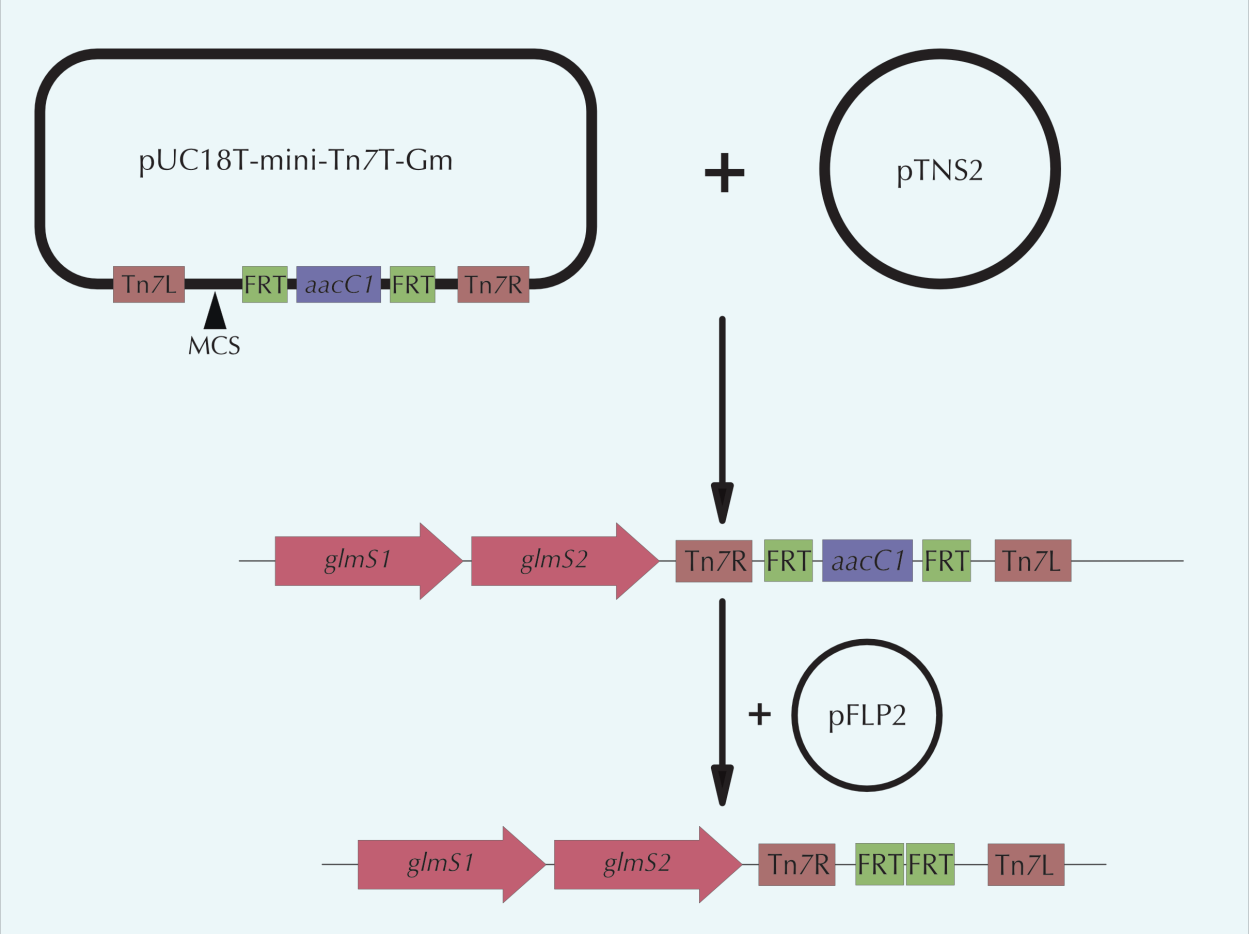

Figure 5. General scheme of mini-Tn*7* plasmid based insertion into *A. baumannii* genome. The gene of interest could be cloned into the multiple cloning site (MCS) of pUC18T-mini-Tn*7*T-Gm plasmid and co-transformed with the pTNS2 plasmid which provides the *tns* genes *in-trans*. After the successful insertion, the gentamicin resistance marker (*aacC1*) could be removed with the use of pFLP2 plasmid encoding the Flp recombinase to obtain a markerless insertion.

1.8.5 CHALLENGES IN GENETIC MANIPULATION OF *A. baumannii*

Emergence of *A. baumannii* as a successful pathogen is hugely dependent on the multi-drug resistance as stated above. In addition to the obstacles associated with this in a clinical setting, it also poses a challenge in laboratory based research involving *A. baumannii* by limiting the useable antibiotic resistance markers for genetic manipulation of *A. baumannii* (Biswas, 2015). Commonly used antibiotic resistance markers in molecular biology approaches coincide with the commonly used antibiotics in the clinic. Hence, the utility of these antibiotic markers are seriously affected when it comes to genetic manipulations of clinical isolates of *A. baumannii* strains that exhibit resistance to those antibiotics (Luna et al., 2017b). Use of non-antibiotic selection markers such as tellurite could be a potential solution for this problem and its use has been demonstrated previously (Amin et al., 2013). Another example is the use of the *pheS** gene in counter selection with p-chlorophenylalanine (A. R. Barrett et al., 2008; Chandler et al., 2009). The utility of these markers could be hindered by the lack of variety in such selectable markers as compared to the many different antibiotic markers available currently. Therefore, much interest in antibiotic markers that are not commonly used in a clinical setting has been seen in recent years (Luna et al., 2017b).Two such antibiotic resistance markers are *aac(3)-IV* which confers resistance to apramycin (Apr^R) and the *ble* (bleomycin resistance) gene which confers resistance to zeocin (Zeo^R). Both Apr^R and Zeo^R have been demonstrated to be effective selection markers against MDR *A. baumannii* strains (Kang et al., 2017; Lucidi et al., 2018b).

The lack of antibiotic selection markers that are usable against MDR strains of *A. baumannii* is shared by the mini-Tn*7* vectors as well due to the presence of a gentamicin resistance marker in the currently available mini-Tn*7* vectors. Therefore, introduction of antibiotic markers that are not commonly used in the clinic such as Apr^R and Zeo^R into the current mini-Tn*7* vectors will

rejuvenate them and enhance the utility of these vectors. This will help bridge the gap that limits molecular tools available for genetic manipulations of antibiotic resistant clinical isolates of *A. baumannii*.

1.9 HYPOTHESIS AND OBJECTIVES

TCSs in *A. baumannii* aid in sensing and adapting to the environmental changes in its surroundings. Adaptation to these changing environments can result in changes in the cellular processes in *A. baumannii*. Antibiotic susceptibility and virulence is modulated by various environmental conditions in *A. baumannii*. Therefore, we hypothesize that understanding these changes will better elucidate antibiotic susceptibility and virulence associated mechanisms of *A. baumannii*.

Therefore, the objectives of this thesis were to;

a) Assess the effect of incubation temperature on the antibiotic susceptibility and virulence associated phenotypes of *A. baumannii* and examine the effect of NaCl on surface associated motility of *A. baumannii* in conjunction with AdeRS TCS
b) Characterize the role(s) of orphan response regulator, A1S_2006 with regards to the antibiotic susceptibility and virulence associated phenotypes of *A. baumannii*
c) Finally, to address the current lack of molecular tools available for genetic manipulations of *A. baumannii* in laboratory settings; creation and utilization of novel plasmid vectors that can be used in genetic manipulations of antibiotic resistant clinical isolates of *A. baumannii*.

CHAPTER 2

MATERIALS AND METHODS

This chapter describes the routine material and methods used for the experiments described in this thesis. Materials and methods specific to each chapter are described in the respective chapters.

2.1 BACTERIAL STRAINS, PLASMIDS, AND OLIGONUCLEOTIDES

A complete list of bacterial strains, plasmids, and oligonucleotides are listed in Tables 1 and 2 respectively.

2.2 MEDIA AND GROWTH CONDITIONS

Lysogeny Broth (LB) Lennox and LB agar was routinely used for culturing the bacterial strains described here unless otherwise stated. Both LB and LB agar was obtained from Difco, Becton Dickinson, Sparks, MD, USA. The routine culture conditions for liquid medium was at 37˚C shaking at 250 rpm unless otherwise stated and static incubation at 37˚C was used for solid media unless otherwise stated.

2.3 GENOMIC AND PLASMID DNA EXTRACTION

Genomic DNA (gDNA) extractions of *A. baumannii* strains were carried out using 1 mL of overnight liquid culture with the Norgen bacterial DNA isolation kit (Norgen Biotek Corp, ON, Canada) using the manufacturer's instructions and solutions except for 95% ethanol which were supplied locally. The final elution of the gDNA from the silica column was performed using 35 μL of the supplied elution buffer.

Plasmid DNA extractions from overnight *E. coli* liquid cultures were performed using BioBasic Plasmid Miniprep Kit (BioBasic Inc. Markham, ON, Canada) following manufacturer's instructions and provided solutions. Once again the elution of plasmid DNA was carried out using 35 μL of the supplied elution buffer.

2.4 DNA MANIPULATIONS

2.4.1 General PCR

Genomic DNA and plasmids extracted using the above mentioned protocols were used as templates for general PCR reactions. Taq DNA polymerase (Froggabio, ON, Canada) or Q5

DNA polymerase (NEB, Pickering, Canada) were used in all reactions following the manufacturers' recommendations.

2.4.2 Splice Overlap Extension PCR (SOEing PCR)

Splice Overlap Extension (SOEing) PCR was the choice of PCR technique for constructing the knockout cassettes for the gene deletions in *A. baumannii*. SOEing PCR was carried out following a previously described method (K. H. Choi & Schweizer, 2005) with slight modifications using the primers listed in Table 2. Briefly, the forward set of primers amplifying a ~1kb upstream region of the desired gene and the reverse set of primers amplifying a ~1kb downstream region of the desired gene were used in two separate PCR reactions with Q5 DNA polymerase. The *aacC1* (Gm^R) gene conferred resistance to gentamicin along with the FRT sites were also amplified using Q5 DNA polymerase and each fragment was gel extracted. These fragments were used as templates for the SOEing PCR reaction using Q5 DNA polymerase. The reaction mixture consisted of 50ng of each fragment as template and regular contents of a Q5 DNA polymerase PCR reaction mixture with the exception of primers. This PCR was cycled for 3 times with an annealing temperature of 55˚C after which the PCR reaction was paused and the upstream forward and the downstream reverse primers were added and cycled for 30 times with an annealing temperature specific to the primers used to facilitate the amplification of the ~3kb knockout cassette. The knockout cassette was then gel extracted and used to ligate into the suicide vector used.

2.5 COMPLEMENTATION OF GENE DELETION

2.5.1 Construction of the plasmid vector

Complementation of the deleted genes were carried out using the previously described pUC18T-mini-Tn*7*T-Gm plasmid vector (K. H. Choi et al., 2005). The deleted gene with its native

promoter was amplified using gDNA from *A. baumannii* ATCC 17978 as the template with the primers containing suitable restriction sites. The PCR product was then gel extracted and digested with their respective enzymes and the digested product was gel extracted. The plasmid vector was digested with the same enzymes and gel extracted. Ligation reactions with the vector and the insert were set up using T4 DNA ligase (Thermo Scientific, Vilnius, Lithuania) following the manufacturer's guidelines and ligation mixtures were incubated at 16˚C overnight before transforming into chemically competent *E. coli* DH5α cells.

2.5.2 Creating the complemented strain

Four parental conjugations were setup to introduce the plasmid vector to the *A. baumannii* strain that carried the gene deletion as described before (Kumar et al., 2010b). The positive colonies for the insertion were screened initially based on their growth on gentamicin 50µg/mL and then confirmed by PCR using the primers listed in Table 2. The positive colonies were electroporated with pFLP2 to excise the Gm^R cassette and selected on carbenicillin 200µg/mL plates. The colonies that grew on carbenicillin were then cross patched onto gentamicin plates to confirm the excision of the Gm^R cassette and the colonies that grew on carbenicillin but not on gentamicin were selected for streaking onto LB+10% (w/v) sucrose plates. This was done to cure the pFLP2 plasmid using the *sacB* gene from *Bacillus subtilis* encoding a toxic levansucrase in the presence of sucrose. The colonies from the LB+10% sucrose plate were cross patched onto gentamicin 50µg/mL, carbenicillin 200µg/mL, and LB plates to confirm the loss of Gm^R marker and pFLP2 plasmid. The resulting colonies had the full length gene with its native promoter inserted into the *att*Tn*7* site that is downstream of the *glmS* gene and it was further confirmed using PCR using the primers glmS F and Tn7R listed in Table 2. The expression of the inserted gene was confirmed using qRT-PCR before using the strain in phenotypic experiments.

2.6 PREPARATION OF COMPETENT CELLS

2.6.1 Chemically competent cells

Chemically competent cells were prepared from *E. coli* DH5α and SM10 cells using the same protocol and stored at -80˚C for future use. Overnight cultures of *E. coli* cells were diluted 1:100 (v/v) in 125 mL of fresh LB and grown to A_{600} of 0.4-0.6. The entire culture was centrifuged at 5000 x g for 5 minutes at 4˚C and the supernatant was discarded. The cell pellet was resuspended in 50 mL of sterile ice-cold TFB1 buffer (100 mM rubidium chloride, 50 mM manganese chloride, 30 mM potassium acetate, 10 mM calcium chloride, and 15% w/v glycerol; pH 5.8) and incubated for 5 minutes on ice. The cell suspension was centrifuged again at 5000 x g for 5 minutes at 4˚C and the supernatant was discarded. The cell pellet was resuspended in 5 mL of sterile ice-cold TFB2 buffer (10mM MOPS, 10 mM rubidium chloride, 75 mM calcium chloride, and 15% w/v glycerol; pH 6.5) and incubated on ice for 30 – 45 minutes. 125 μL aliquots of the cells were then placed onto pre-chilled 1.5 mL microfuge tubes and frozen immediately in a dry ice/ethanol bath for 20 – 30 seconds. The frozen cells were immediately transferred to the -80˚C freezer and stored there until used.

2.6.2 Electrocompetent cells

Electrocompetent cells were prepared for *A. baumannii* strains as and when needed for the experiments and were always made immediately prior to the experiments and never stored for later use. *A. baumannii* cells were grown overnight and 1 mL of the overnight culture was transferred to a 1.5 mL microfuge tube and centrifuged at 13000 x g for 2 minutes. The supernatant was discarded and the cells were resuspended in 1 mL of sterile ice-cold distilled water and centrifuged again at 13000 x g for 2 minutes. This was repeated for another two

rounds and the final cell pellet was resuspended in 100 µL of sterile ice-cold distilled water and placed on ice until use.

2.7 TRANSFORMATION OF BACTERIAL CELLS

2.7.1 Electroporation

Freshly made electrocompetent *A. baumannii* cells were transferred into 2 mm electroporation cuvette and then mixed with 50-100 ng of the plasmid DNA to be transformed. The mixture was incubated on ice for 20 minutes and then electroporated at 1.8 kV after which 900 µL of sterile LB was added and the entire contents of the cuvette was transferred into a 1.5 mL microfuge tube. The time constant was observed for each electroporation and any cuvette with less than 5 ms time constant was discarded. The microfuge tubes were then incubated for 1 hour at 37˚C with shaking to facilitate the outgrowth of transformed cells. The microfuge tubes were then centrifuged at 13000 x g for 2 minutes and the supernatant was discarded. The cell pellet was resuspended in 100 µL of sterile LB and spread plated onto LB agar plates with the appropriate antibiotics.

2.7.2 Chemical transformation

Chemical transformation carried out with either *E. coli* DH5α and SM10 were performed with chemically competent cells that were previously made and stored at -80˚C. The cells were allowed to thaw on ice for 10 minutes and 50 μL of competent cells were incubated with 50-100 ng of plasmid DNA to be transformed for 15 minutes before heat shock. A dry bath set at 42˚C was used for heat shock and the tubes containing the cells and the plasmid was placed in the 42˚C dry bath for 45 seconds and were immediately placed on ice for 2 minutes. 900 μL of pre-warmed sterile LB was added into the transformation tubes and incubated at 37˚C with shaking for 1 hour to facilitate the outgrowth of transformed cells. The tubes were then centrifuged at

13000 x g for 2 minutes and the cell pellet was resuspended in 100 μL of sterile LB and spread plated onto LB agar plates containing the appropriate antibiotic.

2.8 IN-FRAME GENE DELETIONS IN *A. baumannii*

2.8.1 Conjugation

The gene deletions were carried out based on a homologous recombination method previously described with minor modifications (Amin et al., 2013). The suicide vector, pMO130 carrying the knockout cassette for the appropriate gene was transformed into *E. coli* SM10 cells prior to conjugation. Then 100µL of overnight cultures of the SM10 cells carrying the suicide vector and *A. baumannii* ATCC 17978 were mixed in a 1.5mL centrifuge tube. The mixture was then centrifuged at 13000 x g for 2 minutes to pellet the cells and the supernatant was discarded. The cell pellet was washed three times using sterile LB to remove residual antibiotics from the overnight growth medium. After the final wash, the cell pellet was resuspended in 10 µL of sterile LB and spotted onto a sterile nitrocellulose filter paper square placed on a LB agar plate with no antibiotics. The spot was allowed to dry and then incubated at 30˚C for 16 hours to facilitate conjugation. After the incubation period, the nitrocellulose filter paper was carefully removed from the LB agar plate and placed into a 1.5mL centrifuge tube containing 300µL of sterile 0.85% saline. The conjugation spot was carefully mixed with the saline to remove it from the nitrocellulose paper into the saline. The nitrocellulose paper was then removed and the the saline containing the conjugation mixture was then plated onto Simmons citrate agar (Sigma-Aldrich, St. Louise, MO, USA) plates supplemented with kanamycin 50µg/mL. These plates were then incubated at 37˚C for 24 hours or until colonies appeared. Simmons citrate media act as a selective medium for *A. baumannii* using citrate as the carbon source hence the *E. coli* cells in the conjugation mixture are unable to grow on Simmons citrate.

2.8.2 Homologous recombination

The colonies growing on Simmons citrate were the colonies that underwent first homologous recombination with the knockout cassette in the suicide vector. This was phenotypically confirmed by patching those colonies onto LB agar supplemented with 50µg/mL kanamycin (for the presence of plasmid backbone from the suicide vector) and LB agar supplemented with 50µg/mL gentamicin (for the presence of knockout cassette). The colonies that were able to grow on both gentamicin and kanamycin were then streaked onto VBMM minimal media supplemented with 10% sucrose and 30µg/mL gentamicin to facilitate the second crossover of the knockout cassette and removal of the suicide vector backbone where *sacB* is present. The resulting colonies were cross patched onto LB agar supplemented with 50µg/mL kanamycin and 50µg/mL gentamicin separately. The successful second cross over was phenotypically confirmed by the absence of growth on kanamycin indicating the loss of suicide vector backbone and growth on gentamicin indicating the successful insertion of the knockout cassette. Gene disruptions were further confirmed by PCR using the primers flanking the target gene with a PCR product of ~3kb as compared to the size of the wild type gene.

2.8.3 Excision of the Gm^R marker

Conjugations were set up with *E. coli* SM10 harbouring pFLP2 plasmid and the *A. baumannii* strains with the genes disrupted with the knockout cassette containing the Gm^R marker. Conjugations were carried out as described above with overnight cultures of both strains and conjugation mixtures were incubated for 16 hours at 30˚C. After the incubation period, the conjugation mixtures were plated onto Simmons citrate agar supplemented with 200µg/mL carbenicillin to select for the *A. baumannii* colonies with the pFLP2 plasmid present. These colonies were cross patched onto LB agar supplemented with 50µg/mL gentamicin and LB agar

supplemented with 200µg/mL carbenicillin to screen for the loss of Gm^R marker. Colonies that were only able to grow on carbenicillin were streaked onto LB+10% sucrose to facilitate the curing of the pFLP2 plasmid. The colonies from the LB+10% sucrose were then cross patched onto 50µg/mL gentamicin, 200µg/mL carbenicillin, and LB agar to phenotypically reconfirm the loss of Gm^R marker as well as pFLP2 plasmid.

2.9 RNA EXTRACTION AND QUANTITATIVE REAL TIME PCR (qRT-PCR)

2.9.1 RNA extraction and cDNA synthesis

Bacterial cultures were grown in LB at 37˚C or 28˚C with shaking overnight then sub cultured into fresh media (1:100 v/v) and grown to an A_{600} = 0.6 to 0.8 (mid – log phase). 1.5 mL of the mid – log phase cultures were centrifuged at 13000 x g for 2 minutes to pellet the cells and the cell pellets were frozen immediately for 3-5 hours at -80˚C before extracting RNA. RNA extraction was carried out using RNeasy mini kit (Qiagen) according to the manufacturer's instructions. RNA concentrations after the extraction was measured using NanoDrop Lite (Thermo Scientific). 1 µg of extracted RNA was then subjected to DNase I (Qiagen) treatment to remove the carryover genomic DNA contamination before proceeding further. DNase treated RNA was used as the template to synthesise cDNA using SuperScript VILO cDNA sysnthesis kit (Invotrogen) according to the manufacturer's instructions in a 20 µL total volume. The cDNA was diluted either 1:3 or 1:5 using nuclease free water based on the target gene for qRT-PCR.

2.9.2 qRT-PCR

Expression of genes were quantified using SYBR Select master mix (Life Technologies) following manufacturer's guidelines. The primers that were used in the qRT-PCR reactions are listed in Table 2 and were designed to have a 100-200 bp amplicons. The primers were standardised using 10-fold dilutions of *A. baumannii* genomic DNA before using in qRT-PCR

reactions to confirm 95-100% efficiency. The reaction mixtures for qRT-PCR had a total volume of 8 µL per well which consisted of 2.7 µL of cDNA template in 5.3 µL of SYBR Select master mix. All qRT-PCR reactions were carried out in a StepOne Plus (Applied Biosystems) machine using the following cycling conditions; initial denaturation at 95˚C for 2 minutes followed by 40 cycles of 95˚C for 15 seconds, 60˚C for 1 minute. Product specificity was analysed using a melt curve of 95˚C for 10 seconds, 60˚C for 5 seconds, 95˚C for 10 seconds. 16S rRNA gene was used as the internal reference for all reactions and the expression of target genes were normalised to the expression levels of 16S rRNA using the Pfaffl method for calculating relative expression (Pfaffl, 2001). The expression values were then plotted in GrpahPad Prism v6.07 (La Jolla, CA, USA) and statistically analysed using the inbuilt statistical modules of GrpahPad Prism.

2.10 ANTIMICROBIAL SUSCEPTIBILITY TESTING

2.10.1 Broth dilution method

Minimum Inhibitory Concentration (MIC) determination by two-fold broth dilution method was carried out according to the guidelines of the Clinical Laboratory Standards Institute (CLSI). Briefly, an isolated colony of each of the bacterial strains to be tested were grown overnight in LB broth at 37˚C with shaking at 250 rpm. The overnight cultures were then diluted in sterile 0.85% saline to the 0.5 McFarland standard using the DensiChek™ Plus instrument (Biomérieux, Montréal, Canada). The standardised cells were used to make the inoculum for the MIC assay by adding 120 µL of the standardised cells into 10 mL of Muller Hinton Broth (MHB) (Oxoid, Basingstoke, Hants, UK). 50 µL of sterile MHB was added in triplicate into the wells corresponding to each dilution of the antibiotic except the highest concentration on a sterile 96 well plate (Sarstedt, Montréal, QC, Canada). 100 µL of two times the desired highest

concentration of the antibiotic dissolved in MHB was added to the wells corresponding to the highest concentration on the plate. Then by using a multi-channel pipette, 50 µL of MHB from those wells was drawn up and dispensed into the wells corresponding to the next highest concentration and mixed thoroughly by pipetting. 50 µL from those wells were again drawn up and transferred to the wells corresponding to the next highest concentration and this was repeated through the entire plate. 50 µL of MHB from the last set of wells was removed and discarded. This resulted in a two-fold dilution series of the antibiotic to be tested in a total volume of 50 µL per well in a 96 well plate. 50 µL from the cell inoculum prepared earlier was added into each well of the two-fold dilution series to make the final volume of each well 100 µL. The 96 well plates were then incubated at 37 ˚C for 16-18 hours in dark. The readings were obtained by visually observing cell growth in each of the wells and the MIC was determined as the lowest concentration at which the growth is inhibited. The assays were repeated with independent biological replicates at least twice before concluding the MIC value for each strain.

2.10.2 E-test method

MIC determination by E-test method was carried out using E-Strips (Biomérieux, Montréal, Canada) following manufacturer's guidelines. Briefly, an isolated colony of each of the bacterial strains to be tested were grown overnight in LB broth at 37˚C with shaking at 250 rpm. The overnight cultures were then diluted in sterile 0.85% saline to the 0.5 McFarland standard using the DensiChek™ Plus instrument (Biomérieux, Montréal, Canada) to prepare the inoculum. This inoculum was then used to make a lawn of bacteria on a Muller Hinton Agar (MHA) plate with the help of a sterile cotton tipped applicator. The lawn was allowed to dry briefly and the E-Strip for the desired antibiotic was placed carefully in the centre of the bacterial lawn. The MHA plates were then incubated at 37˚C for 16-18 hours in dark and the MIC values were determined

by the zone of inhibition using the scale provided on the E-Strips. The assays were repeated with independent biological replicates at least twice before concluding the MIC value for each strain.

2.11 BIOFILM ASSAY

Biofilm formation by the *A. baumannii* strains were assayed by using a slightly modified version of a previously described method (Iwashkiw et al., 2012). Briefly, bacterial cultures were grown overnight in sterile LB with shaking at 37˚C or 28˚C and the cell density was adjusted to a similar A_{600nm} value based on the lowest value using sterile LB. Those cultures were then diluted to 10% (v/v) in LB and aliquots of 100 μL were dispensed into individual wells of a 96-well polystyrene plate (Sarstedt, Montreal, QC, Canada). The plates were then incubated without shaking at 37˚C or 28˚C for 48 hours in dark before measuring the bacterial growth based on the A_{600nm} values using a SpectraMax M2 reader (Molecular Devices). The media along with the loosely bound cells were carefully removed from each well of the 96-well plate and the wells were washed with dH_2O three times before staining the biofilm biomass with 1% (w/v) crystal violet (Fisher Scientific, New Jersey, USA). The stained biofilm biomass was solubilised using 95% ethanol: Acetone (2:1) and quantified based on the A_{580nm} using the SpectraMax M2 reader. The biofilm biomass formation was normalised to the bacterial growth by using the ratio of A_{580nm}/A_{600nm} for each strain. The assays were carried out in at lease two biological replicates.

Alternatively, a biofilm assay was also carried out using glass test tubes. The culture volume used in each of the glass tubes was 2mL. The inoculated glass tubes were incubated in the dark without shaking at 37˚C for 48 hours similar to the 96-well plates. The washing and staining steps were similar to the ones used in the 96-well plate assay while the tubes were only photographed for visual biofilm formation confirmation. The assay was carried out in triplicate with two biological replicates for each strain.

2.12 SURFACE – ASSOCIATED MOTILITY ASSAY

Surface associated motility was measured based on a previously described method (Harding et al., 2013) with slight modifications. Motility media which consisted of 5 g/L tryptone, 2.5 g/L sodium chloride, and 3 g/L agarose was autoclaved and allowed to cool to ~55˚C. Sodium chloride concentrations were adjusted where applicable, the pH of the media was adjusted using either acetic acid or potassium hydroxide when needed, and either 0.3M or 0.5M sucrose was added to the motility media when needed. 20 mL of motility media was poured into each petri plate after which it was allowed to cool motility media plates were made fresh each time for the assays. Bacterial cultures were grown overnight in LB at 37˚C or 28˚C with shaking and the cell density was adjusted to the lowest A_{600nm} value using sterile LB prior to the assay. A 3 µL aliquot of each strain was stab-inoculated into the centre of the motility media plates and allowed to dry for 10 minutes before incubating for 16 – 18 hours at the appropriate temperature. After the incubation period, the diameters of the motility zones were measured and representative plates were photographed. The assays were carried out in triplicate and at least two biological replicates were performed for each assay.

2.13 VIRULENCE ASSAY

The virulence model of choice for the experiments in this thesis was *Galleria mellonella* (wax moth) larvae, which has been used with *A. baumannii* previously (Peleg et al., 2009). The last instar larvae, which develop from the eggs in about 5 weeks were ordered from a commercial pet store (The Worm Lady, Ontario, Canada) and stored at 16˚C prior to the assays. Virulence assays were conducted based on a previously described protocol (Peleg et al., 2009) with slight modifications. Briefly, the bacterial strains to be tested were grown at either 37˚C or 28˚C overnight in LB and standardised to a 0.5 McFarland standard in sterile 0.85% saline using the

DensiChek™ Plus instrument (Biomérieux, Montréal, Canada). These standards were further diluted 1:100 (v/v) in sterile 0.85% saline and used as the inoculum for the virulence assay. Healthy larvae were removed from the 16˚C incubator, cleaned, and placed on ice for 10 minutes prior to the injection to slow down the physical movement of the larvae. 10 µL of the bacterial inoculum was injected into the second right proleg of each larvae and 10 larvae were used in each experimental condition. Sterile 0.85% saline was injected into a control group of larvae to rule out physical injuries as well as use as the negative control for each experimental condition. The infected larvae were incubated at either 37˚C or 28˚C and monitored for 72 hours with live/dead readings taken every 6 hours. Larvae were considered alive if they displayed movement upon touch and dead if they displayed no movement upon touch. Melanisation of the larvae and appearance of distinctive black spots were a visual indicator of the deteriorating health of the larvae upon infection. The counts of dead and alive larvae were input into GraphPad Prism and survival curves were generated for each experimental condition. Statistical analysis using Kaplan-Meier and log-rank test were performed using the inbuilt modules of GraphPad Prism for each experimental condition.

2.14 RNA – SEQUENCING (RNA-Seq) AND DATA ANALYSIS

RNA extraction of the bacterial cultures for RNA-Seq was performed as described earlier for qRT-PCR and two biological replicates were prepared for each bacterial strain. The RNA samples were shipped on ice to Children's Hospital Research Institute of Manitoba (CHRIM) for enrichment and sequencing using the Illumina MiSeq platform. Raw reads from sequencing were received and analysed for quality of the reads using FastQC (Andrews S. (2010). FastQC: a quality control tool for high throughput sequence data. Available online at: http://www.bioinformatics.babraham.ac.uk/projects/fastqc) and the reads were imported to the

commercially available Geneious R11 (https://www.geneious.com) for further analysis using the built-in plugins of the Geneious software. Briefly, the short reads obtained from the sequencing were aligned to the publicly available complete genome sequence of *A. baumannii* ATCC 17978 (GenBank accession number CP000521.1) using the Bowtie2 plugin module (Langmead & Salzberg, 2012). Differential expression of the genes along with the statistical significance of the said differential expression was calculated using the built-in modules of Geneious R11. The output of the differentially expressed genes, their statistical significance, and other relevant metadata were exported into a Microsoft Excel spreadsheet for further analysis. A $\log_2$ 1.5-fold change with a $P<0.05$ was used as a cut-off to select the significant genes that were either up or downregulated to be analysed further. These genes were then manually classified into the Clusters of Orthologous Groups (COGs) using the web – based interface of EggNOG version 4.5.1 database (Huerta-Cepas et al., 2016).

2.15 PROTEOMIC ANALYSIS

Overnight cultures of ATCC 17978 were diluted 1:100 in 500 ml of LB and incubated at 28°C and 37°C to an A600 of ~0.8. Cells were harvested by centrifugation at 6,000 × g for 15 min at 4°C, and pellets were stored at −80°C until used. Three biological replicates were used for each growth condition. Cell pellets were homogenized in sterile Milli-Q water, mixed with 100 µl of 0.1-mm glass beads (Scientific Industries Inc., Bohemia, NY, USA), heated for 5 min at 95°C, and vortex-mixed vigorously for 3 min, followed by centrifugation and removal of the supernatant into a 15-ml conical tube. Cold sterile Milli-Q water was added to the beads, followed by vortex-mixing and centrifugation to wash the beads and to extract protein (total of six wash/extraction steps); the supernatants from each step were pooled, mixed thoroughly, and stored at −80°C.

Protein was quantified using a bicinchoninic acid (BCA) protein assay kit, with bovine serum albumin (BSA) as the standard (Pierce Protein Research Products; Thermo Fisher Scientific). A total of 100 μg of protein from each sample in triplicate for cultures of ATCC 17978 grown at 28°C and 37°C was used for each digestion/labeling reaction. Protein samples were digested with trypsin (Promega, Madison, WI, USA) overnight using a filter-assisted sample preparation (FASP) method described previously (Wisniewski, Zougman, Nagaraj, & Mann, 2009). iTRAQ labeling with 4-plex kits was performed according to the manufacturer's recommended protocol (Sciex, Framingham, MA, USA). Peptides from each of the three replicates of ATCC 17978 grown at 28°C and 37°C, respectively, were labeled and three sets prepared by mixing peptides from one replicate grown at 37°C and one grown at 28°C each in a 1:1 ratio. The mixture was vacuum dried and rehydrated using offline liquid chromatography (LC) buffer A (20 mM ammonium formate [pH 10]). Each set was then resolved using high pH reversed-phase liquid chromatography to yield 16 fractions per set. Each fraction was dissolved in nanoLC buffer A (2% acetonitrile [vol/vol, in mass spectrometry grade water], 0.1% formic acid) for mass spectrometry analysis.

Each peptide fraction was analyzed using a nano-flow Easy nLC II system in line with an LTQ Orbitrap Velos mass spectrometer (Thermo Fisher Scientific). The peptide sample (1 μg) was loaded onto a C18 reverse-phase analytical column (length, 20 cm; inner diameter, 75 μm; particle size, 2.4 μm) with 100% nano-LC buffer A, and peptides were eluted using a 217-min linear gradient of 2 to 30% nano-LC buffer B (98% acetonitrile, 0.1% formic acid, vol/vol in mass spectrometry-grade water). The total nano-LC-tandem mass spectrometry (MS/MS) run time was 260 min. A data-dependent acquisition method was used, dynamically choosing the top 10 abundant precursor ions from each survey scan (m/z 300 to 1,700) for fragmentation by high-

energy collision dissociation (HCD). MS2 scans were acquired in the Orbitrap with a target resolution of 7,500 at 400 m/z over a dynamic m/z range.

Mascot 2.5 (Matrix Science, Boston, MA, USA) was used for peptide identification, searching against the sequence of the wild-type parent strain ATCC 17978 as the reference (accession number GCA_000015425.1) (3,803 sequences, including 1,121,966 residues); Scaffold Q+ 4 (Proteome Software, Portland, OR, USA) was used for protein filtering (protein false discovery rate [FDR] set to 1.0% and peptide FDR set to 0.1%, with a 2-peptide minimum) and for quantification of the iTRAQ labels. The Benjamini-Hochberg correction method was used to filter proteins with *P* values of <0.05. Final data analysis was carried out using ratios of ATCC 17978 protein data from bacteria grown at 37°C and 28°C, in Microsoft Excel software.

Table 1. Bacterial strains and plasmids used in this study

Strain/Plasmid	Relevant characteristics	Reference/Source
A. baumannii		
17978	Wild type	ATCC
AB030	XDR clinical isolate from Winnipeg, MB	(Loewen, Alsaadi, Fernando, & Kumar, 2014b)
AB031	Clinical isolate from Toronto, ON	(Loewen, Alsaadi, Fernando, & Kumar, 2014a)
LAC-4	MDR clinical isolate from Los Angeles County, CA	(H.-Y. Ou et al., 2015)
AB154	17978:Δ*adeRS*	This study
AB104	17978:Δ*A1S_2006*	This study
AB239	AB104::*A1S_2006*	This study
AB256	AB104::mini-Tn*7*	This study
AB234	17978::mini-Tn*7*T-Apr-LAC	This study
AB235	17978::mini-Tn*7*T-Zeo-LAC	This study
AB240	LAC-4::mini-Tn*7*T-Zeo –LAC	This study
AB241	AB031::mini-Tn*7*T-Zeo-LAC	This study
AB242	AB030::mini-Tn*7*T-Apr-LAC	This study
AB243	AB031::mini-Tn*7*T-Apr-LAC	This study
AB244	LAC-4::mini-Tn*7*T-Apr-LAC	This study
AB271	17978:mini-Tn*7*T-Apr-mCherry2	This study
AB272	LAC-4:mini-Tn*7*T-Apr-mRuby2	This study
AB273	AB030:mini-Tn*7*T-Apr-sfGFP	This study
AB274	AB030:mini-Tn*7*T-Apr-mTurquoise2	This study
E. coli		
DH5α	F– Φ80lacZΔM15 Δ(lacZYA-argF) U169 recA1 endA1 hsdR17 (rK–, mK+) phoA supE44 λ– thi-1 gyrA96 relA1	Invitrogen
SM10	thi thr leu tonA lacY supE recA::RP4-2-Tc::Mu Km λpir	Kumar Lab collection
HB101	F- mcrB mrr hsdS20(rB- mB-) recA13 leuB6 ara-14 proA2 lacY1 galK2 xyl-5 mtl-1 rpsL20(SmR) glnV44 λ-	Kumar Lab collection
Plasmids		
pGEM®-T Easy	PCR cloning vector, *bla*	Promega
pMO130	Suicide vector, *aph(3')*, *sacB*	(Hamad,

		Zajdowicz, Holmes, & Voskuil, 2009)
pFLP2[ab]	pFLP2 (Hoang, Karkhoff-Schweizer, Kutchma, & Schweizer, 1998) containing origin of replication from pWH1266 (Hunger, Schmucker, Kishan, & Hillen, 1990), *bla*	Kumar Lab collection
pPLS176	pGEM®-T Easy-Δ*adeRS*:GmFRT	This study
pPLS181	pMO130-Δ*adeRS*:GmFRT	This study
pPLS156	pGEM®-T Easy-Δ*A1S_2006*:GmFRT	This study
pPLS160	pMO130-Δ*A1S_2006*:GmFRT	This study
pPS1464	pUC18T-mini-Tn*7*T-Gm	(K. H. Choi et al., 2005)
pPLS255	pUC18T-mini-Tn*7*T-Gm-*A1S_2006*	This study
	pUC18T-mini-Tn*7*T-LAC-Gm	(K. H. Choi et al., 2005)
pPLS268	pUC18T-mini-Tn*7*T-LAC-Apr	This study
pPLS267	pUC18T-mini-Tn*7*T-LAC-Zeo	This study
pPLS294	pUC18T-mini-Tn*7*T-Apr	This study
pPLS295	pUC18T-mini-Tn*7*T-Zeo	This study
pPLS337	pFLP2A, *aac(3)-IV*	This study
pPLS338	pFLP2Z, *ble*	This study
pPLS266	pFAM1, *aac(3)-IV*	Schweizer Lab collection
pPLS265	pFZE1, *ble*	Schweizer Lab collection
pTNS2	tnsABCD, *bla*	Kumar Lab collection
pRK2013	Helper plasmid for conjugation, kan[R]	Kumar Lab collection
pPLS296	pFPV-mCherry2	Chao Lab collection
pPLS298	pFPV-mTurquoise2	Chao Lab collection
pPLS297	pFPV-mRuby2	Chao Lab collection
pPLS339	pUC57-sfGFP	This study
pPLS331	pUC18T-mini-Tn7T-Apr-mCherry2	This study
pPLS330	pUC18T-mini-Tn7T-Apr-mRuby2	This study
pPLS334	pUC18T-mini-Tn7T-Apr-sfGFP	This study
pPLS332	pUC18T-mini-Tn7T-Apr-mTurquoise2	This study

Table 2. List of oligonucleotides used in this study

Primer name	Sequence	Target gene/purpose	Reference
adeB qRT F	GGATTATGGCGACTGAAGGA	*adeB*, Gene expression	Kumar Lab collection
adeB qRT R	AATACTGCCGCCAATACCAG		Kumar Lab collection
adeG qRT F	CGTAACTATGCGGTGCTCAA	*adeG*, Gene expression	Kumar Lab collection
adeG qRT R	ATCGCGTAGTCACCAGAACC		Kumar Lab collection
adeJ qRT F	CATCGGCTGAAACAGTTGAA	*adeJ*, Gene expression	Kumar Lab collection
adeJ qRT R	GCCTGACCATTACCAGCACT		Kumar Lab collection
16S qRT F	CTTCGGACCTTGCGCTAATA	16S, Reference gene expression	Kumar Lab collection
16S qRT R	ATCCTCTCAGACCCGCTACA		Kumar Lab collection
adeRS up F	CTTTATCAATCTGTTGAATAGTTGC	Amplify upstream fragment of *adeRS* knockout cassette	This study
adeRS up R GmFRT	TCAGAGCGCTTTTGAAGCTAATTCGCATGATCACGGGAGTC TGAGC		This study
adeRS down F GmFRT	AGGAACTTCAAGATCCCCAATTCGATTGAGGATGAAGGCCC TGGC	Amplify downstream fragment of *adeRS* knockout cassette	This study
adeRS down R	GCATAATCTTTGGCTAAAGCGAAAG		This study
Gm FRT F	CGAATTAGCTTCAAAAGCGCTCTGA	Amplify GmFRT fragment of knockout cassettes	Kumar Lab collection
Gm FRT R	CGAATTGGGGATCTTGAAGTTCCT		Kumar Lab collection
adeRS Full F	GCGTATGATGAGTTGAAGCAC	*adeRS*, Full length	This study

adeRS Full R	ATGGCGAGAAGAGATTCGTAG	screening	This study
A1S_0092 qRT F	ACGTGCCAATACCCAAGAAC	*A1S_0092*, Gene expression	This study
A1S_0092 qRT R	CATGAGCCACTGCTAAACGA		This study
A1S_0116 qRT F	CAGCCACAAGTGTTGGAGAA	*A1S_0116*, Gene expression	This study
A1S_0116 qRT R	CTCGATACCTTTCGCCTGAC		This study
A1S_1708 qRT F	CGCTGCAGATTTACTTCGTG	*A1S_1708*, Gene expression	This study
A1S_1708 qRT R	TGCCAACTTTAAGCATGCAA		This study
csuA qRT F	TTTGGTGAAGCTACCACAGC	*csuA*, Gene expression	This study
csuA qRT R	CCAGCACACTCGATCTGAAA		This study
paaK qRT F	CGCTTAGGTGCAACGGTTAT	*paaK*, Gene expression	This study
paaK qRT R	TGGCGTAACCATAATTGCAG		This study
ompA qRT F	TCAAGGTTTCTTGGCGACTT	*A1S_1193*, Gene expression	This study
ompA qRT R	GGTAAAAGCAGCCGCATAAG		This study
A1S_2006 up F	AGTCAAATGTACGCGGTCATATGC	Amplify upstream fragment of *A1S_2006* knockout cassette	This study
A1S_2006 up R GmFRT	TCAGAGCGCTTTTGAAGCTAATTCGATCGAGCAAGATGACA TCGGC		This study
A1S_2006 down F GmFRT	AGGAACTTCAAGATCCCCAATTCGTGGTTTACCTGAAGACA CAGC	Amplify downstream fragment of *A1S_2006* knockout cassette	This study
A1S_2006 down R	GCTGAAATAACCAATGGAAATCTT		This study
A1S_2006 Full F	CGCGTCGAATTGGCGCATTT	*A1S_2006*, Full length screening	This study
A1S_2006 Full R	GCCGAGTTGCAATTGAGTC		This study
A1S_2006 Full F BamHI	TACGTggatccGAATGGCACTAATCTTGCTT	*A1S_2006*, Amplify full length gene with native promoter and restriction sites	This study
A1S_2006 Full R HindIII	GCTACaagcttGAATATAGCCGAGTTGCAAT		This study
ABglmS_F_N	TATGGAAGAAGTTCAGGCTC	Screening primers for insertion from mini-Tn*7* vectors into *att*Tn*7* site	This study
Tn7R	CACAGCATAACTGGACTGATTTC		(K. H. Choi et al., 2005)
ompA 2840 qRT F	CTATGCTTGTTGCTGCTCCA	*ompA*(*A1S_2840*), Gene	This study

ompA 2840 qRT R	CCATTGTTGTGTTGGCTGTC	expression	This study
A1S_2006 qRT F	GCCCGCTTACATACCATTTT	*A1S_2006*, Gene expression	This study
A1S_2006 qRT R	TGC CAG TTT GGT TTG AGC TT		This study
pFAM F SacII	TGCATccgcggTAGATAATTCGGCTTCTCC	Amplify *aac(3)-IV* gene from pFAM1 plasmid with restriction sites	This study
pFAM R BsrGI	CAGTGtgtacaATTCCCTTTGTCAACAGCAAT		This study
pFZE F BsrGI	CGCTGtgtacaAATTCTAGATATTCGGCTTCG	Amplify *ble* gene from pFZE1 plasmid with restriction sites	This study
pFZE R SacII	TAGTAccgcggTCTCTGATGTTACATTGCAC		This study

*Note: Restriction enzyme recognition sites in the oligonucleotides are shown in lowercase

CHAPTER 3

Section 3.1 of this chapter was originally published in Journal of Membrane Biology, 2018: P. Malaka De Silva and Ayush Kumar., Effect of sodium chloride on surface-associated motility of *Acinetobacter baumannii* and the role of AdeRS two-component system. doi: 10.1007/s00232-017-9985-7

Section 3.2 of this chapter was originally published in Antimicrobial Agents and Chemotherapy, 2018: P. Malaka De Silva, Patrick Chong, Dinesh M. Fernando, Garrett Westmacott, and Ayush Kumar (2018). Effect of incubation temperature on antibiotic resistance and virulence factors of *Acinetobacter baumannii* ATCC 17978. doi: 10.1128/AAC.01514-17

3.1 EFFECT OF SODIUM CHLORIDE ON SURFACE-ASSOCIATED MOTILITY OF *Acinetobacter baumannii* AND THE ROLE OF AdeRS TWO-COMPONENT SYSTEM

This section of the chapter was published in *Journal of Membrane Biology*, 2018: P. Malaka De Silva and Ayush Kumar (2018). Effect of sodium chloride on surface-associated motility of *Acinetobacter baumannii* and the role of AdeRS two-component system. doi: 10.1007/s00232-017-9985-7.

Note: This chapter has been modified from the original publication such that the majority of materials and methods has been described in Chapter 2.

3.1.1 INTRODUCTION

Acinetobacter baumannii is an opportunistic pathogen that is commonly associated with hospital-acquired infections such as ventilator-associated pneumonia, catheter-associated bacteraemia, and a wide variety of skin and soft tissue infections (Antunes et al., 2014). It has recently established itself as a prominent source of infections in hospital settings and routinely displays multidrug- and pandrug-resistant phenotypes limiting treatment options (Peleg & Paterson, 2006). As a result, a recent report by the World Health Organization classified *A. baumannii* under the category of 'critical' organisms that need urgent attention to develop new antibiotics (http://www.who.int/medicines/publications/WHO-PPL-Short_Summary_25Feb-ET_NM_WHO.pdf).

There are a number of factors that contribute to the success of *A. baumannii* to prevail and cause infections within hospital settings. These include but are not limited to its capability to survive in harsh hospital environments, its ability to form potent biofilms on both biological surfaces and

innate surfaces of medical equipment, and most importantly the possession of both intrinsic and acquired antibiotic resistance mechanisms (Peleg, Seifert, et al., 2008). Increased expression of efflux pumps, in particular those belonging to the resistance-nodulation-division or RND family, that extrude an extensive range of molecules including antibiotics is a key strategy of *A. baumannii* to survive antibiotic treatments (Kumar & Schweizer, 2005).

To date, three different RND efflux pumps, AdeABC (Marchand et al., 2004), AdeFGH (Cortez-Cordova & Kumar, 2011; Coyne, Rosenfeld, Lambert, Courvalin, & Perichon, 2010), and AdeIJK (Damier-Piolle, Magnet, Bremont, Lambert, & Courvalin, 2008), have been characterized in *A. baumannii*. Together, these three pumps are capable of effluxing almost all classes of antibiotics currently used for the treatment of *A. baumannii* infections (Coyne, Courvalin, & Perichon, 2011; Yoon et al., 2016).

Considering the important role RND efflux pumps play in the antibiotic resistance of *A. baumannii*, it is imperative to investigate the underlying regulatory mechanisms of RND efflux pumps. The AdeFGH and AdeIJK pumps are under the transcriptional control of a LysR-type transcriptional regulator, AdeL (Coyne et al., 2010), and TetR-type transcriptional regulator, AdeN (Rosenfeld, Bouchier, Courvalin, & Perichon, 2012), respectively. The AdeABC pump, on the other hand, is positively regulated by a Two-Component System (TCS) AdeRS that is encoded directly upstream of the *adeABC* operon (Marchand et al., 2004). Mutations in *adeRS* that cause increased expression of the AdeABC pump and consequently result in reduced susceptibility of *A. baumannii* to antibiotics are commonly seen in clinical isolates of *A. baumannii* (Yoon et al., 2013).

TCSs are known to regulate a multitude of phenotypic traits in bacterial species in response to environmental perturbations. Most abundant in bacteria, any given TCS can regulate a myriad of

pathways in response to an environmental stimuli (Hoch, 2000; Stock et al., 2000). While the role of AdeRS in controlling the expression of the AdeABC pump is well established, environmental signals that stimulate its activity are not known. In this work, we show that AdeRS is involved in the response of *A. baumannii* to the salt concentration in the growth medium.

3.1.2 SPECIFIC EXPERIMENTAL PROCEDURES AND MODIFICATIONS

3.1.2.1 Motility assay

Motility media base was composed of 0.5% tryptone (Becton, Dickenson and Company, MD, USA), NaCl (BioShop Canada Inc., Burlington, ON, Canada), and 0.3% agarose (BioBasic Canada Inc, Markham, ON, Canada). Three different concentrations of NaCl (0.125, 0.25, and 0.5% w/v) were used to test motility. When needed, the pH of the medium was altered using either acetic acid or potassium hydroxide and osmolarity altered using sucrose (0.3 and 0.5 M). To measure the surface-associated motility, we used a previously described protocol (Harding et al. 2013) with slight modifications. A 3 µL aliquot of an overnight culture was stabbed into the freshly poured and solidified motility medium and incubated for 18 h at 37 °C before recording the diameter of the area with bacterial growth.

3.1.2.2 Growth curves

For generating growth curves overnight bacterial cultures grown in 3 mL volumes were standardized to an absorbance of 1.0 at 600 nm (A_{600}) and diluted 1:100 in fresh medium containing varying concentrations of NaCl (0.125, 0.25, and 0.5% w/v). One hundred µL of diluted culture was dispensed into the wells of a sterile 96-well polystyrene plate (Sarstedt, Montreal, QC, Canada) and growth monitored for 18 h at 37˚C using a SpectraMax M2 microplate reader (Molecular Devices, CA, USA) with continuous shaking. A_{600} readings were

taken every 15 min. Results were plotted and statistically analysed using GraphPad Prism v.6.07 (La Jolla, CA, USA).

3.1.3 RESULTS

3.1.3.1 Deletion of *adeRS* and *adeB* expression

As expected, we observed decreased expression of *adeB* (RND component-encoding gene of AdeABC efflux pump) in the in-frame *adeRS* deletion mutant, AB154 (Figure 6). Expression of *adeG* and *adeJ* was not affected by the deletion of *adeRS*, suggesting that downregulation of AdeAB pump does not result in compensatory upregulation of other RND pumps.

3.1.3.2 Antibiotic susceptibility of the *adeRS* deletion mutant

Results of antibiotic susceptibility assays are shown in Table 3. Small but reproducible increases in susceptibility to doxycycline, tigecycline, gentamicin, and cefepime were observed in the *adeRS* deletion mutant AB154. There was no change in the susceptibility of two fluoroquinolones (moxifloxacin and ciprofloxacin) tested.

3.1.3.3 Biofilm formation and virulence of *adeRS* deletion mutant

We noticed that AB154 formed significantly less biofilms compared to the wild-type parent strain (Figure 7). However, we did not observe any differences in the virulence of AB154 and that of the wild-type parent strain when tested in the *G. mellonella* model (Figure 8).

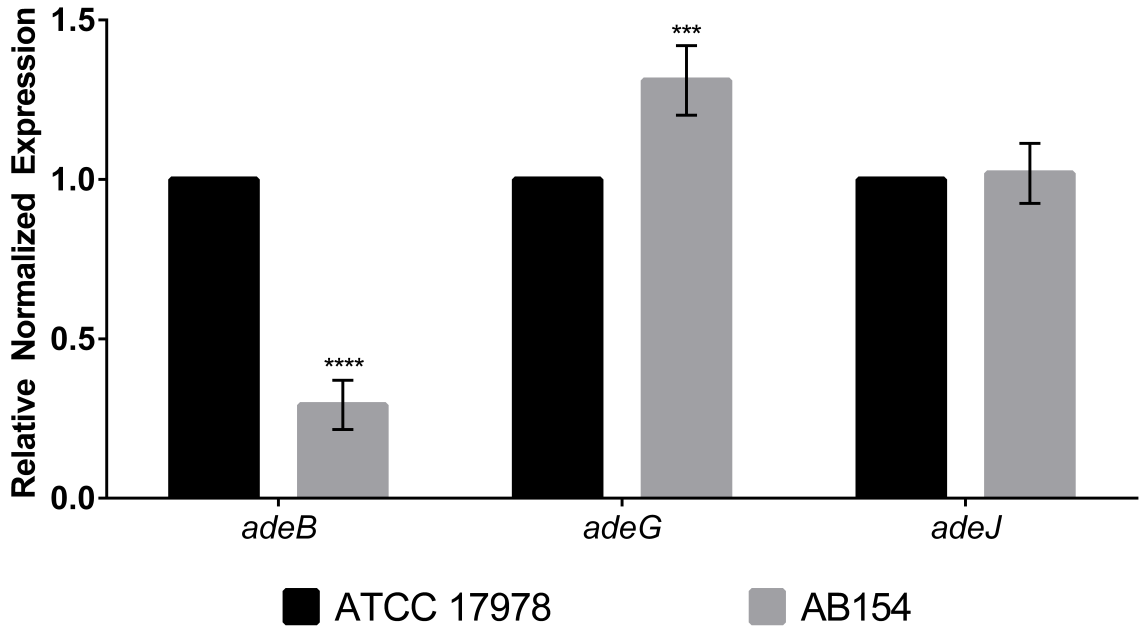

Figure 6. Expression of RND efflux pumps in *A. baumannii* AB154. Expression of RND efflux pump genes (*adeB, adeG, adeJ*) in *A. baumannii* AB154 relative to that in *A. baumannii* ATCC 17978. 16S rRNA gene was used as the housekeeping control. Error bars represent standard deviation. **** indicates $P<0.0001$ and *** indicates $P = 0.0003$.

Table 3. Antibiotic susceptibilities of *A. baumannii* strains ATCC 17978 and AB154. Data expressed in μg/mL as determined by E-strip method and representative of two independent biological replicates.

Antibiotic	**ATCC 17978**	**AB154**
Tigecycline	0.064	0.032
Doxycycline	0.19	0.125
Gentamicin	0.75	0.38
Cefepime	1.5	0.75
Ciprofloxacin	0.064	0.064
Moxifloxacin	0.016	0.016

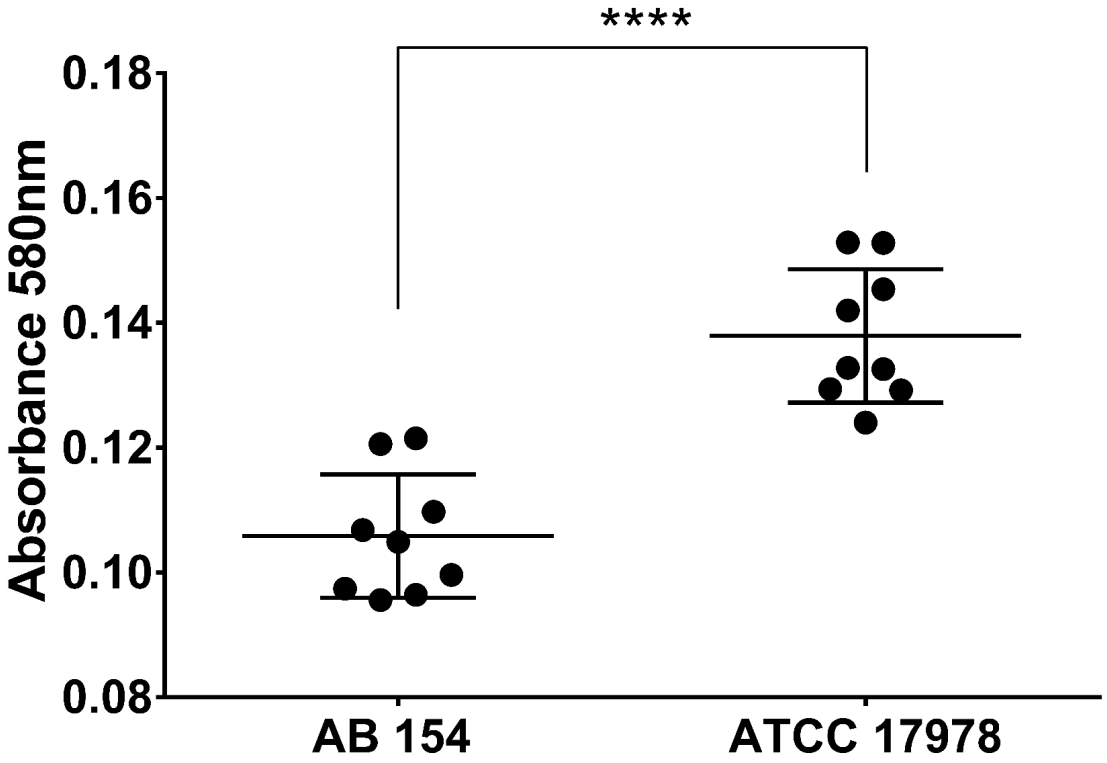

Figure 7. Biofilm formation by *A. baumannii* AB154 and *A. baumannii* ATCC 17978. Biofilm formation was determined after 48 h on plastic surfaces in regular LB, and biofilm biomass was quantified by measuring the optical density at 580 nm. Significant difference ($P < 0.0001$) in biofilm formation by *A. baumannii* AB154 and *A. baumannii* ATCC 17978 was confirmed by student's t-test and is indicated by asterisks. Data shown are representative of two independent assays.

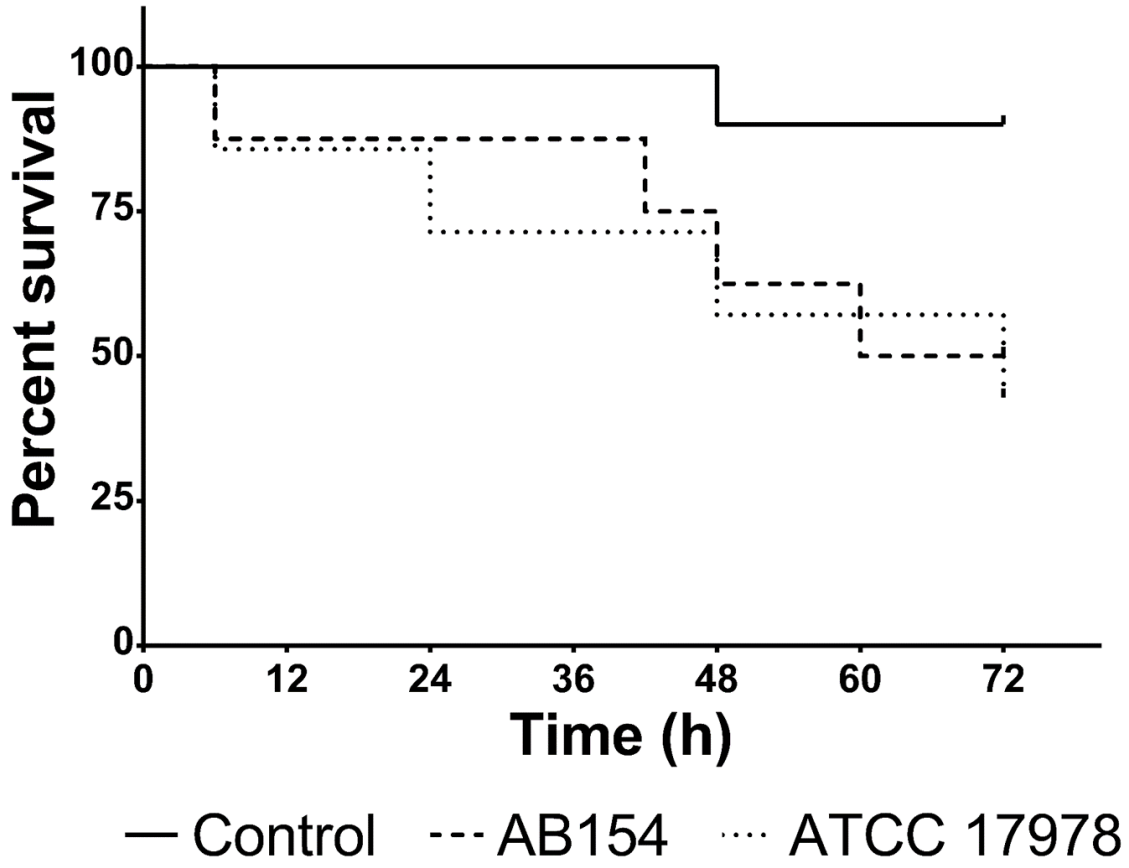

Figure 8. Survival curve of *G. mellonella* larvae when infected with *A. baumannii* strains. Virulence of *A. baumannii* AB154 (dashed line) and *A. baumannii* ATCC 17978 (dotted line) in *Galleria mellonella* infection assays. *G mellonella* larvae were injected into the left proleg with 10 μL of a 10^6 CFU/mL bacterial suspension in 0.85% saline and incubated at 37 °C. An equal volume of 0.85% sterile saline was injected to the control larvae group (solid line) and the viability of the infected larvae was assessed at every 6 h for a total of 72 h. GraphPad Prism v.6.07 was used for statistical analyses where there was no statistical significance between the strains tested.

3.1.3.4 Motility of *adeRS* deletion mutant

On 0.3% agarose plates, AB154 displayed a marked decrease in motility as compared to the wild-type parent strain after 18 h of incubation (Figures 9a, b). Increased expression levels of *adeA* among other changes was previously reported in response to NaCl (Coyne et al., 2011). The routinely used motility medium contains 0.25% NaCl; we then tested the motility of AB154 in the presence of 0.125% and 0.5% NaCl, which amounts to 0.5× and 2× concentrations of NaCl used routinely in the motility medium. Interestingly, we observed that the difference in motility between AB154 and ATCC 17978 was less pronounced in the lower NaCl concentration (0.125%) (Figures 9a, b). However, the surface motility of AB154 was completely abolished in the presence of higher NaCl concentration (0.5%). There was no significant difference in the motility of the parent strain ATCC 17978 in different salt concentrations. In order to determine whether the differences in the motility of AB154 in varying NaCl concentrations were due to the changes in osmolarity or the pH of the medium, we compared its motility with the wild-type parent in two different concentrations of sucrose as well as three different pHs. Supplementing the motility medium with sucrose as well as altering its pH had the same effect on both ATCC 17978 and AB154 with motility completely abolished (Figures 10a, b).

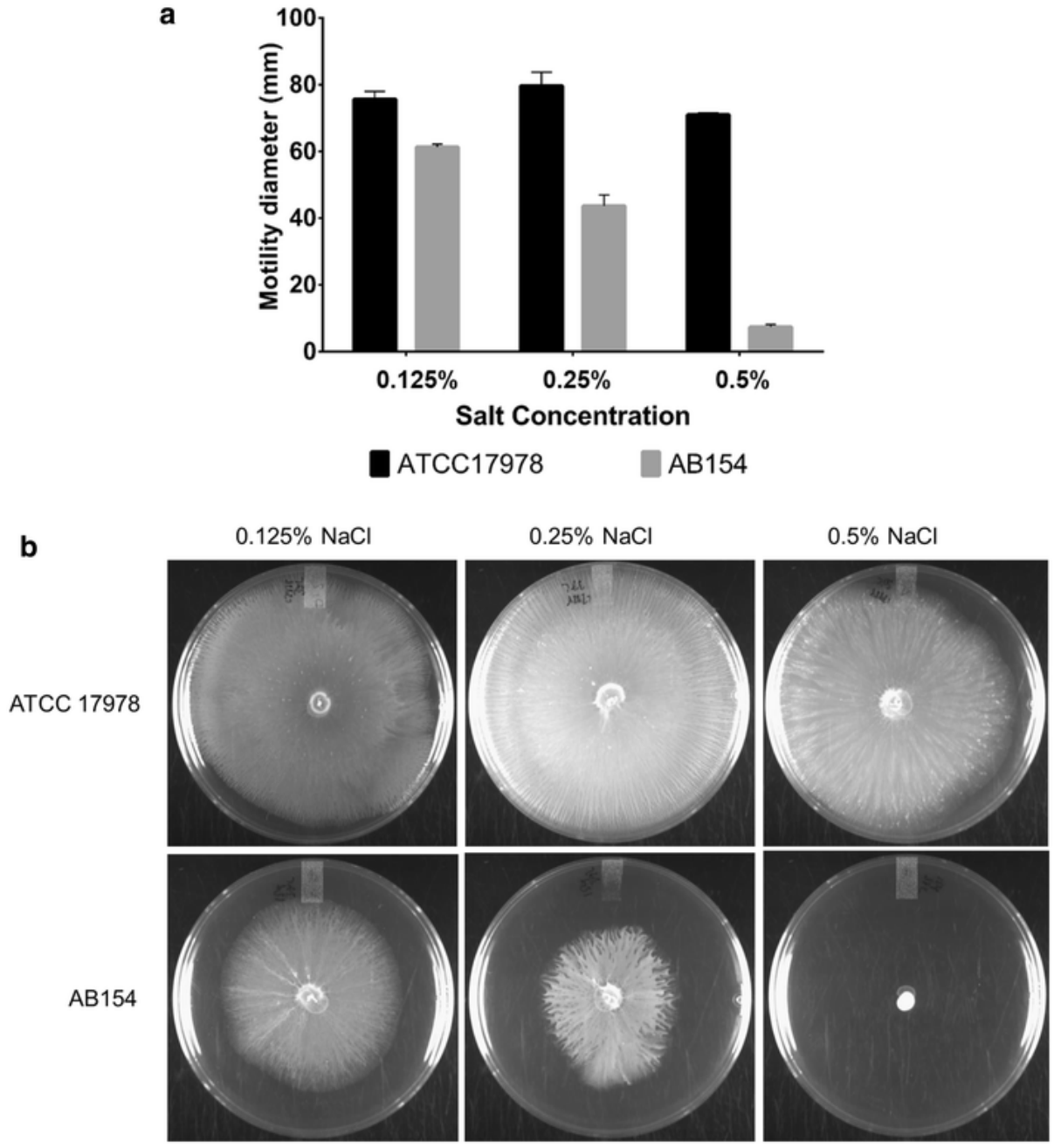

Figure 9. Surface-associated motility of *A. baumannii* AB154 and ATCC 17978 in varying NaCl concentrations. (a) Cell motility of *A. baumannii* AB154 and *A. baumannii* ATCC 17978 on semi-solid agar in varying NaCl concentrations. Each bar represents the diameter of the area of bacterial growth. Error bars represent standard deviation. (b) Plates show the motility of two strains and are representative of 3 biological replicates.

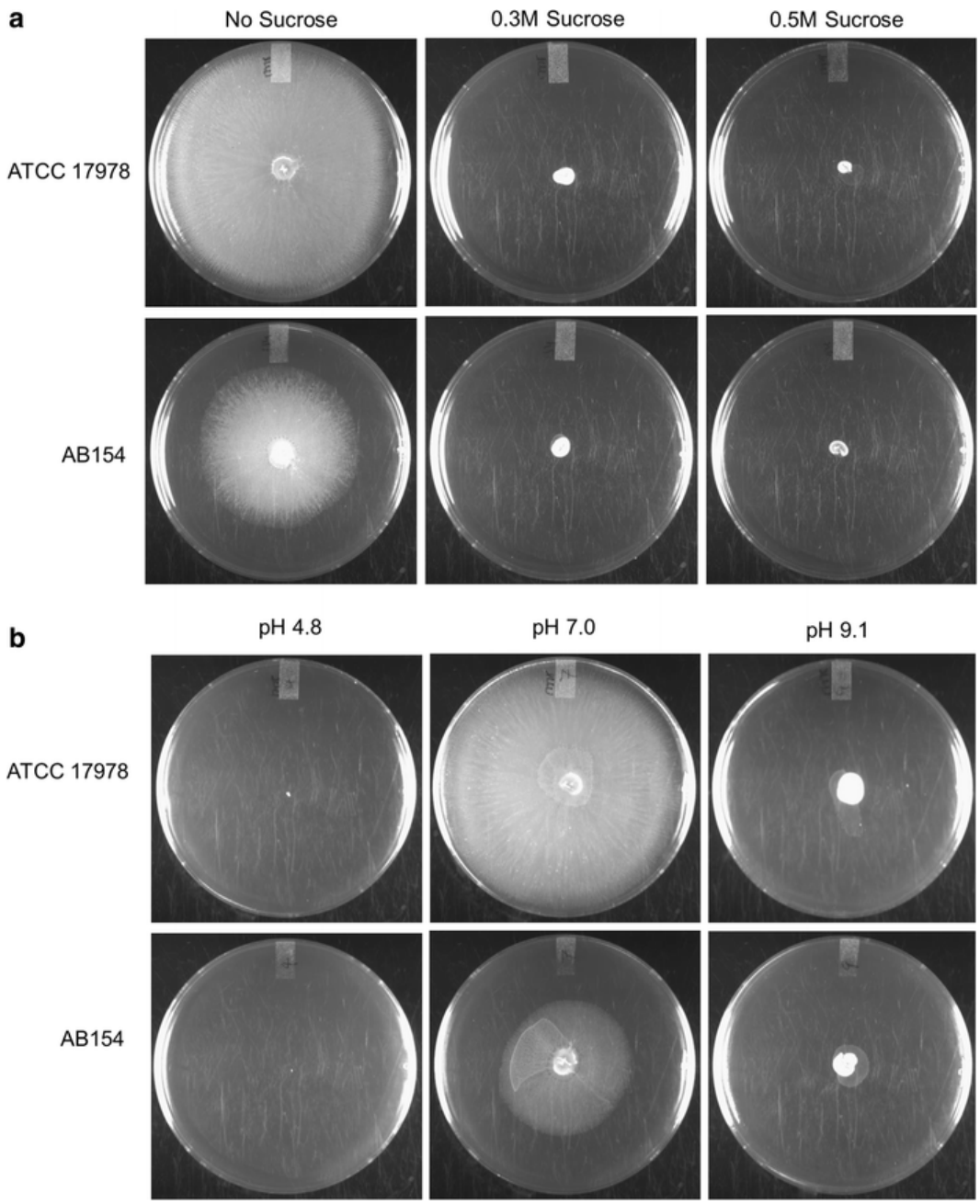

Figure 10. Surface-associated motility of *A. baumannii* AB154 and ATCC 17978 in varying sucrose concentrations and pH. Cell motility of *A. baumannii* AB154 and *A. baumannii* ATCC 17978 in varying sucrose concentration (a) and pH (b). Plates are representative of 3 biological replicates where the NaCl concentration was maintained at 0.25%.

3.1.3.5 Growth of *adeRS* deletion mutant in varying NaCl concentrations

To rule out the fact that the observed differences in surface motility were due to a defect in growth at different NaCl concentrations, we carried out growth assays in LB medium containing 0.125, 0.25, and 0.5% of NaCl. We observed that at all three concentrations tested, AB154 displayed relatively slower growth compared to the parent ATCC 17978 (Figures 11a–c). However, a comparison of growth of AB154 in different NaCl concentrations did not display any significant difference.

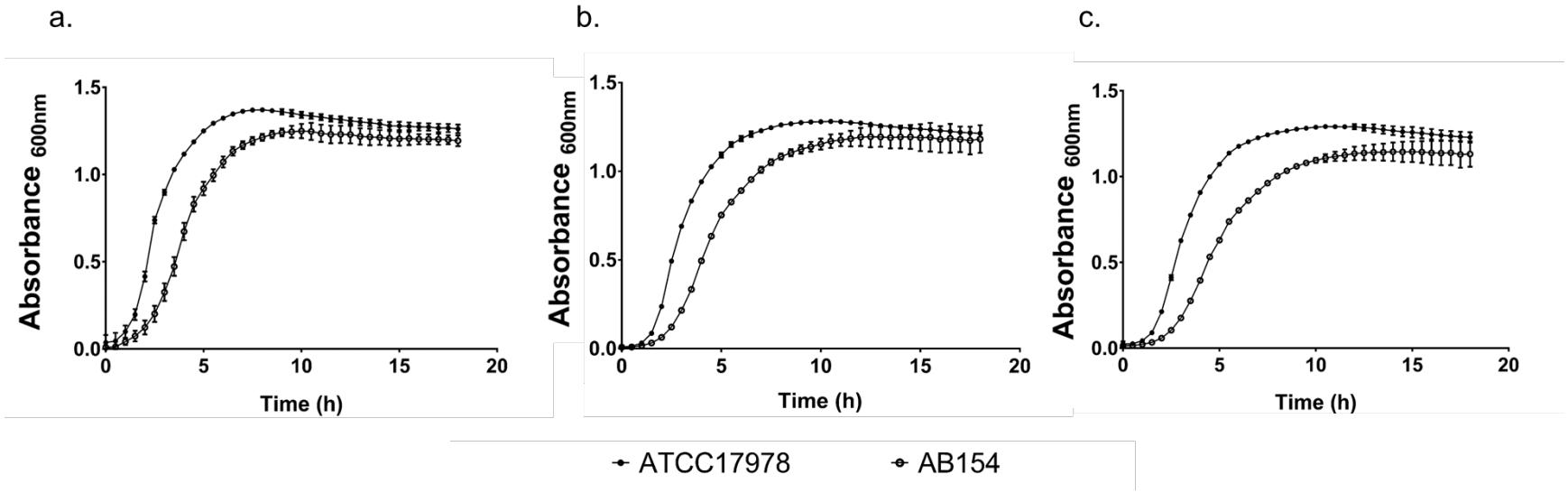

Figure 11. Growth curves of A. *baumannii* AB154 and ATCC 17978 in varying NaCl concentrations. Growth of *A. baumannii* AB154 and *A. baumannii* ATCC 17978 in LB medium supplemented with 0.125% (a), 0.25% (b), and 0.5% (c) NaCl. Growth was monitored for 18 h with shaking.

3.1.4 DISCUSSION

The AdeABC pump of *A. baumannii* is one of the key determinants of its reduced susceptibility to a number of antibiotics. The role of the AdeRS two-component regulatory system is well established in the regulation of the AdeABC pump (Hornsey et al., 2010; Ruzin et al., 2007; Yoon et al., 2013). There is evidence that in addition to regulating the expression of the AdeABC pump, the AdeRS system can influence virulence of *A. baumannii* and biofilm formation on mucosal tissue, albeit in a strain-dependent manner (Richmond et al., 2016). However, it is still not clear to what environmental signals does the AdeRS system respond to. In this study, we provide evidence that the AdeRS system is part of *A. baumannii*'s response to saline stress.

As expected, knocking-out AdeRS system in ATCC 17978 resulted in a decreased expression of the AdeAB pump (Figure 6), concurrently we also observed small but reproducible increases in the susceptibility of AB154 to antibiotics with the exception of fluoroquinolones (Table 3). Antibiotics to which AB154 showed an increased susceptibility, for example tigecycline, gentamicin, and cefepime, have previously been described as substrates of the AdeABC efflux pump (Yoon et al., 2013). However, the type strain ATCC 17978 lacks *adeC* which encodes the outer membrane protein of the AdeABC complex and the observed changes in the susceptibility could suggest that the AdeAB pump recruits an outer membrane protein from another RND system. It is likely that the AdeAB pump perhaps forms the tripartite complex with another, yet unknown, outer membrane protein in ATCC 17978 although there is no definitive evidence for that as yet.

The ability to form biofilm is an important virulence factor in bacterial pathogens (de Breij et al., 2010; Hoiby, Bjarnsholt, Givskov, Molin, & Ciofu, 2010; Parsek & Singh, 2003). Reduced biofilm formation by the *adeRS* deletion mutants of *A. baumannii* has been described previously,

albeit only on mucosal tissue and not on plastic surface (Richmond et al., 2016). Our results show that deletion of the AdeRS system in ATCC 17978 reduces its capability to form biofilm on the polystyrene surface as well (Figure 7). Therefore, our data demonstrating a decreased biofilm formation on abiotic surfaces further confirm a previous finding where biofilm formation on plastic surfaces was affected by the deletion of *adeRS* in *A. baumannii* strain AYE and not in strain S1 (Richmond et al., 2016) showing that the AdeRS system's role in biofilm formation can be strain specific in *A. baumannii*.

We then studied the virulence of AB154 in *G. mellonella*, a well-established virulence model for *A. baumannii* (Peleg et al., 2009). We did not observe any significant differences between the virulence of AB154 and ATCC 17978, indicating that AdeRS does not play a role in ATCC 17978's virulence. These results are also consistent with previously published work (Richmond et al., 2016), where AdeABC but not AdeRS was shown to be involved in the virulence of some strains *A. baumannii*.

A. baumannii displays twitching motility, an important virulence factor, using its type IV pili on semi-solid media (Fernandez, Breidenstein, Song, & Hancock, 2012; McQueary et al., 2012; O'Toole & Kolter, 1998). We assessed the role of the AdeRS system on the surface motility of *A. baumannii* ATCC 17978. We observed that AB154 had a marked decrease in motility as compared to the wild-type strain (Figures 9a, b). Intriguingly, we observed that decreased motility in AB154 was dependent on the NaCl concentration in the medium as the difference in the motility between AB154 and ATCC 17978 was more pronounced in the presence of higher concentration of NaCl (Figures 9a, b). This difference in the surface motility between AB154 and ATCC 17978 was not observed when we altered the osmolarity or the pH of the medium (Figure 10a, b). In fact, both ATCC 17978 and AB154 were non-motile only when the

osmolarity and the pH of the medium were altered while the NaCl was maintained at 0.125% suggesting that while the lack of motility in the presence of NaCl is AdeRS-dependent, in high osmolarity or altered pH it is not. Since we did not observe any differences in the fitness of AB154 under different NaCl concentrations (Figures 11a–c), the altered motility of AB154 is not due to a growth defect under these conditions.

Sodium chloride has been shown to affect the surface motility of organisms like *Burkholderia pseudomallei* (Pumirat et al., 2017) and *Pseudomonas aeruginosa* (Yang, Tang, Si, & Tang, 2017). It has been suggested that adaptation to salt stress is associated with the pathogenicity of organisms such as *B. pseudomallei* (Pumirat et al., 2017). No association between motility, a virulence factor, and NaCl stress has been shown in *A. baumannii* previously. Our data suggest that NaCl can impact the surface motility of *A. baumannii* ATCC 17978 in the absence of AdeRS. It is therefore possible that AdeRS is a part of the *A. baumannii*'s response to salinity stress. However, this needs to be further investigated.

3.1.5 CONCLUSIONS

In conclusion, our work demonstrates that the AdeRS two-component system is not only involved in the regulation of the AdeAB efflux pump but also in biofilm formation on the plastic surface in *A. baumannii* ATCC 17978. The most notable finding from our study is that AdeRS regulates the surface-motility and possibly aids in the adaptation of *A. baumannii* under high salt concentrations. Hence, this study provides evidence of the involvement of the AdeRS TCS in regulatory processes of surface – associated motility when *A. baumannii* is challenged with a high concentration of NaCl.

3.2 EFFECT OF INCUBATION TEMPERATURE ON ANTIBIOTIC RESISTANCE AND VIRULENCE FACTORS OF *Acinetobacter baumannii* ATCC 17978

This section of the chapter was published in *Antimicrobial Agents and Chemotherapy*, 2018: P. Malaka De Silva, Patrick Chong, Dinesh M. Fernando, Garrett Westmacott, and Ayush Kumar (2018). Effect of incubation temperature on antibiotic resistance and virulence factors of *Acinetobacter baumannii* ATCC 17978. doi: 10.1128/AAC.01514-17.

Note: This chapter has been modified from the original publication such that the materials and methods has been described in Chapter 2.

3.2.1 INTRODUCTION

Acinetobacter baumannii is an organism of significant interest due to its ability to resist the action of various antibiotics (Doi, Murray, & Peleg, 2015; Peleg & Paterson, 2006). *A. baumannii* displays a variety of intrinsic and acquired mechanisms of resistance to antibiotics, making treatment of infections often very difficult. While *Acinetobacter* spp. are commonly found in the environment, natural habitats of *A. baumannii* remain to be properly defined. It was thought that *A. baumannii* tends to persist primarily within hospital environments (Peleg, Seifert, et al., 2008); however, a number of recent studies have isolated and characterized *A. baumannii* from different environmental niches, although it is not clear whether human activity within those niches is responsible for the presence of *A. baumannii* (Fernando et al., 2016; Hamouda, Findlay, Al Hassan, & Amyes, 2011; Lupo, Vogt, Seiffert, Endimiani, & Perreten, 2014).

A. baumannii has been reported to cause a variety of infections in hospital settings, including pneumonia, urinary tract infections, osteomyelitis, skin and soft tissue infections, bloodstream

infections, and meningitis (Peleg, Seifert, et al., 2008). It has spread rapidly in hospital settings globally, and some estimates suggest that *A. baumannii* causes 5 to 10% of hospital-acquired infections worldwide (Timsit et al., 2014). It has been suggested that *A. baumannii* is responsible for disproportionately high incidences of pneumonia and bloodstream infections in hospital settings; a recent study demonstrated that, although *A. baumannii* was responsible for only 6% of all hospital-acquired infections, it was implicated in 60% of pneumonia cases and 25% of bloodstream infections (Cornejo-Juarez et al., 2015). This finding speaks to the tremendous success of *A. baumannii* in causing hospital-acquired pneumonia and bloodstream infections.

An important characteristic of *A. baumannii* that partially explains its success as a hospital-acquired pathogen is its ability to persist on various environmental surfaces (Maragakis & Perl, 2008; McDonald, Banerjee, & Jarvis, 1999). Therefore, the adaptation of *A. baumannii* to various environments may serve as a trigger to modulate its virulence factors. However, it is not clear how adaptation to different environmental conditions affects modulation of the antibiotic resistance and virulence of *A. baumannii*. Among these environmental conditions, temperature is likely to be one of the important environmental changes that *A. baumannii* experiences as it makes its way into the human host from the hospital environments. The purpose of this work was to study the effects of temperature on the antibiotic resistance and virulence of *A. baumannii*, using a combination of phenotypic and proteomic approaches.

3.2.2 RESULTS AND DISCUSSION

A. baumannii displays a very impressive propensity to cause multidrug-resistant infections in hospital settings; therefore, it has been studied quite extensively recently (Castanheira, Mendes, & Jones, 2014; Doi et al., 2015; Kassamali, Jain, & Danziger, 2015; Lin & Lan, 2014). *A.*

baumannii uses a variety of mechanisms to resist the activity of antibiotics, but antibiotic resistance is not the only factor contributing to the persistence of *A. baumannii* as an opportunistic nosocomial pathogen. It also contains a wide array of virulence factors (Cerqueira et al., 2014; Eijkelkamp et al., 2013; G. Harris et al., 2013; McConnell et al., 2013; Tilley, Law, Warren, Samis, & Kumar, 2014) and a tremendous ability to adapt to environmental stress, leading to its persistence in hospital settings (Gayoso et al., 2014; Wright et al., 2014).

For a pathogen like *A. baumannii*, temperature is an important environmental change that it experiences as it makes its way into its host. We observed rather fortuitously that *A. baumannii* ATCC 17978 displays reduced levels of surface-associated motility at 28°C, compared with those at 37°C. This suggests that the incubation temperature can affect the phenotype of *A. baumannii* ATCC 17978, which could modulate its virulence. Production of virulence factors by several bacterial species has been shown to be induced at 37°C. The underlying mechanisms of thermoregulation of virulence factor production and/or antibiotic resistance can be diverse. For example, in *Pseudomonas aeruginosa*, this phenomenon has been shown to be mediated by RNA thermometers that result in increased production of virulence factors such as rhamnolipids, pyocyanin, and elastase at 37°C (Grosso-Becerra et al., 2014). Further, a recent study suggested the involvement of a putative diguanylate cyclase in the thermoregulation of biofilm formation in *Burkholderia pseudomallei* (Plumley et al., 2017).

We pursued our findings further in order to study how differently *A. baumannii* ATCC 17978 behaves at different incubation temperatures. We carried out a comparison of the phenotypes (in particular, antibiotic resistance and virulence) of *A. baumannii* ATCC 17978, followed by proteomic analysis in order to understand, at the molecular level, the differences in the phenotypes.

3.2.2.1 Incubation temperature modulates the antibiotic susceptibility of *A. baumannii* ATCC 17978

We initiated our study by comparing the growth of *A. baumannii* ATCC 17978 at 28°C and 37°C (Figure 12). The initial growth of *A. baumannii* ATCC 17978 was slower at 28°C than at 37°C, as the absorbance at 600 nm (A_{600}) of *A. baumannii* ATCC 17978 at 28°C was only about 40% of that at 37°C after 4 h of incubation (Figure 12). This difference became less pronounced after 12 h of incubation, with the growth rate at 28°C being about 92% of that at 37°C (Figure 12). This suggests that *A. baumannii* grows faster at 37°C than at 28°C, at least during the early log phase of the growth cycle.

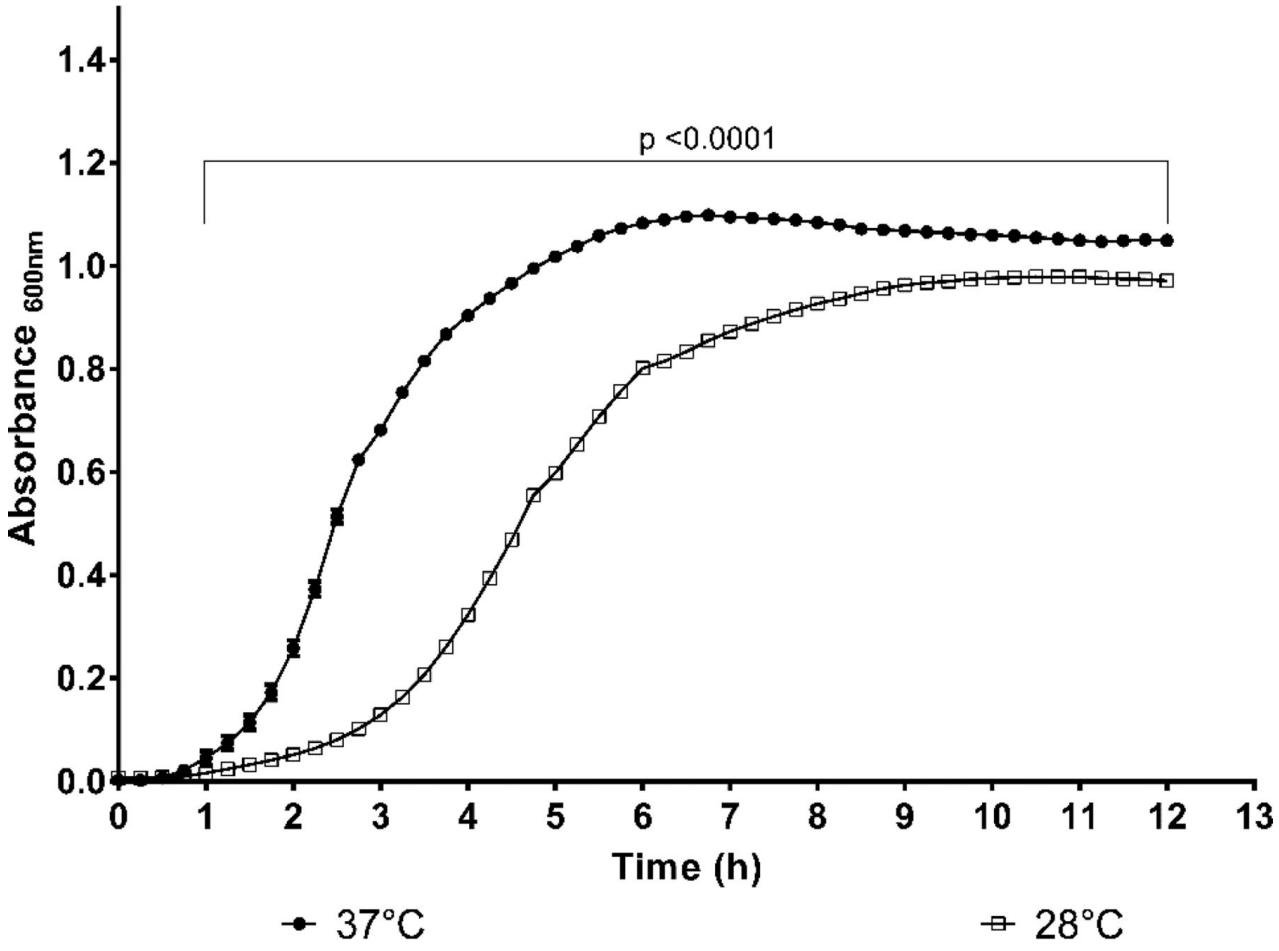

Figure 12. Relative growth of *A. baumannii* ATCC 17978 at 28˚C and 37˚C over 12 hours. The difference in growth was most pronounced after 1hour of incubation; however, the difference was less pronounced after 6 hours, and growth rates were almost the same after 8 hours of incubation. Data shown are the mean of two independent assays.

Antibiotic susceptibility of *A. baumannii* ATCC 17978 was compared at 28 and 37°C (Table 4). *A. baumannii* ATCC 17978 was 4-fold less susceptible to aztreonam at 28°C, but its susceptibility to trimethoprim-sulfamethoxazole was 8-fold higher at 28°C than at 37°C. Small but reproducible changes in susceptibility to some other antibiotics were also observed (Table 4). It seems unlikely that the changes in susceptibility to aztreonam and trimethoprim-sulfamethoxazole were due to the differences in growth rates at the two temperatures tested, because there were little or no changes in susceptibility to the other antibiotics tested. However, in order to rule out the possibility that the differences in susceptibility to aztreonam and trimethoprim-sulfamethoxazole at 28°C and 37°C were due to possible differences in the diffusion of the antibiotics at these temperatures, we carried out susceptibility testing for the two antibiotics using the 2-fold broth dilution method. The results obtained using the broth dilution method showed the same trend as those obtained using the E-test method. *A. baumannii* ATCC 17978 was 4-fold less susceptible to aztreonam at 28°C, and its susceptibility to trimethoprim-sulfamethoxazole was 2-fold higher at 28°C than at 37°C. Currently, we are not sure why we observed opposite responses to aztreonam and trimethoprim-sulfamethoxazole at 28°C versus 37°C.

Table 4. Susceptibilities of *A. baumannii* ATCC 17978 to various antibiotics at 28˚C and 37˚C. Minimum Inhibitory Concentration data expressed in μg/mL as determined by E-test method and representative of at least two independent biological replicates.

.

Antibiotic	**MIC at 37˚C**	**MIC at 28˚C**
Piperacillin-tazobactam	<0.016	<0.016
Ceftriaxone	6	8
Cefepime	0.75	1
Ceftazidime	1	1
Imipenem	0.125	0.094
Doripenem	0.094	0.094
Ciprofloxacin	0.064	0.047
Moxifloxacin	0.012	0.012
Aztreonam	2	8
Trimethoprim-sulfamethoxazole	4	0.5
Gentamicin	0.19	0.25

3.2.2.2 Temperature modulates biofilm formation and surface motility of *A. baumannii* ATCC 17978

Biofilm formation by bacterial pathogens is an important virulence factor. Formation of biofilm by *A. baumannii* is partly responsible for its ability to cause persistent and difficult-to-treat infections (Roca, Espinal, Vila-Farres, & Vila, 2012; Stacy, Welsh, Rather, & Blackwell, 2012). Intriguingly, we observed that *A. baumannii* ATCC 17978 formed more biofilm at 28°C than at 37°C (Figure13), which indicates that the slower growth at 28°C does not have an impact on the ability of *A. baumannii* ATCC 17978 to form biofilm. Whether the thermoregulation of biofilm formation is mediated by a factor similar to that observed in *B. pseudomallei* (Plumley et al., 2017) remains to be investigated.

We also repeated the motility assays in order to confirm our initial observations that *A. baumannii* ATCC 17978 was less motile at 28°C. At 37°C, *A. baumannii* ATCC 17978 displayed surface-associated motility and covered the entire surface of the agarose medium 18 h after incubation (Figure 14). Similar to our initial observations, it was less motile at 28°C, with levels of motility significantly different from those displayed at 37°C. This is an interesting observation, because at 28°C *A. baumannii* ATCC 17978 is less motile on agar surfaces but still forms more biofilm. Previous studies showed that, at least for some strains of *A. baumannii*, the ability to form biofilm is not dependent on the ability to display surface-associated twitching motility (Tomaras et al., 2003), which may be the case for *A. baumannii* ATCC 17978 as well.

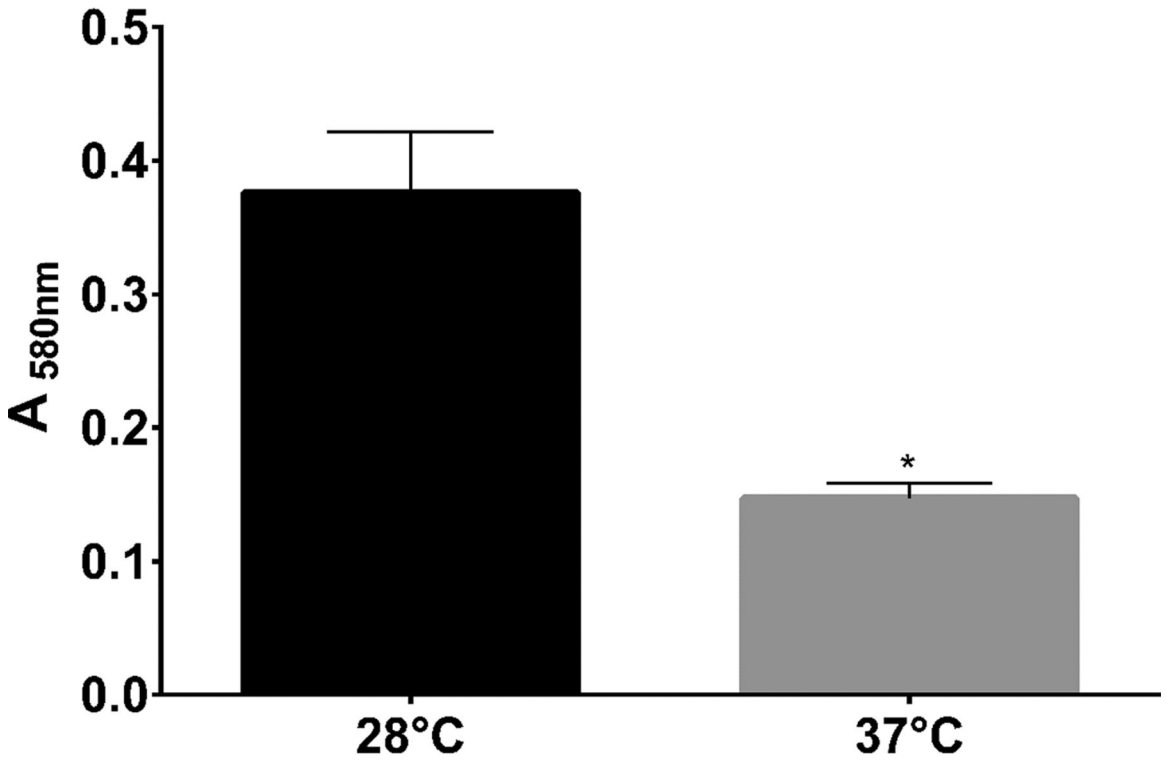

Figure 13. Comparison of biofilm formation by *A. baumannii* ATCC 17978 at 28˚C and 37˚C. Biofilm formation was determined after 48 h, and biofilms were quantified by measuring the optical density at 580 nm. Biofilm formation was significantly greater at 28˚C than at 37˚C. Statistical analysis was carried out using two-way ANOVA. *, *P*=0.001

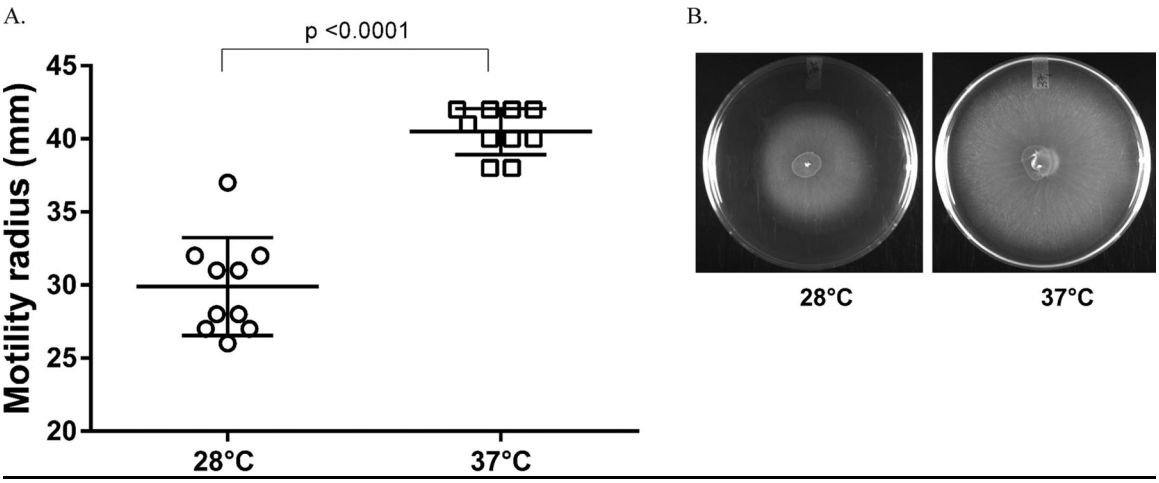

Figure 14. Comparison of twitching motility of *A. baumannii* ATCC 17978 at 28˚C and 37˚C. (A) The bacterial were able to cover the entire surface of the plate after 18 hours of incubation at 37˚C, but growth was significantly less at 28˚C than at 37˚C. Each data point represents a biological replicate. (B) The picture shows representative plates inoculated with *A. baumannii* ATCC 17978 and incubated at 28˚C and 37˚C. Statistical analysis was carried out using paired t-test.

3.2.2.3 Virulence of *A. baumannii* ATCC 17978 in *Galleria mellonella* is not affected by temperature

The virulence of *A. baumannii* ATCC 17978 in *G. mellonella*, a well-accepted infection model for this bacterium (Peleg et al., 2009), was tested at 28°C and 37°C. The results of the virulence assays are shown in Figure 15. Data suggest that, in spite of the phenotypic differences in *A. baumannii* ATCC 17978 grown at 28°C and 37°C, there was no statistically significant difference in the virulence of *A. baumannii* ATCC 17978 in *G. mellonella* at these two temperatures.

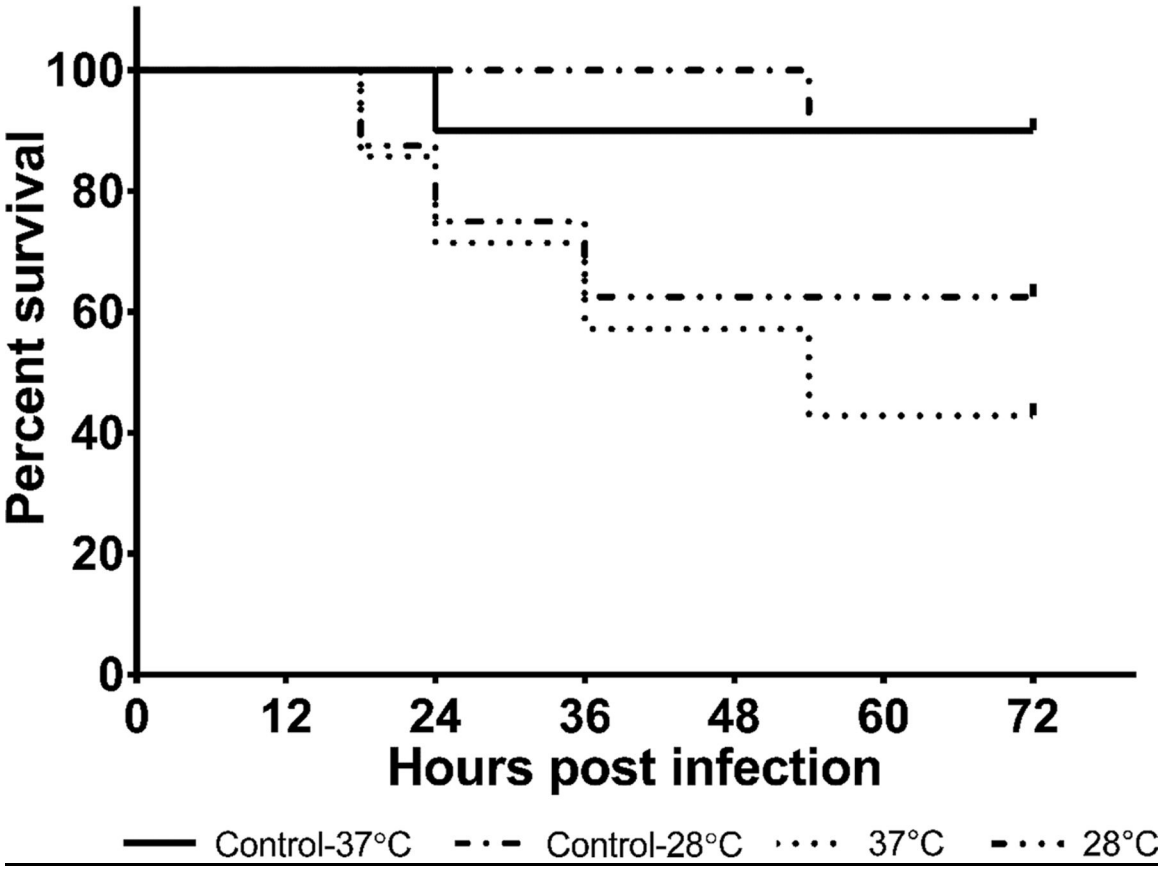

Figure 15. Survival of *Galleria mellonella* inoculated with *A. baumannii* at 28˚C and 37˚C. A 10 µL inoculum (grown overnight at 28˚C or 37˚C) containing 1 X 10^6 CFU/mL in saline was injected into the second right proleg of the worm. 10 µL of saline was injected into the worms used as controls. Injected worms were incubated at 28˚C and 37˚C, respectively, and monitored for 72 hours. The Mantel-Cox test was used for statistical analysis ($P = 0.0838$). Data shown are representative of two independent assays.

3.2.2.4 Proteomic analysis shows that expression of various proteins involved in antibiotic resistance and virulence is altered at different incubation temperatures

Proteomic analysis was used to help understand the molecular basis of phenotypic differences displayed by *A. baumannii* at different growth temperatures. Of 2,446 proteins identified (Appendix I and II), 629 proteins were differentially expressed, with 366 proteins being upregulated and 263 being downregulated at 28°C, compared to 37°C (Figure 16) (the list of proteins whose expression was altered is provided in Appendix I and II). The largest subset of proteins that could be classified whose expression was upregulated or downregulated was those involved in metabolic and enzymatic processes (Appendix I and II). Proteins involved in RNA binding, processing, and translation were found to be largely upregulated at 28°C.

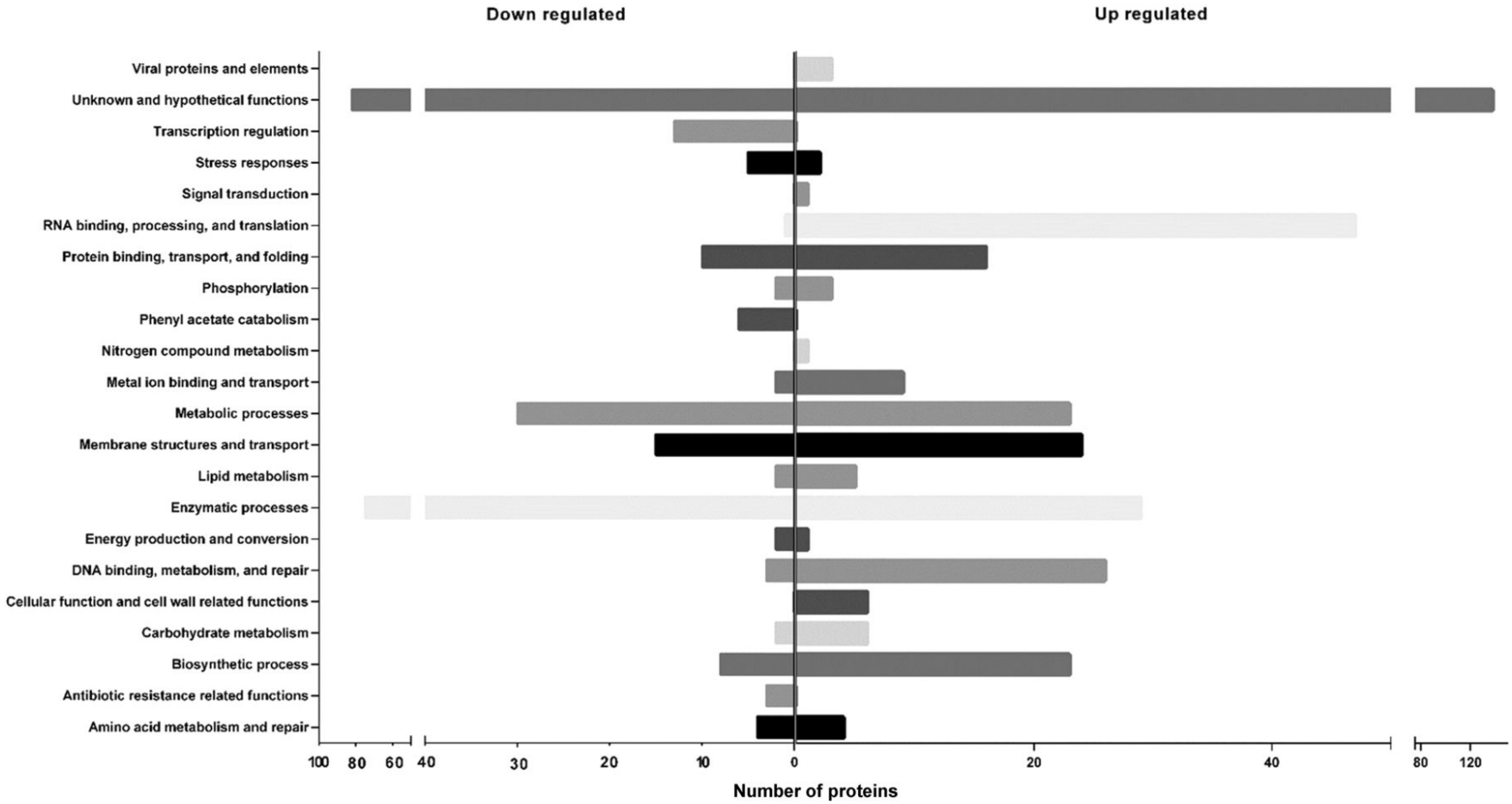

Figure 16. Clusters of Orthologous Genes (COG) analysis of proteins whose expression in *A. baumannii* ATCC 17978 is altered at 28˚C versus 37˚C. Statistical significance of the protein expression was calculated using the Benjamini-Hochberg correction method to filter proteins with $P<0.05$.

The expression of a number of membrane proteins potentially involved in antibiotic resistance was altered at 28°C, compared to 37°C (Table 5); these include proteins that are part of the resistance-nodulation-division (RND) efflux systems, such as A1S_0116, A1S_0908, AdeA, AdeK, A1S_3219, and A1S_0774. There was also differential expression of outer membrane porin proteins, such as A1S_1968 and OmpA. OmpA, which is considered the major porin in *A. baumannii* (Sugawara & Nikaido, 2012), has also been shown to be an important virulence factor that plays a role in the interaction of *A. baumannii* with eukaryotic cells (Gaddy et al., 2009).

We also observed downregulation of a β-lactamase protein (A1S_1708) at 28°C (Table 5). Expression of this protein appears to be at least partly regulated by the histone-like nucleoid-structuring (H-NS) protein, which regulates various virulence-associated genes in *A. baumannii* (Eijkelkamp et al., 2013). In our study, downregulation of A1S_1708 at 28°C may explain small but reproducible increases in the susceptibility of *A. baumannii* to imipenem at this temperature (Table 4). However, the role of A1S_1708 in the antibiotic susceptibility of *A. baumannii* needs to be studied further.

Among the proteins overexpressed at 28°C, of note were those encoded by the *csu* operon. The *csuA/BABCDE* operon was shown to be involved in pilus formation and in the early steps of biofilm formation in *A. baumannii* ATCC 19606 (Tomaras et al., 2003). We observed upregulation of CsuA/B, CsuA, CsuB, CsuC, CsuD, and CsuE (Table 5). Overexpression of the fimbrial protein A1S_1510 was also observed. A1S_1510 has been shown to play a role in biofilm formation by *A. baumannii* (Nait Chabane et al., 2014). This is consistent with our observation that *A. baumannii* ATCC 17978 forms more biofilm at 28°C than at 37°C, perhaps due to upregulation of the *csu* operon at 28°C.

Interestingly, we also observed that proteins involved in phenyl acetate catabolism were

downregulated at 28°C. The genes that encode these proteins are found in the *paa* operon, and PaaC, PaaJ, PaaK, PaaN, and PaaX were detected in our data set. Paa proteins were recently shown to be important for the virulence of *A. baumannii* in a zebra fish infection model (Bhuiyan et al., 2016). However, we did not observe any statistically significant differences in the virulence in *G. mellonella* of *A. baumannii* ATCC 17978 grown at two different temperatures. Therefore, the impact of altered expression of the *paa* operon under different conditions on the virulence of *A. baumannii* ATCC 17978 in *G. mellonella* needs to be investigated further.

Another intriguing observation in this study was the upregulation at 28°C of numerous iron uptake proteins, namely, A1S_0092, A1S_1631, A1S_1921, A1S_2080, A1S_2081, A1S_2570, and A1S_3324. Our data suggest that growth at 28°C may mimic the response of *A. baumannii* to iron-limiting conditions, which may be due to lower iron transport efficiency at this temperature. Iron is one of the most important micronutrients that plays a key role in the success of a pathogen in a host (Carpenter, Whitmire, & Merrell, 2009); it serves as an important signal for the expression of various genes, including those involved in virulence, in pathogenic bacteria such as *A. baumannii* (Nwugo, Gaddy, Zimbler, & Actis, 2011). Therefore, it is possible that temperature serves as an additional signal for the expression of iron uptake proteins in *A. baumannii*.

Table 5. Select proteins whose expression was altered at 28˚C versus 37˚C

Locus tag	Protein annotation	Log_2 fold change	Potential Involvement in
A1S_0116	RND superfamily-like exporter	3.95	Antibiotic susceptibility
A1S_0908	RND family multidrug resistance secretion protein	2.09	Antibiotic susceptibility
A1S_1752	AdeA membrane fusion protein	1.37	Antibiotic susceptibility
A1S_3219	Putative RND family drug transporter	0.58	Antibiotic susceptibility
A1S_0774	Putative RND family drug transporter	-0.7	Antibiotic susceptibility
A1S_2737	AdeK	0.67	Antibiotic susceptibility
A1S_1708	beta-lactamase-like protein	-0.99	Antibiotic susceptibility
A1S_1968	putative outer membrane protein (OmpH)	0.79	Virulence Factors
A1S_1193	OmpA/MotB	-1.27	Virulence Factors
A1S_1343	PaaC	-3.33	Virulence Factors
A1S_1345	PaaK	-3.09	Virulence Factors
A1S_1347	PaaX	-1.04	Virulence Factors
A1S_2213	CsuE	1.6	Biofilm formation
A1S_2214	CsuD	1.33	Biofilm formation
A1S_2215	CsuC	2.07	Biofilm formation
A1S_2216	CsuB	1.69	Biofilm formation
A1S_2217	CsuA	0.73	Biofilm formation
A1S_2218	CsuA/B	1.5	Biofilm formation
A1S_1510	Fimbrial protein	1.16	Biofilm formation
A1S_0092	Putative ferric siderophore receptor protein	0.64	Iron uptake
A1S_1631	Iron-binding protein	0.82	Iron uptake
A1S_1921	Ferrichrome-iron receptor	0.95	Iron uptake
A1S_2080	Putative siderophore receptor	0.82	Iron uptake
A1S_2081	TonB-dependent siderophore receptor	0.79	Iron uptake
A1S_2570	Putative siderophore biosynthesis protein; Putative acetyltransferase	0.84	Iron uptake
A1S_3324	Putative ferric siderophore receptor protein	0.61	Iron uptake
A1S_2664	Chaperone Hsp60	-0.97	Stress response
A1S_2665	Chaperone Hsp10	-1.05	Stress response

In order to determine whether the altered protein expression at 28°C versus 37°C is also displayed by clinical isolates of *A. baumannii*, we tested the expression of *ompA*, *csuA*, *A1S_0116* (an RND transporter-encoding gene), *A1S_1708* (a β-lactamase), *paaK*, and *A1S_0092* (a putative ferrichrome receptor-encoding gene) in clinical isolates of *A. baumannii* using quantitative real-time reverse transcription-PCR (qRT-PCR). These genes encode a subset of proteins whose expression was altered in our proteomic analysis (Table 5). We tested gene expression in three different clinical isolates, i.e., AB030 (P. C. Loewen et al., 2014b), AB031 (P. C. Loewen et al., 2014a), and LAC-4 (H. Y. Ou et al., 2015). These clinical isolates represent antibiotic-resistant and hypervirulent isolates of *A. baumannii*. We observed that the expression pattern of the genes at the two different temperatures in clinical isolates generally agreed with our observations in ATCC 17978 (Figure 17). For example, the expression of *paaK* and *ompA/motB* in the clinical isolates was similar to that observed for ATCC 17978. Interestingly though, we did not detect *paaK* in AB031, and further analysis using endpoint PCR and genome analysis confirmed the absence of the gene in this strain. Furthermore, we did not observe any statistically significant changes in the expression of *A1S_0092* (a putative ferrichrome receptor gene) at the two different temperatures in ATCC 17978 or the clinical isolates tested. Finally, we did not detect *A1S_0116* transcripts in any of the clinical strains. Therefore, our observations from the expression analysis of a limited subset of genes suggest that the altered expression of proteins we observed at the two different incubation temperatures is likely to be a combination of regulation at the transcription and translation levels. The data also suggest that the altered expression of proteins in response to changes in the incubation temperature is likely to be present in the clinical isolates of *A. baumannii* as well.

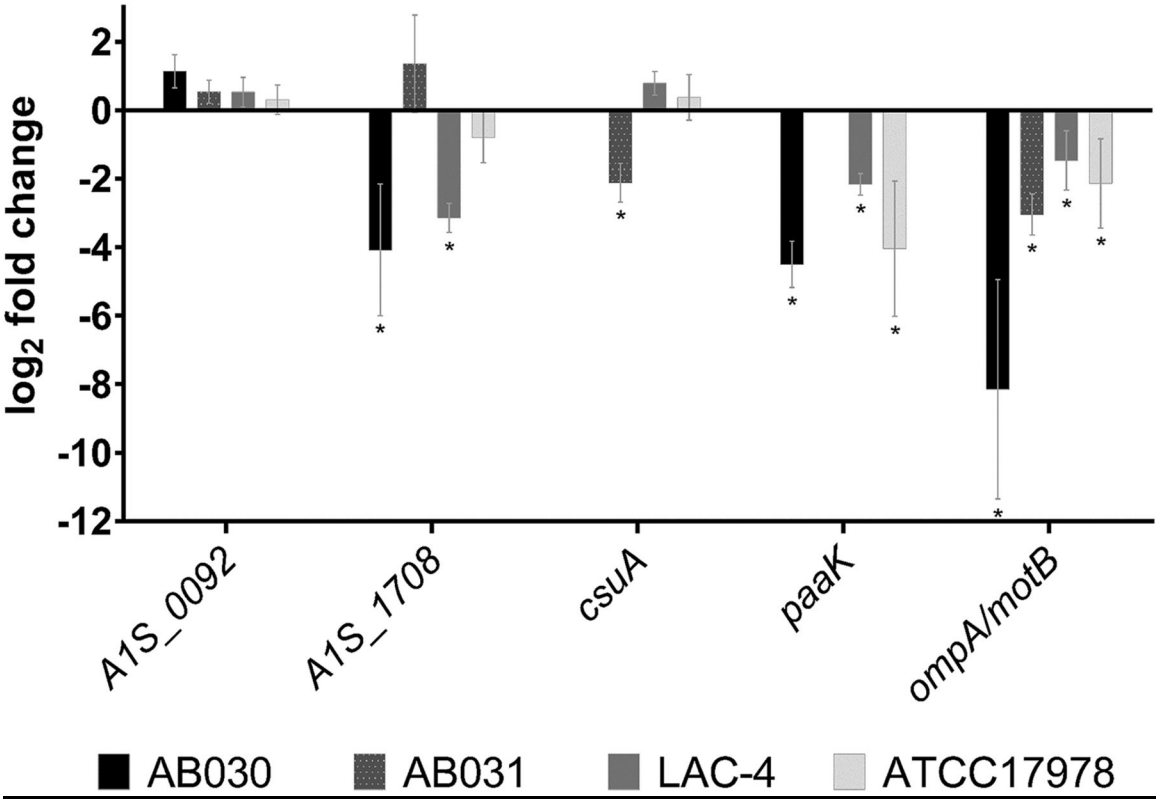

Figure 17. Expression of *A1S_0092*, *A1S_1708*, *csuA*, *paaK*, and *ompA/motB* in *A. baumannii* ATCC 17978 and the clinical isolates AB030, LAC-4, and AB031. Expression was determined using qRT-PCR and 16S rRNA gene was used as the housekeeping control. Data shown are the relative levels of expression of each gene at 28˚C versus 37˚C for the respective isolate and are representative of at least two biological replicates. The *csuA* and *paaK* genes were not detected in AB030 and AB031 respectively. The *paaK* gene was found to be absent in AB031, which was confirmed using the endpoint PCR as well as analysis of the genome sequence. *, $P<0.05$.

3.2.3 CONCLUSIONS

In conclusion, we show that traits such as antibiotic resistance, biofilm formation, and twitching motility can be thermoregulated in *A. baumannii* ATCC 17978. To our knowledge, this is the first study to report such findings. Using proteomic analysis, we identified >600 different proteins whose expression was altered in *A. baumannii* ATCC 17978 in response to the incubation temperature. We were able to establish that the expression of virulence factors such as OmpA and Paa proteins was greater at 37°C than at 28°C, which is suggestive of *A. baumannii* expressing virulence factors in response to the changes in growth temperature as it moves into the human host. We also observed changes in the expression of antibiotic resistance genes in response to the temperature changes. Our work shows that temperature can influence the virulence and antibiotic resistance of *A. baumannii*. We think that our work will lead to a better understanding of how the environment, specifically temperature, can have an impact on the antibiotic resistance and virulence of this important pathogen.

CHAPTER 4

CHARACTERIZATION OF ORPHAN RESPONSE REGULATOR A1S_2006 IN *Acinetobacter baumannii* ATCC 17978

4.1 INTRODUCTION

Acinetobacter baumannii is a Gram-negative coccobaccillus, which is a well-known opportunistic pathogen in hospital settings (Antunes et al., 2014; Peleg, Seifert, et al., 2008). During the last couple of decades, *A. baumannii* has gained considerable attention as an important hospital-acquired infections (Dijkshoorn et al., 2007; Wong et al., 2017). Due to its increasing potential to display multidrug resistance (MDR) phenotypes and virulence-associated phenotypes in clinical settings, it is classified as a "serious" level threat to public health according to the Centre of Disease Control (CDC) report in 2013. *A. baumannii* accounts for 7,300 MDR infections and 500 deaths annually in the United States alone (https://www.cdc.gov/drugresistance/pdf/ar-threats-2013-508.pdf). *A. baumannii* also implicates a considerable burden on the health care systems around the globe due to its increase in MDR strains rendering the current arsenal of antibiotics impotent (C. R. Lee et al., 2017). In addition to that, a more recent World Health Organization (WHO) report in 2016 (https://www.who.int/medicines/publications/WHO-PPL-Short_Summary_25Feb-ET_NM_WHO.pdf) classified MDR *A. baumannii* at the very top of its list of priority pathogens, which imposes a dire need of research and development of new antibiotics against (Tacconelli et al., 2018).

In addition to its MDR phenotypes, success of *A. baumannii* as a human pathogen is also a result of its ability to sense and adapt to the harsh environmental conditions present in hospital settings (Antunes, Imperi, Carattoli, & Visca, 2011; Jawad et al., 1998; Peleg et al., 2012). Two-Component Systems (TCSs), comprised of a membrane bound histidine kinase (HK) and a

cytosolic response regulator (RR) protein, in bacterial species are the major mechanism by which sensing and adaptation to dynamic environmental conditions are achieved (Alm et al., 2006). *A. baumannii* is no exception to this phenomenon and in fact, TCSs in *A. baumannii* help not only to sense and adapt to environmental changes but also helps it to modulate phenotypes relevant to antibiotic susceptibility and virulence (Cerqueira et al., 2014; Kroger et al., 2016; Marchand et al., 2004; Richmond et al., 2016; Tomaras et al., 2008). *A. baumannii* possess 20 genes/operons annotated as TCSs in the genome of the widely studied type strain, ATCC17978 and six out of the 20 TCSs are characterised for its function to date (De Silva & Kumar, 2019).

In this study, we characterise A1S_2006, an orphan RR that spans 591 nucleotides which encode for a predicted 22 kDa protein to gain insights into the regulatory networks that control the virulence and antibiotic resistance-associated traits in *A. baumannii*.

4.2 SPECIFIC EXPERIMENTAL PROCEDURES AND MODIFICATIONS

4.2.1 Creation of deletion mutants and complementation

A. baumannii ATCC 17978 was used as the type strain in this study and was grown and maintained as described in materials and methods unless otherwise mentioned. Deletion of *A1S_2006* was created using the homologous recombination method as previously described (Amin et al., 2013). An unmarked deletion of *A1S_2006* was achieved using the flp recombinase and the FRT sites to excise the Gm^R marker as previously described (K. H. Choi & Schweizer, 2005) and the strain was termed AB104. The deletion of *A1S_2006* was complemented using the pUC18T-mini-Tn*7*T-Gm (K. H. Choi et al., 2005) as described in materials and methods and introduced as a single copy into the genome of AB104 resulting in the complemented strain AB239. An empty vector control strain (AB256) was created by introducing the pUC18T-mini-

Tn*7*T-Gm plasmid without any insertions at the multiple cloning site into the genome of AB104 to be used in the experiments described.

4.2.2 A549 adhesion and invasion assay

Adhesion and invasion capabilities of the *A. baumannii* strains used in this study were determined similar assays described elsewhere (Alvarez-Fraga et al., 2016; Gaddy et al., 2009) with slight modifications. Briefly, human lung epithelial cell line A549 cells (ATCC CCL-185) (Giard et al., 1973) were propagated in tissue-culture treated T75 flasks (Sarstedt) in Dulbecco Modified Eagle Medium (DMEM) containing L-glutamine, 4.5g/L glucose, and sodium pyruvate (Corning Cellgro) supplemented with 10% heat-inactivated fetal bovine serum (FBS) (Seradigm) and 1x Penicillin-Streptomycin (Pen-Strep) antibiotic supplement (Corning) and grown at 37°C and 5% CO_2. Confluent cells were split by washing with prewarmed 1x PBS (Corning Cellgro), then trypsinized with 2mL 0.25% trypsin with 2.21mM EDTA (Corning Cellgro) for 3-4 minutes until detached then diluted 5-10x in fresh prewarmed DMEM + 10% FBS + Pen-Strep into new T75 flasks. To prepare cells for experiments, confluent monolayers were washed and trypsinized as before, but resuspension and subsequent steps omitted Pen-Strep from the DMEM + 10% FBS. Cells were stained with Trypan Blue (Gibco) prior to counting on a hemocytometer, then diluted to $1x10^5$ viable cells/mL in DMEM + 10% FBS. 1mL of this suspension was applied to each well of a 24 well tissue-culture treated plate (Costar), allowed to adhere, and grown a further 1-2 days at 37°and 5% CO_2 until confluent in the wells.

The bacterial strains were grown overnight with shaking in LB and washed twice in sterile 0.85% saline to remove residual media and standardised to a 0.5 McFarland standard using a DensiCHEK™ Plus Instrument (bioMerieux). These cell suspensions were diluted in DMEM +

10% FBS to 10^6 CFU/mL and used to infect A549 monolayers which were prewashed three times with sterile 0.85% saline with a total of 1mL in each well of the 24-well plate. The infected cells were incubated at 37˚C with 5% CO_2 for 3 hours and 24 hours for the adhesion assay and invasion assay, respectively. For adhesion assays, following the 3-hour incubation, the wells were washed three times with sterile 0.85% saline followed by addition of 1mL of sterile cold H_2O to each well to facilitate the lysis of A549 cells. The lysates were collected immediately and were serially diluted and plated on LB agar plates to count colony forming units for each strain. For the invasion assays, the media from each well was carefully removed after 24 hours and replaced with DMEM + 10% FBS supplemented with 512 μg/mL gentamicin and incubated for a further 2 hours to kill the attached bacteria on the surface of the A549 cells. After the 2-hour incubation the wells were treated similarly to as described above for the adhesion assay and the lysates were serially diluted and plated. The resulting CFU/mL counts were then normalised to the growth of each strain and plotted and statistically analysed using GraphPad Prism v6.07 (La Jolla, CA, USA).

4.2.3 BIOLOG™ phenotypic microarray

All the phenotypic microarray plates along with the inoculation fluids were purchased from Biolog™ (Biolog Inc, Hayward, CA, USA). Strains to be tested were grown on a LB agar plates overnight and isolated colonies were used to inoculate the inoculation fluid provided according to the manufacturer's instructions. The inoculums for each strain was added to individual PM3B phenotypic microarray plates as specified by the manufacturer and incubated at 37˚C for 18 hours. Absorbance at 590nm was measured using SpectraMax M2 plate reader for all plates after the incubation period and data were analysed using Microsoft Excel.

4.3 RESULTS

4.3.1 Deletion of *A1S_2006* affects surface associated motility of *A. baumannii*

A. baumannii displays surface associated twitching motility via type IV pili (Tomaras et al., 2003) that is an important virulence factor in the arsenal of *A. baumannii*. When tested for its motility phenotype, AB104 showed decreased motility as compared to the type strain ATCC 17978 after 16 hours of incubation at 37˚C. The complemented strain, AB239 showed partial complementation of the motility phenotype with almost type strain levels of surface associated motility with the empty vector control strain, AB256 showed similar levels of motility to that of the deletion strain (Figure 18). This suggested that the deletion of *A1S_2006* impacts the motility of *A. baumannii*.

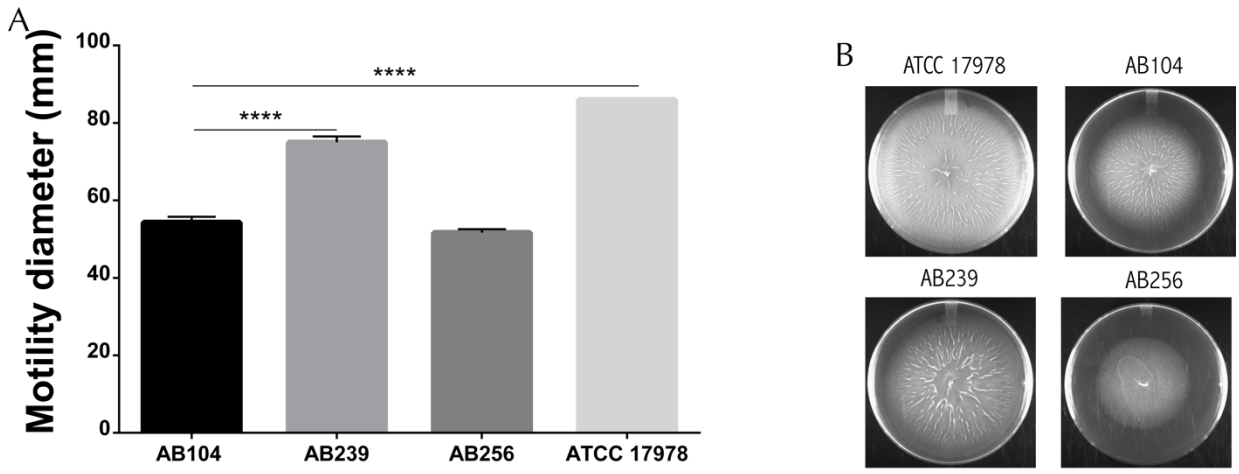

Figure 18. Comparison of surface associated motility of *A. baumannii* strains. (A) Surface associated motility of the strains as tested on 0.3% agarose after 16 hours of incubation at 37˚C and (B) photographs of representative plates. The assay was carried out in biological duplicates with three technical replicates. Average values of each strain was plotted with standard deviation and statistically analysed using one-way ANOVA with Turkey's multiple comparison test. **** denotes $P<0.0001$.

4.3.2 Deletion of *A1S_2006* results in reduced biofilm formation on abiotic surfaces

We used a crystal violet staining based method to determine the effect on biofilm forming capabilities of *A. baumannii* on abiotic surfaces. Both plastic surfaces and glass surfaces have been used previously to assay the biofilm formation by *A. baumannii* (Loehfelm, Luke, & Campagnari, 2008; Tomaras et al., 2003). On this instance we used both these materials where initially we used 96-well polystyrene plates to assess the biofilm formation of the *A. baumannii* strains where we observed that AB104 has a diminished capability to form biofilms compared to ATCC 17978 and AB239. To further confirm this, we used static bacterial cultures grown in glass test tubes to visually assess the biofilm formation which can be distinguished by a "ring of biofilm" formed at the air-liquid interface. The deletion of *A1S_2006* resulted in a visible decrease in biofilms that were formed in the air-liquid interface and this defect was restored in the complemented strain (Figure 19B). Quantification of the biofilms formed in each strain was measured using the absorbance at 580nm of the crystal violet retained by the biofilm and was then normalised relative to the growth of each strain using the absorbance at 600nm values measured after the 48-hour growth. AB104 showed a significant decrease in biofilm formation (~15-fold) as compared to the type strain and AB239 had restored biofilm formation (Figure 19A).

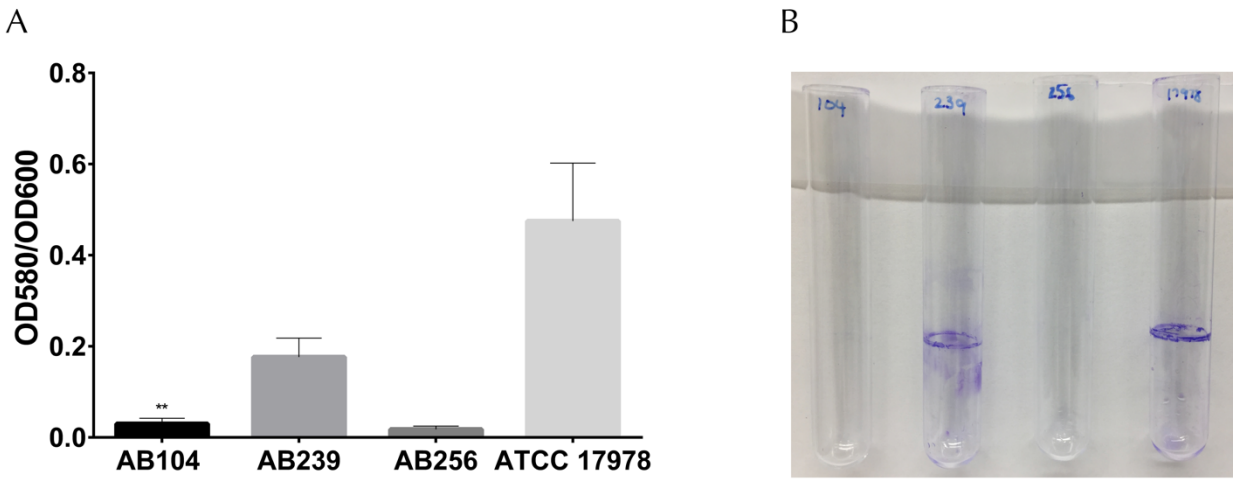

Figure 19. Comparison of biofilm forming capabilities of *A. baumannii* strains on abiotic surfaces. (A) Levels of biofilm formation on plastic surfaces after a static 48-hour incubation at 37˚C and (B) photographs of representative glass tubes used to visually determine biofilm formation capabilities on glass surfaces. The assays were carried out with three biological replicates. Average values of each strain was plotted with standard deviation and statistically analysed using one-way ANOVA with Turkey's multiple comparison test. ** denotes $P<0.05$.

4.3.3 Effect of the deletion of *A1S_2006* on virulence in a *G. mellonella* model

In line with the differences observed for other virulence traits such as motility and biofilm formation, we investigated virulence of AB104, AB239, and ATCC 17978 in *G. mellonella* model. *G. mellonella* larvae were monitored for 72 hours post infection and at the end of the 72-hour period, we observed that both the wild type and AB239 had induced 30% higher mortality of larvae as compared to AB104 (Figure 20 B). Interestingly though, the Kaplan-Meier survival curves of the strains did not indicate a statistical significance between the strains (Figure 20 A). However, the differences in the end-point survival of the infected larvae suggested that the deletion of *A1S_2006* indeed confers reduced virulence of *A. baumannii* in a *G. mellonella* model.

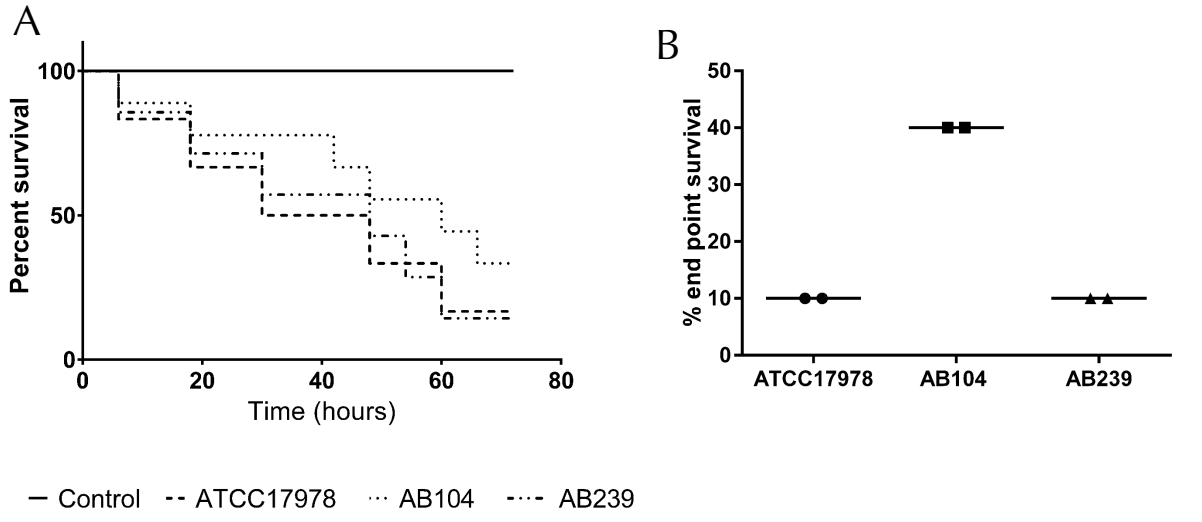

Figure 20. Survival of *G. mellonella* infected with *A. baumannii* strains. (A) Kaplan – Meier survival curves of the virulence of *A. baumannii* AB104, AB239, and ATCC 17978 in *Galleria mellonella* infection assays. (B) End – point survival of the *G. mellonella* larvae infected with the same strains after 72 hours. *G mellonella* larvae were injected into the left proleg with 10 µL of a 10^6 CFU/mL bacterial suspension in 0.85% saline and incubated at 37 °C. An equal volume of 0.85% sterile saline was injected to the control larvae group (solid line) and the viability of the infected larvae was assessed at every 6 h for a total of 72 h. GraphPad Prism v.6.07 was used for statistical analyses.

4.3.4 Deletion of *A1S_2006* results in increased attachment to A549 cells

In this study, we employed A549 human alveolar epithelial cell adhesion and invasion assay using AB104, AB239, and ATCC 17978 to determine the implications of *A1S_2006* deletion on both adhesion to and the invasion of A549 human alveolar epithelial cells. A 3-hour infection of the A549 cells using the different *A. baumannii* strains were used to assess the adhesion capabilities while a 24-hour infection of the A549 cells were used to assess the invasion capabilities of the strains tested. Growth of the *A. baumannii* strains used in this assay in the DMEM + 10% FBS media that is used to culture A549 cells was determined prior to the assay by counting the CFU/mL of each strain after 3 hours and 24 hours of growth in DMEM +10% FBS mimicking the growth conditions of the assay. We did not find any growth defects for any of the strains in DMEM +10% FBS as determined by counting the CFU/mL of each strain grown for either 3 hours or 24 hours. In contrast to the results of the biofilm formation assay on plastic surfaces, we observed a significant increase of ~4-fold in the attachment of AB104 to A549 cells during the 3-hour attachment assay compared to ATCC 17978 (Figure 21). AB239, the complemented strain, displayed attachment levels comparable to ATCC 17978 However, we did not observe a significant change in the invasion levels of the strains tested after the 24-hour incubation of the strains with A549 cells (Figure 21).

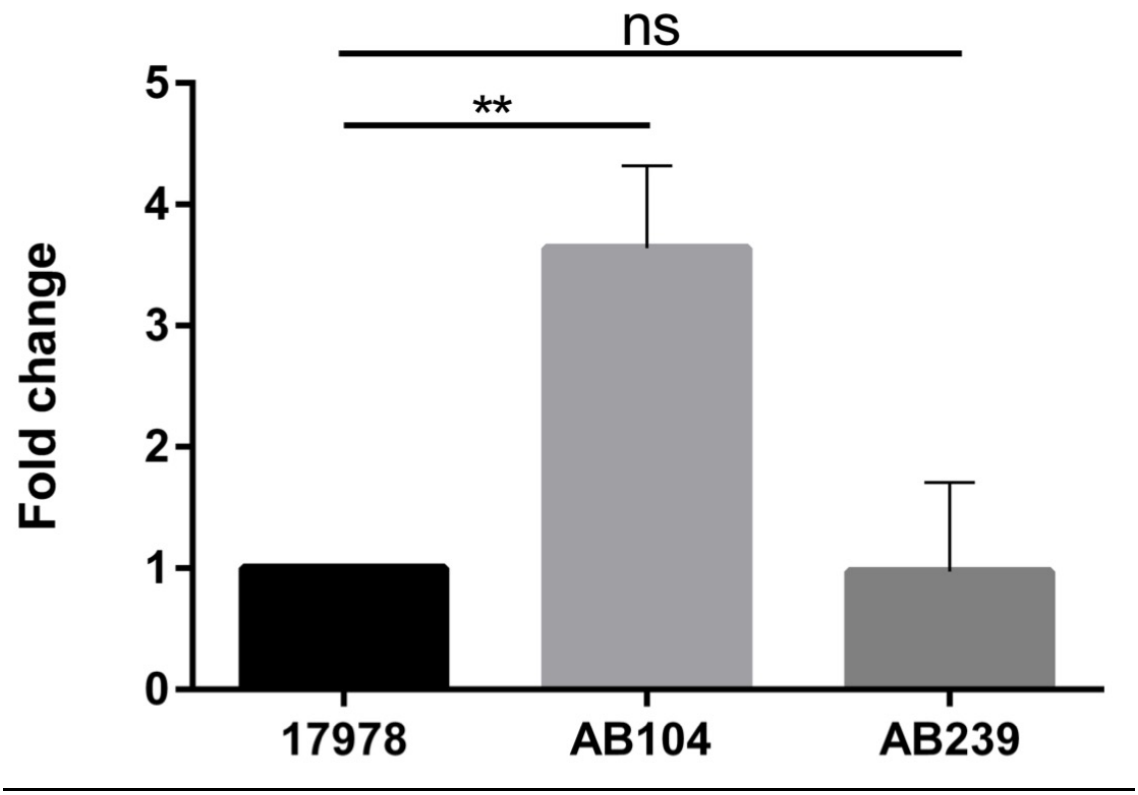

Figure 21. Attachment and adhesion of *A. baumannii* strains into A549 cells. Fold change of attachment levels of AB104, AB239, and ATCC 17978 to A549 cells after a 3-hour incubation. AB104 showed a statistically significant increase in the attachment compared to wild type and AB239. However, there was no statistically significant change in the invasion levels of any of the strains after 24 hours of incubation. ** denotes P=0.0033 as determined by Turkey's multiple comparison test.

4.3.5 *A1S_2006* deletion causes differential expression of gene groups in *A. baumannii*

We performed RNA-Seq on AB104 and ATCC 17978 to understand the changes in expression of the genes resulting from the deletion of *A1S_2006* and also to infer insights into the changes of the global transcriptomic landscape resulting from the deletion of *A1S_2006*. We found that the expression of 116 genes were upregulated and the expression of 42 genes were downregulated in AB104 compared to ATCC 17978 (Appendix III and IV). These genes were selected with an expression level cut-off of $\log_2$ 1.5 fold with a statistical significance of $P<0.05$. The selected genes were further classified into clusters of orthologous groups (COGs) using the web – based interface of EggNOG version 4.5.1 database (http://eggnogdb.embl.de/#/app/home) (Huerta-Cepas et al., 2016) to seek correlations with the phenotypes observed (Figure 22). A number of these genes were annotated as hypothetical proteins reflecting a relatively larger unknown amount of genes in *A. baumannii*. Furthermore, a large proportion of the upregulated genes could not be matched to any COG category orthologs using the EggNOG database. The genes that could not be matched with an ortholog were comparatively shorter in length. This could be due to the viral and other components which are a common feature in *A. baumannii* genomes. The raw data from the RNA-Seq study has been deposited in ArrayExpress under the accession number E-MTAB-7815.

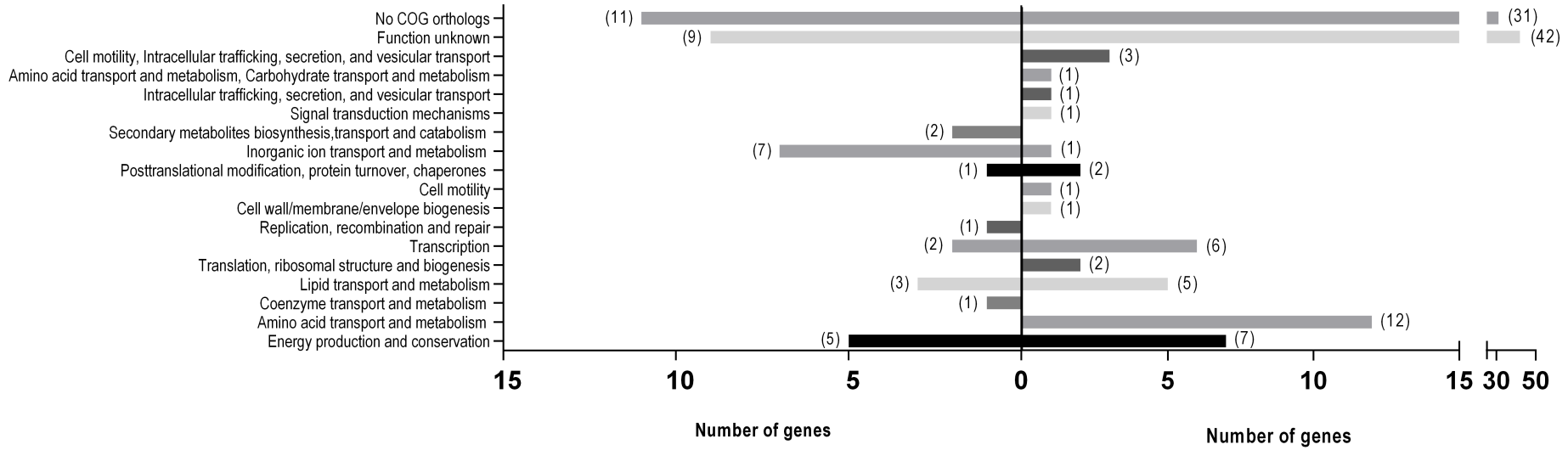

Figure 22. Clusters of Orthologous Genes (COG) analysis of genes whose expression in *A. baumannii* ATCC 17978 was altered in the absence of *A1S_2006.*

4.3.6 Expression levels of Outer Membrane Protein A (OmpA) and susceptibility to meropenem

We noticed reduced expression levels of *ompA* (*A1S_2840*) in AB104 as compared to ATCC 17978 in our RNA-Seq data albeit at a lower level than the cut-off values we used to screen for the differentially expressed genes ($\log_2$ 0.2-fold). Therefore, we performed quantitative real time PCR (qRT – PCR) to confirm the expression levels we observed with RNA-Seq data. We observed similar expression levels of *A1S_2840* with the qRT – PCR where there was reduced expression in AB104 compared to ATCC 17978 and the expression levels were partially restored in AB239 to ATCC 17978 levels (Figure 23A). To determine whether this translates into changes in susceptibility, we used E-test strips to determine the MICs of carbapenem drugs imipenem, meropenam, and doripenem. We observed small but reproducible changes in susceptibility to meropenem as shown in Figure 23B and we did not observe any changes in susceptibility to the other antibiotics.

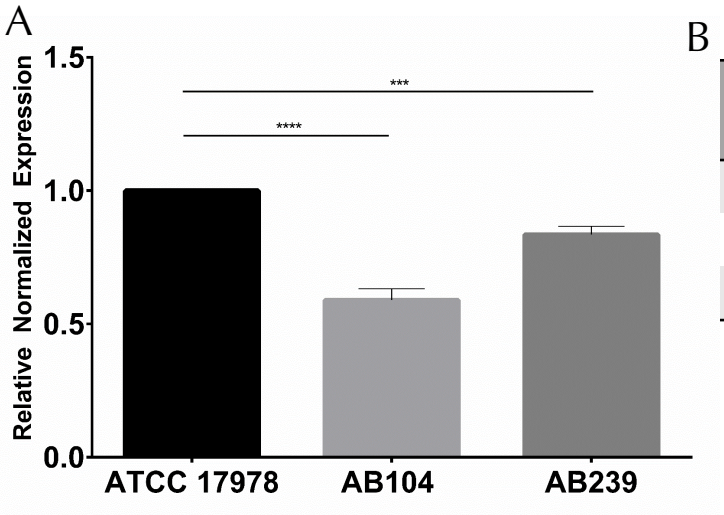

Strain	Meropenem MIC (μg/ml)
AB104	0.38
AB239	0.25
ATCC17978	0.25

Figure 23. Expression levels of *ompA* and resulting susceptibility changes to meropenem. (A) Relative normalized expression of *ompA* of AB104 and AB239. 16S rRNA gene was used as the internal control. **** denotes $P<0.0001$ and *** denotes $P=0.0003$ as determined by two-way ANOVA using Sidak's multiple comparison test. (B) Minimum Inhibitory Concentrations of meropenem as determined by E-test strips. Results are indicative of three independent biological replicates.

4.3.7 Deletion of *A1S_2006* affects utilization of certain N sources

Growth of AB104 and AB239 after 18 hours were normalised to ATCC 17978 growth levels for each of the nitrogen source on the Biolog™ phenotypic microarray plate and used as an indicator of utilization of that particular nitrogen source. We observed growth of AB104 in the presence of certain N sources to be adversely affected during the Biolog assay. The complete list of nitrogen sources with the percentage growth as compared to ATCC 17978 for AB104 and AB239 is provided in Appendix V. We observed AB104 had less than 80% of growth compared to ATCC 17978 for six nitrogen sources from the phenotypic microarray (Table 6). AB239 showed partial restoration of growth to wild type levels for all six nitrogen sources.

Table 6. Growth percentages of AB104 in different nitrogen sources relative to ATCC 17978. The numbers correspond to the A_{590nm} values obtained after an 18-hour incubation period at 37˚C in a Biolog™ phenotypic microarray PM3B plate with different nitrogen sources. Percentage of growth was obtained by normalising the values for AB104 with ATCC 17978 values. The values for AB239 shows partial complementation of the growth defect in each of the nitrogen sources.

Nitrogen Source	ATCC 17978	AB104	AB239	% of growth of AB104 relative to ATCC 17978	% of growth of AB239 relative to ATCC 17978
N-Acetyl-L-Glutamic Acid	1.5261	1.1022	1.4560	72.22%	95.40%
D-Serine	1.5538	1.1451	1.3318	73.69%	85.71%
L-Histidine	1.6835	1.2480	1.4864	74.13%	88.29%
D-Aspartic Acid	1.2553	0.9519	1.3637	75.83%	108.63%
L-Isoleucine	1.3155	1.0211	1.3275	77.62%	100.91%
L-Arginine	1.3511	1.0503	1.3547	77.73%	100.26%

4.4 DISCUSSION

The fact that *A1S_2006* is organised as an orphan RR in the genome of *A. baumannii* ATCC 17978 with a cognate HK absent directly up or downstream is unique and defies the conventional TCSs architecture (Casino et al., 2009; Laub & Goulian, 2007) (Casino et al., 2009). However, the presence of orphan response regulators has been reported before and owing to the phosphorylation capabilities of RRs by non-cognate HKs, the orphan RRs usually have their HK partners located elsewhere in the genome and possibly share the signal specificity with other RRs (Desai & Kenney, 2017).

In-silico analysis of the amino acid sequence of A1S_2006 revealed the conserved aspartate residue required for the phosphorylation of a RR at amino acid position 55. Also, when we carried out the conserved domain analysis of A1S_2006 using ScanProsite online tool, we were able to retrieve a positive hit for an ANTAR (AmiR and NasR transcription antitermination regulators) domain spanning amino acids 122 to 183. A1S_2006 was the only RR regulator annotated in the genome of *A. baumannii* ATCC 17978 to possess an ANTAR domain as its effector domain (De Silva & Kumar, 2019). Proteins with ANTAR domain have previously been shown to be involved in transcription antitermination (Shu & Zhulin, 2002). For example, AmiR of *P. aeruginosa*, prevents the formation of the termination stem-loop structure and functions as a transcription antiterminator of the amidase operon (Wilson, Wachira, Norman, Pearl, & Drew, 1996) It is characteristic for the ANTAR domain to be located C-terminally to a signalling/sensing domain (Boudes et al., 2012; Ramesh et al., 2012; Stewart & van Tilbeurgh, 2012). However, when we performed *in-silico* protein folding of A1S_2006 using the Phyre2 server (Kelley, Mezulis, Yates, Wass, & Sternberg, 2015), we retrieved a 27% sequence identity with a 100% confidence to CheY-like superfamily of proteins. Therefore, the actual effector

domain of A1S_2006 remains ambiguous and warrants both structural as well as phenotypic studies.

Here we have shown that a response regulator, A1S_2006 is involved in regulating a number of clinically relevant phenotypes of *A. baumannii*. We used a deletion mutant of *A1S_2006* (AB104) and the chromosomally complemented strain of AB104 with *A1S_2006* (AB239) to assess the phenotypic variations arising from the loss of *A1S_2006* to unravel the regulatory mechanisms that A1S_2006 is potentially involved in.

Surface associated motility and biofilm formation of *A. baumannii* on abiotic surfaces has been previously shown to be dependent on the pili formation (Tomaras et al., 2003). The *csu* operon which consists of *csuE*, *csuD*, *csuC*, *csuB*, *csuA*, and *csuA/B* genes is primiarily responsible for the pili formation of *A. baumannii*. In our RNA-Seq data, we observed that the *csu* operon was indeed downregulated. Specifically, *csuE*, *csuD*, *csuC*, and *csuA/B* were downregulated by $\log_2$ 1.1, 0.3, 0, and 0.3 folds respectively while *csuA* showed a slight upregulation of $\log_2$ 0.1. However, we did not detect any transcripts of *csuB* in AB104, which led us to believe that the whole operon is affected by the deletion of *A1S_2006*. This is evident on our results obtained for surface associated motility and biofilm formation assays where AB104 was less motile and formed less biofilm compared to ATCC 17978. While there may be other factors affecting the phenotypes relating to biofilm formation and surface associated motility, the downregulation of the *csu* operon as a result of the deletion of *A1S_2006* suggests that A1S_2006 is involved in modulating these phenotypes in *A. baumannii*.

Even though we observed that the deletion of *A1S_2006* causes *A. baumannii* to form less biofilms on plastic or glass surfaces suggesting the attachment to abiotic surfaces was adversely affected, the A549 adhesion assay showed that AB104 had a significantly increased capability of

attaching onto A549 human alveolar epithelial cells. This can be independent of influence of *csu* operon as it has been previously suggested that attachment of *A. baumannii* to biotic surfaces are independent of CsuA/BABCDE-mediated pili (Gaddy et al., 2009). However, an involvement of a separate gene, *A1S_2091* was recently associated with having a role in attachment of *A. baumannii* to A549 cells in *A. baumannii* strain MAR002 (Alvarez-Fraga et al., 2016). According to Alvarez-Fraga *et al*., inactivation of *A1S_2091* (*LH92_11085* in *A. baumannii* MAR002) led to decreased attachment to A549 cells. Our RNA-Seq data showed a $\log_2$ 0.7-fold downregulation (*P*-value = 0.17) of *A1S_2091*, which is the homologue of *LH92_11085*. This suggests that there may be additional factors involved in the ability of *A. baumannii* to adhere to A549 cells. There have been suggestions of the involvement of small RNAs in adhesion of *A. baumannii* to A549 cells (Alvarez-Fraga et al., 2017) adding to the complexity and attesting to the multi-factorial nature of the interaction of *A. baumannii* with eukaryotic cells. Further investigations into the exact molecular mechanisms involved in adhesion of *A. baumannii* onto eukaryotic cells are warranted. The dataset obtained in our RNA-Seq study could provide a platform and could be of interest to future research providing insights into the different genes with potential involvement. Furthermore, we were not able to detect significant alterations in the invasion capability of *A. baumannii* strains into A549 human alveolar epithelial cells in our study even though there were significant differences in the adhesion assay between the strains. This could potentially be attributed to the relatively low numbers of *A. baumannii* cells that were able to adhere to the A549 cells.

Outer membrane protein A (*ompA*) of *A. baumannii*, which is a highly conserved beta-barrel porin (Smith, Mahon, Lambert, & Fagan, 2007), has been reported to play a key role in several of the virulence traits as well as antibiotic susceptibility of *A. baumannii* (Gaddy et al., 2009)

(Kwon et al., 2017). We observed a slight downregulation ($\log_2$ 0.2-fold, $P<0.05$) of *ompA*. We confirmed the downregulation of *A1S_2840* (*ompA*) using qRT-PCR. Antibiotics and other small molecules have been demonstrated to selectively permeate through OmpA of *A. baumannii* (Iyer, Moussa, Durand-Reville, Tommasi, & Miller, 2018), which results in OmpA-dependent antibiotic susceptibility. Deletion of *ompA* has been previously associated with varied levels (often less than 2-fold) of increased susceptibility to a variety of antibiotics (trimethoprim, ciprofloxacin, colistin, gentamicin, imipenem, aztreonam, ceftazidime, and nalidixic acid) with a possible interaction with efflux pump systems (Kwon et al., 2017). We observed similar changes in susceptibility to ciprofloxacin and colistin between AB104 and ATCC 17978 but not for the other antibiotics. This could potentially be due to the reduced expression of *ompA* rather than a deletion as described by Kwon *et al*. OMPs are often associated with susceptibility to carbapenem drugs (del Mar Tomas et al., 2005) (Limansky, Mussi, & Viale, 2002) and therefore, we further investigated additional carbapenem drugs doripenem and meropenem to determine their susceptibility profile between AB104 and ATCC17978. Pronounced decreased susceptibility was only observed for meropenem where we observed a less than two-fold but consistent reduction in susceptibility in AB104. While this could be due to the downregulation of *ompA* gene, further exploration into our RNA-Seq data revealed a downregulation of $\log_2$ 1.1-fold ($P<0.05$) of A1S_2538 which is annotated as outer membrane protein CarO precursor in *A. baumannii* ATCC17978. CarO OMP of *A. baumannii* has been previously characterised for its role in modulating carbapenem drug susceptibility (Mussi, Limansky, & Viale, 2005). Therefore, it is possible that the change in meropenem susceptibility in AB104 compared to ATCC17978 could be attributed to a combination of *ompA* and *carO* being downregulated as a result of *A1S_2006* deletion.

Our RNA-Seq data analysis showed 42 genes to be downregulated and 116 genes to be upregulated in the absence of *A1S_2006* (Appendix III and IV). Organising those genes into COG categories allowed us to have a broader overview of the potential involvements of A1S_2006 in the transcriptomic regulon of *A. baumannii*. Unsurprisingly, we observed that the major portion of the differentially expressed genes to be either of unknown function or there was no ortholog to be found in the COG database. This is due to the plasticity of the *A. baumannii* genome and poor characterisation and annotation of the published *A. baumannii* genomes to date. In a way, this substantiates the fact that considerable amount of research is still needed in deciphering the roles of a large number of genes in *A. baumannii* genome. However, it was interesting to see that there were more than twice as many upregulated genes than downregulated genes in the absence of *A1S_2006* albeit most of them with unknown function or with no COG ortholog. Genes involved in amino acid transportation and metabolism had the highest number of genes upregulated with 12 genes and genes involved in energy production and conservation had the second highest number of genes upregulated with 7 genes. Interestingly, there were 6 upregulated genes involved in transcription and three of them were putative transcriptional regulators belonging to TetR family (*A1S_0548*, *A1S_0625*, and *A1S_2042*) and one belonged to the acrR family (*A1S_1377*). This could potentially reflect on the regulatory networks affected by A1S_2006 and further investigation is required to decipher whether A1S_2006 plays a role in the regulatory networks controlled by these transcriptional regulators.

We also observed that a predicted operon for a taurine ABC transporter consisting of four genes (*A1S_1442-44*) to have statistically significant downregulation. *A1S_1443* that encodes for a predicted taurine ATP-binding transport system component has previously been associated with an involvement of surface-associated motility and virulence of *A. baumannii* (Perez-Varela et

al., 2017) where the deletion of *A1S_1443* abolished motility and was less virulent in a *C. elegans* model. The downregulation of this operon in AB104 could have a potential contribution to the surface-associated motility and the virulence phenotypes we observed albeit to a lesser extent than in the deletion as observed by Perez-Varela *et al*.

Genomic location of *A1S_2006* where it is neighboured by a nitrite reductase and a nitrate transport protein warranted us to examine the growth of AB104 in different nitrogen sources in comparison to the wild type strain. The phenotypic microarray assays using Biolog™ plates demonstrated that AB104 could not utilise certain nitrogen sources as effectively (Table 6). This is a preliminary finding and there needs to be further investigations as to the metabolic mechanisms associated with the utilisation of these nitrogen sources and the relationship with A1S_2006.

Taken together, our data shows the involvement of A1S_2006 in several clinically relevant phenotypes of *A. baumannii*. Given the complex nature of TCS signalling, the effects we observed for the deletion of *A1S_2006* may result from direct or indirect involvement of the orphan RR A1S_2006. While the cognate HK is still undiscovered for A1S_2006, the possibility of A1S_2006 acting together with other HK proteins are a plausible possibility. Further research into the structural and biochemical aspects of A1S_2006 will facilitate more light to be shed onto the specific regulons that A1S_2006 is involved in. However, we believe that our phenotypic data and especially our transcriptomic data will serve as an ideal platform to the said studies.

CHAPTER 5

NEXT GENERATION OF Tn*7*-BASED SINGLE COPY INSERTION ELEMENTS FOR USE IN MULTI- AND PAN-DRUG RESISTANT STRAINS OF *Acinetobacter baumannii*

This section of the chapter was published in *Applied and Environmental Microbiology*, 2019: Kaleigh Ducas-Mowchun‡, P. Malaka De Silva‡, Leandro Crisostomo, Dinesh M. Fernando, Tzu-Chiao Chao, Peter Pelka, Herbert P. Schweizer, and Ayush Kumar (2019). Next generation of Tn7-based single copy insertion elements for use in multi- and pandrug resistant strains of *Acinetobacter baumannii*. doi: 10.1128/AEM.00066-19.

‡Authors contributed equally

Note: This chapter has been modified from the original publication such that the majority of materials and methods has been described in Chapter 2

5.1 INTRODUCTION

Acinetobacter baumannii is an opportunistic, Gram-negative coccobacillus that has become a serious health concern due to an increasing incidence of multidrug resistant (MDR) hospital acquired infections (Howard, O'Donoghue, Feeney, & Sleator, 2012). Recently, the WHO listed *A. baumannii* as a global priority pathogen for which research and development of antibiotics is critically needed (http://www.who.int/mediacentre/news/releases/2017/bacteria-antibiotics-needed/en/). In order to study the resistance and virulence mechanisms of *A. baumannii,* availability of effective molecular tools for genetic manipulation in this species is necessary. However, one of the major challenges in studying *A. baumannii* in the laboratory setting is the scarcity of molecular tools available for genetic manipulation in this important pathogen (Yildirim, Thompson, Jacobs, Zurawski, & Kirkup, 2016).

Clinical isolates of *Acinetobacter* present an even greater challenge to researchers as far as genetic manipulations are concerned as these strains often display decreased susceptibility to most commonly used antibiotics. This makes such antibiotic markers impractical in genetic manipulation procedures. A promising set of molecular tools for use in MDR strains of *Acinetobacter* are mini-Tn*7* vectors, a collection of Tn*7* transposon-based plasmids, that were first used in other Gram-negative bacteria such as *Pseudomonas* spp. and *Burkholderia* spp. (K. H. Choi et al., 2006; K. H. Choi et al., 2005; K. H. Choi et al., 2008b; K. H. Choi & Schweizer, 2006b).

Mini-Tn*7* vectors can be used for a range of applications including single copy gene complementation, molecular tagging and promoter analysis (Kumar, Dalton, Cortez-Cordova, & Schweizer, 2010a). The major advantages of these vectors include the ability to offer site specific, single copy chromosomal insertion at a neutral location within the genome thus bypassing the need for continued antibiotic selection, in addition to their broad-host-range capabilities (K. H. Choi & Schweizer, 2006b; Kumar et al., 2010a). With rare exceptions (K. H. Choi & Schweizer, 2006a), chromosomal insertion of mini-Tn*7* occurs downstream of the *glmS* gene that encodes glutamine-fructose-6-phosphate aminotransferase a highly conserved essential enzyme of bacteria (J.E. Peters & N.L. Craig, 2001). Bacteria with multiple *glmS* genes contain multiple Tn*7* insertion (*att*Tn*7*) sites (K. H. Choi et al., 2006; K. H. Choi et al., 2008b). Unmarked insertions can be obtained by introduction of a site-specific excision vector that encodes a source of Flp recombinase, an enzyme that recognizes the Flp recombinase target (*FRT*) sites flanking the selectable marker in mini-Tn*7* and allows for its excision (Hoang et al., 1998; Kumar et al., 2010a).

A limitation of mini-Tn*7* vectors currently available is the lack of antibiotic resistance markers for use in MDR bacteria. Versions of mini-Tn*7* vectors shown for use thus far in *A. baumannii* utilized gentamicin, tetracycline, and trimethoprim resistance markers for selection (K. H. Choi & Schweizer, 2006b; Kumar et al., 2010a). Using these selection markers in genetic manipulations of *A. baumannii* clinical isolates is often impractical as clinical strains can be highly resistant to these antibiotics (Liu et al., 2014; Maraki, Mantadakis, Mavromanolaki, Kofteridis, & Samonis, 2016).

However, antibiotics/antimicrobials that are not widely used clinically can be utilized for selection purposes, since incidences of resistance against them are likely to be very low due to the lack of selection pressure. Zeocin (Zeo) resistance markers have recently been shown to be useful for selection purposes in MDR clinical isolates of *A. baumannii* (Lucidi et al., 2018a; Luna et al., 2017a). Similarly, apramycin (Apr) has also been shown to have promising activity against MDR *A. baumannii* strains (Kang et al., 2017). Although apramycin is used in veterinary medicine, both apramycin and zeocin are antibiotics that are not used in human clinical settings (Luna et al., 2017a; E. Paget & J. Davies, 1996), and therefore are less prone to already acquired resistance due to lack of selective pressure.

The objective of this study was to create a set of mini-Tn*7* insertion vectors and Flp-recombinase excision vectors containing apramycin (Apr^r) and zeocin (Zeo^r) resistance markers that can be used to carry out genomic manipulations in clinical isolates of *A. baumannii* displaying MDR and XDR phenotypes. The tools developed in this study include mini-Tn*7* vectors containing apramycin or zeocin selection markers that allow for both inducible and constitutive expression of target gene, as well as a pFLP2A (Apr^r) and pFLP2Z (Zeo^r) site specific excision vectors that

can be used to obtain unmarked insertions. Finally, we also created mini-Tn*7* vectors with fluorescent markers to be used in MDR *A. baumannii* isolates.

5.2 SPECIFIC EXPERIMENTAL PROCEDURES AND MODIFICATIONS.

5.2.1 Determination of *att*Tn*7* site in *A. baumannii* clinical isolates

Genome sequences of *A. baumannii* ATCC 17978 (Michael G. Smith et al., 2007), AB030 (Loewen, Alsaadi, Fernando, & Kumar, 2014b), AB031 (Loewen, Alsaadi, Fernando, & Kumar, 2014a) and LAC-4 (H.-Y. Ou et al., 2015) were used to determine the presence of *att*Tn*7* associated sequences as determined previously (Kumar et al., 2010a). Alignment was carried out using Clustal Omega Multiple Sequence Alignment Tool (https://www.ebi.ac.uk/Tools/msa/clustalo/). The aligned sequences were visualized using GeneDoc Multiple Sequence Alignment Editor & Shading Utility v 2.7.000 (Nicholas, Karl B., and Nicholas, Hugh, B. Jr., 1997, GeneDoc: a tool for editing and annotating multiple sequence alignments. Distributed by the author).

5.2.2 Construction of mini-Tn*7* vectors with Apr- and Zeo-resistance markers

Strategy for the construction of mini-Tn*7* plasmids is summarized in Figure 24. The Gm^r marker from pUC18T-mini-Tn*7*T-LAC-Gm was excised using BsrGI and SacII (New England Biolabs, ON, Canada), leaving the *FRT* sites in the plasmid backbone intact. The resulting plasmid backbone (5,374 bp fragment) was purified from agarose gel using the E.Z.N.A.® gel extraction kit (Omega Bio-tek, GA, USA) according to the manufacturer's protocol. The 998 bp *aac(3)-IV* (Apr^r) and 569 bp *ble* (Zeo^r) containing fragments were PCR amplified from pFAM1 and pFZE1 plasmids (primer sequences are provided in Table 2), respectively; and purified from agarose gel using the E.Z.N.A.® gel extraction kit (Omega Bio-tek). PCR products were digested with BsrGI

and SacII (New England Biolabs) and the fragments ligated into the mini-Tn*7* plasmid backbone digested with the same enzymes described above. The ligated plasmids were transformed into *E. coli* DH5α and colonies were selected on LB + 30 μg/mL Apr (Apr^{30}) for pUC18T-mini-Tn*7*T-LAC-Apr transformants or LB + 25 μg/mL Zeo (Zeo^{25}) for pUC18T-mini-Tn*7*T-LAC-Zeo transformants. Construction of pUC18T-mini-Tn*7*T-LAC-Apr and pUC18T-mini-Tn*7*T-LAC-Zeo was initially confirmed by colony PCR as well as restriction digestion. Further confirmation was carried out by sequencing both plasmids by Illumina Hi-Seq next generation sequencing (MGH CCIB DNA Core Facility, Cambridge, MA, USA).

For construction of pUC18T-mini-Tn*7*T plasmids with Apr^r- and Zeo^r-resistance markers, the Apr^r and Zeo^r genes (*aac(3)-IV* and *ble*, respectively) were obtained using the restriction enzymes BsrGI and SacII, from pUC18T-mini-Tn*7*T-LAC-Apr and pUC18T-mini-Tn*7*T-LAC-Zeo, respectively. The resistance genes were extracted from agarose gel using the E.Z.N.A.® gel extraction kit (Omega Bio-tek) and ligated to pUC18T-mini-Tn*7*-Gm digested with BsrGI and SacII [to remove *aacC*1 (Gm^r-marker)]. The ligated plasmids were transformed into *E. coli* DH5α and colonies were selected on LB + Apr^{30} for pUC18T-mini Tn*7*T-Apr transformants or LB + Zeo^{25} for pUC18T-mini Tn*7*T-Zeo transformants. Both pUC18T-mini Tn7T-Apr and pUC18T-mini Tn7T-Zeo were confirmed using restriction digestion.

All plasmid maps were created using SnapGene® software (from GSL Biotech; available at snapgene.com)

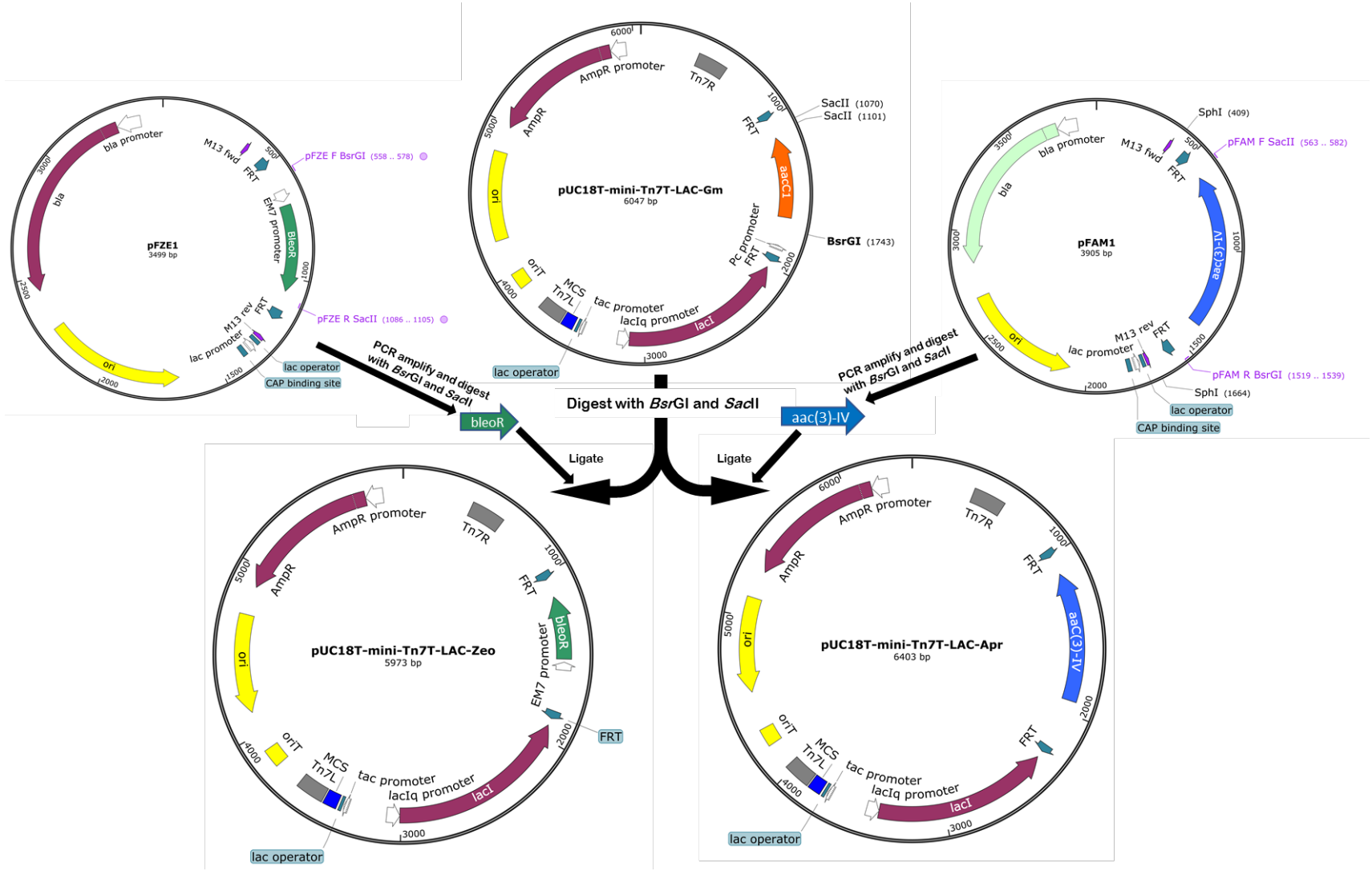

Figure 24. Overview of the strategy in replacing the Gm^R marker with Apr^R and Zeo^R markers.

5.2.3 construction of pFLP2A and pFLP2Z

Plasmid pFLP2^{ab} was created by cloning the *Acinetobacter* compatible origin of replication from the plasmid pWH1266 (Hunger et al., 1990) into pFLP2 plasmid (K. H. Choi et al., 2005). pFLP2A and pFLPZ plasmids were created by cloning *aac(3)-IV* (Apr^r) and *ble* (Zeo^r) genes into pFLP2^{ab}. Briefly, pFLP2^{ab} was extracted from *E. coli* DH5α using the EZ-10 Spin Column kit (Biobasic) and *bla*-gene excised using AhdI and XmnI (New England Biolabs). *aac(3)-IV* (Apr^r) and *ble* (Zeo^r) fragments were PCR amplified with Q5 DNA polymerase (New England Biolabs) using pFAM1 and pFZE1 as templates, respectively. The PCR products were cloned into pFLP2^{ab} plasmid backbone (10,041 bp) using T4 DNA ligase (Thermo Scientific). Transformants were selected on LB+Apr^{30} or LB+Zeo^{25}, respectively. The resulting pFLP2A and pFLP2Z plasmids were confirmed by restriction digestion.

5.2.4 optimizing GFP for expression in *A. baumannii*

Nucleotide sequence for the codon-optimized sfGFP for use in *Acinetobacter sp.* was obtained from Dr. Marek Basler (The Center for Molecular Life Sciences, University of Basel). This sequence was used to construct constitutively expressed synthetic *sfGFP* gene. Briefly, the nucleotide sequence of the *tac*-promoter (P_{tac}) along with a 47 bp downstream region from the pUC18T-mini-Tn*7*T-Gm-LAC vector was fused upstream of the *sfGFP* gene to create the synthetic gene. Restriction enzyme recognition sites for KpnI, NotI, and HindIII were introduced immediately upstream of P_{tac}, immediately upstream of the sfGFP start codon, and immediately downstream of the sfGFP stop codon, respectively. The synthetic construct was cloned into the pUC57 plasmid using the commercial gene synthesis service offered by BioBasic Inc. The synthetic *sfGFP* was excised from pUC57 by restriction-digestion using KpnI and HindIII. The

gene was gel purified and ligated into the pUC18T-mini-Tn*7*T-Apr vector digested with the same enzymes to be used in further experiments.

5.2.5 Construction of pUC18T-mini-Tn*7*T-Apr vectors containing fluorescent genes sfGFP, mRuby, mCherry, and mTurquoise

The fluorescent genes along with their native promoters were excised from their parent plasmids (Table 1) using HindIII and KpnI (New England Biolabs) and, ligated to pUC18T-mini-Tn*7*T-Apr digested with the same enzymes before transformation into *E. coli* DH5α. Colonies were selected on LB + Apr^{30}. The constructs were confirmed *via* restriction digestion.

5.2.6 Insertion of mini-Tn*7* vectors into *A. baumannii* strains

Delivery of mini-Tn*7* vectors into *A. baumannii* was carried out either via electroporation (K. H. Choi & Schweizer, 2006b) or four-parental mating (Kumar et al., 2010a) methods. For electroporation, cells were incubated in 4 mL LB broth culture overnight at 37˚C, aliquoted into microcentrifuge tubes and centrifuged at 13,000 xg for 2 minutes. The cell pellet was washed three-times with sterile ice-cold water. The washed pellets were pooled in 100 µL cold distilled water, and incubated on ice for 15 min with 100 ng each of mini-Tn*7* and pTNS2 helper plasmids. pTNS2 plasmid (K. H. Choi et al., 2005) provides the TnsABC+D *in-trans* in order to facilitate the high frequency integration of the mini-Tn*7* vector into *att*Tn*7*. The plasmid is non-replicative in *A. baumannii* and is spontaneously lost by cells. Following incubation on ice, cells were electroporated using the Eppendorf Electroporator 2510 at the following settings: 25 µF, 200 Ω, and 2.0 kV. One mL of SOC broth (BioBasic) was added immediately to the cell suspension. Cells were recovered for 1 hour at 37 ˚C with shaking (250 rpm). Recovered cells were plated on LB + Apr^{100} or LB + Zeo^{100} plates and resulting colonies screened for the mini-Tn*7* insert by colony PCR as described below.

Occasionally depending on plasmid/strain combinations, a four-parental conjugation method, as described previously (Kumar et al., 2010a), was used with minor modifications. Briefly, 100 µL each of overnight (37 ˚C) cultures of *E. coli* DH5α/mini-Tn*7* donor strain, the respective *A. baumannii* recipient strain, *E. coli* DH5α/pTNS2 and *E. coli* HB101/pRK2013 helper strains were added to 600 µL LB broth and centrifuged at 13,000 xg for 2 minutes. The cells were washed three times using 1 mL LB broth by centrifuging at 13,000 xg for 2 minutes. The pellet was resuspended in 10 µL LB broth and spotted onto a 2 x 2 cm sterile nitrocellulose filter paper placed on a pre-warmed (37˚C) LB agar plate. Following incubation at 30 ˚C for 24 h, the cells were washed off the nitrocellulose filter paper with 0.85% sterile saline and plated on Simmons citrate agar (Sigma–Aldrich, St. Louis, MO, USA) supplemented with Apr^{100} or Zeo^{100}. Colonies from the Simmons citrate plates were patched onto LB agar supplemented with Apr^{100} or Zeo^{100} and screened for the mini-Tn*7* insert by colony PCR as described below.

Colonies from LB + Apr^{100} or LB + Zeo^{100} plates were resuspended in 20 µL sterile water and incubated for 10 minutes at 100˚C to lyse cells. One µL of cell lysate was used as the template in each PCR reaction. PCR was set up using *Taq* DNA polymerase (Froggabio), ABglmS_F_N and Tn7R primers (Table 2), and the following cycle conditions: 94˚C denaturing for 30 seconds, 48˚C annealing for 30 seconds, 72˚C extension for 30 seconds. Successful insertion produced a PCR product of 368 bp (Figure 25).

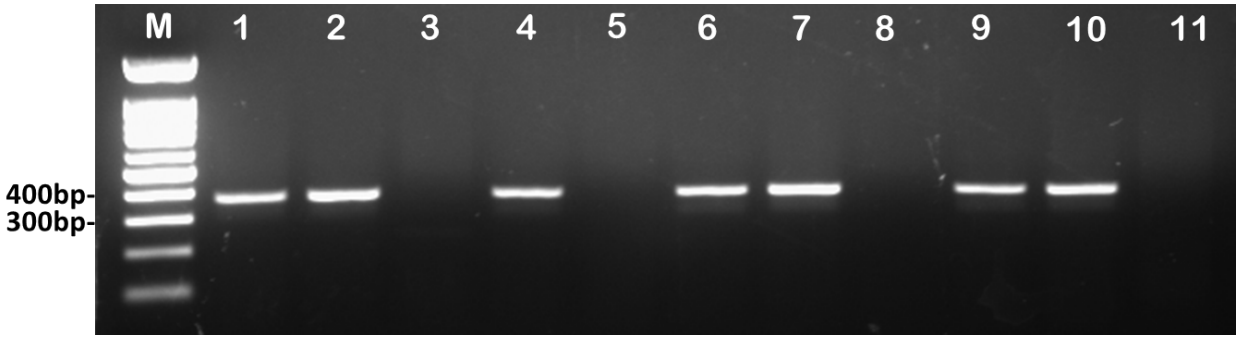

Figure 25. Confirmation of insertion of the mini-Tn*7* vectors into the genomes of *A. baumannii* strains. The mini-Tn*7*T-Apr-LAC and mini-Tn*7*T-Zeo-LAC genomic insertions in *A. baumannii* strains were confirmed using ABglmS_F_New and Tn7R primers gives expected 368 bp band. M: 100 bp molecular weight marker (New England Biolabs). Lane 1, *A. baumannii* ATCC17978::mini-Tn*7*T- Apr-LAC, Lane 2, *A. baumannii* ATCC17978::mini-Tn*7*T-Zeo-LAC, respectively; Lane 3, negative control for *A. baumannii* ATCC17978; Lane 4, *A. baumannii* AB030::mini-Tn*7*T-Apr -LAC; Lane 5, negative control for *A. baumannii* AB030; Lane 6, *A. baumannii* AB031::mini-Tn*7*T-Apr-LAC; Lane 7, *A. baumannii* AB031:: mini-Tn*7*T-Zeo-LAC; Lane 8, negative control for *A. baumannii* AB031; Lane 9, *A. baumannii* LAC-4::mini-Tn*7*T-Apr-LAC; Lane 10, *A. baumannii* LAC-4::mini-Tn*7*T-Zeo-LAC; Lane 11, negative control for *A. baumannii* LAC-4.

5.2.7 Removal of Apr^r/Zeo^r markers from mini-Tn*7* insertions in *A. baumannii*

The removal of *aac(3)-IV* (Apr^r-marker) from miniTn*7*T-Apr-LAC or *ble* (Zeo^r-marker) from mini-Tn*7*T-Zeo-LAC genomic insertions in *A. baumannii* strains was achieved using pFLP2Z or pFLP2A excision vectors, respectively. Briefly, for the removal of resistance marker, 100 ng of pFLP2Z or pFLP2A plasmid DNA was used for electroporation. After recovery following electroporation, cells were plated either on LB agar supplemented with Apr^{100} (for pFLP2A) or Zeo^{100} (for pFLP2Z) and incubated overnight at 37˚C. Colonies from these plates were cross patched onto LB + Zeo^{100} and LB + Apr^{100} plates. Colonies that were apramycin-susceptible and zeocin-resistant (indicating loss of the Apr^r marker from the genome) or Zeo-susceptible and Apr-resistant (indicating loss of the Zeo^r marker from the genome) were confirmed by colony PCR for the loss of respective resistance gene. The pFLP2Z or pFLP2A plasmids were cured by streaking cells on LB agar supplemented with 10% sucrose and incubating overnight at 37˚C. Loss of pFLP2Z or pFLP2A was confirmed by cross patching onto LB agar and LB agar supplemented with appropriate antibiotic (Zeo or Apr), followed by PCR using the primers for Zeo^r or Apr^r-resistance genes (Table 2) to confirm the loss of the resistance gene (Figures 26a, b, and c).

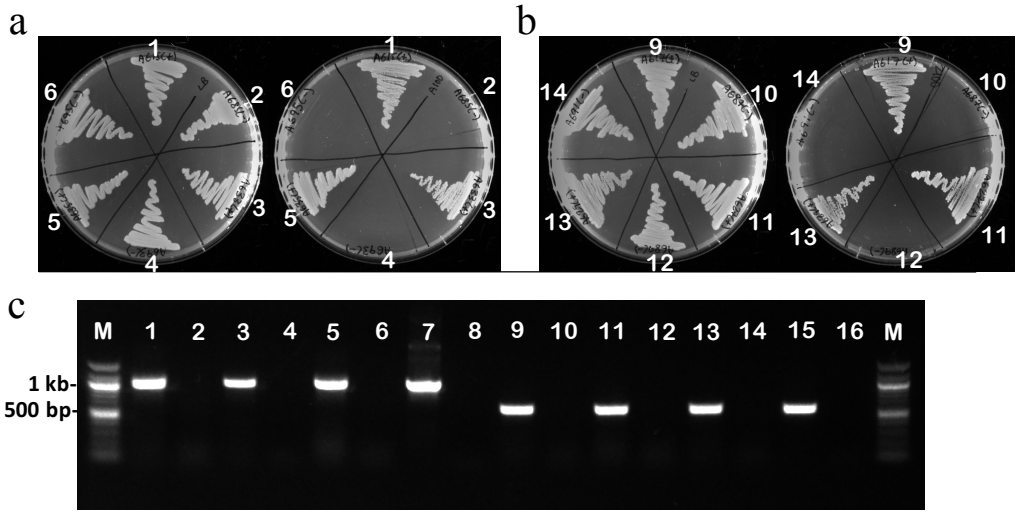

Figure 26. Removal of apramycin- or zeocin-resistance markers from *A. baumannii* using pFLP2A. (**a**) Photographs of the LB agar plate (left) and the LB agar plate supplemented with 100 µg/mL of apramycin (right) to screen for the loss of Apr^r-resistance gene by using pFLP2Z encoding Flp recombinase. Absence of growth on LB + Apr medium confirms the loss of *aac(3)-IV* (Apr^r-marker). (**b**) Photographs of the LB agar plate (left) and the LB agar plate supplemented with 100 µg/mL of zeocin (right) to screen for the loss of Zeo^r-resistance gene. Absence of growth LB + Zeo medium confirms the loss of *ble* (Zeo^r-marker). The loss of the relevant resistance markers was further confirmed with PCR as shown in (**c**) where lanes 1,3, and 5 show the 998 bp band corresponding to the *aac(3)-IV* gene in ATCC17978, LAC-4, and AB031 respectively and lanes 2,4, and 6 depict the loss of the said band in the pFLP2Z treated ATCC17978, LAC-4, and AB031 strains. Lane 7 is the positive control for the 998 bp *aac(3)-IV* band while lane 8 is the negative control. Lanes 9, 11, and 13 show the 569 bp band corresponding to the *ble* gene in ATCC17978, LAC-4, and AB031 respectively and lanes 10, 12, and 14 depict the loss of the said band in the pFLP2A treated ATCC17978, LAC-4, and AB031 strains. Lane 15 is the positive control for the 569 bp *ble* band while lane 16 is the negative control. Lanes marked with M show the 100 bp molecular weight marker.

5.2.8 Fluorescent image acquisition

Image acquisition was conducted using the ImageXpress Micro 4 High-Content Imaging System from Molecular Devices. Bacterial cultures for image acquisition were grown in LB broth overnight and 10 µL of the overnight culture was placed on a clean glass slide and spread using a coverslip. The sample was air-dried and heat fixed after which the coverslip was placed on the slide before imaging. Images were taken using the 40X super Plan Fluor ELWD objective and sCMOS camera. Images of fluorescence tagged proteins were mTurquoise, eGFP, mCherry and Ruby Red. The following filter cubes were used to visualize the cells: TL10 (Transmitted light), DAPI (excitation: 377/50 nm and emission: 447/60 nm, for mTurquoise), FITC (excitation: 424/27 nm and emission: 520/35 nm for eGFP), TEXAS RED (excitation: 562/40 nm and emission: 624/40 nm, for mCherry and Ruby Red). The software used to analyze images was MetaXpress version 6.2.3.733 from Molecular Devices (San Jose, CA, USA).

5.3 RESULTS AND DISCUSSION

Genetic manipulations in bacteria require the use of selection markers. Frequently, selection markers confer resistance to antibiotics that are or have been used in clinical settings. This presents a challenge for organisms that display reduced susceptibility to these antibiotics. *A. baumannii* is one such organism. Clinical isolates of *A. baumannii* display resistance to majority of antibiotics, making treatment of infections a challenge. Thus, there is an urgent need to understand the molecular mechanisms of antibiotic resistance of *A. baumannii*. These efforts frequently require genetic manipulations in clinical isolates of *A. baumannii*, but paradoxically it is the antibiotic resistance of clinical isolates that hinders the molecular characterization of antibiotic resistance mechanisms in *A. baumannii*. One solution to this problem is the use of

selection markers that confer resistance to antibiotics that are not used clinically. In this work, we constructed mini-Tn*7*-based vectors containing Zeo or Apr resistance markers and demonstrated their application in multi- and pan-drug resistant isolates of *A. baumannii*. Zeocin is a glycopeptide antibiotic that causes cell death by intercalating into DNA and causing its cleavage (Utashima, Yamashita, Arima, & Masaki, 2017). Apramycin is an aminoglycoside that inhibits translation by binding the 30S rRNA (E Paget & J Davies, 1996). Due to its widespread toxicity, zeocin is not used therapeutically in humans (Utashima et al., 2017). Apramycin, on the other hand, has been used widely in animals but not as an antibiotic in humans (E Paget & J Davies, 1996).

In this study, three different clinical isolates of *A. baumannii* were used: AB030, AB031, and LAC-4. Both LAC-4 and AB030 are resistant to gentamicin, while AB031 is susceptible (Table 7). High resistance of LAC-4 (64 μg/mL) and AB030 ($\geq$ 1024 μg/mL) to gentamicin means that the Gm^r-marker is not ideal in these strains. Conversely, all three strains had relatively low MIC values for Apr and Zeo (Table 7). Therefore, both these resistance markers are suitable for genetic manipulations in multidrug resistant isolates of *A. baumannii*. Using Apr and Zeo resistance markers, we created site-specific mini-Tn*7*-based gene insertion systems. Further, plasmids that express yeast Flp recombinase were also modified by cloning Apr- or Zeo-resistance genes, allowing for the creation of unmarked insertions

Table 7. Minimum inhibitory concentrations (µg/mL) of *A. baumannii* wild type strain and clinical isolates against gentamicin, apramycin, and zeocin as determined by broth dilution method. Data are from of two independent replicates and discrepancies between replicates are shown with two values.

Strain	Gentamicin[a]	Apramycin	Zeocin
ATCC17978	1 (S)	2-4	16
AB030	>1024 (R)	16-32	128-256
AB031	2 (S)	8	16
LAC-4	64 (R)	8	4-8

Note: R, resistant; S; susceptible.

[a]Gentamicin susceptibility results interpreted using CSLI guidelines (standard M100-27; CSLI 2017).

.

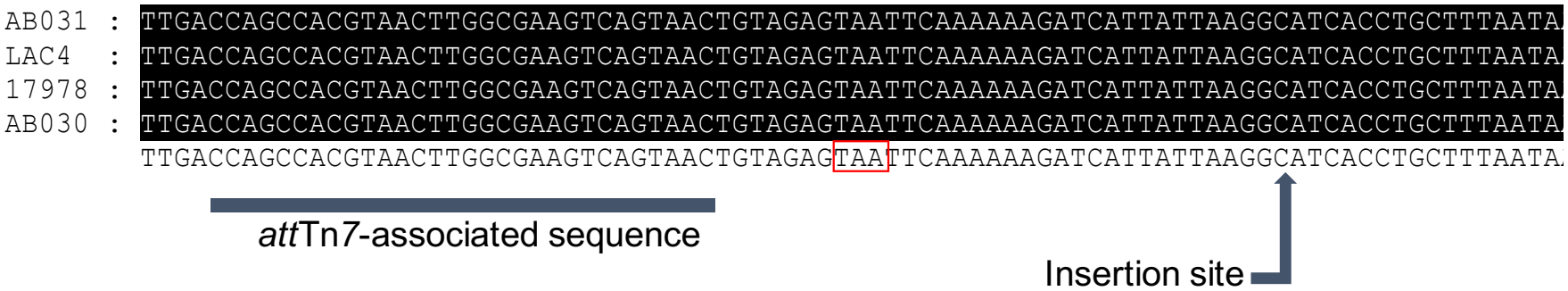

Figure 27. Sequence alignment of the *att*Tn*7*-associated sequence and the Tn*7* insertion site of *Acinetobacter baumannii* ATCC17978 and clinical isolates used. This shows the highly conserved sequence homology between the strains. The insertion site is located 24 bp downstream of the *glmS2* gene in a neutral location (as shown by the arrow). The stop codon of the *glmS2* gene is outlined in the red box. Consensus sequence is shown at the bottom of the alignment displays a 100% identity

Utility of single copy gene expression systems using the mini-Tn*7*-based plasmids has been recognized in various bacterial species (K. H. Choi et al., 2005; K. H. Choi et al., 2008b; K. H. Choi & Schweizer, 2006b; Crepin, Harel, & Dozois, 2012; Kumar et al., 2010a). We recently showed the utility of mini-Tn*7* vectors with an inducible promoter (P_{tac}) where the expression was controlled by addition of IPTG (Ducas-Mowchun, De Silva, Patidar, Schweizer, & Kumar, 2019). The Tn*7* *tnsABCD* genes encode the site-specific transposition pathway and mediate insertion into the chromosome at *att*Tn*7* sites (J.E. Peters & N.L. Craig, 2001). The chromosomal sequence recognized by TnsD resides in the 3' terminal portion of the bacterial *glmS* gene, however insertion occurs at the *att*Tn*7* insertion site usually located in an intergenic region downstream of *glmS* (J.E. Peters & N.L. Craig, 2001) . The *glmS* genes appear to be highly conserved in a diversity of bacterial genomes, conferring broad host range to the Tn*7* transposition pathway of mini-Tn*7* vectors (K. H. Choi et al., 2005). Although *A. baumannii* has two *glmS* genes, only one (*glmS2*) contains the *att*Tn*7* associated sequence (Kumar et al., 2010a). Sequence alignment of the *att*Tn*7*-associated sequence and the Tn*7* insertion site of *A. baumannii* type strain ATCC 17978 and clinical isolates AB030, AB031 and LAC-4 showed 100% conserved sequence homology between the strains (Figure 27). This represents the versatility of mini-Tn*7* vectors for genomic manipulation in *A. baumannii* clinical isolates.

Once the feasibility of using mini-Tn*7* plasmids with Apr or Zeo-resistance markers was confirmed, mini-Tn*7* plasmids were constructed for use in multidrug resistant *A. baumannii* isolates. First, we created pUC18T-mini-Tn*7*T-Apr-LAC and pUC18T-mini-Tn*7*T-Zeo-LAC-plasmids, that contain the inducible IPTG-inducible *E. coli trp-lac* hybrid promoter P_{tac} and the *lacI*^{q} gene (Figure 24). These new mini-Tn*7* plasmids share the following relevant

characteristics: i) origin of transfer for conjugation (*oriT*), ii) high copy number ColE1 origin of replication for *E. coli* maintenance but not in *A. baumannii*, iii) ampicillin resistance gene for *E. coli* selection (*bla*); and iv) within the Tn*7* transposon left and right ends (Tn*7*L, Tn*7*R): a multiple cloning site (MCS) for cloning of sequences under control of the *tac* promoter, a *lac* operator, the *lac* repressor (*lacI*) gene under control of the $lacI^q$ promoter, and an *FRT* cassette flanking Apr or Zeo resistance markers. Utility of mini-Tn*7* vectors containing inducible promoters has previously been shown in various organisms (K. H. Choi et al., 2008b; Kumar, Chua, & Schweizer, 2006). Such plasmids are particularly useful for genetic complementation studies, as they allow regulated expression of genes in single copy and thus avoiding undesirable 'multicopy effects' that may result from plasmid-based gene expression.

Two other versions of mini-Tn*7* plasmids were created that lack the inducible P_{tac} promoters. These two plasmids, pUC18T-mini-Tn*7*T-Apr and pUC18T-mini-Tn*7*T-Zeo, allow for the cloning of the genes with their native promoters. Alternatively, these can also be used for tagging of *A. baumannii* isolates using fluorescent markers as we show below.

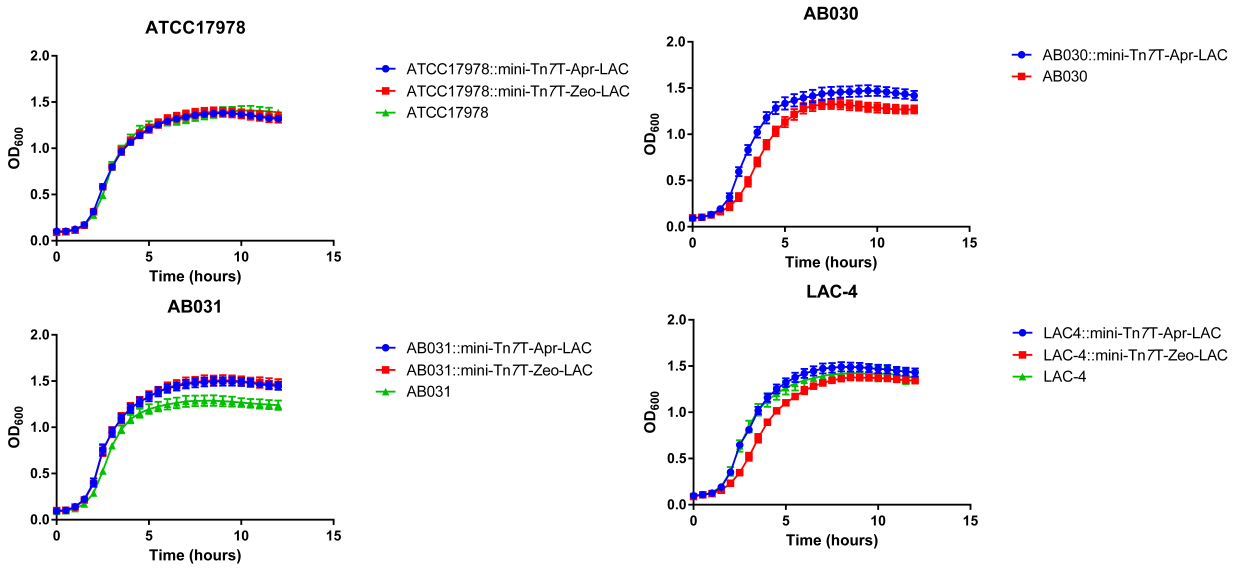

Figure 28. Growth curve analysis of the mini-Tn*7* insertion strains as compared with their respective parent strain. Overnight cultures of each strain was grown in LB at 37˚C with 250 rpm shaking and diluted 1:100 (v/v) in fresh LB to be used as the inoculum for the growth curves. Growth assays were conducted by using 100 µL of the inoculum in each well of a 96-well plate and the A_{600} values were recorded using a SprectraMax M2 microplate reader (Molecular Devices) every 15 minutes with continuous shaking. The resulting values were plotted and statistically analyzed using GraphPad Prism v6.07 (La Jolla, CA, USA). No statistical significance was observed between the strains in each graph as determined by either one-way ANOVA or unpaired t-test (for AB030). All assays were conducted in triplicate with at least two biological replicates.

One of the salient features of mini-Tn*7*-based systems is the unmarked insertion of the plasmid in the chromosome (K. H. Choi & Schweizer, 2006b). Unmarked insertions are often desired to avoid complicating the study of mutant strains with an antibiotic resistance marker and can be obtained by introducing a source of Flp recombinase into the mini-Tn*7* insertion mutant. This allows for excision of the resistance marker through *FRT* site-specific recognition. The site-specific excision vector pFLP2 created for such a purpose in manipulations of *Pseudomonas aeruginosa* (Hoang et al., 1998) was modified for *A. baumannii* by insertion of the origin of replication from the plasmid pWH1266 (Hunger et al., 1990). The pFLP2A and pFLP2Z plasmids created in this study were made using this modified plasmid, pFLP2^{ab}. Both pFLP2A and pFLP2Z, therefore, share the following relevant characteristics: Flp recombinase encoding gene, pWH1266 origin of replication, and *sacB* counter-selectable marker for curing of pFLP. These plasmids differ with respect to the selection marker; pFLP2Z contains a Zeo^r marker and pFLP2A contains an Apr^r marker. These two plasmids were created with the intention of providing a compatible source of Flp recombinase to obtain markerless insertions when using either the Apr or the Zeo mini-Tn*7* constructs created in this study. For example, in an MDR or XDR clinical isolate where the MICs for Zeo and Apr are of practical use for selection purposes, the mini-Tn*7* Apr construct may be used for insertion and the pFLP2Z excision vector can be used subsequently to obtain the markerless insert. Some clinical isolates may not be susceptible to Apr or Zeo, which will hinder achieving markerless insertions. For example, AB030 is resistant to Zeo and as a result we were not able to create makerless insertions in the strain using pFLP2Z plasmid. Nevertheless, we were able to achieve marked insertions of the fluorescent proteins in AB030 (Figure 29). Thus the insertion system can still have wide applications in

clinical isolates, as long as they are susceptible to at least one of the two antibiotics i.e. Apr or Zeo.

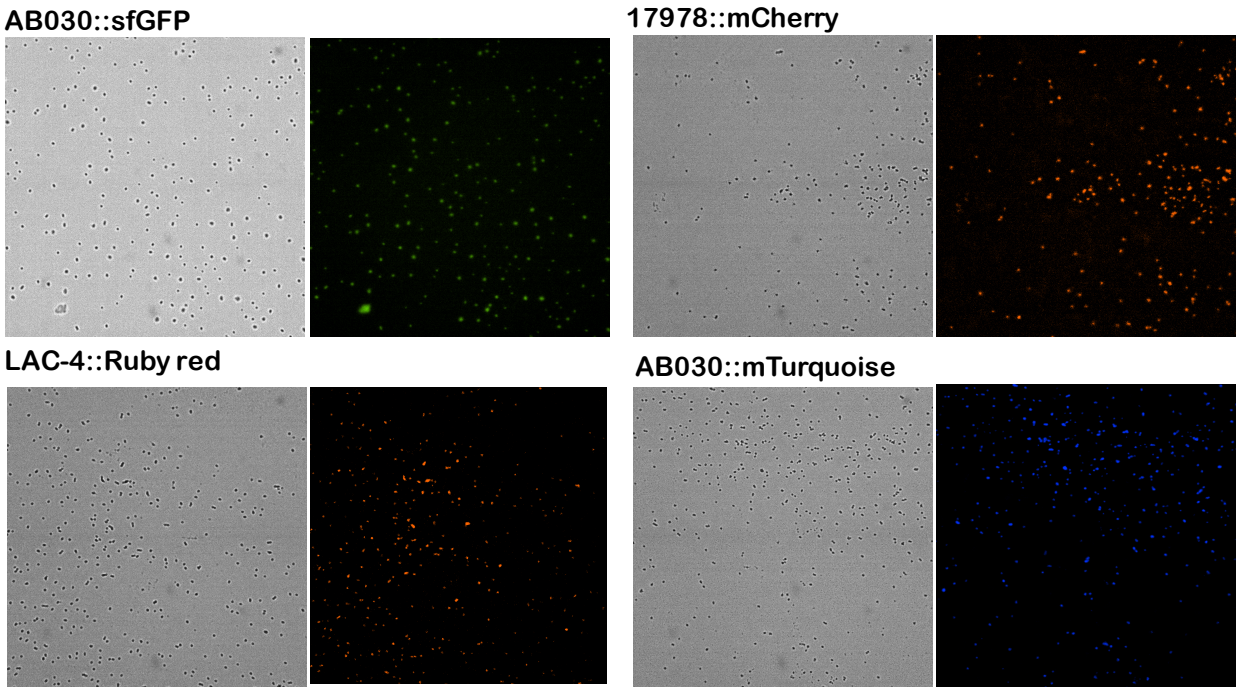

Figure 29. Visualization of the inserted fluorescent protein genes in different *A. baumannii* strains. Images were obtained using ImageXpress Micro 4 High-Content Imaging System with a 40X objective. Images for LAC-4::Ruby Red and 17978::mCherry was acquired using Texas Red filter while AB030::sfGFP was acquired using FITC filter and AB030::mTurquoise was acquired using DAPI filter. The images acquired using the filters were compared to the bright field images of the same to observe the presence and distribution of cells. Emission and excitation wavelengths are provided in Materials and Methods

To test the utility of the plasmids constructed, we cloned fluorescent markers in the pUC18T-mini-Tn*7*T-Apr. Four different plasmids were created containing different fluorescent markers as listed in Table 1. This was followed by inserting pUC18T-mini-Tn*7*T-Apr-sfGFP in AB030, pUC18T-mini-Tn*7*T-Apr-mRuby in LAC-4, pUC18T-mini-Tn*7*T-Apr-mCherry in ATCC 17978, and pUC18T-mini-Tn*7*T-Apr-mTurquoise in AB030. The cells were visualized using a fluorescent imager. As seen in Figure 29, single copy expression of fluorescent genes can be effectively used to visualize *A. baumannii* strains. There are a number of applications of such a system, for example fluorescent-labeled cells can be used in virulence studies (such as in infection models), monitoring biofilm growth, fitness competition assays, etc.

In conclusion, availability of diverse molecular tools for effective genetic manipulation is necessary to study pathogens such as *A. baumannii* that demonstrate high degrees of genetic variability and resistance. The single copy gene expression systems created in this study aid in genetic manipulations in MDR and XDR isolates of *A. baumannii* in a highly efficient and reproducible manner.

CHAPTER 6

CONCLUSIONS AND FUTURE DIRECTIONS

The overall objective of the work presented here is to examine the environmental determinants of antibiotic resistance and virulence in *A. baumannii* and to address the lack of molecular tools available for genetic manipulations of *A. baumannii*. As a successful pathogen in hospital settings, *A. baumannii* has the ability to adapt to the fluctuating environmental conditions it encounters and it is vital to its survival as well as to its ability to cause infections. For example, persistence of *A. baumannii* on hospital surfaces and inside a human host require *A. baumannii* to express different virulence factors according to its surroundings. Therefore, it is of paramount importance for *A. baumannii* to sense and adapt to the environmental conditions surrounding it. As in all other bacteria, TCSs play a key role in this aspect and it is essential to its survival and success as a potent pathogen. Since TCSs can be involved in a multitude of complex regulatory networks, a better understanding of the molecular mechanisms of TCS signalling in *A. baumannii* is essential for finding novel and innovative treatment options when the current antibiotic arsenal becomes incompetent.

AdeRS is an important TCS in *A. baumannii* as it is involved in modulating the expression of AdeABC efflux pump (Marchand et al., 2004). A deletion mutant of *adeRS* displayed reduced expression of *adeB* inline with previous observations (Richmond et al., 2016) and more importantly AdeRS deletion resulted in complete abolishment of surface-associated motility at higher NaCl concentrations. This observation coupled with no changes in motility when pH and osmolarity was altered suggests that AdeRS is involved in salinity stress response of *A. baumannii*. This is the first observation of AdeRS TCS triggered by NaCl and future work regarding the interaction between AdeS and NaCl is required to further understand the molecular mechanisms of sensing NaCl by *A. baumannii*.

Changes in the proteome of *A. baumannii* was observed depending on the incubation temperatures of 28˚C and 37˚C. Adaptation to different temperatures is critical for *A. baumannii* as and when it enters a host system for infection from ambient environments. Changes in clinically relevant phenotypes such as biofilm formation were observed at 28˚C versus 37˚C and this correlates with the proteomic data where Csu operon, which initiates early steps of biofilm formation, was upregulated at 28˚C. General agreement of the expression patterns in the subset of genes tested by qRT-PCR in clinical isolates with the changes observed in wild type ATCC 17978 suggests that there is a general consensus of expression patterns between clinical isolates and type strain of *A. baumannii*. The rather large data set obtained by the proteomic analysis provides a number of clues to the regulatory networks displayed by *A. baumannii* at different temperatures. Therefore, it serves as a foundation for future studies into specific molecular mechanisms of antibiotic resistance and virulence associated phenotypes observed with changes in temperature. These individual regulatory networks that play a part in either susceptibility to antibiotics and / or virulence could be studied further to decipher the complex regulatory networks functioning in response to changes in temperature. One such example is the upregulation of cyclic-di-GMP related proteins at 28˚C. These could be ideal targets for future studies following their traditional role in modulating clinically relevant phenotypes such as biofilm formation and motility.

In an attempt to characterise the as yet uncharacterised TCSs in *A. baumannii*, the orphan response regulator, *A1S_2006* was deleted from wild type *A. baumannii* ATCC 17978. The defects observed in clinically relevant phenotypes of the deletion mutant such as biofilm formation, surface-associated motility, and virulence towards a *G. mellonella* model suggests that A1S_2006 is a part of the regulatory networks that govern these clinically important

phenotypes. Interestingly, *A1S_2006* is located with a nitrite reductase upstream and a nitrate transport protein gene downstream and the inability of the deletion mutant to utilise some nitrogen sources suggest that A1S_2006 could potentially be involved in nitrogen metabolism related functions as well. This warrants further investigations and future studies into this could benefit from the datasets available from Biolog™ phenotypic microarray and RNA-seq. Another direction that future studies could be directed is to investigate the histidine kinase partner of A1S_2006. Being an orphan response regulator, it is entirely possible that A1S_2006 could be phosphorylated by a histidine kinase from another TCS and finding out the histidine kinase partner of A1S_2006 could shed more light into the regulatory networks and environmental stimuli that activate A1S_2006.

Finally, the modified plasmid vectors created to address the lack of molecular tools available for genetic manipulations of *A. baumannii* would benefit the current laboratory based research especially in clinical strains of *A. baumannii* with reduced susceptibility to commonly used antibiotics. These tools provide a feasible way to insert a single copy of genes of interest into a known location of the *A. baumannii* genome. This provides a variety of applications such as insertion of fluorescent markers to identify strains in phenotypic studies such as tracking the progression of infection in animal models. Future studies into making the armoury of molecular tools stronger could benefit from using Apramycin and zeocin as selection markers. One such example world be modifying the commonly used suicide vector pMO130 with these selection markers to be used in achieving gene deletions in clinical strains of *A. baumannii* displaying reduced susceptibility to the current selection markers present in pMO130.

CHAPTER 7

REFERENCES

Adams, M. D., Nickel, G. C., Bajaksouzian, S., Lavender, H., Murthy, A. R., Jacobs, M. R., & Bonomo, R. A. (2009). Resistance to colistin in *Acinetobacter baumannii* associated with mutations in the PmrAB two-component system. *Antimicrob Agents Chemother, 53*(9), 3628-3634. doi:10.1128/AAC.00284-09

Agodi, A., Auxilia, F., Barchitta, M., Brusaferro, S., D'Alessandro, D., Montagna, M. T., . . . Gisio. (2010). Building a benchmark through active surveillance of intensive care unit-acquired infections: the Italian network SPIN-UTI. *J Hosp Infect, 74*(3), 258-265. doi:10.1016/j.jhin.2009.08.015

Albanesi, D., Martin, M., Trajtenberg, F., Mansilla, M. C., Haouz, A., Alzari, P. M., . . . Buschiazzo, A. (2009). Structural plasticity and catalysis regulation of a thermosensor histidine kinase. *Proc Natl Acad Sci U S A, 106*(38), 16185-16190. doi:10.1073/pnas.0906699106

Alm, E., Huang, K., & Arkin, A. (2006). The evolution of two-component systems in bacteria reveals different strategies for niche adaptation. *PLoS Comput Biol, 2*(11), e143. doi:10.1371/journal.pcbi.0020143

Alon, U., Camarena, L., Surette, M. G., Aguera y Arcas, B., Liu, Y., Leibler, S., & Stock, J. B. (1998). Response regulator output in bacterial chemotaxis. *EMBO J, 17*(15), 4238-4248. doi:10.1093/emboj/17.15.4238

Alvarez-Fraga, L., Perez, A., Rumbo-Feal, S., Merino, M., Vallejo, J. A., Ohneck, E. J., . . . Poza, M. (2016). Analysis of the role of the LH92_11085 gene of a biofilm hyper-producing *Acinetobacter baumannii* strain on biofilm formation and attachment to eukaryotic cells. *Virulence, 7*(4), 443-455. doi:10.1080/21505594.2016.1145335

Alvarez-Fraga, L., Rumbo-Feal, S., Perez, A., Gomez, M. J., Gayoso, C., Vallejo, J. A., . . . Poza, M. (2017). Global assessment of small RNAs reveals a non-coding transcript involved in biofilm formation and attachment in *Acinetobacter baumannii* ATCC 17978. *PLoS One, 12*(8), e0182084. doi:10.1371/journal.pone.0182084

Amin, I. M., Richmond, G. E., Sen, P., Koh, T. H., Piddock, L. J., & Chua, K. L. (2013). A method for generating marker-less gene deletions in multidrug-resistant *Acinetobacter baumannii*. *BMC Microbiol, 13*, 158. doi:10.1186/1471-2180-13-158

Andrews, B. J., Proteau, G. A., Beatty, L. G., & Sadowski, P. D. (1985). The FLP recombinase of the 2 micron circle DNA of yeast: interaction with its target sequences. *Cell, 40*(4), 795-803.

Antunes, L. C., Imperi, F., Carattoli, A., & Visca, P. (2011). Deciphering the multifactorial nature of *Acinetobacter baumannii* pathogenicity. *PLoS One, 6*(8), e22674. doi:10.1371/journal.pone.0022674

Antunes, L. C., Visca, P., & Towner, K. J. (2014). *Acinetobacter baumannii*: evolution of a global pathogen. *Pathog Dis, 71*(3), 292-301. doi:10.1111/2049-632X.12125

Arroyo, L. A., Herrera, C. M., Fernandez, L., Hankins, J. V., Trent, M. S., & Hancock, R. E. (2011). The pmrCAB operon mediates polymyxin resistance in *Acinetobacter baumannii* ATCC 17978 and clinical isolates through phosphoethanolamine modification of lipid A. *Antimicrob Agents Chemother, 55*(8), 3743-3751. doi:10.1128/AAC.00256-11

Bainton, R. J., Kubo, K. M., Feng, J. N., & Craig, N. L. (1993). Tn7 transposition: target DNA recognition is mediated by multiple Tn7-encoded proteins in a purified in vitro system. *Cell, 72*(6), 931-943.

Barakat, M., Ortet, P., & Whitworth, D. E. (2011). P2CS: a database of prokaryotic two-component systems. *Nucleic Acids Res, 39*(Database issue), D771-776. doi:10.1093/nar/gkq1023

Barrett, A. R., Kang, Y., Inamasu, K. S., Son, M. S., Vukovich, J. M., & Hoang, T. T. (2008). Genetic tools for allelic replacement in *Burkholderia* species. *Appl Environ Microbiol, 74*(14), 4498-4508. doi:10.1128/AEM.00531-08

Barrett, J. F., & Hoch, J. A. (1998). Two-component signal transduction as a target for microbial anti-infective therapy. *Antimicrob Agents Chemother, 42*(7), 1529-1536.

Barth, P. T., Datta, N., Hedges, R. W., & Grinter, N. J. (1976). Transposition of a deoxyribonucleic acid sequence encoding trimethoprim and streptomycin resistances from R483 to other replicons. *J Bacteriol, 125*(3), 800-810.

Beceiro, A., Llobet, E., Aranda, J., Bengoechea, J. A., Doumith, M., Hornsey, M., . . . Woodford, N. (2011). Phosphoethanolamine modification of lipid A in colistin-resistant variants of *Acinetobacter baumannii* mediated by the pmrAB two-component regulatory system. *Antimicrob Agents Chemother, 55*(7), 3370-3379. doi:10.1128/AAC.00079-11

Beceiro, A., Moreno, A., Fernandez, N., Vallejo, J. A., Aranda, J., Adler, B., . . . Bou, G. (2014). Biological cost of different mechanisms of colistin resistance and their impact on virulence in *Acinetobacter baumannii*. *Antimicrob Agents Chemother, 58*(1), 518-526. doi:10.1128/AAC.01597-13

Bertrand, J. J., West, J. T., & Engel, J. N. (2010). Genetic analysis of the regulation of type IV pilus function by the Chp chemosensory system of *Pseudomonas aeruginosa*. *J Bacteriol, 192*(4), 994-1010. doi:10.1128/JB.01390-09

Bhate, M. P., Molnar, K. S., Goulian, M., & DeGrado, W. F. (2015). Signal transduction in histidine kinases: insights from new structures. *Structure, 23*(6), 981-994. doi:10.1016/j.str.2015.04.002

Bhuiyan, M. S., Ellett, F., Murray, G. L., Kostoulias, X., Cerqueira, G. M., Schulze, K. E., . . . Peleg, A. Y. (2016). *Acinetobacter baumannii* phenylacetic acid metabolism influences infection outcome through a direct effect on neutrophil chemotaxis. *Proc Natl Acad Sci U S A, 113*(34), 9599-9604. doi:10.1073/pnas.1523116113

Biswas, I. (2015). Genetic tools for manipulating *Acinetobacter baumannii* genome: an overview. *J Med Microbiol, 64*(7), 657-669. doi:10.1099/jmm.0.000081

Bonomo, R. A., & Szabo, D. (2006). Mechanisms of multidrug resistance in *Acinetobacter* species and *Pseudomonas aeruginosa*. *Clin Infect Dis, 43 Suppl 2*, S49-56. doi:10.1086/504477

Bou, G., Cervero, G., Dominguez, M. A., Quereda, C., & Martinez-Beltran, J. (2000). Characterization of a nosocomial outbreak caused by a multiresistant *Acinetobacter baumannii* strain with a carbapenem-hydrolyzing enzyme: high-level carbapenem resistance in *A. baumannii* is not due solely to the presence of beta-lactamases. *J Clin Microbiol, 38*(9), 3299-3305.

Boudes, M., Lazar, N., Graille, M., Durand, D., Gaidenko, T. A., Stewart, V., & van Tilbeurgh, H. (2012). The structure of the NasR transcription antiterminator reveals a one-component system with a NIT nitrate receptor coupled to an ANTAR RNA-binding effector. *Mol Microbiol, 85*(3), 431-444. doi:10.1111/j.1365-2958.2012.08111.x

Brackett, C. M., Furlani, R. E., Anderson, R. G., Krishnamurthy, A., Melander, R. J., Moskowitz, S. M., . . . Melander, C. (2016). Second Generation Modifiers of Colistin

Resistance Show Enhanced Activity and Lower Inherent Toxicity. *Tetrahedron, 72*(25), 3549-3553. doi:10.1016/j.tet.2015.09.019
Brown, S., & Amyes, S. (2006). OXA (beta)-lactamases in *Acinetobacter*: the story so far. *J Antimicrob Chemother, 57*(1), 1-3. doi:10.1093/jac/dki425
Brown, S., Young, H. K., & Amyes, S. G. (2005). Characterisation of OXA-51, a novel class D carbapenemase found in genetically unrelated clinical strains of *Acinetobacter baumannii* from Argentina. *Clin Microbiol Infect, 11*(1), 15-23. doi:10.1111/j.1469-0691.2004.01016.x
Cai, Y., Chai, D., Wang, R., Liang, B., & Bai, N. (2012). Colistin resistance of *Acinetobacter baumannii*: clinical reports, mechanisms and antimicrobial strategies. *J Antimicrob Chemother, 67*(7), 1607-1615. doi:10.1093/jac/dks084
Cardona, S. T., Choy, M., & Hogan, A. M. (2018). Essential Two-Component Systems Regulating Cell Envelope Functions: Opportunities for Novel Antibiotic Therapies. *J Membr Biol, 251*(1), 75-89. doi:10.1007/s00232-017-9995-5
Carpenter, B. M., Whitmire, J. M., & Merrell, D. S. (2009). This is not your mother's repressor: the complex role of fur in pathogenesis. *Infect Immun, 77*(7), 2590-2601. doi:10.1128/IAI.00116-09
Casino, P., Rubio, V., & Marina, A. (2009). Structural insight into partner specificity and phosphoryl transfer in two-component signal transduction. *Cell, 139*(2), 325-336. doi:10.1016/j.cell.2009.08.032
Casino, P., Rubio, V., & Marina, A. (2010). The mechanism of signal transduction by two-component systems. *Curr Opin Struct Biol, 20*(6), 763-771. doi:10.1016/j.sbi.2010.09.010
Castanheira, M., Mendes, R. E., & Jones, R. N. (2014). Update on *Acinetobacter* species: mechanisms of antimicrobial resistance and contemporary in vitro activity of minocycline and other treatment options. *Clin Infect Dis, 59 Suppl 6*, S367-373. doi:10.1093/cid/ciu706
Cerqueira, G. M., Kostoulias, X., Khoo, C., Aibinu, I., Qu, Y., Traven, A., & Peleg, A. Y. (2014). A global virulence regulator in *Acinetobacter baumannii* and its control of the phenylacetic acid catabolic pathway. *J Infect Dis, 210*(1), 46-55. doi:10.1093/infdis/jiu024
Chandler, J. R., Duerkop, B. A., Hinz, A., West, T. E., Herman, J. P., Churchill, M. E., . . . Greenberg, E. P. (2009). Mutational analysis of *Burkholderia thailandensis* quorum sensing and self-aggregation. *J Bacteriol, 191*(19), 5901-5909. doi:10.1128/JB.00591-09
Chen, R., Lv, R., Xiao, L., Wang, M., Du, Z., Tan, Y., . . . Song, Y. (2017). A1S_2811, a CheA/Y-like hybrid two-component regulator from *Acinetobacter baumannii* ATCC17978, is involved in surface motility and biofilm formation in this bacterium. *Microbiologyopen, 6*(5). doi:10.1002/mbo3.510
Cheng, H. Y., Chen, Y. F., & Peng, H. L. (2010). Molecular characterization of the PhoPQ-PmrD-PmrAB mediated pathway regulating polymyxin B resistance in *Klebsiella pneumoniae* CG43. *J Biomed Sci, 17*, 60. doi:10.1186/1423-0127-17-60
Chin, C. Y., Tipton, K. A., Farokhyfar, M., Burd, E. M., Weiss, D. S., & Rather, P. N. (2018). A high-frequency phenotypic switch links bacterial virulence and environmental survival in *Acinetobacter baumannii*. *Nat Microbiol, 3*(5), 563-569. doi:10.1038/s41564-018-0151-5
Choi, C. H., Lee, E. Y., Lee, Y. C., Park, T. I., Kim, H. J., Hyun, S. H., . . . Lee, J. C. (2005). Outer membrane protein 38 of *Acinetobacter baumannii* localizes to the mitochondria

and induces apoptosis of epithelial cells. *Cell Microbiol, 7*(8), 1127-1138. doi:10.1111/j.1462-5822.2005.00538.x

Choi, C. H., Lee, J. S., Lee, Y. C., Park, T. I., & Lee, J. C. (2008). *Acinetobacter baumannii* invades epithelial cells and outer membrane protein A mediates interactions with epithelial cells. *BMC Microbiol, 8*, 216. doi:10.1186/1471-2180-8-216

Choi, K. H., DeShazer, D., & Schweizer, H. P. (2006). mini-Tn*7* insertion in bacteria with multiple *glmS*-linked *att*Tn*7* sites: example *Burkholderia mallei* ATCC 23344. *Nat Protoc, 1*(1), 162-169. doi:nprot.2006.25 [pii]
10.1038/nprot.2006.25

Choi, K. H., Gaynor, J. B., White, K. G., Lopez, C., Bosio, C. M., Karkhoff-Schweizer, R. R., & Schweizer, H. P. (2005). A Tn7-based broad-range bacterial cloning and expression system. *Nat Methods, 2*(6), 443-448.

Choi, K. H., Mima, T., Casart, Y., Rholl, D., Kumar, A., Beacham, I. R., & Schweizer, H. P. (2008a). Genetic tools for select-agent-compliant manipulation of *Burkholderia pseudomallei*. *Appl Environ Microbiol, 74*(4), 1064-1075. doi:10.1128/AEM.02430-07

Choi, K. H., Mima, T., Casart, Y., Rholl, D., Kumar, A., Beacham, I. R., & Schweizer, H. P. (2008b). Genetic tools for select-agent-compliant manipulation of *Burkholderia pseudomallei*. *Appl. Environ. Microbiol., 74*(4), 1064-1075. doi:AEM.02430-07 [pii]
10.1128/AEM.02430-07

Choi, K. H., & Schweizer, H. P. (2005). An improved method for rapid generation of unmarked *Pseudomonas aeruginosa* deletion mutants. *BMC Microbiol, 5*, 30. doi:10.1186/1471-2180-5-30

Choi, K. H., & Schweizer, H. P. (2006a). mini-Tn7 insertion in bacteria with secondary, non-glmS-linked *att*Tn*7* sites: example *Proteus mirabilis* HI4320. *Nat Protoc, 1*(1), 170-178. doi:10.1038/nprot.2006.26

Choi, K. H., & Schweizer, H. P. (2006b). mini-Tn7 insertion in bacteria with single *att*Tn*7* sites: example *Pseudomonas aeruginosa*. *Nat Protoc, 1*(1), 153-161. doi:10.1038/nprot.2006.24

Choi, K. Y., Spencer, J. M., & Craig, N. L. (2014). The Tn7 transposition regulator TnsC interacts with the transposase subunit TnsB and target selector TnsD. *Proc Natl Acad Sci U S A, 111*(28), E2858-2865. doi:10.1073/pnas.1409869111

Chu, Y. W., Afzal-Shah, M., Houang, E. T., Palepou, M. I., Lyon, D. J., Woodford, N., & Livermore, D. M. (2001). IMP-4, a novel metallo-beta-lactamase from nosocomial *Acinetobacter* spp. collected in Hong Kong between 1994 and 1998. *Antimicrob Agents Chemother, 45*(3), 710-714. doi:10.1128/AAC.45.3.710-714.2001

Cornejo-Juarez, P., Vilar-Compte, D., Perez-Jimenez, C., Namendys-Silva, S. A., Sandoval-Hernandez, S., & Volkow-Fernandez, P. (2015). The impact of hospital-acquired infections with multidrug-resistant bacteria in an oncology intensive care unit. *Int J Infect Dis, 31*, 31-34. doi:10.1016/j.ijid.2014.12.022

Cortez-Cordova, J., & Kumar, A. (2011). Activity of the efflux pump inhibitor phenylalanine-arginine beta-naphthylamide against the AdeFGH pump of *Acinetobacter baumannii*. *Int J Antimicrob Agents, 37*(5), 420-424. doi:10.1016/j.ijantimicag.2011.01.006

Corvec, S., Caroff, N., Espaze, E., Giraudeau, C., Drugeon, H., & Reynaud, A. (2003). AmpC cephalosporinase hyperproduction in *Acinetobacter baumannii* clinical strains. *J Antimicrob Chemother, 52*(4), 629-635. doi:10.1093/jac/dkg407

Coyne, S., Courvalin, P., & Perichon, B. (2011). Efflux-mediated antibiotic resistance in *Acinetobacter* spp. *Antimicrob Agents Chemother, 55*(3), 947-953. doi:10.1128/AAC.01388-10

Coyne, S., Rosenfeld, N., Lambert, T., Courvalin, P., & Perichon, B. (2010). Overexpression of resistance-nodulation-cell division pump AdeFGH confers multidrug resistance in *Acinetobacter baumannii*. *Antimicrob Agents Chemother, 54*(10), 4389-4393. doi:10.1128/AAC.00155-10

Craig, N. L. (1991). Tn7: a target site-specific transposon. *Mol Microbiol, 5*(11), 2569-2573.

Crepin, S., Harel, J., & Dozois, C. M. (2012). Chromosomal complementation using Tn7 transposon vectors in Enterobacteriaceae. *Appl Environ Microbiol, 78*(17), 6001-6008. doi:10.1128/AEM.00986-12

Da Silva, G. J., & Domingues, S. (2017). Interplay between Colistin Resistance, Virulence and Fitness in *Acinetobacter baumannii*. *Antibiotics (Basel), 6*(4). doi:10.3390/antibiotics6040028

Damier-Piolle, L., Magnet, S., Bremont, S., Lambert, T., & Courvalin, P. (2008). AdeIJK, a resistance-nodulation-cell division pump effluxing multiple antibiotics in *Acinetobacter baumannii*. *Antimicrob Agents Chemother, 52*(2), 557-562. doi:10.1128/AAC.00732-07

de Breij, A., Dijkshoorn, L., Lagendijk, E., van der Meer, J., Koster, A., Bloemberg, G., . . . Nibbering, P. (2010). Do biofilm formation and interactions with human cells explain the clinical success of *Acinetobacter baumannii*? *PLoS One, 5*(5), e10732. doi:10.1371/journal.pone.0010732

de Breij, A., Gaddy, J., van der Meer, J., Koning, R., Koster, A., van den Broek, P., . . . Dijkshoorn, L. (2009). CsuA/BABCDE-dependent pili are not involved in the adherence of *Acinetobacter baumannii* ATCC19606(T) to human airway epithelial cells and their inflammatory response. *Res Microbiol, 160*(3), 213-218. doi:10.1016/j.resmic.2009.01.002

De Silva, P. M., & Kumar, A. (2017). Effect of Sodium Chloride on Surface-Associated Motility of *Acinetobacter baumannii* and the Role of AdeRS Two-Component System. *J Membr Biol*. doi:10.1007/s00232-017-9985-7

De Silva, P. M., & Kumar, A. (2019). Signal Transduction Proteins in *Acinetobacter baumannii*: Role in Antibiotic Resistance, Virulence, and Potential as Drug Targets. *Front Microbiol, 10*, 49. doi:10.3389/fmicb.2019.00049

del Mar Tomas, M., Beceiro, A., Perez, A., Velasco, D., Moure, R., Villanueva, R., . . . Bou, G. (2005). Cloning and functional analysis of the gene encoding the 33- to 36-kilodalton outer membrane protein associated with carbapenem resistance in *Acinetobacter baumannii*. *Antimicrob Agents Chemother, 49*(12), 5172-5175. doi:10.1128/AAC.49.12.5172-5175.2005

Desai, S. K., & Kenney, L. J. (2017). To ~P or Not to ~P? Non-canonical activation by two-component response regulators. *Mol Microbiol, 103*(2), 203-213. doi:10.1111/mmi.13532

Dijkshoorn, L., Nemec, A., & Seifert, H. (2007). An increasing threat in hospitals: multidrug-resistant *Acinetobacter baumannii*. *Nat Rev Microbiol, 5*(12), 939-951. doi:10.1038/nrmicro1789

Doi, Y., Murray, G. L., & Peleg, A. Y. (2015). *Acinetobacter baumannii*: evolution of antimicrobial resistance-treatment options. *Semin Respir Crit Care Med, 36*(1), 85-98. doi:10.1055/s-0034-1398388

Dorsey, C. W., Tomaras, A. P., & Actis, L. A. (2002). Genetic and phenotypic analysis of *Acinetobacter baumannii* insertion derivatives generated with a transposome system. *Appl Environ Microbiol, 68*(12), 6353-6360.

Draughn, G. L., Milton, M. E., Feldmann, E. A., Bobay, B. G., Roth, B. M., Olson, A. L., . . . Cavanagh, J. (2018). The Structure of the Biofilm-controlling Response Regulator BfmR from *Acinetobacter baumannii* Reveals Details of Its DNA-binding Mechanism. *J Mol Biol, 430*(6), 806-821. doi:10.1016/j.jmb.2018.02.002

Ducas-Mowchun, K., De Silva, P. M., Patidar, R., Schweizer, H. P., & Kumar, A. (2019). Tn7-Based Single-Copy Insertion Vectors for *Acinetobacter baumannii*. In I. Biswas & P. N. Rather (Eds.), *Acinetobacter baumannii: Methods and Protocols* (pp. 135-150). New York, NY: Springer New York.

Eijkelkamp, B. A., Stroeher, U. H., Hassan, K. A., Elbourne, L. D., Paulsen, I. T., & Brown, M. H. (2013). H-NS plays a role in expression of *Acinetobacter baumannii* virulence features. *Infect Immun, 81*(7), 2574-2583. doi:10.1128/IAI.00065-13

Esterly, J. S., Richardson, C. L., Eltoukhy, N. S., Qi, C., & Scheetz, M. H. (2011). Genetic Mechanisms of Antimicrobial Resistance of *Acinetobacter baumannii*. *Ann Pharmacother, 45*(2), 218-228. doi:10.1345/aph.1P084

Fabret, C., & Hoch, J. A. (1998). A two-component signal transduction system essential for growth of *Bacillus subtilis*: implications for anti-infective therapy. *J Bacteriol, 180*(23), 6375-6383.

Fernandez, L., Breidenstein, E. B., Song, D., & Hancock, R. E. (2012). Role of intracellular proteases in the antibiotic resistance, motility, and biofilm formation of *Pseudomonas aeruginosa*. *Antimicrob Agents Chemother, 56*(2), 1128-1132. doi:10.1128/AAC.05336-11

Fernando, D. M., Khan, I. U., Patidar, R., Lapen, D. R., Talbot, G., Topp, E., & Kumar, A. (2016). Isolation and Characterization of *Acinetobacter baumannii* Recovered from Campylobacter Selective Medium. *Front Microbiol, 7*, 1871. doi:10.3389/fmicb.2016.01871

Finn, J. A., Parks, A. R., & Peters, J. E. (2007). Transposon Tn7 directs transposition into the genome of filamentous bacteriophage M13 using the element-encoded TnsE protein. *J Bacteriol, 189*(24), 9122-9125. doi:10.1128/JB.01451-07

Fournier, P. E., Vallenet, D., Barbe, V., Audic, S., Ogata, H., Poirel, L., . . . Claverie, J. M. (2006). Comparative genomics of multidrug resistance in *Acinetobacter baumannii*. *PLoS Genet, 2*(1), e7. doi:10.1371/journal.pgen.0020007

Gaddy, J. A., Arivett, B. A., McConnell, M. J., Lopez-Rojas, R., Pachon, J., & Actis, L. A. (2012). Role of acinetobactin-mediated iron acquisition functions in the interaction of *Acinetobacter baumannii* strain ATCC 19606T with human lung epithelial cells, *Galleria mellonella* caterpillars, and mice. *Infect Immun, 80*(3), 1015-1024. doi:10.1128/IAI.06279-11

Gaddy, J. A., Tomaras, A. P., & Actis, L. A. (2009). The *Acinetobacter baumannii* 19606 OmpA protein plays a role in biofilm formation on abiotic surfaces and in the interaction of this pathogen with eukaryotic cells. *Infect Immun, 77*(8), 3150-3160. doi:10.1128/IAI.00096-09

Gales, A. C., Tognim, M. C., Reis, A. O., Jones, R. N., & Sader, H. S. (2003). Emergence of an IMP-like metallo-enzyme in an *Acinetobacter baumannii* clinical strain from a Brazilian teaching hospital. *Diagn Microbiol Infect Dis, 45*(1), 77-79.

Gary, P. A., Biery, M. C., Bainton, R. J., & Craig, N. L. (1996). Multiple DNA processing reactions underlie Tn7 transposition. *J Mol Biol, 257*(2), 301-316.
Gay, N. J., Tybulewicz, V. L., & Walker, J. E. (1986). Insertion of transposon Tn7 into the *Escherichia coli* glmS transcriptional terminator. *Biochem J, 234*(1), 111-117.
Gayoso, C. M., Mateos, J., Mendez, J. A., Fernandez-Puente, P., Rumbo, C., Tomas, M., . . . Bou, G. (2014). Molecular mechanisms involved in the response to desiccation stress and persistence in *Acinetobacter baumannii*. *J Proteome Res, 13*(2), 460-476. doi:10.1021/pr400603f
Geisinger, E., & Isberg, R. R. (2015). Antibiotic modulation of capsular exopolysaccharide and virulence in *Acinetobacter baumannii*. *PLoS Pathog, 11*(2), e1004691. doi:10.1371/journal.ppat.1004691
Geisinger, E., Mortman, N. J., Vargas-Cuebas, G., Tai, A. K., & Isberg, R. R. (2018). A global regulatory system links virulence and antibiotic resistance to envelope homeostasis in *Acinetobacter baumannii*. *PLoS Pathog, 14*(5), e1007030. doi:10.1371/journal.ppat.1007030
Giard, D. J., Aaronson, S. A., Todaro, G. J., Arnstein, P., Kersey, J. H., Dosik, H., & Parks, W. P. (1973). In vitro cultivation of human tumors: establishment of cell lines derived from a series of solid tumors. *J Natl Cancer Inst, 51*(5), 1417-1423.
Gooderham, W. J., & Hancock, R. E. (2009). Regulation of virulence and antibiotic resistance by two-component regulatory systems in *Pseudomonas aeruginosa*. *FEMS Microbiol Rev, 33*(2), 279-294. doi:10.1111/j.1574-6976.2008.00135.x
Gordon, N. C., Png, K., & Wareham, D. W. (2010). Potent synergy and sustained bactericidal activity of a vancomycin-colistin combination versus multidrug-resistant strains of *Acinetobacter baumannii*. *Antimicrob Agents Chemother, 54*(12), 5316-5322. doi:10.1128/AAC.00922-10
Gordon, N. C., & Wareham, D. W. (2010). Multidrug-resistant *Acinetobacter baumannii*: mechanisms of virulence and resistance. *Int J Antimicrob Agents, 35*(3), 219-226. doi:10.1016/j.ijantimicag.2009.10.024
Gotoh, Y., Doi, A., Furuta, E., Dubrac, S., Ishizaki, Y., Okada, M., . . . Utsumi, R. (2010). Novel antibacterial compounds specifically targeting the essential WalR response regulator. *J Antibiot (Tokyo), 63*(3), 127-134. doi:10.1038/ja.2010.4
Gotoh, Y., Eguchi, Y., Watanabe, T., Okamoto, S., Doi, A., & Utsumi, R. (2010). Two-component signal transduction as potential drug targets in pathogenic bacteria. *Curr Opin Microbiol, 13*(2), 232-239. doi:10.1016/j.mib.2010.01.008
Grosso-Becerra, M. V., Croda-Garcia, G., Merino, E., Servin-Gonzalez, L., Mojica-Espinosa, R., & Soberon-Chavez, G. (2014). Regulation of *Pseudomonas aeruginosa* virulence factors by two novel RNA thermometers. *Proc Natl Acad Sci U S A, 111*(43), 15562-15567. doi:10.1073/pnas.1402536111
Guardabassi, L., Dijkshoorn, L., Collard, J. M., Olsen, J. E., & Dalsgaard, A. (2000). Distribution and in-vitro transfer of tetracycline resistance determinants in clinical and aquatic *Acinetobacter* strains. *J Med Microbiol, 49*(10), 929-936. doi:10.1099/0022-1317-49-10-929
Guarnieri, M. T., Zhang, L., Shen, J., & Zhao, R. (2008). The Hsp90 inhibitor radicicol interacts with the ATP-binding pocket of bacterial sensor kinase PhoQ. *J Mol Biol, 379*(1), 82-93. doi:10.1016/j.jmb.2008.03.036

Gunn, J. S. (2008). The *Salmonella* PmrAB regulon: lipopolysaccharide modifications, antimicrobial peptide resistance and more. *Trends Microbiol, 16*(6), 284-290. doi:10.1016/j.tim.2008.03.007

Hamad, M. A., Zajdowicz, S. L., Holmes, R. K., & Voskuil, M. I. (2009). An allelic exchange system for compliant genetic manipulation of the select agents *Burkholderia pseudomallei* and *Burkholderia mallei*. *Gene, 430*(1-2), 123-131. doi:10.1016/j.gene.2008.10.011

Hamouda, A., Findlay, J., Al Hassan, L., & Amyes, S. G. (2011). Epidemiology of *Acinetobacter baumannii* of animal origin. *Int J Antimicrob Agents, 38*(4), 314-318. doi:10.1016/j.ijantimicag.2011.06.007

Hancock, L., & Perego, M. (2002). Two-component signal transduction in *Enterococcus faecalis*. *J Bacteriol, 184*(21), 5819-5825.

Harding, C. M., Tracy, E. N., Carruthers, M. D., Rather, P. N., Actis, L. A., & Munson, R. S., Jr. (2013). *Acinetobacter baumannii* strain M2 produces type IV pili which play a role in natural transformation and twitching motility but not surface-associated motility. *MBio, 4*(4). doi:10.1128/mBio.00360-13

Harris, G., Kuo Lee, R., Lam, C. K., Kanzaki, G., Patel, G. B., Xu, H. H., & Chen, W. (2013). A mouse model of *Acinetobacter baumannii*-associated pneumonia using a clinically isolated hypervirulent strain. *Antimicrob Agents Chemother, 57*(8), 3601-3613. doi:10.1128/AAC.00944-13

Harris, T. L., Worthington, R. J., Hittle, L. E., Zurawski, D. V., Ernst, R. K., & Melander, C. (2014). Small molecule downregulation of PmrAB reverses lipid A modification and breaks colistin resistance. *ACS Chem Biol, 9*(1), 122-127. doi:10.1021/cb400490k

Henis, Y., Tagari, H., & Volcani, R. (1964). Effect of water extracts of carob pods, tannic acid, and their derivatives on the morphology and growth of microorganisms. *Appl Microbiol, 12*, 204-209.

Henry, R., Vithanage, N., Harrison, P., Seemann, T., Coutts, S., Moffatt, J. H., . . . Boyce, J. D. (2012). Colistin-resistant, lipopolysaccharide-deficient *Acinetobacter baumannii* responds to lipopolysaccharide loss through increased expression of genes involved in the synthesis and transport of lipoproteins, phospholipids, and poly-beta-1,6-N-acetylglucosamine. *Antimicrob Agents Chemother, 56*(1), 59-69. doi:10.1128/AAC.05191-11

Hoang, T. T., Karkhoff-Schweizer, R. R., Kutchma, A. J., & Schweizer, H. P. (1998). A broad-host-range Flp-FRT recombination system for site-specific excision of chromosomally-located DNA sequences: application for isolation of unmarked *Pseudomonas aeruginosa* mutants. *Gene, 212*(1), 77-86.

Hoch, J. A. (2000). Two-component and phosphorelay signal transduction. *Curr Opin Microbiol, 3*(2), 165-170.

Hoiby, N., Bjarnsholt, T., Givskov, M., Molin, S., & Ciofu, O. (2010). Antibiotic resistance of bacterial biofilms. *Int J Antimicrob Agents, 35*(4), 322-332. doi:10.1016/j.ijantimicag.2009.12.011

Hong, H. J., Hutchings, M. I., Buttner, M. J., Biotechnology, & Biological Sciences Research Council, U. K. (2008). Vancomycin resistance VanS/VanR two-component systems. *Adv Exp Med Biol, 631*, 200-213.

Hornsey, M., Ellington, M. J., Doumith, M., Thomas, C. P., Gordon, N. C., Wareham, D. W., . . . Woodford, N. (2010). AdeABC-mediated efflux and tigecycline MICs for epidemic

clones of *Acinetobacter baumannii*. *J Antimicrob Chemother, 65*(8), 1589-1593. doi:10.1093/jac/dkq218
Howard, A., O'Donoghue, M., Feeney, A., & Sleator, R. D. (2012). *Acinetobacter baumannii*: an emerging opportunistic pathogen. *Virulence, 3*(3), 243-250. doi:10.4161/viru.19700
Hsing, W., & Silhavy, T. J. (1997). Function of conserved histidine-243 in phosphatase activity of EnvZ, the sensor for porin osmoregulation in *Escherichia coli*. *J Bacteriol, 179*(11), 3729-3735.
Huerta-Cepas, J., Szklarczyk, D., Forslund, K., Cook, H., Heller, D., Walter, M. C., . . . Bork, P. (2016). eggNOG 4.5: a hierarchical orthology framework with improved functional annotations for eukaryotic, prokaryotic and viral sequences. *Nucleic Acids Res, 44*(D1), D286-293. doi:10.1093/nar/gkv1248
Hunger, M., Schmucker, R., Kishan, V., & Hillen, W. (1990). Analysis and nucleotide sequence of an origin of DNA replication in *Acinetobacter calcoaceticus* and its use for *Escherichia coli* shuttle plasmids. *Gene, 87*(1), 45-51.
Igarashi, M., Watanabe, T., Hashida, T., Umekita, M., Hatano, M., Yanagida, Y., . . . Nomoto, A. (2013). Waldiomycin, a novel WalK-histidine kinase inhibitor from *Streptomyces* sp. MK844-mF10. *J Antibiot (Tokyo), 66*(8), 459-464. doi:10.1038/ja.2013.33
Iwashkiw, J. A., Seper, A., Weber, B. S., Scott, N. E., Vinogradov, E., Stratilo, C., . . . Feldman, M. F. (2012). Identification of a general O-linked protein glycosylation system in *Acinetobacter baumannii* and its role in virulence and biofilm formation. *PLoS Pathog, 8*(6), e1002758. doi:10.1371/journal.ppat.1002758
Iyer, R., Moussa, S. H., Durand-Reville, T. F., Tommasi, R., & Miller, A. (2018). *Acinetobacter baumannii* OmpA Is a Selective Antibiotic Permeant Porin. *ACS Infect Dis, 4*(3), 373-381. doi:10.1021/acsinfecdis.7b00168
Jacoby, G. A. (2009). AmpC beta-lactamases. *Clin Microbiol Rev, 22*(1), 161-182, doi:10.1128/CMR.00036-08
Jawad, A., Seifert, H., Snelling, A. M., Heritage, J., & Hawkey, P. M. (1998). Survival of *Acinetobacter baumannii* on dry surfaces: comparison of outbreak and sporadic isolates. *J Clin Microbiol, 36*(7), 1938-1941.
Ji, Q., Chen, P. J., Qin, G., Deng, X., Hao, Z., Wawrzak, Z., . . . He, C. (2016). Structure and mechanism of the essential two-component signal-transduction system WalKR in *Staphylococcus aureus*. *Nat Commun, 7*, 11000. doi:10.1038/ncomms11000
Joly-Guillou, M. L., Wolff, M., Pocidalo, J. J., Walker, F., & Carbon, C. (1997). Use of a new mouse model of *Acinetobacter baumannii* pneumonia to evaluate the postantibiotic effect of imipenem. *Antimicrob Agents Chemother, 41*(2), 345-351.
Kallipolitis, B. H., & Ingmer, H. (2001). *Listeria monocytogenes* response regulators important for stress tolerance and pathogenesis. *FEMS Microbiol Lett, 204*(1), 111-115.
Kang, A. D., Smith, K. P., Eliopoulos, G. M., Berg, A. H., McCoy, C., & Kirby, J. E. (2017). Invitro Apramycin Activity against multidrug-resistant *Acinetobacter baumannii* and *Pseudomonas aeruginosa. Diagn Microbiol Infect Dis, 88*(2), 188-191. doi:10.1016/j.diagmicrobio.2017.03.006
Kassamali, Z., Jain, R., & Danziger, L. H. (2015). An update on the arsenal for multidrug-resistant *Acinetobacter* infections: polymyxin antibiotics. *Int J Infect Dis, 30*, 125-132. doi:10.1016/j.ijid.2014.10.014

Kelley, L. A., Mezulis, S., Yates, C. M., Wass, M. N., & Sternberg, M. J. (2015). The Phyre2 web portal for protein modeling, prediction and analysis. *Nat Protoc, 10*(6), 845-858. doi:10.1038/nprot.2015.053

Kenney, L. J. (2010). How important is the phosphatase activity of sensor kinases? *Curr Opin Microbiol, 13*(2), 168-176. doi:10.1016/j.mib.2010.01.013

Kim, C., Hesek, D., Zajicek, J., Vakulenko, S. B., & Mobashery, S. (2006). Characterization of the bifunctional aminoglycoside-modifying enzyme ANT(3")-Ii/AAC(6')-IId from *Serratia marcescens*. *Biochemistry, 45*(27), 8368-8377. doi:10.1021/bi060723g

Knapp, S., Wieland, C. W., Florquin, S., Pantophlet, R., Dijkshoorn, L., Tshimbalanga, N., . . . van der Poll, T. (2006). Differential roles of CD14 and toll-like receptors 4 and 2 in murine *Acinetobacter* pneumonia. *Am J Respir Crit Care Med, 173*(1), 122-129. doi:10.1164/rccm.200505-730OC

Kroger, C., Kary, S. C., Schauer, K., & Cameron, A. D. (2016). Genetic Regulation of Virulence and Antibiotic Resistance in *Acinetobacter baumannii*. *Genes (Basel), 8*(1). doi:10.3390/genes8010012

Kubo, K. M., & Craig, N. L. (1990). Bacterial transposon Tn7 utilizes two different classes of target sites. *J Bacteriol, 172*(5), 2774-2778.

Kumar, A., Chua, K. L., & Schweizer, H. P. (2006). Method for regulated expression of single-copy efflux pump genes in a surrogate *Pseudomonas aeruginosa* strain: identification of the BpeEF-OprC chloramphenicol and trimethoprim efflux pump of *Burkholderia pseudomallei* 1026b. *Antimicrob. Agents Chemother., 50*(10), 3460-3463.

Kumar, A., Dalton, C., Cortez-Cordova, J., & Schweizer, H. P. (2010a). Mini-Tn7 vectors as genetic tools for single copy gene cloning in *Acinetobacter baumannii*. *J. Microbiol. Meth., 82*(3), 296-300. doi:S0167-7012(10)00233-2 [pii]
10.1016/j.mimet.2010.07.002

Kumar, A., Dalton, C., Cortez-Cordova, J., & Schweizer, H. P. (2010b). Mini-Tn7 vectors as genetic tools for single copy gene cloning in *Acinetobacter baumannii*. *J Microbiol Methods, 82*(3), 296-300. doi:10.1016/j.mimet.2010.07.002

Kumar, A., & Schweizer, H. P. (2005). Bacterial resistance to antibiotics: active efflux and reduced uptake. *Adv Drug Deliv Rev, 57*(10), 1486-1513. doi:10.1016/j.addr.2005.04.004

Kwon, H. I., Kim, S., Oh, M. H., Na, S. H., Kim, Y. J., Jeon, Y. H., & Lee, J. C. (2017). Outer membrane protein A contributes to antimicrobial resistance of *Acinetobacter baumannii* through the OmpA-like domain. *J Antimicrob Chemother, 72*(11), 3012-3015. doi:10.1093/jac/dkx257

Labarca, J. A., Salles, M. J., Seas, C., & Guzman-Blanco, M. (2016). Carbapenem resistance in *Pseudomonas aeruginosa* and *Acinetobacter baumannii* in the nosocomial setting in Latin America. *Crit Rev Microbiol, 42*(2), 276-292. doi:10.3109/1040841X.2014.940494

Lakemeyer, M., Zhao, W., Mandl, F. A., Hammann, P., & Sieber, S. A. (2018). Thinking Outside the Box-Novel Antibacterials To Tackle the Resistance Crisis. *Angew Chem Int Ed Engl, 57*(44), 14440-14475. doi:10.1002/anie.201804971

Lange, R., Wagner, C., de Saizieu, A., Flint, N., Molnos, J., Stieger, M., . . . Amrein, K. E. (1999). Domain organization and molecular characterization of 13 two-component systems identified by genome sequencing of *Streptococcus pneumoniae*. *Gene, 237*(1), 223-234.

Langmead, B., & Salzberg, S. L. (2012). Fast gapped-read alignment with Bowtie 2. *Nat Methods, 9*(4), 357-359. doi:10.1038/nmeth.1923

Laub, M. T., & Goulian, M. (2007). Specificity in two-component signal transduction pathways. *Annu Rev Genet, 41*, 121-145. doi:10.1146/annurev.genet.41.042007.170548

Lean, S. S., Yeo, C. C., Suhaili, Z., & Thong, K. L. (2015). Comparative Genomics of Two ST 195 Carbapenem-Resistant *Acinetobacter baumannii* with Different Susceptibility to Polymyxin Revealed Underlying Resistance Mechanism. *Front Microbiol, 6*, 1445. doi:10.3389/fmicb.2015.01445

Leblanc, S. K., Oates, C. W., & Raivio, T. L. (2011). Characterization of the induction and cellular role of the BaeSR two-component envelope stress response of *Escherichia coli*. *J Bacteriol, 193*(13), 3367-3375. doi:10.1128/JB.01534-10

Lee, C. R., Lee, J. H., Park, M., Park, K. S., Bae, I. K., Kim, Y. B., . . . Lee, S. H. (2017). Biology of *Acinetobacter baumannii*: Pathogenesis, Antibiotic Resistance Mechanisms, and Prospective Treatment Options. *Front Cell Infect Microbiol, 7*, 55. doi:10.3389/fcimb.2017.00055

Lee, J. Y., & Ko, K. S. (2014). Mutations and expression of PmrAB and PhoPQ related with colistin resistance in *Pseudomonas aeruginosa* clinical isolates. *Diagn Microbiol Infect Dis, 78*(3), 271-276. doi:10.1016/j.diagmicrobio.2013.11.027

Leung, D. W., Chen, E., Cachianes, G., & Goeddel, D. V. (1985). Nucleotide sequence of the partition function of *Escherichia coli* plasmid ColE1. *DNA, 4*(5), 351-355. doi:10.1089/dna.1985.4.351

Li, J., Rayner, C. R., Nation, R. L., Owen, R. J., Spelman, D., Tan, K. E., & Liolios, L. (2006). Heteroresistance to colistin in multidrug-resistant *Acinetobacter baumannii*. *Antimicrob Agents Chemother, 50*(9), 2946-2950. doi:10.1128/AAC.00103-06

Li, J., Swanson, R. V., Simon, M. I., & Weis, R. M. (1995). The response regulators CheB and CheY exhibit competitive binding to the kinase CheA. *Biochemistry, 34*(45), 14626-14636.

Limansky, A. S., Mussi, M. A., & Viale, A. M. (2002). Loss of a 29-kilodalton outer membrane protein in *Acinetobacter baumannii* is associated with imipenem resistance. *J Clin Microbiol, 40*(12), 4776-4778.

Lin, M. F., & Lan, C. Y. (2014). Antimicrobial resistance in *Acinetobacter baumannii*: From bench to bedside. *World J Clin Cases, 2*(12), 787-814. doi:10.12998/wjcc.v2.i12.787

Lin, M. F., Lin, Y. Y., & Lan, C. Y. (2015). The Role of the Two-Component System BaeSR in Disposing Chemicals through Regulating Transporter Systems in *Acinetobacter baumannii*. *PLoS One, 10*(7), e0132843. doi:10.1371/journal.pone.0132843

Lin, M. F., Lin, Y. Y., Yeh, H. W., & Lan, C. Y. (2014). Role of the BaeSR two-component system in the regulation of *Acinetobacter baumannii* adeAB genes and its correlation with tigecycline susceptibility. *BMC Microbiol, 14*, 119. doi:10.1186/1471-2180-14-119

Liu, F., Zhu, Y., Yi, Y., Lu, N., Zhu, B., & Hu, Y. (2014). Comparative genomic analysis of *Acinetobacter baumannii* clinical isolates reveals extensive genomic variation and diverse antibiotic resistance determinants. *BMC Genomics, 15*, 1163. doi:10.1186/1471-2164-15-1163

Loehfelm, T. W., Luke, N. R., & Campagnari, A. A. (2008). Identification and characterization of an *Acinetobacter baumannii* biofilm-associated protein. *J Bacteriol, 190*(3), 1036-1044. doi:10.1128/JB.01416-07

Loewen, P. C., Alsaadi, Y., Fernando, D., & Kumar, A. (2014a). Genome Sequence of a Tigecycline-Resistant Clinical Isolate of *Acinetobacter baumannii* Strain AB031

Obtained from a Bloodstream Infection. *Genome Announc, 2*(5). doi:10.1128/genomeA.01036-14
Loewen, P. C., Alsaadi, Y., Fernando, D., & Kumar, A. (2014a). Genome sequence of a tigecycline-resistant clinical isolate of *Acinetobacter baumannii* strain AB031 obtained from a bloodstream infection. *Genome Announc., 2*(5), e01036-01014. doi:10.1128/genomeA.01036-14
Loewen, P. C., Alsaadi, Y., Fernando, D., & Kumar, A. (2014b). Genome sequence of an extremely drug-resistant clinical isolate of *Acinetobacter baumannii* strain AB030. *Genome Announc., 2*(5), e01035-01014. doi:10.1128/genomeA.01035-14
Loewen, P. C., Alsaadi, Y., Fernando, D., & Kumar, A. (2014b). Genome Sequence of an Extremely Drug-Resistant Clinical Isolate of *Acinetobacter baumannii* Strain AB030. *Genome Announc, 2*(5). doi:10.1128/genomeA.01035-14
Lopez-Redondo, M. L., Moronta, F., Salinas, P., Espinosa, J., Cantos, R., Dixon, R., . . . Contreras, A. (2010). Environmental control of phosphorylation pathways in a branched two-component system. *Mol Microbiol, 78*(2), 475-489.
Lucidi, M., Runci, F., Rampioni, G., Frangipani, E., Leoni, L., & Visca, P. (2018a). New Shuttle Vectors for Gene Cloning and Expression in Multidrug-Resistant *Acinetobacter* Species. *Antimicrob Agents Chemother, 62*(4), pii: e02480-02417. doi:10.1128/AAC.02480-17
Lucidi, M., Runci, F., Rampioni, G., Frangipani, E., Leoni, L., & Visca, P. (2018b). New Shuttle Vectors for Gene Cloning and Expression in Multidrug-Resistant *Acinetobacter* Species. *Antimicrob Agents Chemother, 62*(4). doi:10.1128/AAC.02480-17
Luna, B. M., Ulhaq, A., Yan, J., Pantapalangkoor, P., Nielsen, T. B., Davies, B. W., . . . Spellberg, B. (2017a). Selectable Markers for Use in Genetic Manipulation of Extensively Drug-Resistant (XDR) *Acinetobacter baumannii* HUMC1. *mSphere, 2*(2), e00140-00117. doi:10.1128/mSphere.00140-17
Luna, B. M., Ulhaq, A., Yan, J., Pantapalangkoor, P., Nielsen, T. B., Davies, B. W., . . . Spellberg, B. (2017b). Selectable Markers for Use in Genetic Manipulation of Extensively Drug-Resistant (XDR) *Acinetobacter baumannii* HUMC1. *mSphere, 2*(2). doi:10.1128/mSphere.00140-17
Lupo, A., Vogt, D., Seiffert, S. N., Endimiani, A., & Perreten, V. (2014). Antibiotic resistance and phylogenetic characterization of *Acinetobacter baumannii* strains isolated from commercial raw meat in Switzerland. *J Food Prot, 77*(11), 1976-1981. doi:10.4315/0362-028X.JFP-14-073
Magnet, S., Courvalin, P., & Lambert, T. (2001). Resistance-nodulation-cell division-type efflux pump involved in aminoglycoside resistance in *Acinetobacter baumannii* strain BM4454. *Antimicrob Agents Chemother, 45*(12), 3375-3380. doi:10.1128/AAC.45.12.3375-3380.2001
Maragakis, L. L., & Perl, T. M. (2008). *Acinetobacter baumannii*: epidemiology, antimicrobial resistance, and treatment options. *Clin Infect Dis, 46*(8), 1254-1263. doi:10.1086/529198
Maraki, S., Mantadakis, E., Mavromanolaki, V. E., Kofteridis, D. P., & Samonis, G. (2016). A 5-year Surveillance Study on Antimicrobial Resistance of *Acinetobacter baumannii* Clinical Isolates from a Tertiary Greek Hospital. *Infect Chemother, 48*(3), 190-198. doi:10.3947/ic.2016.48.3.190
Marchand, I., Damier-Piolle, L., Courvalin, P., & Lambert, T. (2004). Expression of the RND-type efflux pump AdeABC in *Acinetobacter baumannii* is regulated by the AdeRS two-

component system. *Antimicrob Agents Chemother, 48*(9), 3298-3304. doi:10.1128/AAC.48.9.3298-3304.2004
Marque, S., Poirel, L., Heritier, C., Brisse, S., Blasco, M. D., Filip, R., . . . Nordmann, P. (2005). Regional occurrence of plasmid-mediated carbapenem-hydrolyzing oxacillinase OXA-58 in *Acinetobacter* spp. in Europe. *J Clin Microbiol, 43*(9), 4885-4888. doi:10.1128/JCM.43.9.4885-4888.2005
Martin, P. K., Li, T., Sun, D., Biek, D. P., & Schmid, M. B. (1999). Role in cell permeability of an essential two-component system in *Staphylococcus aureus*. *J Bacteriol, 181*(12), 3666-3673.
McConnell, M. J., Actis, L., & Pachon, J. (2013). *Acinetobacter baumannii*: human infections, factors contributing to pathogenesis and animal models. *FEMS Microbiol Rev, 37*(2), 130-155. doi:10.1111/j.1574-6976.2012.00344.x
McDonald, L. C., Banerjee, S. N., & Jarvis, W. R. (1999). Seasonal variation of *Acinetobacter* infections: 1987-1996. Nosocomial Infections Surveillance System. *Clin Infect Dis, 29*(5), 1133-1137. doi:10.1086/313441
McKenzie, G. J., & Craig, N. L. (2006). Fast, easy and efficient: site-specific insertion of transgenes into enterobacterial chromosomes using Tn7 without need for selection of the insertion event. *BMC Microbiol, 6*, 39. doi:10.1186/1471-2180-6-39
McKown, R. L., Orle, K. A., Chen, T., & Craig, N. L. (1988). Sequence requirements of *Escherichia coli att*Tn*7*, a specific site of transposon Tn7 insertion. *J Bacteriol, 170*(1), 352-358.
McQueary, C. N., Kirkup, B. C., Si, Y., Barlow, M., Actis, L. A., Craft, D. W., & Zurawski, D. V. (2012). Extracellular stress and lipopolysaccharide modulate *Acinetobacter baumannii* surface-associated motility. *J Microbiol, 50*(3), 434-443. doi:10.1007/s12275-012-1555-1
Metzgar, D., Bacher, J. M., Pezo, V., Reader, J., Doring, V., Schimmel, P., . . . de Crecy-Lagard, V. (2004). *Acinetobacter* sp. ADP1: an ideal model organism for genetic analysis and genome engineering. *Nucleic Acids Res, 32*(19), 5780-5790. doi:10.1093/nar/gkh881
Miller, S. I., Kukral, A. M., & Mekalanos, J. J. (1989). A two-component regulatory system (phoP phoQ) controls *Salmonella typhimurium* virulence. *Proc Natl Acad Sci U S A, 86*(13), 5054-5058.
Milton, M. E., Minrovic, B. M., Harris, D. L., Kang, B., Jung, D., Lewis, C. P., . . . Cavanagh, J. (2018). Re-sensitizing Multidrug Resistant Bacteria to Antibiotics by Targeting Bacterial Response Regulators: Characterization and Comparison of Interactions between 2-Aminoimidazoles and the Response Regulators BfmR from *Acinetobacter baumannii* and QseB from Francisella spp. *Front Mol Biosci, 5*, 15. doi:10.3389/fmolb.2018.00015
Moffatt, J. H., Harper, M., Harrison, P., Hale, J. D., Vinogradov, E., Seemann, T., . . . Boyce, J. D. (2010). Colistin resistance in *Acinetobacter baumannii* is mediated by complete loss of lipopolysaccharide production. *Antimicrob Agents Chemother, 54*(12), 4971-4977. doi:10.1128/AAC.00834-10
Moffatt, J. H., Harper, M., Mansell, A., Crane, B., Fitzsimons, T. C., Nation, R. L., . . . Boyce, J. D. (2013). Lipopolysaccharide-deficient *Acinetobacter baumannii* shows altered signaling through host Toll-like receptors and increased susceptibility to the host antimicrobial peptide LL-37. *Infect Immun, 81*(3), 684-689. doi:10.1128/IAI.01362-12
Moon, D. C., Choi, C. H., Lee, J. H., Choi, C. W., Kim, H. Y., Park, J. S., . . . Lee, J. C. (2012). *Acinetobacter baumannii* outer membrane protein A modulates the biogenesis of outer membrane vesicles. *J Microbiol, 50*(1), 155-160. doi:10.1007/s12275-012-1589-4

Moon, K. H., Weber, B. S., & Feldman, M. F. (2017). Subinhibitory Concentrations of Trimethoprim and Sulfamethoxazole Prevent Biofilm Formation by *Acinetobacter baumannii* through Inhibition of Csu Pilus Expression. *Antimicrob Agents Chemother, 61*(9). doi:10.1128/AAC.00778-17

Morris, F. C., Dexter, C., Kostoulias, X., Uddin, M. I., & Peleg, A. Y. (2019). The Mechanisms of Disease Caused by *Acinetobacter baumannii*. *Front Microbiol, 10*, 1601. doi:10.3389/fmicb.2019.01601

Mu, X., Wang, N., Li, X., Shi, K., Zhou, Z., Yu, Y., & Hua, X. (2016). The Effect of Colistin Resistance-Associated Mutations on the Fitness of *Acinetobacter baumannii*. *Front Microbiol, 7*, 1715. doi:10.3389/fmicb.2016.01715

Mussi, M. A., Limansky, A. S., & Viale, A. M. (2005). Acquisition of resistance to carbapenems in multidrug-resistant clinical strains of *Acinetobacter baumannii*: natural insertional inactivation of a gene encoding a member of a novel family of beta-barrel outer membrane proteins. *Antimicrob Agents Chemother, 49*(4), 1432-1440. doi:10.1128/AAC.49.4.1432-1440.2005

Nait Chabane, Y., Marti, S., Rihouey, C., Alexandre, S., Hardouin, J., Lesouhaitier, O., . . . De, E. (2014). Characterisation of pellicles formed by *Acinetobacter baumannii* at the air-liquid interface. *PLoS One, 9*(10), e111660. doi:10.1371/journal.pone.0111660

Nemec, A., Dolzani, L., Brisse, S., van den Broek, P., & Dijkshoorn, L. (2004). Diversity of aminoglycoside-resistance genes and their association with class 1 integrons among strains of pan-European *Acinetobacter baumannii* clones. *J Med Microbiol, 53*(Pt 12), 1233-1240. doi:10.1099/jmm.0.45716-0

Ni, W., Han, Y., Zhao, J., Wei, C., Cui, J., Wang, R., & Liu, Y. (2016). Tigecycline treatment experience against multidrug-resistant *Acinetobacter baumannii* infections: a systematic review and meta-analysis. *Int J Antimicrob Agents, 47*(2), 107-116. doi:10.1016/j.ijantimicag.2015.11.011

Nixon, B. T., Ronson, C. W., & Ausubel, F. M. (1986). Two-component regulatory systems responsive to environmental stimuli share strongly conserved domains with the nitrogen assimilation regulatory genes ntrB and ntrC. *Proc Natl Acad Sci U S A, 83*(20), 7850-7854.

Njoroge, J., & Sperandio, V. (2009). Jamming bacterial communication: new approaches for the treatment of infectious diseases. *EMBO Mol Med, 1*(4), 201-210. doi:10.1002/emmm.200900032

Nordmann, P., & Poirel, L. (2005). Emergence of plasmid-mediated resistance to quinolones in Enterobacteriaceae. *J Antimicrob Chemother, 56*(3), 463-469. doi:10.1093/jac/dki245

Nwugo, C. C., Gaddy, J. A., Zimbler, D. L., & Actis, L. A. (2011). Deciphering the iron response in *Acinetobacter baumannii*: A proteomics approach. *J Proteomics, 74*(1), 44-58. doi:10.1016/j.jprot.2010.07.010

O'Hara, J. A., Ambe, L. A., Casella, L. G., Townsend, B. M., Pelletier, M. R., Ernst, R. K., . . . Doi, Y. (2013). Activities of vancomycin-containing regimens against colistin-resistant *Acinetobacter baumannii* clinical strains. *Antimicrob Agents Chemother, 57*(5), 2103-2108. doi:10.1128/AAC.02501-12

O'Toole, G. A., & Kolter, R. (1998). Flagellar and twitching motility are necessary for *Pseudomonas aeruginosa* biofilm development. *Mol Microbiol, 30*(2), 295-304.

Oddo, A., Thomsen, T. T., Kjelstrup, S., Gorey, C., Franzyk, H., Frimodt-Moller, N., . . . Hansen, P. R. (2015). An Amphipathic Undecapeptide with All d-Amino Acids Shows

Promising Activity against Colistin-Resistant Strains of *Acinetobacter baumannii* and a Dual Mode of Action. *Antimicrob Agents Chemother, 60*(1), 592-599. doi:10.1128/AAC.01966-15

Okada, A., Igarashi, M., Okajima, T., Kinoshita, N., Umekita, M., Sawa, R., . . . Utsumi, R. (2010). Walkmycin B targets WalK (YycG), a histidine kinase essential for bacterial cell growth. *J Antibiot (Tokyo), 63*(2), 89-94. doi:10.1038/ja.2009.128

Ou, H.-Y., Kuang, S. N., He, X., Molgora, B. M., Ewing, P. J., Deng, Z., . . . Xu, H. H. (2015). Complete genome sequence of hypervirulent and outbreak-associated *Acinetobacter baumannii* strain LAC-4: epidemiology, resistance genetic determinants and potential virulence factors. *Sci. Rep., 5*, 8643. doi:10.1038/srep08643

Ou, H. Y., Kuang, S. N., He, X., Molgora, B. M., Ewing, P. J., Deng, Z., . . . Xu, H. H. (2015). Complete genome sequence of hypervirulent and outbreak-associated *Acinetobacter baumannii* strain LAC-4: epidemiology, resistance genetic determinants and potential virulence factors. *Sci Rep, 5*, 8643. doi:10.1038/srep08643

Pachon-Ibanez, M. E., Docobo-Perez, F., Lopez-Rojas, R., Dominguez-Herrera, J., Jimenez-Mejias, M. E., Garcia-Curiel, A., . . . Pachon, J. (2010). Efficacy of rifampin and its combinations with imipenem, sulbactam, and colistin in experimental models of infection caused by imipenem-resistant *Acinetobacter baumannii*. *Antimicrob Agents Chemother, 54*(3), 1165-1172. doi:10.1128/AAC.00367-09

Paget, E., & Davies, J. (1996). Apramycin resistance as a selective marker for gene transfer in mycobacteria. *J Bacteriol, 178*(21), 6357-6360.

Paget, E., & Davies, J. (1996). Apramycin resistance as a selective marker for gene transfer in mycobacteria. *Journal of Bacteriology, 178*(21), 6357-6360. doi:10.1128/jb.178.21.6357-6360.1996

Pakharukova, N., Tuittila, M., Paavilainen, S., Malmi, H., Parilova, O., Teneberg, S., . . . Zavialov, A. V. (2018). Structural basis for *Acinetobacter baumannii* biofilm formation. *Proc Natl Acad Sci U S A*. doi:10.1073/pnas.1800961115

Park, Y. K., Choi, J. Y., Shin, D., & Ko, K. S. (2011). Correlation between overexpression and amino acid substitution of the PmrAB locus and colistin resistance in *Acinetobacter baumannii*. *Int J Antimicrob Agents, 37*(6), 525-530. doi:10.1016/j.ijantimicag.2011.02.008

Parsek, M. R., & Singh, P. K. (2003). Bacterial biofilms: an emerging link to disease pathogenesis. *Annu Rev Microbiol, 57*, 677-701. doi:10.1146/annurev.micro.57.030502.090720

Payne, D. E., Martin, N. R., Parzych, K. R., Rickard, A. H., Underwood, A., & Boles, B. R. (2013). Tannic acid inhibits *Staphylococcus aureus* surface colonization in an IsaA-dependent manner. *Infection and Immunity, 81*(2), 496-504. doi:10.1128/iai.00877-12

Peleg, A. Y., de Breij, A., Adams, M. D., Cerqueira, G. M., Mocali, S., Galardini, M., . . . Dijkshoorn, L. (2012). The success of *Acinetobacter* species; genetic, metabolic and virulence attributes. *PLoS One, 7*(10), e46984. doi:10.1371/journal.pone.0046984

Peleg, A. Y., Jara, S., Monga, D., Eliopoulos, G. M., Moellering, R. C., Jr., & Mylonakis, E. (2009). *Galleria mellonella* as a model system to study *Acinetobacter baumannii* pathogenesis and therapeutics. *Antimicrob Agents Chemother, 53*(6), 2605-2609. doi:10.1128/AAC.01533-08

Peleg, A. Y., & Paterson, D. L. (2006). Multidrug-resistant *Acinetobacter*: a threat to the antibiotic era. *Intern Med J, 36*(8), 479-482. doi:10.1111/j.1445-5994.2006.01130.x

Peleg, A. Y., Seifert, H., & Paterson, D. L. (2008). *Acinetobacter baumannii*: emergence of a successful pathogen. *Clin Microbiol Rev, 21*(3), 538-582. doi:10.1128/CMR.00058-07

Peleg, A. Y., Tampakakis, E., Fuchs, B. B., Eliopoulos, G. M., Moellering, R. C., Jr., & Mylonakis, E. (2008). Prokaryote-eukaryote interactions identified by using *Caenorhabditis elegans*. *Proc Natl Acad Sci U S A, 105*(38), 14585-14590. doi:10.1073/pnas.0805048105

Perez, F., Hujer, A. M., Hujer, K. M., Decker, B. K., Rather, P. N., & Bonomo, R. A. (2007). Global challenge of multidrug-resistant *Acinetobacter baumannii*. *Antimicrob Agents Chemother, 51*(10), 3471-3484. doi:10.1128/AAC.01464-06

Perez-Varela, M., Corral, J., Vallejo, J. A., Rumbo-Feal, S., Bou, G., Aranda, J., & Barbe, J. (2017). Mutations in the beta-Subunit of the RNA Polymerase Impair the Surface-Associated Motility and Virulence of *Acinetobacter baumannii*. *Infect Immun, 85*(8). doi:10.1128/IAI.00327-17

Peters, J. E. (2014). Tn7. *Microbiol Spectr, 2*(5). doi:10.1128/microbiolspec.MDNA3-0010-2014

Peters, J. E., & Craig, N. L. (2001a). Tn7 recognizes transposition target structures associated with DNA replication using the DNA-binding protein TnsE. *Genes Dev, 15*(6), 737-747. doi:10.1101/gad.870201

Peters, J. E., & Craig, N. L. (2001b). Tn7: smarter than we thought. *Nat Rev Mol Cell Biol, 2*(11), 806-814. doi:10.1038/35099006

Peters, J. E., & Craig, N. L. (2001). Tn*7*: smarter than we thought. *Nat. Rev. Mol. Cell Biol., 2*, 806-814.

Peterson, A. A., Fesik, S. W., & McGroarty, E. J. (1987). Decreased binding of antibiotics to lipopolysaccharides from polymyxin-resistant strains of *Escherichia coli* and *Salmonella typhimurium*. *Antimicrob Agents Chemother, 31*(2), 230-237. doi:10.1128/aac.31.2.230

Pfaffl, M. W. (2001). A new mathematical model for relative quantification in real-time RT-PCR. *Nucleic Acids Res, 29*(9), e45.

Plumley, B. A., Martin, K. H., Borlee, G. I., Marlenee, N. L., Burtnick, M. N., Brett, P. J., . . . Borlee, B. R. (2017). Thermoregulation of Biofilm Formation in *Burkholderia pseudomallei* Is Disrupted by Mutation of a Putative Diguanylate Cyclase. *J Bacteriol, 199*(5). doi:10.1128/JB.00780-16

Pumirat, P., Vanaporn, M., Boonyuen, U., Indrawattana, N., Rungruengkitkun, A., & Chantratita, N. (2017). Effects of sodium chloride on heat resistance, oxidative susceptibility, motility, biofilm and plaque formation of *Burkholderia pseudomallei*. *Microbiologyopen, 6*(4). doi:10.1002/mbo3.493

Quale, J., Bratu, S., Landman, D., & Heddurshetti, R. (2003). Molecular epidemiology and mechanisms of carbapenem resistance in *Acinetobacter baumannii* endemic in New York City. *Clin Infect Dis, 37*(2), 214-220. doi:10.1086/375821

Quesada, A., Porrero, M. C., Tellez, S., Palomo, G., Garcia, M., & Dominguez, L. (2015). Polymorphism of genes encoding PmrAB in colistin-resistant strains of *Escherichia coli* and *Salmonella enterica* isolated from poultry and swine. *J Antimicrob Chemother, 70*(1), 71-74. doi:10.1093/jac/dku320

Raetz, C. R., Reynolds, C. M., Trent, M. S., & Bishop, R. E. (2007). Lipid A modification systems in gram-negative bacteria. *Annu Rev Biochem, 76*, 295-329. doi:10.1146/annurev.biochem.76.010307.145803

Ramesh, A., DebRoy, S., Goodson, J. R., Fox, K. A., Faz, H., Garsin, D. A., & Winkler, W. C. (2012). The mechanism for RNA recognition by ANTAR regulators of gene expression. *PLoS Genet, 8*(6), e1002666. doi:10.1371/journal.pgen.1002666

Rasko, D. A., Moreira, C. G., Li de, R., Reading, N. C., Ritchie, J. M., Waldor, M. K., . . . Sperandio, V. (2008). Targeting QseC signaling and virulence for antibiotic development. *Science, 321*(5892), 1078-1080. doi:10.1126/science.1160354

Reis, A. O., Luz, D. A., Tognim, M. C., Sader, H. S., & Gales, A. C. (2003). Polymyxin-resistant *Acinetobacter* spp. isolates: what is next? *Emerg Infect Dis, 9*(8), 1025-1027. doi:10.3201/eid0908.030052

Renckens, R., Roelofs, J. J., Knapp, S., de Vos, A. F., Florquin, S., & van der Poll, T. (2006). The acute-phase response and serum amyloid A inhibit the inflammatory response to *Acinetobacter baumannii* Pneumonia. *J Infect Dis, 193*(2), 187-195. doi:10.1086/498876

Ribera, A., Ruiz, J., & Vila, J. (2003). Presence of the Tet M determinant in a clinical isolate of *Acinetobacter baumannii*. *Antimicrob Agents Chemother, 47*(7), 2310-2312. doi:10.1128/aac.47.7.2310-2312.2003

Richmond, G. E., Evans, L. P., Anderson, M. J., Wand, M. E., Bonney, L. C., Ivens, A., . . . Piddock, L. J. (2016). The *Acinetobacter baumannii* Two-Component System AdeRS Regulates Genes Required for Multidrug Efflux, Biofilm Formation, and Virulence in a Strain-Specific Manner. *MBio, 7*(2), e00430-00416. doi:10.1128/mBio.00430-16

Robicsek, A., Sahm, D. F., Strahilevitz, J., Jacoby, G. A., & Hooper, D. C. (2005). Broader distribution of plasmid-mediated quinolone resistance in the United States. *Antimicrob Agents Chemother, 49*(7), 3001-3003. doi:10.1128/AAC.49.7.3001-3003.2005

Roca, I., Espinal, P., Vila-Farres, X., & Vila, J. (2012). The *Acinetobacter baumannii* Oxymoron: Commensal Hospital Dweller Turned Pan-Drug-Resistant Menace. *Front Microbiol, 3*, 148. doi:10.3389/fmicb.2012.00148

Rodriguez-Bano, J., Cisneros, J. M., Fernandez-Cuenca, F., Ribera, A., Vila, J., Pascual, A., . . . Grupo de Estudio de Infeccion, H. (2004). Clinical features and epidemiology of *Acinetobacter baumannii* colonization and infection in Spanish hospitals. *Infect Control Hosp Epidemiol, 25*(10), 819-824. doi:10.1086/502302

Rodriguez-Hernandez, M. J., Jimenez-Mejias, M. E., Pichardo, C., Cuberos, L., Garcia-Curiel, A., & Pachon, J. (2004). Colistin efficacy in an experimental model of *Acinetobacter baumannii* endocarditis. *Clin Microbiol Infect, 10*(6), 581-584. doi:10.1111/j.1469-0691.2004.00910.x

Rolain, J. M., Diene, S. M., Kempf, M., Gimenez, G., Robert, C., & Raoult, D. (2013). Real-time sequencing to decipher the molecular mechanism of resistance of a clinical pan-drug-resistant *Acinetobacter baumannii* isolate from Marseille, France. *Antimicrob Agents Chemother, 57*(1), 592-596. doi:10.1128/AAC.01314-12

Romero-Jimenez, L., Rodriguez-Carbonell, D., Gallegos, M. T., Sanjuan, J., & Perez-Mendoza, D. (2015). Mini-Tn7 vectors for stable expression of diguanylate cyclase PleD* in Gram-negative bacteria. *BMC Microbiol, 15*, 190. doi:10.1186/s12866-015-0521-6

Rosenfeld, N., Bouchier, C., Courvalin, P., & Perichon, B. (2012). Expression of the resistance-nodulation-cell division pump AdeIJK in *Acinetobacter baumannii* is regulated by AdeN, a TetR-type regulator. *Antimicrob Agents Chemother, 56*(5), 2504-2510. doi:10.1128/AAC.06422-11

Roychoudhury, S., Zielinski, N. A., Ninfa, A. J., Allen, N. E., Jungheim, L. N., Nicas, T. I., & Chakrabarty, A. M. (1993). Inhibitors of two-component signal transduction systems:

inhibition of alginate gene activation in *Pseudomonas aeruginosa*. *Proc Natl Acad Sci U S A, 90*(3), 965-969.
Russo, T. A., Luke, N. R., Beanan, J. M., Olson, R., Sauberan, S. L., MacDonald, U., . . . Campagnari, A. A. (2010). The K1 capsular polysaccharide of *Acinetobacter baumannii* strain 307-0294 is a major virulence factor. *Infect Immun, 78*(9), 3993-4000. doi:10.1128/IAI.00366-10
Ruzin, A., Keeney, D., & Bradford, P. A. (2007). AdeABC multidrug efflux pump is associated with decreased susceptibility to tigecycline in *Acinetobacter calcoaceticus-Acinetobacter baumannii* complex. *J Antimicrob Chemother, 59*(5), 1001-1004. doi:10.1093/jac/dkm058
Sarnovsky, R. J., May, E. W., & Craig, N. L. (1996). The Tn7 transposase is a heteromeric complex in which DNA breakage and joining activities are distributed between different gene products. *EMBO J, 15*(22), 6348-6361.
Seward, R. J., & Towner, K. J. (1998). Molecular epidemiology of quinolone resistance in *Acinetobacter* spp. *Clin Microbiol Infect, 4*(5), 248-254.
Shu, C. J., & Zhulin, I. B. (2002). ANTAR: an RNA-binding domain in transcription antitermination regulatory proteins. *Trends Biochem Sci, 27*(1), 3-5.
Sievert, D. M., Ricks, P., Edwards, J. R., Schneider, A., Patel, J., Srinivasan, A., . . . Participating, N. F. (2013). Antimicrobial-resistant pathogens associated with healthcare-associated infections: summary of data reported to the National Healthcare Safety Network at the Centers for Disease Control and Prevention, 2009-2010. *Infect Control Hosp Epidemiol, 34*(1), 1-14. doi:10.1086/668770
Smith, M. G., Gianoulis, T. A., Pukatzki, S., Mekalanos, J. J., Ornston, L. N., Gerstein, M., & Snyder, M. (2007). New insights into *Acinetobacter baumannii* pathogenesis revealed by high-density pyrosequencing and transposon mutagenesis. *Genes Dev., 21*(5), 601-614. doi:10.1101/gad.1510307
Smith, M. G., Gianoulis, T. A., Pukatzki, S., Mekalanos, J. J., Ornston, L. N., Gerstein, M., & Snyder, M. (2007). New insights into *Acinetobacter baumannii* pathogenesis revealed by high-density pyrosequencing and transposon mutagenesis. *Genes Dev, 21*(5), 601-614. doi:10.1101/gad.1510307
Smith, S. G., Mahon, V., Lambert, M. A., & Fagan, R. P. (2007). A molecular Swiss army knife: OmpA structure, function and expression. *FEMS Microbiol Lett, 273*(1), 1-11. doi:10.1111/j.1574-6968.2007.00778.x
Sperandio, V., Torres, A. G., & Kaper, J. B. (2002). Quorum sensing *Escherichia coli* regulators B and C (QseBC): a novel two-component regulatory system involved in the regulation of flagella and motility by quorum sensing in *E. coli*. *Mol Microbiol, 43*(3), 809-821.
Stacy, D. M., Welsh, M. A., Rather, P. N., & Blackwell, H. E. (2012). Attenuation of quorum sensing in the pathogen *Acinetobacter baumannii* using non-native N-Acyl homoserine lactones. *ACS Chem Biol, 7*(10), 1719-1728. doi:10.1021/cb300351x
Stewart, V., & van Tilbeurgh, H. (2012). Found: the elusive ANTAR transcription antiterminator. *PLoS Genet, 8*(6), e1002773. doi:10.1371/journal.pgen.1002773
Stock, A. M., Robinson, V. L., & Goudreau, P. N. (2000). Two-component signal transduction. *Annu Rev Biochem, 69*, 183-215. doi:10.1146/annurev.biochem.69.1.183
Su, X. Z., Chen, J., Mizushima, T., Kuroda, T., & Tsuchiya, T. (2005). AbeM, an H+-coupled *Acinetobacter baumannii* multidrug efflux pump belonging to the MATE family of

transporters. *Antimicrob Agents Chemother, 49*(10), 4362-4364. doi:10.1128/AAC.49.10.4362-4364.2005

Sugawara, E., & Nikaido, H. (2012). OmpA is the principal nonspecific slow porin of *Acinetobacter baumannii*. *J Bacteriol, 194*(15), 4089-4096. doi:10.1128/JB.00435-12

Sun, J. R., Jeng, W. Y., Perng, C. L., Yang, Y. S., Soo, P. C., Chiang, Y. S., & Chiueh, T. S. (2016). Single amino acid substitution Gly186Val in AdeS restores tigecycline susceptibility of *Acinetobacter baumannii*. *J Antimicrob Chemother, 71*(6), 1488-1492. doi:10.1093/jac/dkw002

Sun, J. R., Perng, C. L., Lin, J. C., Yang, Y. S., Chan, M. C., Chang, T. Y., . . . Chiueh, T. S. (2014). AdeRS combination codes differentiate the response to efflux pump inhibitors in tigecycline-resistant isolates of extensively drug-resistant *Acinetobacter baumannii*. *Eur J Clin Microbiol Infect Dis, 33*(12), 2141-2147. doi:10.1007/s10096-014-2179-7

Szurmant, H., White, R. A., & Hoch, J. A. (2007). Sensor complexes regulating two-component signal transduction. *Curr Opin Struct Biol, 17*(6), 706-715. doi:10.1016/j.sbi.2007.08.019

Tacconelli, E., Carrara, E., Savoldi, A., Harbarth, S., Mendelson, M., Monnet, D. L., . . . Group, W. H. O. P. P. L. W. (2018). Discovery, research, and development of new antibiotics: the WHO priority list of antibiotic-resistant bacteria and tuberculosis. *Lancet Infect Dis, 18*(3), 318-327. doi:10.1016/S1473-3099(17)30753-3

Tamayo, R., Choudhury, B., Septer, A., Merighi, M., Carlson, R., & Gunn, J. S. (2005). Identification of cptA, a PmrA-regulated locus required for phosphoethanolamine modification of the *Salmonella enterica* serovar typhimurium lipopolysaccharide core. *J Bacteriol, 187*(10), 3391-3399. doi:10.1128/JB.187.10.3391-3399.2005

Tamayo, R., Prouty, A. M., & Gunn, J. S. (2005). Identification and functional analysis of *Salmonella enterica* serovar Typhimurium PmrA-regulated genes. *FEMS Immunol Med Microbiol, 43*(2), 249-258. doi:10.1016/j.femsim.2004.08.007

Thompson, R. J., Bobay, B. G., Stowe, S. D., Olson, A. L., Peng, L., Su, Z., . . . Cavanagh, J. (2012). Identification of BfmR, a response regulator involved in biofilm development, as a target for a 2-Aminoimidazole-based antibiofilm agent. *Biochemistry, 51*(49), 9776-9778. doi:10.1021/bi3015289

Tilley, D., Law, R., Warren, S., Samis, J. A., & Kumar, A. (2014). CpaA a novel protease from *Acinetobacter baumannii* clinical isolates deregulates blood coagulation. *FEMS Microbiol Lett, 356*(1), 53-61. doi:10.1111/1574-6968.12496

Timsit, J. F., Soubirou, J. F., Voiriot, G., Chemam, S., Neuville, M., Mourvillier, B., . . . Wolff, M. (2014). Treatment of bloodstream infections in ICUs. *BMC Infect Dis, 14*, 489. doi:10.1186/1471-2334-14-489

Tipton, K. A., & Rather, P. N. (2016). An ompR/envZ Two-Component System Ortholog Regulates Phase Variation, Osmotic Tolerance, Motility, and Virulence in *Acinetobacter baumannii* strain AB5075. *J Bacteriol*. doi:10.1128/JB.00705-16

Tiwari, S., Jamal, S. B., Hassan, S. S., Carvalho, P., Almeida, S., Barh, D., . . . Azevedo, V. (2017). Two-Component Signal Transduction Systems of Pathogenic Bacteria As Targets for Antimicrobial Therapy: An Overview. *Front Microbiol, 8*, 1878. doi:10.3389/fmicb.2017.01878

Tomaras, A. P., Dorsey, C. W., Edelmann, R. E., & Actis, L. A. (2003). Attachment to and biofilm formation on abiotic surfaces by *Acinetobacter baumannii*: involvement of a novel chaperone-usher pili assembly system. *Microbiology, 149*(Pt 12), 3473-3484. doi:10.1099/mic.0.26541-0

Tomaras, A. P., Flagler, M. J., Dorsey, C. W., Gaddy, J. A., & Actis, L. A. (2008). Characterization of a two-component regulatory system from *Acinetobacter baumannii* that controls biofilm formation and cellular morphology. *Microbiology, 154*(Pt 11), 3398-3409. doi:10.1099/mic.0.2008/019471-0

Turton, J. F., Kaufmann, M. E., Gill, M. J., Pike, R., Scott, P. T., Fishbain, J., . . . Pitt, T. L. (2006). Comparison of *Acinetobacter baumannii* isolates from the United Kingdom and the United States that were associated with repatriated casualties of the Iraq conflict. *J Clin Microbiol, 44*(7), 2630-2634. doi:10.1128/JCM.00547-06

Ulijasz, A. T., & Weisblum, B. (1999). Dissecting the VanRS signal transduction pathway with specific inhibitors. *J Bacteriol, 181*(2), 627-631.

Ulrich, L. E., & Zhulin, I. B. (2007). MiST: a microbial signal transduction database. *Nucleic Acids Res, 35*(Database issue), D386-390. doi:10.1093/nar/gkl932

Utashima, Y., Yamashita, S., Arima, T.-H., & Masaki, K. (2017). Codon optimization enables the Zeocin resistance marker's use in the ascomycete yeast *Debaryomyces occidentalis*. *The Journal of General and Applied Microbiology, 63*(4), 254-257. doi:10.2323/jgam.2016.11.003

Vila, J., Ruiz, J., Goni, P., & Jimenez de Anta, T. (1997). Quinolone-resistance mutations in the topoisomerase IV parC gene of *Acinetobacter baumannii*. *J Antimicrob Chemother, 39*(6), 757-762. doi:10.1093/jac/39.6.757

Vila, J., Ruiz, J., Goni, P., Marcos, A., & Jimenez de Anta, T. (1995). Mutation in the gyrA gene of quinolone-resistant clinical isolates of *Acinetobacter baumannii*. *Antimicrob Agents Chemother, 39*(5), 1201-1203. doi:10.1128/aac.39.5.1201

Visca, P., Seifert, H., & Towner, K. J. (2011). *Acinetobacter* infection--an emerging threat to human health. *IUBMB Life, 63*(12), 1048-1054. doi:10.1002/iub.534

Waddell, C. S., & Craig, N. L. (1988). Tn7 transposition: two transposition pathways directed by five Tn7-encoded genes. *Genes Dev, 2*(2), 137-149.

Waddell, C. S., & Craig, N. L. (1989). Tn7 transposition: recognition of the *att*Tn*7* target sequence. *Proc Natl Acad Sci U S A, 86*(11), 3958-3962.

Walker, J. E., Gay, N. J., Saraste, M., & Eberle, A. N. (1984). DNA sequence around the *Escherichia coli* unc operon. Completion of the sequence of a 17 kilobase segment containing asnA, oriC, unc, glmS and phoS. *Biochem J, 224*(3), 799-815.

Walsh, T. R. (2005). The emergence and implications of metallo-beta-lactamases in Gram-negative bacteria. *Clin Microbiol Infect, 11 Suppl 6*, 2-9. doi:10.1111/j.1469-0691.2005.01264.x

Wen, Y., Ouyang, Z., Yu, Y., Zhou, X., Pei, Y., Devreese, B., . . . Zheng, F. (2017). Mechanistic insight into how multidrug resistant *Acinetobacter baumannii* response regulator AdeR recognizes an intercistronic region. *Nucleic Acids Res, 45*(16), 9773-9787. doi:10.1093/nar/gkx624

Whitworth, D. E. (2008). Genomes and knowledge - a questionable relationship? *Trends Microbiol, 16*(11), 512-519. doi:10.1016/j.tim.2008.08.001

Whitworth, D. E., & Cock, P. J. (2008). Two-component systems of the myxobacteria: structure, diversity and evolutionary relationships. *Microbiology, 154*(Pt 2), 360-372. doi:10.1099/mic.0.2007/013672-0

Whitworth, D. E., & Cock, P. J. (2009). Evolution of prokaryotic two-component systems: insights from comparative genomics. *Amino Acids, 37*(3), 459-466. doi:10.1007/s00726-009-0259-2

Wilson, S. A., Wachira, S. J., Norman, R. A., Pearl, L. H., & Drew, R. E. (1996). Transcription antitermination regulation of the *Pseudomonas aeruginosa* amidase operon. *EMBO J, 15*(21), 5907-5916.

Wisniewski, J. R., Zougman, A., Nagaraj, N., & Mann, M. (2009). Universal sample preparation method for proteome analysis. *Nat Methods, 6*(5), 359-362. doi:10.1038/nmeth.1322

Wong, D., Nielsen, T. B., Bonomo, R. A., Pantapalangkoor, P., Luna, B., & Spellberg, B. (2017). Clinical and Pathophysiological Overview of *Acinetobacter* Infections: a Century of Challenges. *Clin Microbiol Rev, 30*(1), 409-447. doi:10.1128/CMR.00058-16

Wright, M. S., Haft, D. H., Harkins, D. M., Perez, F., Hujer, K. M., Bajaksouzian, S., . . . Adams, M. D. (2014). New insights into dissemination and variation of the health care-associated pathogen *Acinetobacter baumannii* from genomic analysis. *MBio, 5*(1), e00963-00913. doi:10.1128/mBio.00963-13

Wuichet, K., Cantwell, B. J., & Zhulin, I. B. (2010). Evolution and phyletic distribution of two-component signal transduction systems. *Curr Opin Microbiol, 13*(2), 219-225. doi:10.1016/j.mib.2009.12.011

Yamamoto, K., Hirao, K., Oshima, T., Aiba, H., Utsumi, R., & Ishihama, A. (2005). Functional characterization in vitro of all two-component signal transduction systems from *Escherichia coli*. *J Biol Chem, 280*(2), 1448-1456. doi:10.1074/jbc.M410104200

Yang, A., Tang, W. S., Si, T., & Tang, J. X. (2017). Influence of Physical Effects on the Swarming Motility of *Pseudomonas aeruginosa*. *Biophys J, 112*(7), 1462-1471. doi:10.1016/j.bpj.2017.02.019

Yildirim, S., Thompson, M. G., Jacobs, A. C., Zurawski, D. V., & Kirkup, B. C. (2016). Evaluation of Parameters for High Efficiency Transformation of *Acinetobacter baumannii*. *Sci Rep, 6*, 22110. doi:10.1038/srep22110

Yoon, E. J., Balloy, V., Fiette, L., Chignard, M., Courvalin, P., & Grillot-Courvalin, C. (2016). Contribution of the Ade Resistance-Nodulation-Cell Division-Type Efflux Pumps to Fitness and Pathogenesis of *Acinetobacter baumannii*. *MBio, 7*(3). doi:10.1128/mBio.00697-16

Yoon, E. J., Courvalin, P., & Grillot-Courvalin, C. (2013). RND-type efflux pumps in multidrug-resistant clinical isolates of *Acinetobacter baumannii*: major role for AdeABC overexpression and AdeRS mutations. *Antimicrob Agents Chemother, 57*(7), 2989-2995. doi:10.1128/AAC.02556-12

Yuhan, Y., Ziyun, Y., Yongbo, Z., Fuqiang, L., & Qinghua, Z. (2016). Over expression of AdeABC and AcrAB-TolC efflux systems confers tigecycline resistance in clinical isolates of *Acinetobacter baumannii* and *Klebsiella pneumoniae*. *Rev Soc Bras Med Trop, 49*(2), 165-171. doi:10.1590/0037-8682-0411-2015

Zschiedrich, C. P., Keidel, V., & Szurmant, H. (2016). Molecular Mechanisms of Two-Component Signal Transduction. *J Mol Biol, 428*(19), 3752-3775. doi:10.1016/j.jmb.2016.08.003

APPENDIX

Appendix I. Conservation of the TCSs in *A. baumannii* in sequenced and publicly available clinical strains

	17978mff CP012004.1		AB030 CP009257.1		Ab04-mff CP012006.1		LAC4 CP007712.1		AB0057 CP001182.2		AB5075-UW CP008706.1		AB031 CP009256.1		AYE CU459141.1	
Gene	Identity	Nucleotide conservation	Identity	Nucleotide conservation	Identity	Nucleotide conservation	Identity	Nucleotide conservation	Identity	Nucleotide conservation	Identity	Nucleotide conservation	Identity	Nucleotide conservation	Identity	Nucleotide conservation
A1S_0234	99%	446/447	98%	438/447	97%	434/447	97%	434/447	98%	437/447	98%	437/447	93%	417/447	98%	437/447
A1S_0235	100%	1524/1524	98%	1497/1524	99%	1505/1524	99%	1506/1524	98%	1501/1524	98%	1501/1524	98%	1500/1524	98%	1501/1524
A1S_0236	100%	636/636	99%	634/636	99%	633/636	99%	632/636	99%	631/636	99%	631/636	99%	631/636	99%	631/636
A1S_0260	100%	1140/1140	99%	1134/1140	99%	1132/1140	99%	1132/1140	99%	1128/1140	99%	1128/1140	99%	1131/1140	99%	1128/1140
A1S_0261	100%	741/741	99%	737/741	99%	736/741	99%	735/741	99%	733/741	99%	733/741	99%	736/741	99%	733/741
A1S_0574	100%	2808/2808	99%	2780/2808	99%	2769/2808	99%	2769/2808	99%	2773/2808	99%	2773/2808	99%	2773/2808	99%	2773/2808
A1S_0748	100%	717/717	99%	713/717	99%	708/717	99%	708/717	99%	713/717	99%	713/717	100%	717/717	99%	713/717
A1S_0749	100%	1593/1593	98%	1564/1593	97%	1550/1593	97%	1550/1593	98%	1566/1593	98%	1566/1593	99%	1587/1593	98%	1566/1593
A1S_1393	100%	3465/3465	94%	3261/3465	94%	3258/3465	94%	3257/3465	95%	3299/3465	95%	3299/3465	95%	3303/3465	95%	3298/3465
A1S_1394	100%	960/960	96%	920/960	99%	952/960	99%	951/960	97%	928/960	97%	928/960	96%	922/960	97%	928/960
A1S_1753	100%	744/744	98%	731/744	-	-	-	-	99%	735/744	99%	735/744	97%	721/744	99%	735/744
A1S_1754	100%	1086/1086	98%	1041/1065	-	-	-	-	97%	1052/1086	97%	1052/1086	disrupted	disrupted	97%	1052/1086
A1S_1977	100%	1110/1110	99%	1094/1110	99%	1094/1110	99%	1094/1110	98%	1093/1110	98%	1093/1110	99%	1096/1110	98%	1093/1110
A1S_1978	100%	1494/1494	97%	1454/1494	97%	1452/1494	97%	1451/1494	97%	1448/1494	97%	1447/1494	97%	1449/1494	97%	1448/1494
A1S_2006	100%	591/591	Disrupted		100%	591/591	100%	591/591	99%	588/591	99%	588/591	99%	588/591	99%	588/591
A1S_2137	100%	717/717	93%	669/717	95%	674/711	95%	673/711	95%	681/717	95%	681/717	98%	703/717	95%	680/717
A1S_2138	100%	2655/2655	95%	2526/2656	94%	2509/2656	95%	2510/2656	96%	2537/2656	96%	2537/2656	94%	2502/2656	96%	2538/2656
A1S_2287	99%	1358/1360	99%	1342/1360	99%	1356/1360	99%	1355/1360	98%	1336/1360	98%	1336/1360	99%	1344/1360	98%	1336/1360
A1S_2750	100%	1335/1335	99%	1318/1335	99%	1330/1335	99%	1330/1335	99%	1316/1335	99%	1316/1335	99%	1318/1335	99%	1316/1335
A1S_2751	100%	675/675	99%	670/675	99%	665/675	99%	665/675	99%	668/675	99%	668/675	99%	671/675	99%	668/675
A1S_2811	100%	4521/4521	98%	4426/4521	98%	4441/4521	98%	4442/4521	98%	4433/4521	98%	4433/4521	98%	4442/4521	98%	4433/4521
A1S_2814	100%	363/363	99%	361/363	99%	362/363	99%	362/363	99%	362/363	99%	362/363	99%	362/363	99%	362/363
A1S_2815	100%	384/384	99%	383/384	99%	381/384	99%	381/384	99%	383/384	99%	383/384	99%	383/384	99%	383/384
A1S_2883	100%	687/687	99%	680/687	99%	684/687	99%	684/687	99%	678/687	99%	678/687	99%	679/687	99%	678/687
A1S_2884	99%	1463/1464	99%	1458/1464	99%	1457/1464	99%	1456/1464	99%	1454/1464	99%	1454/1464	99%	1449/1464	99%	1454/1464
A1S_2906	100%	1269/1269	99%	1250/1269	99%	1256/1269	99%	1256/1269	99%	1255/1269	99%	1255/1269	99%	1255/1269	99%	1255/1269
A1S_2937	100%	684/684	-	-	85%	579/684	100%	684/684	87%	592/684	87%	592/684	-	-	87%	592/684
A1S_2938	100%	1374/1374	-	-	-	-	99%	1372/1374	91%	1256/1377	91%	1256/1377	-	-	91%	1256/1377

A1S_3229	100%	765/765	99%	760/765	99%	757/765	99%	757/765	99%	756/765	99%	756/765	99%	761/765	99%	756/765
A1S_3230	100%	1458/1458	99%	1444/1458	99%	1445/1458	99%	1445/1458	99%	1440/1458	99%	1440/1458	99%	1452/1458	99%	1440/1458
A1S_3302	100%	3498/3498	98%	3441/3498	99%	3450/3498	99%	3450/3498	98%	3434/3498	98%	3434/3498	98%	3432/3498	98%	3434/3498
A1S_3304	100%	651/651	99%	644/651	99%	645/651	99%	645/651	99%	643/651	99%	643/651	99%	645/651	99%	643/651
A1S_3374	100%	164/164	100%	164/164	99%	163/164	99%	163/164	100%	164/164	100%	164/164	100%	164/164	100%	164/164
A1S_3376	100%	1359/1359	99%	1339/1359	98%	1329/1359	98%	1329/1359	98%	1331/1359	98%	1331/1359	99%	1341/1359	98%	1331/1359

Appendix II. List of upregulated proteins at 28˚C in *A. baumannii* ATCC 17978

Locus tag	Name	Log_2 fold change	GO term classification
A1S_0011	hypothetical protein	0.74	Enzymatic processes
A1S_0016	site-specific tyrosine recombinase	0.73	DNA binding, metabolism, and repair
A1S_0035	putative phosphoglycolate phosphatase 2 (PGP 2)	0.6	Enzymatic processes
A1S_0047	FKBP-type 22KD peptidyl-prolyl cis-trans isomerase (rotamase)	0.72	Protein binding, transport, and folding
A1S_0050	putative protein tyrosine phosphatase	0.77	Protein binding, transport, and folding
A1S_0067	L-lactate permease	0.64	Membrane structures and transport
A1S_0087	Short-chain dehydrogenase/reductase SDR	1.88	Unknown and hypothetical functions
A1S_0092	putative ferric siderophore receptor protein	0.64	RNA binding, processing, and translation
A1S_0112	Acyl-CoA synthetase/AMP-acid ligases II	3.18	Metabolic processes
A1S_0113	Acyl-CoA dehydrogenase	3.74	Enzymatic processes
A1S_0115	Amino acid adenylation	2.36	Biosynthetic process
A1S_0116	RND superfamily-like exporter	3.95	Membrane structures and transport
A1S_0133	hypothetical protein	3.58	Unknown and hypothetical functions
A1S_0157	hypothetical protein	2.19	Unknown and hypothetical functions
A1S_0158	hypothetical protein	0.55	Unknown and hypothetical functions
A1S_0183	hypothetical protein	1.31	Metabolic processes
A1S_0189	hypothetical protein	0.8	Unknown and hypothetical functions

A1S_0191	hypothetical protein	1.09	Unknown and hypothetical functions
A1S_0207	hypothetical protein	1.19	Unknown and hypothetical functions
A1S_0209	Transposase	1.13	DNA binding, metabolism, and repair
A1S_0210	Transposase	1.36	DNA binding, metabolism, and repair
A1S_0211	Transposition Helper	1.71	DNA binding, metabolism, and repair
A1S_0223	riboflavin synthase alpha chain	0.54	Unknown and hypothetical functions
A1S_0240	thiol:disulfide interchange protein	0.77	Protein binding, transport, and folding
A1S_0251	thiamine hydroxymethylpyrimidine moiety synthesis	0.61	RNA binding, processing, and translation
A1S_0281	preprotein translocase IISP family membrane subunit	0.8	Unknown and hypothetical functions
A1S_0283	50S ribosomal protein	0.73	Unknown and hypothetical functions
A1S_0284	50S ribosomal protein	0.59	Unknown and hypothetical functions
A1S_0285	50S ribosomal protein	0.54	RNA binding, processing, and translation
A1S_0286	50S ribosomal protein	0.61	RNA binding, processing, and translation
A1S_0302	hypothetical protein	0.72	Unknown and hypothetical functions
A1S_0304	hypothetical protein	1.83	Unknown and hypothetical functions
A1S_0320	hypothetical protein	1.96	Unknown and

			hypothetical functions
A1S_0324	putative tRNA/rRNA methyltransferase	0.83	RNA binding, processing, and translation
A1S_0330	triosephosphate isomerase	0.8	Carbohydrate metabolism
A1S_0334	hypothetical protein	0.61	Biosynthetic process
A1S_0335	transcription termination/antitermination L factor	0.63	RNA binding, processing, and translation
A1S_0344	putative ATP binding site	0.91	Unknown and hypothetical functions
A1S_0345	putative DNA helicase	1.28	DNA binding, metabolism, and repair
A1S_0347	putative oxidoreductase; putative flavoprotein monooxygenase	0.95	Enzymatic processes
A1S_0350	S-adenosylmethionine : 2-DMK methyltransferase and 2-octaprenyl-6-methoxy-14-benzoquinone methylase	0.52	Enzymatic processes
A1S_0361	polyribonucleotide nucleotidyltransferase	0.66	RNA binding, processing, and translation
A1S_0369	general secretion pathway protein F	0.89	Protein binding, transport, and folding
A1S_0390	putative type III effector	0.94	Unknown and hypothetical functions
A1S_0406	putative phosphoglycolate phosphatase protein	1.08	Enzymatic processes
A1S_0407	putative transcriptional regulator	0.54	Unknown and hypothetical functions
A1S_0426	hypothetical protein	0.72	Unknown and hypothetical functions
A1S_0443	putative RNA-binding protein	0.71	Metabolic processes
A1S_0448	50S ribosomal protein L28	0.75	RNA binding, processing, and translation
A1S_0449	coniferyl aldehyde dehydrogenase (CALDH)	1.16	Cellular function and cell wall related functions

A1S_0453	putative biopolymer transport protein (ExbB)	0.86	Protein binding, transport, and folding
A1S_0454	putative biopolymer transport protein (ExbD)	0.68	Protein binding, transport, and folding
A1S_0475	trigger factor septum formation molecular chaperone	0.57	Protein binding, transport, and folding
A1S_0477	ATP-dependent Clp protease ATP-binding subunit	0.67	Protein binding, transport, and folding
A1S_0479	putative signal peptide	2.12	Unknown and hypothetical functions
A1S_0484	hypothetical protein	0.58	Metabolic processes
A1S_0486	thermoresistant gluconokinase	0.71	Carbohydrate metabolism
A1S_0508	putative acyltransferase	0.54	Metabolic processes
A1S_0520	putative oxidoreductase protein; putative dehydrogenase (flavoprotein)	0.6	Enzymatic processes
A1S_0526	hypothetical protein	1.56	Metabolic processes
A1S_0528	protein exporting molecular chaperone	0.44	Protein binding, transport, and folding
A1S_0532	oligoribonuclease	0.71	Unknown and hypothetical functions
A1S_0533	putative membrane protein	0.74	Membrane structures and transport
A1S_0548	putative transcriptional regulator (TetR family)	1.71	DNA binding, metabolism, and repair
A1S_0549	hypothetical protein	1.25	Unknown and hypothetical functions
A1S_0562	tRNA-dihydrouridine synthase A	0.66	RNA binding, processing, and translation
A1S_0564	hypothetical protein	0.62	Unknown and hypothetical functions
A1S_0570	hypothetical protein	1.67	Unknown and hypothetical functions

A1S_0586	3-methyl-2-oxobutanoate hydroxymethyltransferase	0.52	Biosynthetic process
A1S_0594	putative glutathione S-transferase	0.92	Metabolic processes
A1S_0599	hypothetical protein	2.22	Metabolic processes
A1S_0624	putative lipoprotein	0.63	Enzymatic processes
A1S_0626	hypothetical protein	1.21	Unknown and hypothetical functions
A1S_0629	hypothetical protein	0.96	DNA binding, metabolism, and repair
A1S_0630	hypothetical protein	2.31	Unknown and hypothetical functions
A1S_0631	hypothetical protein	1.92	Unknown and hypothetical functions
A1S_0638	hypothetical protein	2.32	Unknown and hypothetical functions
A1S_0640	hypothetical protein	1.46	Unknown and hypothetical functions
A1S_0644	hypothetical protein	2.02	Unknown and hypothetical functions
A1S_0646	IcmB protein	3.09	Unknown and hypothetical functions
A1S_0651	TraB protein	1.41	DNA binding, metabolism, and repair
A1S_0661	phage integrase family protein	0.83	DNA binding, metabolism, and repair
A1S_0685	UDP-N-acetylglucosamine 1-carboxyvinyltransferase	0.63	Unknown and hypothetical functions
A1S_0696	putative MutT/nudix family protein	0.65	Enzymatic processes
A1S_0706	putative hydrolase	0.76	Enzymatic processes
A1S_0736	hypothetical protein	1.5	Unknown and hypothetical functions

A1S_0738	putative flavoprotein oxidoreductase	0.92	Enzymatic processes
A1S_0746	ribonucleoside-diphosphate reductase beta subunit	0.99	DNA binding, metabolism, and repair
A1S_0747	ribonucleoside diphosphate reductase alpha subunit	0.64	DNA binding, metabolism, and repair
A1S_0767	Excalibur	1.18	Unknown and hypothetical functions
A1S_0772	putative oxidoreductase	0.55	Enzymatic processes
A1S_0789	hypothetical protein	0.71	RNA binding, processing, and translation
A1S_0816	50S ribosomal protein L32	0.79	RNA binding, processing, and translation
A1S_0825	aspartate 1-decarboxylase precursor	1.29	Amino acid metabolism and repair
A1S_0828	50S ribosomal protein L25	0.51	RNA binding, processing, and translation
A1S_0841	ribosomal large subunit pseudouridine synthase D	0.65	Biosynthetic process
A1S_0867	30S ribosomal protein S7	0.66	Unknown and hypothetical functions
A1S_0887	phosphomannomutase	0.82	Carbohydrate metabolism
A1S_0891	hemerythrin-like metal-binding protein	1.7	Metal ion binding and transport
A1S_0901	hypothetical protein	0.87	Stress responses
A1S_0906	delta-aminolevulinic acid dehydratase	0.62	Biosynthetic process
A1S_0908	RND family multidrug resistance secretion protein	2.09	Membrane structures and transport
A1S_0923	malate dehydrogenase FAD/NAD(P)-binding domain	1.27	Unknown and hypothetical functions
A1S_0953	hypothetical protein	1.16	Unknown and hypothetical functions
A1S_0979	putative membrane-bound protein in GNT I	0.68	Metal ion binding

	transport system (GntY)		and transport
A1S_0980	ferric enterobactin receptor precursor	0.62	Membrane structures and transport
A1S_0993	estB	0.96	Unknown and hypothetical functions
A1S_1003	hypothetical protein	1.1	Unknown and hypothetical functions
A1S_1014	urease alpha subunit	0.73	Unknown and hypothetical functions
A1S_1055	hypothetical protein	1.73	Unknown and hypothetical functions
A1S_1062	putative FMN oxidoreductase	1.44	Enzymatic processes
A1S_1092	succinylornithine transaminase (carbon starvation protein C)	1.1	RNA binding, processing, and translation
A1S_1130	Pirin-like:Cupin 2 barrel	0.82	Unknown and hypothetical functions
A1S_1138	putative cytochrome	0.57	Energy production and conversion
A1S_1139	putative signal peptide	1.01	Unknown and hypothetical functions
A1S_1140	RNAse HII	1.62	RNA binding, processing, and translation
A1S_1179	adenylosuccinate synthetase	0.58	Biosynthetic process
A1S_1188	putative N-6 Adenine-specific DNA methylase	0.62	RNA binding, processing, and translation
A1S_1189	putative N-6 Adenine-specific DNA methylase	0.8	RNA binding, processing, and translation
A1S_1190	aspartate carbamoyltransferase catalytic subunit	0.53	Unknown and hypothetical functions
A1S_1196	tRNA(guanine-7)methyltransferase	1.18	RNA binding, processing, and translation
A1S_1228	Cold shock protein	3.59	DNA binding,

			metabolism, and repair
A1S_1229	pyrroline-5-carboxylate reductase	1.49	Biosynthetic process
A1S_1250	GCN5-related N-acetyltransferase	0.51	Metabolic processes
A1S_1258	hypothetical protein	3.13	Unknown and hypothetical functions
A1S_1281	TPR domain protein	2.2	Unknown and hypothetical functions
A1S_1296	hypothetical protein	1.11	Unknown and hypothetical functions
A1S_1318	GCN5-related N-acetyltransferase	0.89	Metabolic processes
A1S_1319	hypothetical protein	0.79	Metabolic processes
A1S_1354	(Acyl-carrier protein) phosphodiesterase	1.41	Enzymatic processes
A1S_1406	major membrane protein I (MMP-I)	0.98	Unknown and hypothetical functions
A1S_1435	hypothetical protein	0.96	Unknown and hypothetical functions
A1S_1476	hypothetical protein	1.22	Cellular function and cell wall related functions
A1S_1497	putative acyltransferase	1.11	Metabolic processes
A1S_1510	Fimbrial protein	1.16	Cellular function and cell wall related functions
A1S_1511	biotin synthase	1.36	Biosynthetic process
A1S_1514	holliday junction nuclease	0.67	DNA binding, metabolism, and repair
A1S_1521	transketolase	0.57	Metabolic processes
A1S_1528	hypothetical protein	0.81	DNA binding, metabolism, and repair
A1S_1531	putative cobalamin biosynthetic protein (CobB)	1.45	Biosynthetic process
A1S_1540	putative transcriptional regulator (TetR family)	0.76	DNA binding, metabolism, and repair
A1S_1548	putative phosphotransferase	0.77	Unknown and hypothetical functions

A1S_1578	putative transcriptional regulator	0.92	DNA binding, metabolism, and repair
A1S_1609	heme-binding protein A precursor	0.61	Membrane structures and transport
A1S_1612	ABC-type dipeptide/oligopeptide/nickel transport systems permease component	0.58	Membrane structures and transport
A1S_1616	hypothetical protein	0.74	Unknown and hypothetical functions
A1S_1617	30S ribosomal protein S20	0.56	RNA binding, processing, and translation
A1S_1630	hypothetical protein	1.05	Membrane structures and transport
A1S_1631	iron-binding protein	0.82	Metal ion binding and transport
A1S_1638	peptidyl-prolyl cis-trans isomerase precursor	1.19	Protein binding, transport, and folding
A1S_1677	putative porin precursor	0.83	Membrane structures and transport
A1S_1683	o-succinylhomoserine sulfhydrylase	0.75	Biosynthetic process
A1S_1752	AdeA membrane fusion protein	1.37	Membrane structures and transport
A1S_1811	hypothetical protein	0.81	Unknown and hypothetical functions
A1S_1921	Ferrichrome-iron receptor	0.95	RNA binding, processing, and translation
A1S_1922	putative sugar kinase protein	1.5	Carbohydrate metabolism
A1S_1938	hypothetical protein	0.57	Unknown and hypothetical functions
A1S_1951	hypothetical protein	2.24	Carbohydrate metabolism
A1S_1960	predicted hydrolase (HAD superfamily)	0.95	Metabolic processes
A1S_1962	DNA strand exchange and recombination protein	0.79	Unknown and hypothetical

			functions
A1S_1968	putative outer membrane protein (OmpH)	0.79	Protein binding, transport, and folding
A1S_1970	putative membrane-associated Zn-dependent proteases 1	0.73	Metal ion binding and transport
A1S_1976	hypothetical protein	0.6	RNA binding, processing, and translation
A1S_2042	putative transcriptional regulator (TetR family)	0.77	DNA binding, metabolism, and repair
A1S_2051	putative phosphotyrosine protein phosphatase	1.34	Protein binding, transport, and folding
A1S_2080	putative siderophore receptor	0.82	RNA binding, processing, and translation
A1S_2081	TonB-dependent siderophore receptor	0.79	RNA binding, processing, and translation
A1S_2096	putative 5-carboxymethyl-2-hydroxymuconate delta isomerase	0.83	Unknown and hypothetical functions
A1S_2143	putative 2-amino-4-hydroxy-6-hydroxymethyldihydropteridine pyrophosphokinase	0.61	Biosynthetic process
A1S_2160	haemin storage system HmsR protein	0.67	Metabolic processes
A1S_2161	putative hemin storage signal peptide protein	1.01	Carbohydrate metabolism
A1S_2162	hypothetical protein YcdS precursor	1.01	Membrane structures and transport
A1S_2172	30S ribosomal protein S18	0.68	RNA binding, processing, and translation
A1S_2173	50S ribosomal protein L9	0.6	RNA binding, processing, and translation
A1S_2182	glucose-inhibited division protein A	0.64	RNA binding, processing, and translation
A1S_2186	DNA-binding protein	0.93	DNA binding, metabolism, and repair
A1S_2211	ADP-ribose pyrophosphatase	2.08	Metabolic processes

A1S_2213	CsuE	1.6	Unknown and hypothetical functions
A1S_2214	CsuD	1.33	Membrane structures and transport
A1S_2215	CsuC	2.07	Cellular function and cell wall related functions
A1S_2216	CsuB	1.69	Viral proteins and elements
A1S_2217	CsuA	0.73	Viral proteins and elements
A1S_2218	CsuA/B	1.5	Viral proteins and elements
A1S_2220	hypothetical protein	1.31	Unknown and hypothetical functions
A1S_2232	methylmalonate-semialdehyde dehydrogenase	1.86	Enzymatic processes
A1S_2247	putative signal peptide	0.5	Metal ion binding and transport
A1S_2261	putative cold shock protein	2.89	DNA binding, metabolism, and repair
A1S_2271	rtcb protein	1.94	RNA binding, processing, and translation
A1S_2272	hypothetical protein	2.6	Unknown and hypothetical functions
A1S_2273	3'-terminal phosphate cyclase	1.45	RNA binding, processing, and translation
A1S_2274	aminoacyl-histidine dipeptidase	0.94	Enzymatic processes
A1S_2282	hypothetical protein	0.95	Unknown and hypothetical functions
A1S_2293	ferredoxin--NADP+ reductase	0.65	Enzymatic processes
A1S_2321	hypothetical protein	0.7	Membrane structures and transport
A1S_2322	protein chain elongation factor EF-Ts	0.61	RNA binding, processing, and

			translation
A1S_2337	sensory box protein	0.47	Signal transduction
A1S_2349	4-hydroxybenzoate octaprenyltransferase	0.84	Biosynthetic process
A1S_2370	uroporphyrinogen decarboxylase	0.67	Biosynthetic process
A1S_2371	hypothetical protein	0.65	Metabolic processes
A1S_2397	MoeA	1.67	Biosynthetic process
A1S_2423	50S ribosomal protein L31	0.8	RNA binding, processing, and translation
A1S_2428	putative ATP-dependent protease	0.53	Enzymatic processes
A1S_2430	putative ATP-dependent protease	0.67	Enzymatic processes
A1S_2434	putative signal peptide	0.86	Unknown and hypothetical functions
A1S_2441	adenylosuccinate lyase	0.69	Biosynthetic process
A1S_2444	putative protease (SohB)	1.2	Enzymatic processes
A1S_2446	high-affinity phosphate transport protein	0.7	Membrane structures and transport
A1S_2458	putative fatty acid desaturase	1.11	Lipid metabolism
A1S_2459	putative oxidoreductase	1.33	Membrane structures and transport
A1S_2460	putative transcriptional regulator (tetR family)	0.58	DNA binding, metabolism, and repair
A1S_2463	putative ribosomal large subunit pseudouridine synthase A(RluA-like)	0.63	Biosynthetic process
A1S_2469	hypothetical protein	0.65	Unknown and hypothetical functions
A1S_2470	putative protease	1.56	Metal ion binding and transport
A1S_2472	putative transport protein	1.48	Membrane structures and transport
A1S_2476	putative pseudouridine synthase	0.58	Biosynthetic process
A1S_2479	putative D-ala-D-ala-carboxypeptidase penicillin-binding protein	1.42	Enzymatic processes
A1S_2481	FKBP-type peptidyl-prolyl cis-trans isomerase	1.91	Protein binding, transport, and folding
A1S_2488	hypothetical protein	0.59	Membrane

			structures and transport
A1S_2505	hypothetical protein	0.64	Unknown and hypothetical functions
A1S_2506	putative GGDEF family protein	0.69	Phosphorylation
A1S_2509	putative chaperone	1.21	Membrane structures and transport
A1S_2519	ribonuclease III	0.76	RNA binding, processing, and translation
A1S_2521	leader peptidase	0.77	Enzymatic processes
A1S_2528	thymidylate kinase	0.62	Biosynthetic process
A1S_2559	hypothetical protein	1.36	Unknown and hypothetical functions
A1S_2570	putative siderophore biosynthesis protein; putative acetyltransferase	0.84	Metabolic processes
A1S_2586	deoxyguanosinetriphosphate triphosphohydrolase	0.6	Amino acid metabolism and repair
A1S_2605	phosphoribosylaminoimidazole synthetase	0.64	Biosynthetic process
A1S_2615	hypothetical protein	0.65	Unknown and hypothetical functions
A1S_2643	oxidoreductase short chain dehydrogenase/reductase family	0.94	Enzymatic processes
A1S_2648	Hypothetical protein	1.92	Unknown and hypothetical functions
A1S_2649	putative regulatory protein	0.93	Unknown and hypothetical functions
A1S_2656	hypothetical protein	0.94	RNA binding, processing, and translation
A1S_2668	phosphoenolpyruvate carboxykinase	0.66	Metal ion binding and transport
A1S_2681	cell division protein	0.7	Metal ion binding and transport
A1S_2683	hypothetical protein	0.9	RNA binding, processing, and translation
A1S_2690	hypothetical protein	2.15	Unknown and

			hypothetical functions
A1S_2705	hypothetical protein	1.48	Unknown and hypothetical functions
A1S_2708	hypothetical protein	1.15	Metabolic processes
A1S_2737	AdeK	0.67	Membrane structures and transport
A1S_2756	putative esterase	0.71	Lipid metabolism
A1S_2757	putative membrane protein	0.51	Unknown and hypothetical functions
A1S_2758	putative membrane protease subunit	0.8	Membrane structures and transport
A1S_2774	putative homoserine kinase (ThrH)	0.86	Metabolic processes
A1S_2787	hypothetical protein	1.27	Unknown and hypothetical functions
A1S_2789	putative metallopeptidase	1.16	Enzymatic processes
A1S_2821	putative alkylphosphonate uptake protein (PhnA) in phosphonate metabolism	1.05	Unknown and hypothetical functions
A1S_2825	putative thiol:disulphide interchange protein (DsbC-like)	0.85	Unknown and hypothetical functions
A1S_2835	GTP-binding elongation factor family protein	0.73	Enzymatic processes
A1S_2839	hypothetical protein	0.69	RNA binding, processing, and translation
A1S_2856	putative esterase	1.64	Lipid metabolism
A1S_2878	hypothetical protein	1	Unknown and hypothetical functions
A1S_2881	putative fatty acid desaturase	0.63	Lipid metabolism
A1S_2882	hypothetical protein	0.73	Unknown and hypothetical functions
A1S_2907	hypothetical protein	1.38	DNA binding, metabolism, and repair
A1S_2908	putative integrase	0.97	DNA binding, metabolism, and

			repair
A1S_2911	Uncharacterized membrane protein LemA family	1.22	Unknown and hypothetical functions
A1S_2912	queuine tRNA-ribosyltransferase	0.73	RNA binding, processing, and translation
A1S_2913	putative preprotein translocase IISP family membrane subunit	1.22	Unknown and hypothetical functions
A1S_2921	putative intracellular septation protein (IspZ)	0.84	Membrane structures and transport
A1S_2927	Phage integrase	1.05	DNA binding, metabolism, and repair
A1S_2966	UDP-N-acetylmuramate:L-alanyl-gamma-D-glutamyl- meso-diaminopimelate ligase	0.72	Biosynthetic process
A1S_2976	putative thiol:disulfide interchange protein	1.59	Cellular function and cell wall related functions
A1S_2980	hypothetical protein	0.7	Protein binding, transport, and folding
A1S_2981	Inner membrane protein (IMP) integration factor	0.7	Protein binding, transport, and folding
A1S_2983	RNase P	0.61	RNA binding, processing, and translation
A1S_3000	50S ribosomal protein L13	0.72	RNA binding, processing, and translation
A1S_3001	30S ribosomal protein S9	0.64	Unknown and hypothetical functions
A1S_3003	stringent starvation protein B	0.97	Unknown and hypothetical functions
A1S_3028	putative tRNA-i(6)A37 modification enzyme	0.37	RNA binding, processing, and translation
A1S_3029	putative tRNA-i(6)A37 modification enzyme	0.69	Metal ion binding and transport
A1S_3031	hypothetical protein	1.39	RNA binding, processing, and

			translation
A1S_3047	oligopeptidase A	0.79	Enzymatic processes
A1S_3052	hypothetical protein	1.08	Unknown and hypothetical functions
A1S_3056	RNA polymerase alpha subunit	0.55	RNA binding, processing, and translation
A1S_3057	30S ribosomal protein S4	0.6	Unknown and hypothetical functions
A1S_3058	30S ribosomal protein S11	0.61	Unknown and hypothetical functions
A1S_3059	30S ribosomal protein S13	0.8	RNA binding, processing, and translation
A1S_3061	secretion protein	0.62	Unknown and hypothetical functions
A1S_3062	50S ribosomal protein L15	0.71	RNA binding, processing, and translation
A1S_3064	30S ribosomal protein S5	0.56	Unknown and hypothetical functions
A1S_3065	50S ribosomal protein L18	0.61	Unknown and hypothetical functions
A1S_3066	50S ribosomal protein L6	0.54	Unknown and hypothetical functions
A1S_3067	30S ribosomal protein S8	0.59	Unknown and hypothetical functions
A1S_3069	50S ribosomal protein L5	0.53	Unknown and hypothetical functions
A1S_3072	30S ribosomal protein S17	0.79	RNA binding, processing, and translation
A1S_3074	50S ribosomal protein L16	0.62	Unknown and hypothetical functions
A1S_3078	50S ribosomal protein L23	0.86	RNA binding,

			processing, and translation
A1S_3081	30S ribosomal protein S10	0.79	RNA binding, processing, and translation
A1S_3101	toluene tolerance efflux transporter	0.68	Unknown and hypothetical functions
A1S_3104	putative ATP-dependent RNA helicase	1.75	DNA binding, metabolism, and repair
A1S_3105	inositol-1-monophosphatase	0.83	Phosphorylation
A1S_3110	hypothetical protein	0.54	Unknown and hypothetical functions
A1S_3127	putative signal peptide	0.45	Unknown and hypothetical functions
A1S_3161	50S ribosomal protein L19	0.69	RNA binding, processing, and translation
A1S_3164	30S ribosomal protein S16	0.73	RNA binding, processing, and translation
A1S_3170	guanylate kinase	0.78	Phosphorylation
A1S_3185	glutamate synthase large chain precursor	0.66	Amino acid metabolism and repair
A1S_3206	S-adenosylmethionine methyltransferase	0.74	Enzymatic processes
A1S_3219	Putative RND family drug transporter	0.58	Membrane structures and transport
A1S_3236	putative membrane protein	0.94	Membrane structures and transport
A1S_3263	putative cytoplasmic protein	0.88	Enzymatic processes
A1S_3273	putative peptide signal	1.74	Unknown and hypothetical functions
A1S_3281	4-aminobutyrate aminotransferase PLP-dependent	1.95	Metabolic processes
A1S_3297	putative outer membrane protein	1.39	Membrane structures and transport

A1S_3318	ssDNA exonuclease	1.02	DNA binding, metabolism, and repair
A1S_3321	IMP dehydrogenase	0.71	Amino acid metabolism and repair
A1S_3324	putative ferric siderophore receptor protein	0.61	RNA binding, processing, and translation
A1S_3342	putative arsenate reductase	0.58	Unknown and hypothetical functions
A1S_3350	hypothetical protein	1.03	Metabolic processes
A1S_3355	hypothetical protein	0.94	Cellular function and cell wall related functions
A1S_3377	hypothetical protein	0.94	Lipid metabolism
A1S_3378	phosphatidylserine decarboxylase	0.74	Biosynthetic process
A1S_3380	nicotinate phosphoribosyltransferase	0.84	Biosynthetic process
A1S_3382	Catalase	0.72	Stress responses
A1S_3398	Glutamate racemase	0.83	Nitrogen compound metabolism
A1S_3399	VirP protein	0.57	Metabolic processes
A1S_3435	3-methyl-adenine DNA glycosylase I	0.78	DNA binding, metabolism, and repair
A1S_3436	putative alcohol dehydrogenase	0.63	Enzymatic processes
A1S_3456	methionyl-tRNA formyltransferase	0.56	Biosynthetic process
A1S_3459	hypothetical protein	0.67	Unknown and hypothetical functions
A1S_3464	Cro-like protein	0.96	Unknown and hypothetical functions
A1S_3465	hypothetical protein	2.38	Protein binding, transport, and folding
A1S_3517	hypothetical protein	0.59	Unknown and hypothetical functions
A1S_3519	hypothetical protein	1.11	Unknown and hypothetical functions
A1S_3520	hypothetical protein	0.61	Unknown and hypothetical

			functions
A1S_3522	hypothetical protein	1.94	Unknown and hypothetical functions
A1S_3524	hypothetical protein	0.96	Unknown and hypothetical functions
A1S_3526	hypothetical protein	1.29	Unknown and hypothetical functions
A1S_3533	hypothetical protein	1.54	Unknown and hypothetical functions
A1S_3535	hypothetical protein	2.47	Unknown and hypothetical functions
A1S_3537	hypothetical protein	0.71	Unknown and hypothetical functions
A1S_3540	hypothetical protein	1.75	Unknown and hypothetical functions
A1S_3541	hypothetical protein	4.04	Unknown and hypothetical functions
A1S_3582	hypothetical protein	1.41	Unknown and hypothetical functions
A1S_3631	hypothetical protein	2.44	Unknown and hypothetical functions
A1S_3643	hypothetical protein	0.65	Unknown and hypothetical functions
A1S_3644	hypothetical protein	2.32	Unknown and hypothetical functions
A1S_3653	hypothetical protein	1.69	Unknown and hypothetical functions
A1S_3715	hypothetical protein	0.84	Unknown and hypothetical functions
A1S_3716	hypothetical protein	1.64	Unknown and hypothetical functions

A1S_3732	hypothetical protein	0.84	Unknown and hypothetical functions
A1S_3748	hypothetical protein	2.67	Unknown and hypothetical functions
A1S_3767	hypothetical protein	1.73	Unknown and hypothetical functions
A1S_3774	hypothetical protein	1.05	Unknown and hypothetical functions
A1S_3775	hypothetical protein	0.77	Unknown and hypothetical functions
A1S_3787	hypothetical protein	1.21	Unknown and hypothetical functions
A1S_3794	hypothetical protein	1.7	Unknown and hypothetical functions
A1S_3796	hypothetical protein	0.87	Unknown and hypothetical functions
A1S_3797	hypothetical protein	0.65	Unknown and hypothetical functions
A1S_3804	hypothetical protein	2.06	Unknown and hypothetical functions
A1S_3826	hypothetical protein	1.17	Unknown and hypothetical functions
A1S_3831	hypothetical protein	1.38	Unknown and hypothetical functions
A1S_3834	hypothetical protein	0.99	Unknown and hypothetical functions
A1S_3841	hypothetical protein	1.22	Unknown and hypothetical functions
A1S_3843	hypothetical protein	0.88	Unknown and hypothetical functions
A1S_3857	hypothetical protein	1.08	Unknown and

			hypothetical functions
A1S_3858	hypothetical protein	0.52	Unknown and hypothetical functions
A1S_3859	hypothetical protein	1.74	Unknown and hypothetical functions
A1S_3861	hypothetical protein	2.13	Unknown and hypothetical functions
A1S_3863	hypothetical protein	0.54	Unknown and hypothetical functions
A1S_3880	hypothetical protein	3.98	Unknown and hypothetical functions
A1S_3899	hypothetical protein	1.53	Unknown and hypothetical functions
A1S_3901	hypothetical protein	1.14	Unknown and hypothetical functions
A1S_3902	hypothetical protein	1.59	Unknown and hypothetical functions
A1S_3908	hypothetical protein	1.66	Unknown and hypothetical functions

Appendix III. List of downregulated proteins at 28˚C in *A. baumannii* ATCC 17978

Locus tag	Name	Log2 fold change	GO term classification
A1S_0009	putative RND type efflux pump	-1.34	Unknown and hypothetical functions
A1S_0037	alkali-inducible disulfide interchange protein	-0.68	Enzymatic processes
A1S_0073	putative carboxyphosphonoenolpyruvate phosphonomutase or putative methylisocitrate lyase (PrpB)	-0.55	Enzymatic processes
A1S_0076	aconitate hydratase 1	-1.08	Unknown and hypothetical functions
A1S_0091	hypothetical protein	-1.24	Unknown and hypothetical functions
A1S_0096	alanine racemase 2 PLP-binding, catabolic	-1.51	Biosynthetic process
A1S_0097	hypothetical protein	-1.05	Unknown and hypothetical functions
A1S_0103	3-hydroxyisobutyrate dehydrogenase	-1.84	Enzymatic processes
A1S_0104	putative acetyl-coA synthetase/AMP-(fatty) acid ligase	-1.66	Metabolic processes
A1S_0105	putative acyl-CoA dehydrogenase	-1.33	Enzymatic processes
A1S_0106	putative enoyl-CoA hydratase/isomerase	-1.32	Metabolic processes
A1S_0107	putative enoyl-CoA hydratase/isomerase family protein	-1.36	Metabolic processes
A1S_0128	putative membrane protein	-1.76	Unknown and hypothetical functions
A1S_0132	putative transcriptional regulator	-0.75	Unknown and hypothetical functions
A1S_0136	glutathione S-transferase	-0.95	Protein binding, transport, and folding
A1S_0177	cysteine synthase A/O-acetylserine sulfhydrolase A subunit PLP-dependent	-0.59	Biosynthetic process

	enzyme		
A1S_0181	transcriptional regulator SoxR-family	-0.65	Transcription regulation
A1S_0220	putative transcriptional regulator	-0.6	Transcription regulation
A1S_0252	hypothetical protein	-0.78	Unknown and hypothetical functions
A1S_0253	Transcriptional regulator	-0.66	Transcription regulation
A1S_0261	alginate biosynthesis regulatory protein	-0.91	Biosynthetic process
A1S_0290	hypothetical protein	-0.62	Enzymatic processes
A1S_0293	putative signal peptide	-1.02	Unknown and hypothetical functions
A1S_0299	hypothetical protein	-1.34	Unknown and hypothetical functions
A1S_0372	protein secretion chaperone	-0.9	RNA binding, processing, and translation
A1S_0398	putative short-chain dehydrogenase	-0.63	Unknown and hypothetical functions
A1S_0436	putative Zn-dependent oxidoreductase	-0.86	Enzymatic processes
A1S_0481	phosphate acetyltransferase	-0.88	Metabolic processes
A1S_0482	acetate kinase (propionate kinase)	-1.13	Phosphrylation
A1S_0518	hypothetical protein	-0.92	Protein binding, transport, and folding
A1S_0558	aconitate hydratase 1	-0.87	Metabolic processes
A1S_0571	hydroxypyruvate isomerase	-0.51	Unknown and hypothetical functions
A1S_0591	putative AMP-dependent synthetase/ligase	-1.01	Metabolic processes
A1S_0683	putative sigma(54) modulation protein RpoX	-1.03	Metabolic processes
A1S_0709	putative cation efflux system protein	-0.8	Membrane structures and transport

A1S_0750	hypothetical protein	-0.61	Unknown and hypothetical functions
A1S_0771	putative membrane protein	-1.06	Membrane structures and transport
A1S_0774	Putative RND family drug transporter	-0.7	Protein binding, transport, and folding
A1S_0803	trehalose-6-phosphate synthase	-0.51	Biosynthetic process
A1S_0855	dioxygenase beta subunit	-1.1	Enzymatic processes
A1S_0917	Transcriptional regulator	-0.57	Transcription regulation
A1S_0996	hypothetical protein	-0.97	Unknown and hypothetical functions
A1S_1009	putative lipoprotein	-0.75	Unknown and hypothetical functions
A1S_1042	hypothetical protein	-1.34	Unknown and hypothetical functions
A1S_1084	Glycine/D-amino acid oxidases (deaminating)	-1.49	Enzymatic processes
A1S_1089	hypothetical protein	-1.17	Enzymatic processes
A1S_1110	hydroxybenzaldehyde dehydrogenase	-1.75	Enzymatic processes
A1S_1180	putative Zn-dependent protease with chaperone function	-1.32	Enzymatic processes
A1S_1181	putative oxidoreductase aldo/keto reductase family	-0.89	Enzymatic processes
A1S_1186	ATP-dependent protease Hsp 100	-1.53	Protein binding, transport, and folding
A1S_1193	OmpA/MotB	-1.27	Membrane structures and transport
A1S_1203	o-methyl transferase	-0.77	Enzymatic processes
A1S_1212	short-chain dehydrogenase/reductase SDR	-2.17	Unknown and hypothetical functions
A1S_1213	benzoate 12-dioxygenase electron transfer	-1.66	Enzymatic

	component		processes
A1S_1214	benzoate 12-dioxygenase beta subunit	-2.76	Enzymatic processes
A1S_1215	benzoate 12 dioxygenase alpha subunit	-2.82	Enzymatic processes
A1S_1218	heavy metal regulator HmrR	-0.55	Transcription regulation
A1S_1246	putative universal stress protein	-0.92	Stress responses
A1S_1261	Putative 3-hydroxyacyl-CoA dehydrogenase	-0.75	Enzymatic processes
A1S_1262	GCN5-related N-acetyltransferase	-0.92	Antibiotic resistance related functions
A1S_1307	putative ClpA/B-type chaperone	-0.8	Enzymatic processes
A1S_1310	hypothetical protein	-0.61	Membrane structures and transport
A1S_1334	Iron-sulfur-dependent L-serine dehydratase single chain form	-0.52	Carbohydrate metabolism
A1S_1335	Phenylacetic acid degradation protein paaN	-3.87	Enzymatic processes
A1S_1336	hypothetical protein	-3.7	Phenyl acetate catabolism
A1S_1337	Phenylacetic acid degradation B	-4.13	Unknown and hypothetical functions
A1S_1338	hypothetical protein	-4.05	Phenyl acetate catabolism
A1S_1339	Phenylacetate-CoA oxygenase PaaJ subunit	-2.79	Unknown and hypothetical functions
A1S_1340	Phenylacetate-CoA oxygenase/reductase PaaK subunit	-3.66	Enzymatic processes
A1S_1341	Enoyl-CoA hydratase/carnithine racemase	-4.05	Metabolic processes
A1S_1342	putative enoyl-CoA hydratase II	-3.8	Phenyl acetate catabolism
A1S_1343	PaaC	-3.33	Phenyl acetate catabolism
A1S_1344	Thiolase	-3.76	Enzymatic processes
A1S_1345	PaaK	-3.09	Phenyl acetate catabolism
A1S_1346	phenylacetyl-CoA ligase	-2.82	Phenyl acetate catabolism

A1S_1347	PaaX	-1.04	Transcription regulation
A1S_1348	Carbonic anhydrases/acetyltransferases isoleucine patch superfamily	-2.6	Metabolic processes
A1S_1349	thioesterase domain protein	-1.89	Unknown and hypothetical functions
A1S_1368	Pyruvate ferredoxin/flavodoxin oxidoreductase	-1.43	Enzymatic processes
A1S_1369	putative oxidoreductase protein	-1.04	Enzymatic processes
A1S_1370	Oxidoreductase	-1.27	Enzymatic processes
A1S_1372	hypothetical protein	-0.99	Metabolic processes
A1S_1373	putative acyl-CoA carboxylase alpha chain protein	-0.85	Metabolic processes
A1S_1374	3-methylglutaconyl-CoA hydratase	-1.05	Metabolic processes
A1S_1375	putative propionyl-CoA carboxylase (Beta subunit)	-0.93	Metabolic processes
A1S_1376	Acyl-CoA dehydrogenase	-0.8	Enzymatic processes
A1S_1378	putative long chain fatty-acid CoA ligase	-1.23	Lipid metabolism
A1S_1380	putative protein (DcaP-like)	-1.05	Unknown and hypothetical functions
A1S_1383	surface antigen	-1.05	Unknown and hypothetical functions
A1S_1386	Catalase	-0.72	Enzymatic processes
A1S_1419	anti-sigm factor ChrR	-0.73	Unknown and hypothetical functions
A1S_1430	malonate utilization transcriptional regulator (LysR family)	-0.61	Unknown and hypothetical functions
A1S_1431	malonate utilization transcriptional regulator (LysR family)	-0.66	Transcription regulation
A1S_1451	hypothetical protein	-0.99	Metabolic processes
A1S_1466	glutaminase-asparaginase	-0.62	Amino acid metabolism and transport
A1S_1490	glutamate/aspartate transport protein	-1.62	Unknown and

			hypothetical functions
A1S_1491	glutamate/aspartate transport protein	-0.99	Amino acid metabolism and transport
A1S_1492	glutamate/aspartate transport protein	-0.79	Amino acid metabolism and transport
A1S_1493	glutamate/aspartate transport protein	-0.79	Membrane structures and transport
A1S_1517	beta-lactamase OXA-95	-0.78	Antibiotic resistance related functions
A1S_1523	putative signal peptide	-0.87	Unknown and hypothetical functions
A1S_1533	putative transcriptional regulator (AraC family)	-0.68	Transcription regulation
A1S_1539	putative transcriptional regulator (ArsR family)	-0.68	Transcription regulation
A1S_1560	putative deoxyribonuclease	-0.55	Enzymatic processes
A1S_1614	hypothetical protein	-0.99	Unknown and hypothetical functions
A1S_1642	putative acyl-CoA dehydrogenase	-0.28	Enzymatic processes
A1S_1662	hypothetical protein	-0.65	Phosphrylation
A1S_1680	hypothetical protein	-0.85	Unknown and hypothetical functions
A1S_1682	putative poly(R)-hydroxyalkanoic acid synthase	-0.67	Metabolic processes
A1S_1691	hypothetical protein	-0.66	Unknown and hypothetical functions
A1S_1692	tryptophan synthase subunit beta	-0.65	Unknown and hypothetical functions
A1S_1699	acetoin:26-dichlorophenolindophenol oxidoreductase alpha subunit	-1.15	Enzymatic processes
A1S_1700	acetoin:26-dichlorophenolindophenol oxidoreductase beta subunit	-1.25	Enzymatic processes
A1S_1701	dihydrolipoamide acetyltransferase	-0.72	Metabolic processes

A1S_1702	dihydrolipoamide dehydrogenase	-0.67	Enzymatic processes
A1S_1704	acetoin dehydrogenase	-0.76	Enzymatic processes
A1S_1705	putative (RR)-butanediol dehydrogenase	-1.53	Enzymatic processes
A1S_1708	beta-lactamase-like protein	-0.99	Metabolic processes
A1S_1709	hypothetical protein	-1.68	Enzymatic processes
A1S_1715	(Acyl-carrier protein) phosphodiesterase	-0.76	Enzymatic processes
A1S_1729	putative acetyl-CoA acetyltransferase	-1.54	Metabolic processes
A1S_1731	acetoacetyl-CoA transferase beta subunit	-0.98	Metabolic processes
A1S_1732	acetoacetyl-CoA transferase alpha subunit	-0.98	Metabolic processes
A1S_1737	3-hydroxybutyrate dehydrogenase	-1.44	Enzymatic processes
A1S_1817	Acyl-CoA dehydrogenase	-0.72	Enzymatic processes
A1S_1827	hypothetical protein	-1.01	Unknown and hypothetical functions
A1S_1830	putative dihydrofolate reductase	-0.98	Enzymatic processes
A1S_1834	hypothetical protein	-1.59	Unknown and hypothetical functions
A1S_1842	Cat operon transcriptional regulator (LysR family)	-0.62	Unknown and hypothetical functions
A1S_1843	muconate cycloisomerase I	-1.79	Metabolic processes
A1S_1845	CatA3	-2.17	Enzymatic processes
A1S_1848	Beta-ketoadipyl CoA thiolase	-1.07	Metabolic processes
A1S_1857	vanillate O-demethylase oxidoreductase	-4.48	Enzymatic processes
A1S_1861	benzoate dioxygenase large subunit	-4.89	Enzymatic processes
A1S_1864	Acyl-CoA dehydrogenase-like protein	-4.72	Enzymatic processes
A1S_1865	Glu-tRNA amidotransferase	-4.3	Enzymatic

			processes
A1S_1880	pyrroloquinoline-quinone QuiA	-0.69	Enzymatic processes
A1S_1886	gamma-carboxymuconolactone decarboxylase (CMD)	-0.67	Enzymatic processes
A1S_1891	beta-ketoadipyl CoA thiolase	-1.31	Metabolic processes
A1S_1905	24-dienoyl-CoA reductase	-0.76	Enzymatic processes
A1S_1924	cytochrome d terminal oxidase polypeptide subunit I	-0.63	Enzymatic processes
A1S_1929	putative oxidoreductase	-0.82	Enzymatic processes
A1S_1932	hypothetical protein	-1.4	Membrane structures and transport
A1S_1935	hypothetical protein	-0.73	Enzymatic processes
A1S_1939	putative transcriptional regulator	-0.56	Transcription regulation
A1S_1942	hypothetical protein	-1.13	Unknown and hypothetical functions
A1S_1950	putative universal stress protein	-1.94	Stress responses
A1S_1967	hypothetical protein	-0.61	Biosynthetic process
A1S_1983	putative signal peptide	-0.8	Unknown and hypothetical functions
A1S_1984	D-amino acid dehydrogenase small subunit	-1.64	Enzymatic processes
A1S_2019	hypothetical protein	-0.98	Unknown and hypothetical functions
A1S_2025	hypothetical protein	-0.92	Unknown and hypothetical functions
A1S_2061	putative short-chain dehydrogenase	-0.82	Unknown and hypothetical functions
A1S_2070	P-type ATPase Mg2+ ATPase transporter	-0.64	Metal ion binding and transport
A1S_2074	hypothetical protein	-1.84	Unknown and hypothetical functions
A1S_2098	putative alcohol dehydrogenase	-0.65	Enzymatic

			processes
A1S_2102	aldehyde dehydrogenase 1	-0.54	Enzymatic processes
A1S_2111	oxygen-insensitive NADPH nitroreductase	-0.83	Enzymatic processes
A1S_2119	putative acetyltransferase	-0.64	Antibiotic resistance related functions
A1S_2148	putative acetyl-CoA synthetase/AMP-(fatty) acid ligase	-1.34	Metabolic processes
A1S_2149	putative acyl CoA dehydrogenase oxidoreductase protein	-1	Enzymatic processes
A1S_2150	putative oxidoreductase short-chain dehydrogenase/reductase family	-1.27	Unknown and hypothetical functions
A1S_2158	putative monooxygenase	-1.28	Enzymatic processes
A1S_2177	putative proteasome protease	-0.79	Enzymatic processes
A1S_2179	hypothetical protein	-0.72	Unknown and hypothetical functions
A1S_2196	membrane-associated dicarboxylate transport protein	-0.6	Membrane structures and transport
A1S_2230	hypothetical protein	-1.72	Unknown and hypothetical functions
A1S_2294	hypothetical protein	-1.12	Biosynthetic process
A1S_2308	hypothetical protein	-1.44	Lipid metabolism
A1S_2332	putative 4-carboxymuconolactone decarboxylase	-1.03	Enzymatic processes
A1S_2335	510-methylenetetrahydrofolate reductase	-0.65	Enzymatic processes
A1S_2343	superoxide dismutase	-0.67	Enzymatic processes
A1S_2395	hypothetical protein	-0.99	Unknown and hypothetical functions
A1S_2406	hypothetical protein	-1.1	Metabolic processes
A1S_2417	starvation-induced peptide utilization protein	-0.61	Stress responses
A1S_2450	putative pyruvate decarboxylase	-3.24	Metabolic processes
A1S_2452	NAD-dependent aldehyde dehydrogenase	-2.58	Enzymatic

			processes
A1S_2456	transcriptional regulator lysR family	-0.57	Transcription regulation
A1S_2466	hypothetical protein	-1.17	Membrane structures and transport
A1S_2475	isocitrate dehydrogenase	-0.93	Energy production and conversion
A1S_2478	putative trypsin-like serine protease	-0.67	Protein binding, transport, and folding
A1S_2483	putative membrane protein	-0.65	Membrane structures and transport
A1S_2511	Phenylacetic acid degradation-related protein	-0.69	Unknown and hypothetical functions
A1S_2520	putative signal peptide	-1.04	Unknown and hypothetical functions
A1S_2542	hypothetical protein	-0.36	Biosynthetic process
A1S_2549	hypothetical protein	-0.55	Unknown and hypothetical functions
A1S_2550	Tn7 transposase A	-0.65	DNA binding, metabolism, and repair
A1S_2551	Tn7-like transposition protein B	-0.61	DNA binding, metabolism, and repair
A1S_2552	ATPase	-0.68	Unknown and hypothetical functions
A1S_2589	Metal-dependent hydrolase of the aminoacylase-2/carboxypeptidase-Z family	-0.65	Metabolic processes
A1S_2601	putative outer membrane protein A	-0.7	Unknown and hypothetical functions
A1S_2602	hypothetical protein	-0.73	Unknown and hypothetical functions
A1S_2653	transcription elongation factor GreB	-1.1	Transcription regulation
A1S_2664	chaperone Hsp60	-0.97	Protein binding, transport, and

			folding
A1S_2665	chaperone Hsp10	-1.05	Protein binding, transport, and folding
A1S_2685	hypothetical protein	-2.06	Unknown and hypothetical functions
A1S_2700	putative flavodoxin or tryptophan repressor binding protein	-1.56	Energy production and conversion
A1S_2759	hypothetical protein YbdF	-1.06	Unknown and hypothetical functions
A1S_2773	putative long-chain fatty acid transport protein	-0.62	Unknown and hypothetical functions
A1S_2785	putative protease	-0.91	Unknown and hypothetical functions
A1S_2809	bacteriolytic lipoprotein entericidin B	-0.84	Stress responses
A1S_2823	hypothetical protein	-1.38	Stress responses
A1S_2828	putative FMN oxidoreductase	-0.67	Enzymatic processes
A1S_2843	hypothetical protein	-1.6	Unknown and hypothetical functions
A1S_2850	putative acyl-CoA transferase/carnitine dehydratase	-1.43	Enzymatic processes
A1S_2863	putative antioxidant protein	-0.94	Enzymatic processes
A1S_2880	putative signal peptide	-1.67	Unknown and hypothetical functions
A1S_2924	putative Rhodanese-related sulfurtransferase	-1.19	Unknown and hypothetical functions
A1S_2929	putative cation efflux system protein	-0.92	Membrane structures and transport
A1S_2931	hypothetical protein	-1.09	Unknown and hypothetical functions
A1S_2935	copper resistance protein B precursor	-0.97	Membrane structures and transport
A1S_2936	copper resistance protein A precursor	-0.86	Enzymatic processes

A1S_2939	ATPase E1-E2 type:Copper-translocating P-type ATPase:Heavy metal translocating P-type ATPase	-1.24	Metal ion binding and transport
A1S_2944	hypothetical protein	-1.25	Unknown and hypothetical functions
A1S_2956	esterase	-0.96	Metabolic processes
A1S_2959	Hsp 24 nucleotide exchange factor	-0.83	Protein binding, transport, and folding
A1S_2960	chaperone Hsp70	-0.73	Protein binding, transport, and folding
A1S_2961	hypothetical protein	-1.09	Unknown and hypothetical functions
A1S_2978	hypothetical protein	-0.72	Transcription regulation
A1S_3013	hypothetical protein	-0.71	Unknown and hypothetical functions
A1S_3014	hypothetical protein	-0.91	Metabolic processes
A1S_3024	hypothetical protein	-0.68	Unknown and hypothetical functions
A1S_3053	acyl coenzyme A dehydrogenase	-0.71	Enzymatic processes
A1S_3088	hypothetical protein	-0.78	Metabolic processes
A1S_3112	hypothetical protein	-0.87	Unknown and hypothetical functions
A1S_3143	Cu/Zn superoxide dismutase	-1.19	Enzymatic processes
A1S_3149	hypothetical protein	-0.85	Enzymatic processes
A1S_3155	hypothetical protein	-0.95	Unknown and hypothetical functions
A1S_3180	putative signal peptide	-0.9	Unknown and hypothetical functions
A1S_3207	sulfate transport protein	-0.83	Membrane structures and

			transport
A1S_3224	acyl coenzyme A reductase	-1.21	Enzymatic processes
A1S_3225	putative sulfate permease	-0.81	Membrane structures and transport
A1S_3258	putative NAD(P)H oxidoreductase	-1.02	Enzymatic processes
A1S_3277	putative pirin-like protein	-1.04	Enzymatic processes
A1S_3300	putative sodium:solute symporter	-1.64	Membrane structures and transport
A1S_3301	putative membrane protein	-1.45	Membrane structures and transport
A1S_3303	hypothetical protein	-1.07	Unknown and hypothetical functions
A1S_3309	acetyl-CoA synthetase	-2.13	Biosynthetic process
A1S_3343	hypothetical protein	-0.66	Unknown and hypothetical functions
A1S_3361	hypothetical protein	-0.68	Protein binding, transport, and folding
A1S_3405	histidine ammonia-lyase	-0.63	Amino acid metabolism and transport
A1S_3406	urocanate hydratase	-1.14	Enzymatic processes
A1S_3407	Urocanase	-1.12	Enzymatic processes
A1S_3418	4-hydroxyphenylpyruvate dioxygenase	-0.67	Enzymatic processes
A1S_3428	putative glucose dehydrogenase precursor	-1.99	Carbohydrate metabolism
A1S_3439	aldehyde reductase	-0.69	Enzymatic processes
A1S_3461	DNA replication protein	-1.02	DNA binding, metabolism, and repair
A1S_3473	hypothetical protein	-0.69	Enzymatic processes
A1S_3493	hypothetical protein	-1.19	Unknown and

			hypothetical functions
A1S_3564	hypothetical protein	-2.18	Unknown and hypothetical functions
A1S_3627	hypothetical protein	-1.04	Unknown and hypothetical functions
A1S_3629	hypothetical protein	-0.77	Unknown and hypothetical functions
A1S_3636	hypothetical protein	-1.37	Unknown and hypothetical functions
A1S_3637	hypothetical protein	-0.98	Unknown and hypothetical functions
A1S_3646	hypothetical protein	-0.75	Unknown and hypothetical functions
A1S_3662	hypothetical protein	-1.4	Unknown and hypothetical functions
A1S_3685	hypothetical protein	-0.86	Unknown and hypothetical functions
A1S_3706	hypothetical protein	-0.71	Unknown and hypothetical functions
A1S_3709	hypothetical protein	-0.53	Unknown and hypothetical functions
A1S_3714	hypothetical protein	-1.18	Unknown and hypothetical functions
A1S_3723	hypothetical protein	-0.99	Unknown and hypothetical functions
A1S_3750	hypothetical protein	-2.08	Unknown and hypothetical functions
A1S_3765	hypothetical protein	-0.75	Unknown and hypothetical functions
A1S_3786	hypothetical protein	-1.34	Unknown and hypothetical

			functions
A1S_3887	hypothetical protein	-1	Unknown and hypothetical functions

Appendix IV. List of upregulated genes in *A. baumannii* AB104 compared to ATCC 17978

locus_tag	Name	Differential Expression Log2 Ratio	Differential Expression p-value
A1S_0099	D-serine/D-alanine/glycine transport protein CDS	1.6	2.20E-19
A1S_0371	putative membrane protein CDS	1.8	0.00E+00
A1S_0429	glutamate:aspartate symport protein (DAACS family) CDS	2.5	0.00E+00
A1S_0548	putative transcriptional regulator (TetR family) CDS	1.9	7.60E-25
A1S_0549	hypothetical protein CDS	2	0.00E+00
A1S_0566	pyridine nucleotide transhydrogenase (proton pump) alpha subunit (part1) CDS	2	6.30E-30
A1S_0567	pyridine nucleotide transhydrogenase (proton pump) alpha subunit (part2) CDS	1.8	2.10E-19
A1S_0568	pyridine nucleotide transhydrogenase beta subunit CDS	1.6	1.00E-26
A1S_0624	putative lipoprotein CDS	1.5	1.60E-17
A1S_0625	putative transcriptional regulator (TetR family) CDS	1.7	4.30E-14
A1S_0630	hypothetical protein CDS	2.5	0.00E+00
A1S_0631	hypothetical protein CDS	2.4	0.00E+00
A1S_0632	DNA primase CDS	1.7	3.40E-12
A1S_0633	hypothetical protein CDS	2.4	0.00E+00
A1S_0634	hypothetical protein CDS	2.3	0.00E+00
A1S_0640	hypothetical protein CDS	2.3	0.00E+00
A1S_0641	hypothetical protein CDS	2.4	4.00E-33
A1S_0642	hypothetical protein CDS	2.7	0.00E+00
A1S_0643	hypothetical protein CDS	3.9	0.00E+00
A1S_0644	hypothetical protein CDS	4	0.00E+00
A1S_0645	hypothetical protein CDS	4.2	0.00E+00
A1S_0646	IcmB protein CDS	3	0.00E+00
A1S_0647	IcmO protein CDS	2.2	2.30E-21
A1S_0650	conjugal transfer protein CDS	3	0.00E+00
A1S_1135	putative transporter CDS	1.6	1.70E-25
A1S_1143	hypothetical protein CDS	2	0.0094
A1S_1258	hypothetical protein CDS	2.3	0.00E+00
A1S_1266	putative membrane protein CDS	2.3	0.00E+00
A1S_1267	putative lactam utilization protein CDS	1.6	0.00E+00
A1S_1268	hypothetical protein CDS	1.6	0.00E+00
A1S_1269	putative allophanate hydrolase subunit 1 and 2 CDS	1.6	0.00E+00
A1S_1376	Acyl-CoA dehydrogenase CDS	1.8	0.00E+00
A1S_1377	transcriptional regulator acrR family CDS	1.7	0.00E+00

A1S_1378	putative long chain fatty-acid CoA ligase CDS	1.8	0.00E+00
A1S_1379	putative SAM-dependent methyltransferase CDS	1.8	2.30E-21
A1S_1380	putative protein (DcaP-like) CDS	1.9	4.30E-09
A1S_1466	glutaminase-asparaginase CDS	2.3	0.00E+00
A1S_1467	putative glutamate symport transmembrane protein CDS	2.6	0.00E+00
A1S_1509	pili assembly chaperone CDS	1.9	0.000056
A1S_1510	Fimbrial protein CDS	2.8	0.00E+00
A1S_1530	SSS family major sodium/proline symporter CDS	1.5	0.00E+00
A1S_1590	peptidase U35 phage prohead HK97 CDS	2.3	0.028
A1S_1591	phage major capsid protein HK97 CDS	2.3	0.0011
A1S_1592	putative Phage head-tail adaptor CDS	1.9	0.017
A1S_1594	hypothetical protein CDS	2.6	0.00012
A1S_1595	hypothetical protein CDS	1.7	0.0012
A1S_1730	short-chain fatty acid transporter (scFAT family) CDS	2.1	2.10E-19
A1S_1732	acetoacetyl-CoA transferase alpha subunit CDS	1.6	0.00E+00
A1S_1736	putative membrane protein CDS	2.7	0.00E+00
A1S_1737	3-hydroxybutyrate dehydrogenase CDS	1.6	1.00E-29
A1S_1776	transcriptional regulatory protein CDS	1.6	0.011
A1S_1778	putative methylenetetrahydrofolate reductase CDS	1.6	0.006
A1S_2016	Phage-related lysozyme CDS	4.1	0.00092
A1S_2025	hypothetical protein CDS	1.7	2.50E-12
A1S_2027	hypothetical protein CDS	1.8	2.50E-09
A1S_2028	phage putative head morphogenesis protein CDS	1.8	0.00019
A1S_2031	hypothetical protein CDS	3.2	0.00028
A1S_2032	hypothetical protein CDS	2.6	0.014
A1S_2041	hypothetical protein CDS	1.5	3.60E-28
A1S_2042	putative transcriptional regulator (TetR family) CDS	2	1.10E-16
A1S_2148	putative acetyl-CoA synthetase/AMP-(fatty) acid ligase CDS	1.7	0.0000066
A1S_2280	aerobic C4-dicarboxylate transport protein CDS	2	0.00E+00
A1S_2449	aromatic amino acid transporter (APC family) CDS	1.6	0.0035
A1S_2450	putative pyruvate decarboxylase CDS	2.6	4.00E-16
A1S_2452	NAD-dependent aldehyde dehydrogenase CDS	1.7	1.10E-19
A1S_2793	putative amino-acid transport protein CDS	2.6	0.00E+00
A1S_2912	queuine tRNA-ribosyltransferase CDS	1.5	5.50E-16
A1S_2982	hypothetical protein CDS	1.6	0.00E+00
A1S_3056	RNA polymerase alpha subunit CDS	1.5	0
A1S_3061	secretion protein CDS	1.7	0
A1S_3162	tRNA (guanine-1-)-methyltransferase CDS	1.8	0.00E+00

A1S_3273	putative peptide signal CDS	3.3	0.00E+00
A1S_3283	gamma-aminobutyrate permease CDS	1.5	3.60E-11
A1S_3300	putative sodium:solute symporter CDS	2	0.00E+00
A1S_3301	putative membrane protein CDS	2.3	0.00E+00
A1S_3404	proline transport protein (APC family) CDS	1.6	0.00E+00
A1S_3486	hypothetical protein CDS	1.7	0.033
A1S_3504	hypothetical protein CDS	2	0
A1S_3521	hypothetical protein CDS	1.6	2.40E-12
A1S_3522	hypothetical protein CDS	2.4	0.00E+00
A1S_3523	hypothetical protein CDS	2.4	0.00E+00
A1S_3524	hypothetical protein CDS	1.5	4.00E-08
A1S_3528	hypothetical protein CDS	1.7	0.00E+00
A1S_3532	hypothetical protein CDS	1.6	2.40E-24
A1S_3533	hypothetical protein CDS	1.9	0.00E+00
A1S_3534	hypothetical protein CDS	2.8	0.00E+00
A1S_3535	hypothetical protein CDS	4.2	0.00E+00
A1S_3537	hypothetical protein CDS	1.9	1.50E-24
A1S_3539	hypothetical protein CDS	4.5	0.00E+00
A1S_3540	hypothetical protein CDS	4.2	0.00E+00
A1S_3541	hypothetical protein CDS	4	0.00E+00
A1S_3542	hypothetical protein CDS	3.1	0.00E+00
A1S_3543	hypothetical protein CDS	3	0
A1S_3544	hypothetical protein CDS	3.4	0.00E+00
A1S_3545	hypothetical protein CDS	2.6	1.70E-30
A1S_3546	hypothetical protein CDS	2.7	1.90E-27
A1S_3548	hypothetical protein CDS	2.2	1.90E-18
A1S_3552	hypothetical protein CDS	3.4	0.00E+00
A1S_3553	hypothetical protein CDS	2.5	2.10E-29
A1S_3657	hypothetical protein CDS	1.6	0.011
A1S_3693	hypothetical protein CDS	4.8	0.000083
A1S_3699	hypothetical protein CDS	1.9	0.017
A1S_3700	hypothetical protein CDS	1.8	0.0018
A1S_3717	hypothetical protein CDS	1000000	0.0095
A1S_3754	hypothetical protein CDS	1.5	0.0021
A1S_3755	hypothetical protein CDS	1.7	0.01
A1S_3760	hypothetical protein CDS	2.1	4.50E-07
A1S_3764	hypothetical protein CDS	2	0.033
A1S_3765	hypothetical protein CDS	1.9	0.0000024
A1S_3766	hypothetical protein CDS	1.8	0.000023
A1S_3785	hypothetical protein CDS	1.6	3.80E-13
A1S_3809	hypothetical protein CDS	2.2	8.00E-09

A1S_3836	hypothetical protein CDS	1.6	1.50E-27
A1S_3895	hypothetical protein CDS	1.8	0.00019
A1S_3908	hypothetical protein CDS	2.1	1.30E-27
A1S_3915	hypothetical protein CDS	1.5	0.0000012

Appendix V. List of downregulated genes in *A. baumannii* AB104 compared to ATCC 17978

locus_tag	Name	Differential Expression Log2 Ratio	Differential Expression p-value
A1S_0040	putative oxidoreductase CDS	-1.5	0.00023
A1S_0067	L-lactate permease CDS	-5.7	0.00E+00
A1S_0068	L-lactate utilization transcriptional repressor (GntR family) CDS	-3.1	2.60E-29
A1S_0069	L-lactate dehydrogenase FMN linked CDS	-4	0.00E+00
A1S_0070	D-lactate dehydrogenase NADH independent, FAD-binding domain CDS	-2.9	1.20E-22
A1S_0509	putative acyl carrier protein CDS	-2.4	0.021
A1S_0902	lactoylglutathione lyase-related protein CDS	-1.7	1.40E-08
A1S_1217	heavy metal translocating P-type ATPase CDS	-1.5	6.00E-07
A1S_1224	transposase CDS	-1.5	4.00E-17
A1S_1437	putative acyl-CoA dehydrogenase CDS	-1.6	0.0021
A1S_1442	taurine ABC transporter periplasmic taurine-binding protein CDS	-1.5	0.0000015
A1S_1443	taurine ATP-binding transport system component CDS	-2.9	4.90E-11
A1S_1444	ABC taurine transporter permease subunit CDS	-2.2	0.0000024
A1S_1445	taurine dioxygenase CDS	-1.5	0.00016
A1S_1539	putative transcriptional regulator (ArsR family) CDS	-1.6	5.90E-07
A1S_2183	putative signal peptide CDS	-1.6	0.00E+00
A1S_2347	hypothetical protein CDS	-1.7	0.05
A1S_2407	hypothetical protein CDS	-3.2	0.039
A1S_2458	putative fatty acid desaturase CDS	-1.5	0.00E+00
A1S_2531	sulfate transport protein CDS	-1.6	0.000011
A1S_2532	sulfate transport protein CDS	-1000000	0.037
A1S_2533	putative esterase CDS	-2.1	0.00024
A1S_2551	Tn7-like transposition protein B CDS	-1.6	6.60E-11
A1S_2552	ATPase CDS	-1.6	4.30E-11
A1S_2553	transposition site target selection protein D CDS	-1.7	0.000017
A1S_2664	chaperone Hsp60 CDS	-1.6	0
A1S_2665	chaperone Hsp10 CDS	-1.5	0.00E+00
A1S_2853	putative 3-hydroxybutyryl-CoA epimerase CDS	-1.5	1.40E-07
A1S_3108	coproporphyrinogen III oxidase CDS	-1.7	0.00E+00
A1S_3225	putative sulfate permease CDS	-1.8	0.00011
A1S_3253	putative signal peptide CDS	-1.8	1.70E-33

A1S_3260	hypothetical protein CDS	-2	0.00022
A1S_3317	putative outer membrane protein CDS	-1.6	0.00E+00
A1S_3350	hypothetical protein CDS	-1.7	0
A1S_3511	hypothetical protein CDS	-1.6	0.000029
A1S_3564	hypothetical protein CDS	-1.5	0.00E+00
A1S_3580	hypothetical protein CDS	-1.8	3.30E-39
A1S_3641	hypothetical protein CDS	-1.9	2.30E-15
A1S_3842	hypothetical protein CDS	-2.1	0.0018
A1S_3865	hypothetical protein CDS	-1.6	3.70E-30
A1S_3877	hypothetical protein CDS	-1.5	5.50E-38
A1S_3907	hypothetical protein CDS	-2.8	0.0042

Appendix VI. Data obtained from Biolog™ phenotypic microarray plate PM3B for utilisation of nitrogen sources. The numbers indicate the A_{590nm} values obtained after 18 hours of incubation at 37˚C in a Biolog™ phenotypic microarray plate PM3B. The percentage growth of each strain was calculated by normalising the A_{590nm} values for AB104 and AB239 with ATCC 17978 values. Growth percentages of AB104 were colour coded from red (low) to green (high). AB239 shows partial restoration of the growth defects observed in AB104.

Nitrogen source	ATCC 17978	AB104	AB239	% of growth of AB104 relative to ATCC 17978	% of growth of AB239 relative to ATCC 17978
N-Acetyl-L-Glutamic Acid	1.5261	1.1022	1.456	72.2233143	95.406592
D-Serine	1.5538	1.1451	1.3318	73.6967435	85.7124469
L-Histidine	1.6835	1.248	1.4864	74.1312741	88.2922483
D-Aspartic Acid	1.2553	0.9519	1.3637	75.8304788	108.635386
L-Isoleucine	1.3155	1.0211	1.3275	77.6206765	100.912201
L-Arginine	1.3511	1.0503	1.3547	77.736659	100.26645
D-Alanine	1.3551	1.1021	1.491	81.3297912	110.02878
Allantoin	1.2352	1.0112	1.3816	81.865285	111.852332
Ala-Gly	1.2991	1.0736	1.2775	82.641829	98.3373104
L-Citrulline	1.4252	1.1889	1.4633	83.4198709	102.673309
D-Asparagine	1.2507	1.0455	1.1983	83.5931878	95.8103462
L-Methionine	1.3172	1.108	1.2219	84.1178257	92.764956
Glycine	1.1851	1.006	1.4047	84.8873513	118.530082
Gly-Asn	1.3581	1.155	1.1919	85.0452839	87.762315
Gly-Met	1.2348	1.0567	1.3051	85.5766116	105.69323
D-Lysine	1.2773	1.0934	1.2896	85.6024427	100.962969
Ala-Leu	1.2622	1.0946	1.4075	86.7215972	111.511646
N-Acetyl-D-Mannosamine	1.2834	1.1143	1.3067	86.8240611	101.81549
Guanosine	1.2224	1.0724	1.2057	87.7290576	98.6338351
Thymine	1.1981	1.0529	1.254	87.8808113	104.665721
L-Alanine	1.3273	1.1686	1.3784	88.0433964	103.849921
L-Asparagine	1.4419	1.2738	1.4326	88.3417713	99.3550177
D-Amino-N-Valeric Acid	1.161	1.0259	1.2359	88.3634798	106.451335
Ethylamine	1.2081	1.0768	1.2885	89.1316944	106.655078

Methylamine	1.2484	1.1167	1.2444	89.4504966	99.6795899
Alloxan	1.2344	1.1089	1.3689	89.8331173	110.895982
L-Glutamine	1.7627	1.5903	1.4812	90.2195496	84.030181
e-Amino-N-Caproic Acid	1.1611	1.0504	1.2296	90.4659375	105.899578
Parabanic Acid	1.1208	1.0179	1.3016	90.8190578	116.131335
Gly-Gln	1.2196	1.1093	1.297	90.9560512	106.346343
β-Phenylethyl-amine	0.7721	0.708	0.822	91.6979666	106.462893
Cytosine	1.4315	1.3131	1.4792	91.7289556	103.332169
N-Acetyl-D-Glucosamine	1.1183	1.0386	1.2239	92.873111	109.442904
Uracil	1.3671	1.2717	1.4175	93.0217248	103.686636
γ-Amino-N-Butyric Acid	1.242	1.1561	1.3671	93.0837359	110.072464
Acetamide	1.1425	1.0648	1.2239	93.1991247	107.124726
Biuret	1.2124	1.1314	1.3325	93.3190366	109.905972
Inosine	1.1501	1.0744	1.3536	93.4179637	117.694114
N-Phthaloyl-L-Glutamic Acid	1.2188	1.1388	1.2579	93.4361667	103.208074
L-Phenylalanine	1.4145	1.3284	1.399	93.9130435	98.9042064
Ethanolamine	1.1023	1.0367	1.0875	94.048807	98.6573528
D-Galactosamine	1.2109	1.1425	1.357	94.3513089	112.065406
L-Aspartic Acid	1.4754	1.3952	1.5317	94.564186	103.815914
L-Pyroglutamic Acid	1.3949	1.3205	1.465	94.6662843	105.02545
D-Mannosamine	1.3046	1.2393	1.196	94.9946344	91.6756094
Adenine	0.9839	0.9387	1.0591	95.4060372	107.643053
Adenosine	0.969	0.9259	1.2678	95.5521156	130.835913
Cytidine	1.136	1.0957	1.3174	96.4524648	115.96831
Guanine	0.9548	0.9211	1.1907	96.470465	124.706745
Thymidine	1.1134	1.0787	1.2553	96.8834202	112.744746
Glucuronamine	1.1573	1.1276	1.1804	97.4336818	101.996025
L-Serine	1.1988	1.1777	1.3966	98.2399066	116.499833
D-Valine	1.0454	1.0287	1.3577	98.4025253	129.873733
L-Proline	1.3761	1.3617	1.6612	98.9535644	120.717971
Uric Acid	1.04	1.0312	1.1667	99.1538462	112.182692
N-Amylamine	1.0354	1.0289	1.1605	99.3722233	112.082287
Met-Ala	1.2568	1.2495	1.3406	99.4191598	106.667728
L-Lysine	1.1231	1.1171	1.3624	99.4657644	121.307096
Ala-Thr	1.0956	1.0908	1.2215	99.5618839	111.49142
D,L-Lactamide	1.0745	1.0706	1.2645	99.6370405	117.682643
Ala-Asp	1.2012	1.2003	1.2734	99.9250749	106.010656
Ala-His	1.1616	1.1773	1.3175	101.351584	113.421143
Tyramine	0.9424	0.9562	1.0854	101.464346	115.174024

Formamide	1.0373	1.0542	1.2893	101.62923	124.29384
Ala-Glu	1.042	1.0624	1.3665	101.957774	131.142035
Agmatine	1.0669	1.0883	1.0867	102.005811	101.855844
N-Acetyl-D-Galactosamine	1.085	1.1118	1.1275	102.470046	103.917051
Ala-Gln	1.2008	1.2309	1.3134	102.506662	109.377082
Xanthosine	1.0325	1.0585	1.2164	102.51816	117.811138
L-Glutamic Acid	1.3105	1.3532	1.6012	103.258298	122.182373
Ammonia	1.0196	1.0536	1.186	103.334641	116.320126
D-Glutamic Acid	1.4315	1.4836	1.782	103.639539	124.484806
D,L-a-Amino-Caprylic Acid	1.1989	1.2426	1.2587	103.645008	104.987906
Gly-Glu	1.0041	1.0488	1.2115	104.451748	120.655313
L-Leucine	1.2246	1.2864	1.3119	105.046546	107.128858
D,L-a-Amino-N-Butyric Acid	1.1059	1.1634	1.2237	105.199385	110.651958
Urea	1.0155	1.0791	1.243	106.262925	122.402757
L-Homoserine	0.9713	1.0323	1.3239	106.280243	136.301863
Histamine	0.9378	1.0001	1.4166	106.643208	151.055662
L-Tryptophan	1.1926	1.2726	1.4576	106.708033	122.220359
Putrescine	1.3901	1.4853	1.3844	106.848428	99.5899576
L-Ornithine	1.0186	1.0902	1.4853	107.029256	145.817789
L-Tyrosine	0.9645	1.0342	1.1876	107.226542	123.131156
L-Cysteine	1.0787	1.1571	1.1772	107.268008	109.131362
Xanthine	1.1176	1.2198	1.401	109.144596	125.35791
N-Butylamine	1.0057	1.1008	1.2052	109.4561	119.83693
L-Valine	1.1315	1.2421	1.1335	109.774635	100.176757
Nitrite	0.9679	1.0822	1.1837	111.809071	122.295692
L-Threonine	1.0879	1.2261	1.4483	112.703373	133.128045
Nitrate	1.0484	1.1882	1.3163	113.334605	125.553224
D-Glucosamine	0.9683	1.1027	1.4133	113.879996	145.956832
Uridine	1.0009	1.1736	1.3991	117.254471	139.784194
Ethylenediamine	1.1657	1.3671	1.3543	117.277173	116.17912
Hydroxylamine	0.5998	0.7104	0.8579	118.43948	143.03101
α-Amino-N-Valeric Acid	0.9285	1.1237	1.2193	121.023156	131.319332

Appendix VII. Plasmid map of pFLP2A

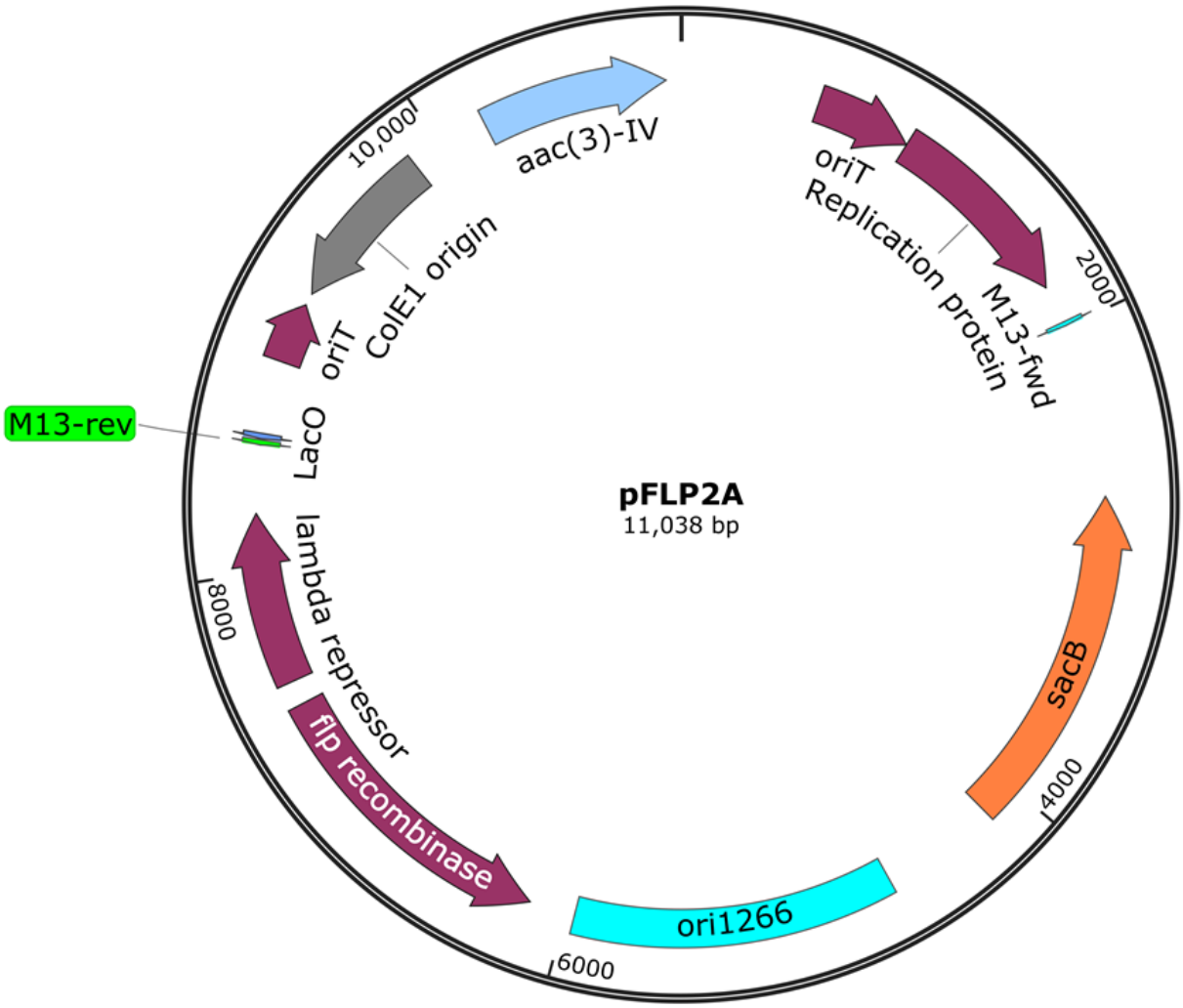

Appendix VIII. Plasmid map of pFLP2Z

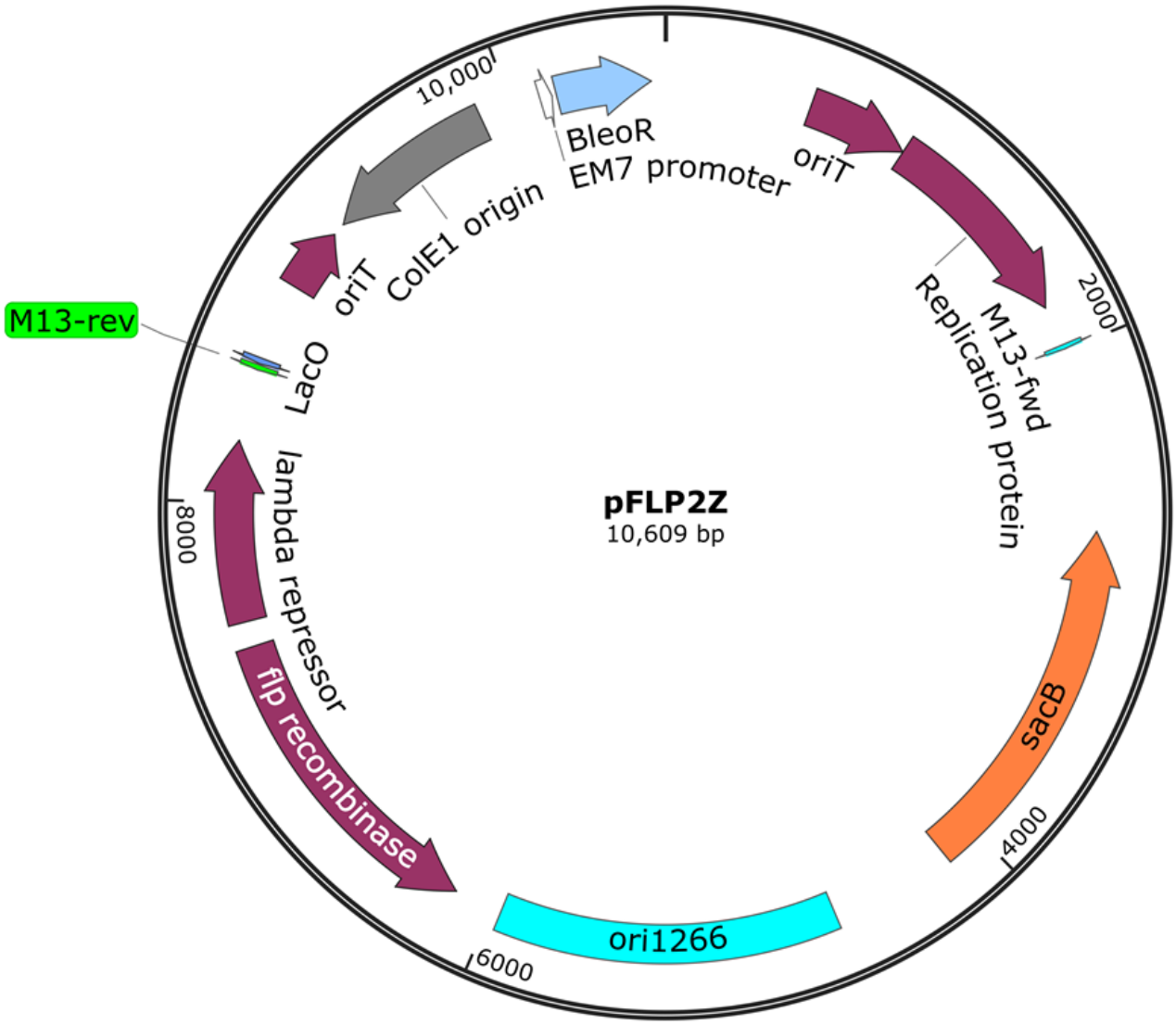

Appendix IX. Plasmid map of pUC18T-mini-Tn*7*T-Apr-mCherry2

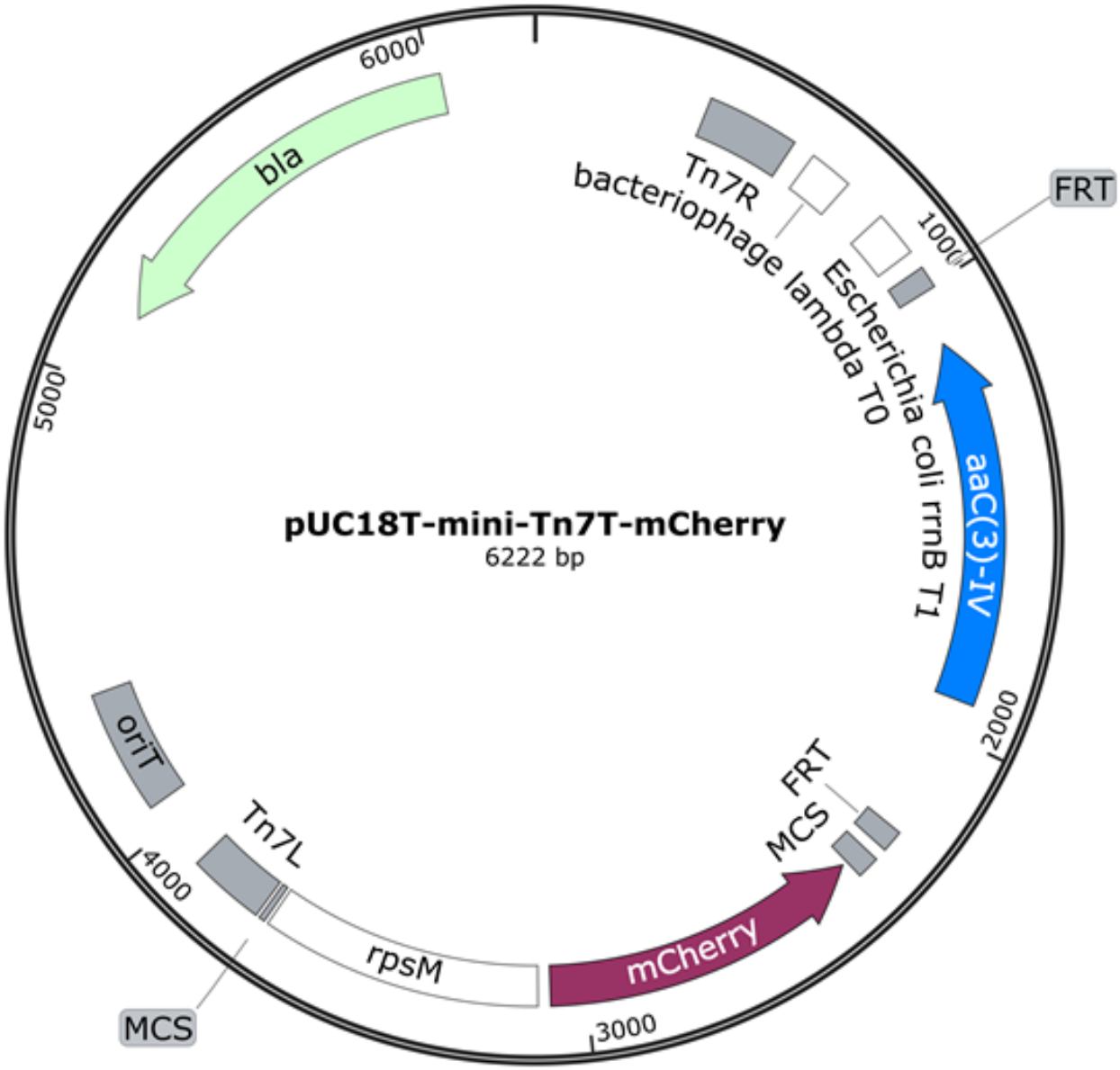

Appendix X. Plasmid map of pUC18T-mini-Tn7T-Apr-mRuby2

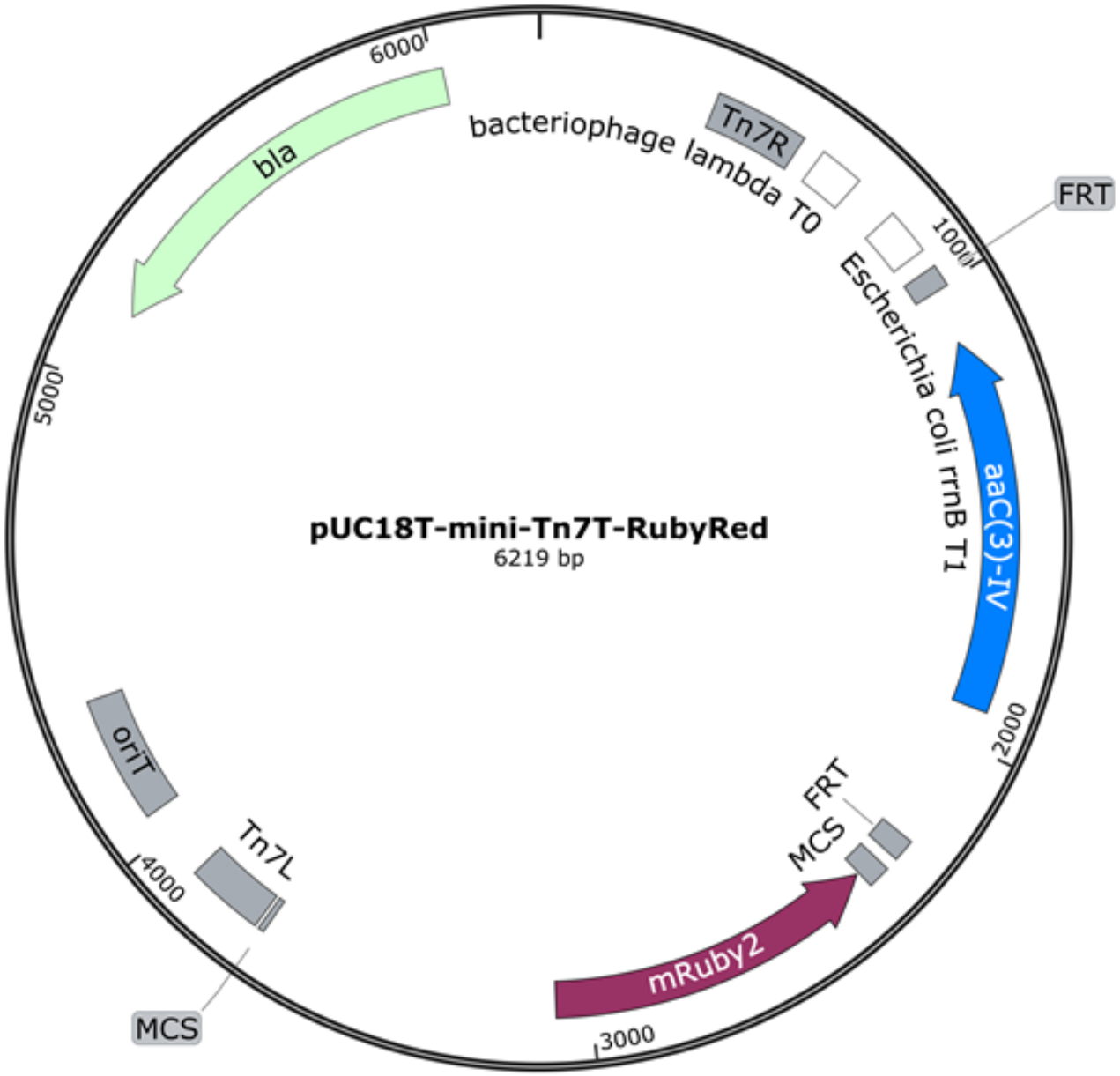

Appendix XI. Plasmid map of pUC18T-mini-Tn*7*T-Apr-sfGFP

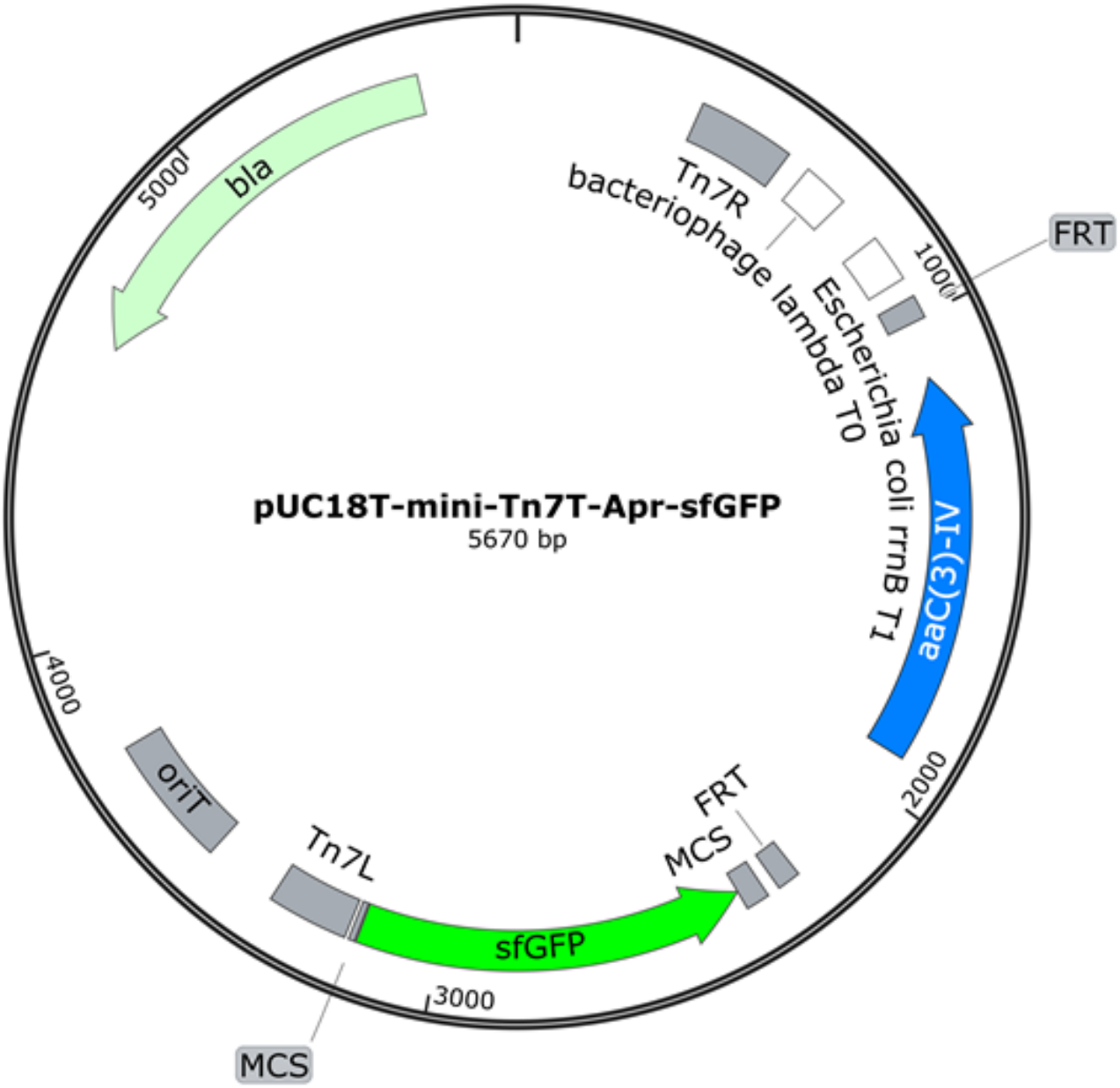

Appendix XII. Plasmid map of pUC18T-mini-Tn*7*T-Apr-mTurquoise2